

UC Berkeley

UC Berkeley Electronic Theses and Dissertations

Title

Insight into the Genetic Basis of Craniofacial Morphological Variation in the Domestic Dog, *Canis familiaris*

Permalink

<https://escholarship.org/uc/item/3hw582pm>

Author

Rizk, Oliver Torres

Publication Date

2012

Peer reviewed|Thesis/dissertation

Insight into the Genetic Basis of Craniofacial Morphological Variation in the
Domestic Dog, *Canis familiaris*

By

Oliver Torres Rizk

A dissertation submitted in partial satisfaction of the
requirements for the degree of

Doctor of Philosophy

in

Integrative Biology

in the

Graduate Division

of the

University of California, Berkeley

Committee in charge:

Professor Leslea Hlusko, Chair
Professor Montgomery Slatkin
Professor Katharine Milton
Professor Tim D. White

Fall 2012

Insight into the Genetic Basis of Craniofacial Morphological Variation in the
Domestic Dog, *Canis familiaris*

Copyright © 2012
by
Oliver Torres Rizk

Abstract

Insight into the Genetic Basis of Craniofacial Morphological Variation in the Domestic Dog, *Canis familiaris*

by

Oliver Torres Rizk

Doctor of Philosophy in Integrative Biology

University of California, Berkeley

Professor Leslea Hlusko, Chair

The domestic dog, *Canis familiaris*, presents a unique opportunity to identify and study the relationship between genotype and phenotype. Over the approximately 15,000 years since its domestication from the gray wolf, *Canis lupus*, the dog has undergone intense artificial selection for a variety of functional and aesthetic forms, resulting in hundreds of modern breeds that exhibit a wide range of behavior and morphology. Restrictive breeding histories have rendered each breed as a distinct genetic unit, facilitating the genetic mapping of breed-specific phenotypes.

Brachycephaly, or a short, wide head, is a phenotype that is observed across a variety of breeds. However, brachycephaly has not been consistently defined or quantified and it remains unclear whether different forms of brachycephaly exist across breeds. The inclusion of brachycephalic breeds within two genetically distant breed groups, the toy dogs and the Mastiff-like dogs, supports the possibility that distinctions within the brachycephalic category exist. In addition, mouse developmental gene expression studies demonstrate that multiple genetic pathways can be manipulated to produce a brachycephalic mouse, suggesting that distinctions between brachycephalic dog breeds may correspond to different genetic mechanisms.

The objectives of this dissertation are to identify patterns of morphological distinction between brachycephalic dog breeds and to draw connections between these patterns and genetic relationships among breeds and craniofacial developmental genetics in mice. The following three research questions are addressed:

- (1) Are there significant distinctions in the patterns of shape differences between the crania of various brachycephalic breeds and the ancestral gray wolf cranium?
- (2) Do any distinctions in patterns of shape differences correspond to genetic relationships between breeds?
- (3) Are these patterns of shape differences comparable to genetic pathways identified in mouse developmental genetic studies?

Three-dimensional landmark coordinates representing craniofacial shape variation were collected from 527 adult dog crania, representing sixty-nine breeds. Dog breed crania were compared to a

sample of 120 adult gray wolf crania from Alaska. Comparison of average cranial shape between groups was performed using a geometric morphometric approach, wherein landmark coordinate configurations were superimposed to remove the effects of size and orientation. Principal component and discriminant function analyses were implemented to describe the major axes of variation within each group and to identify the shape differences from the gray wolf characterizing each breed.

Three distinct patterns of canine brachycephaly were observed across breeds. First, the Boxer and Bulldog breeds share a pattern of facial shortening, which, relative to the gray wolf, includes a more rostro-dorsal position of the frontal bones and a reduction in length and a dorsal tilt of the rostral nasal bones. The short snout of these breeds is also proportionally wider. Second, the Pug, Pekingese, and French Bulldog breeds exhibit a pattern that is distinct from the Boxer and Bulldog. Relative to the gray wolf, these breeds display an even greater degree of reduction in the length of the rostral-most snout elements than observed in the Boxer and Bulldog. This reduction is combined with extremely dished nasal bones at the midface. Finally, the Chihuahua presents a third form of brachycephaly in which, relative to the gray wolf, the rostral snout is neither tilted dorsally nor proportionally increased in width.

These patterns do not correspond to recently determined genetic relationships between breeds. The presence of different forms of brachycephaly within the toy dog and Mastiff-like dog groups suggests that the overall genetic similarity between breeds may not reflect shared genetic mechanisms for individual traits that are part of complex breeding histories.

Three candidate genes for canine brachycephaly were identified from the mouse developmental genetic literature. Mouse mutant phenotypes for each gene were compared with the patterns of brachycephaly observed in dog breeds. Mouse haploinsufficient for the gene *Tcof1* exhibit brachycephalic features resembling the Pug/Pekingese/French Bulldog pattern, whereas mice lacking *Msx1* and *Msx2* alleles present a phenotype most similar to the Boxer/Bulldog pattern. Finally, loss- and gain-of-function mutations in the gene *Fgfr2c* in mice produce a form of brachycephaly that parallels that seen in the Chihuahua.

By quantifying variation in the brachycephalic phenotype and identifying candidate genes that may underlie this variation, these findings provide direction for future studies of genetic association. This insight into the relationship between genetic variation and craniofacial phenotypic variation in the dog can also be applied to our understanding of the processes of natural selection that have produced brachycephalic forms in the canid fossil record, as well as throughout vertebrate evolution.

I dedicate this dissertation to my parents.

Table of Contents

Dedication.....	i
Table of Contents.....	ii
Acknowledgments.....	v
Chapter 1: The Domestic Dog as a Model Organism.....	1
1.1 Connecting genotype and phenotype.....	1
1.2 The brachycephalic dog phenotype.....	2
1.3 Research questions.....	8
1.4 Dissertation overview.....	10
1.5 Origin of the domestic dog.....	11
1.5.1 Domestication.....	11
1.5.1.A Evolutionary scenarios.....	11
1.5.1.B Selection for behavior.....	12
1.5.1.C Characters of domestication.....	13
1.5.2 Archaeology.....	16
1.5.3 Molecular studies.....	18
1.5.3.A Karyology and serology.....	19
1.5.3.B Mitochondrial DNA.....	19
1.5.3.C Nuclear DNA.....	21
1.6 Craniofacial variation in the domestic dog.....	22
1.6.1 With respect to archaeology.....	22
1.6.2 As an expression of cranial metrics and indices.....	22
1.6.2.A The Hirnstammbasis.....	23
1.6.2.B Facial angle.....	23
1.6.2.C Other anatomical traits.....	23
1.6.3 In relation to size (static allometry).....	24
1.6.3.A Body size.....	24
1.6.3.B Brain size.....	25
1.6.4 In relation to growth (ontogenetic allometry).....	25
1.6.4.A Ontogeny.....	25
1.6.4.B Heterochrony.....	23
1.6.5 In relation to morphological integration.....	28
1.7 The genetic basis for craniofacial variation in the domestic dog.....	28
1.7.1 Studies of inheritance.....	28
1.7.2 The genome of the domestic dog.....	30
1.7.3 Studies of genetic association.....	30
Chapter 2: Materials and Methods.....	33
2.1 Materials.....	33
2.1.1 <i>Canis lupus</i>	33
2.1.2 <i>Canis familiaris</i>	33
2.2 Methods.....	36
2.2.1 Introduction to geometric morphometrics.....	36

2.2.1.A	Early origins of geometric morphometric approaches.....	36
2.2.1.B	Landmark-based methods.....	41
2.2.1.B.i	Coordinate-based approaches.....	42
2.2.1.B.i.a	Superimposition: Generalized Procrustes analysis.....	43
2.2.1.B.i.b	Superimposition: Two-point and edge-matching registration.....	45
2.2.1.B.i.c	Deformation: Finite-element scaling analysis.....	45
2.2.1.B.i.d	Deformation: Thin-plate spline.....	47
2.2.1.B.ii	Coordinate-free approaches: Euclidean distance matrix analysis.....	48
2.2.1.C	Non-landmark-based approaches.....	49
2.2.1.C.i	Eigenshape and Fourier analyses.....	50
2.2.1.C.ii	Geodesic distance analysis.....	51
2.2.1.D	Rationale for the techniques applied in this study.....	52
2.2.2	Data collection.....	53
2.2.3	Data formatting.....	55
2.2.4	Measurement error.....	55
2.2.4.A	Error assessment in geometric morphometric studies.....	55
2.2.4.B	Error assessment for canid crania digitization.....	57
2.2.5	MorphoJ analyses.....	57

Chapter 3: Craniofacial Shape Differences between Domestic Dog Breeds and the Gray Wolf..... 58

3.1	Introduction.....	58
3.2	Principal component analyses.....	58
3.2.1	<i>Canis lupus</i>	58
3.2.2	<i>Canis familiaris</i>	62
3.2.3	Comparison of <i>C. lupus</i> and <i>C. familiaris</i>	65
3.2.4	Dolichocephalic breeds.....	68
3.2.5	Mesaticephalic breeds.....	68
3.2.6	Brachycephalic breeds.....	68
3.3	Discriminant function analyses.....	76
3.3.1	Dolichocephalic breed differences from the gray wolf.....	76
3.3.2	Mesaticephalic breed differences from the gray wolf.....	79
3.3.3	Brachycephalic breed differences from the gray wolf.....	79
3.4	Discussion.....	86
3.4.1	Differences between brachycephalic breeds.....	86
3.4.2	The genetic relationship between brachycephalic breeds.....	89

Chapter 4: Candidate Genes for Canine Brachycephaly..... 93

4.1	Introduction.....	93
4.2	Development of the vertebrate head.....	93
4.2.1	Evolutionary origins of the components of the skull.....	94
4.2.2	Embryonic tissue origins of the components of the skull.....	94
4.2.3	Genetic regulation of embryonic head development.....	95
4.2.3.A	Neural crest induction.....	96
4.2.3.B	Neural crest migration.....	96
4.2.3.C	Patterning of the facial prominences.....	97

4.2.3.D	Outgrowth of the face	97
4.2.4	Genetic regulation of skeletogenesis	98
4.3	Candidate genes for brachycephaly based on mouse models	99
4.3.1	<i>Tcofl</i>	100
4.3.1.A	The role of <i>Tcofl</i> in neural crest cell generation and proliferation.....	100
4.3.1.B	The craniofacial phenotype of <i>Tcofl</i> haploinsufficiency.....	100
4.3.1.C	<i>Tcofl</i> as a candidate gene for canine brachycephaly	101
4.3.2	<i>Msx1</i> and <i>Msx2</i>	102
4.3.2.A	The role of <i>Msx1</i> and <i>Msx2</i> in frontal bone development	102
4.3.2.B	The craniofacial phenotype of <i>Msx1</i> and <i>Msx2</i> null mutants	102
4.3.2.C	<i>Msx1</i> and <i>Msx2</i> as candidate genes for canine brachycephaly	103
4.3.3	<i>Fgfr2c</i>	103
4.3.3.A	The role of <i>Fgfr2c</i> in osteoblast development and cranial suture fusion.....	103
4.3.3.B	The craniofacial phenotype of <i>Fgfr2c</i> mutants.....	104
4.3.3.C	<i>Fgfr2c</i> as a candidate gene for canine brachycephaly	104
4.4	Discussion.....	104
Chapter 5: Conclusion		107
5.1	Research questions.....	107
5.2	Findings	107
5.2.1	Response to research question 1	107
5.2.2	Response to research question 2	108
5.2.3	Response to research question 3	108
5.3	Future directions	109
5.3.1	Genetic association	109
5.3.2	The canid fossil record.....	109
References.....		111
Appendix 1: <i>Canis lupus</i> sample		143
Appendix 2: <i>Canis familiaris</i> sample		146
Appendix 3: Cranial landmark definitions.....		158
Appendix 4: Landmark coordinate standard deviations (gray wolf, 20 trials)		161
Appendix 5: Focus breed second principal components of shape variation.....		163
Appendix 6: Discriminant function shape deformations: additional focus breeds.....		170
Appendix 7: Additional measures of disparity between breeds.....		179

Acknowledgments

I thank my dissertation committee for their guidance in this project from its earliest conception to completion. There is no way to sufficiently thank my advisor and dissertation committee chair Leslea Hlusko for her endless support and encouragement. I am very fortunate to have had an advisor who was always so readily available to help me and ensure that the best opportunities and resources were available to me. Tim White, Katie Milton, and Monty Slatkin donated considerable time and energy to reading my thesis and helping me to improve it. I thank my entire committee for their patience and thoughtfulness.

The formulation and execution of this dissertation was influenced and aided by a number of other scientists, who all played indispensable advisory roles during my graduate career. I thank Nina Jablonski, David DeGusta, F. Clark Howell, Bill Clemens, Tony Barnosky, Ellen Simms, Jim Patton, Jackson Njau, Henry Gilbert, and Charles Marshall for their contributions.

It would have been impossible to accomplish anything as a graduate student in Integrative Biology without the help of Mei Griebenow, whom I depended on in all matters of funding and filing. The entire Integrative Biology staff was a tremendous resource. I especially thank Michael Schneider for his help in coordinating all of the travel required for my data collection, and Susan Gardner for her assistance applying for funding.

So much of this work has depended on access to museum collections and I am indebted to the curators and collections managers of all of the institutions that I visited. In particular I thank Marc Nussbaumer at the Naturhistorisches Museum der Burgergemeinde Bern in Switzerland and Link Olson at the University of Alaska Museum of the North for hosting my lengthy stay at each location. I also thank Chris Conroy at the Museum of Vertebrate Zoology at Berkeley, Moe Flannery at the California Academy of Sciences, Jim Dines at the Los Angeles County Museum of Natural History, Kristof Zyskowski at the Yale Peabody Museum of Natural History, Judy Chupasko at the Harvard Museum of Comparative Zoology, Eileen Westwig at the American Museum of Natural History, Linda Gordon at the National Museum of Natural History, Susan Woodward at the Royal Ontario Museum, and Ray Bandar, for access to his private collection in San Francisco, California.

I was fortunate to have the opportunity to take the geometric morphometrics shortcourse offered at Berkeley every summer by Mimi Zeldtich and Don Swiderski. I am thankful for their expertise and assistance in designing and implementing the geometric morphometric approach taken in this study. I also thank Sabrina Sholts, Rebecca Jabbour, and Gary Richards for their help with the digitization process.

My experience was greatly enhanced by the community of wonderful researchers I worked alongside in the Hlusko lab and the Human Evolution Research Center. It has been a privilege to work with Sarah Amugongo, Theresa Grieco, Jackie Moustakas, Josh Carlson, and Monica Carr. I also have appreciated the support of Kyle Brudvik, Denise Su, Alexis Lainoff, Michael Holmes, Tesla Monson, Liz Bates, Arta Zowghi, Julia Addiss, Josh Cohen, Priscilla Lee, Jeff Yoshihara, Nick Do, Zach Fletcher, Tina Koh, and Kara Timmins. I thank my colleagues in the departments of Integrative Biology and Environmental Science and Policy Management, particularly Andrew Rush, Mike Wasserman, Bryan Kraatz, Sarah Werning, Katie Brakora, Alan Shabel, Andrew Ritchie, Maya deVries, Charlene Ng, Michael Shuldman, Nick Pyenson and Susumu Tomiya. Outside of Berkeley, I thank many close friends for their kindness and support: Michael Leyton, Julian Wass, Chris Yamaoka, Janet Kim, Derek Yu, Evan Hayden, Noah Cates and Kate Pruitt.

I also thank my family, whose support and love have been the driving force behind the completion of this dissertation. I thank my parents, my brother, and my grandparents for fostering my love for science as a child and for supporting me through all of my studies.

Last, but not least, I thank my girlfriend Patricia Pei for being such an incredible partner. Patricia has assisted in the completion of this dissertation in countless ways, including her Excel spreadsheet magic, extraordinary proofreading, and all-around enthusiasm for dogs. I thank Patricia for keeping me motivated at all times and for making it all worth it in the end.



Chapter 1: The Domestic Dog as a Model Organism

1.1 Connecting genotype and phenotype

Understanding the relationship between genotype and phenotype is central to the study of the evolution of skeletal morphology. By linking variation in the DNA sequence inherited over generations to variation in the morphology selected for by the environment, researchers have been able to answer questions about how the genetic organization of morphology has evolved over time at the population level and on larger scales.

For example, Cheverud and colleagues employed a quantitative genetic approach to test Olson and Miller's (1958) hypothesis of morphological integration between developmentally and functionally related traits in primate and mouse crania (e.g., Cheverud 1982, 1995, 1996; Leamy *et al.* 1999). Work of this nature has proven increasingly informative for our understanding of which phenotypes are heritable (see, for example, Richtsmeier and McGrath's (1986) study of cranial nonmetric trait heritability and etiology) as well as the degree to which phenotypes are genetically independent from each other (see the analysis of molar cusp patterning by Hlusko *et al.* (2004)). Marroig and Cheverud (2005) also demonstrated that estimates of genetic variance and covariance between traits could be used to characterize past evolutionary forces in their study of size as a line of least evolutionary resistance in the evolution of New World monkeys.

Shapiro *et al.* (2004, 2006) elegantly combined quantitative genetics, gene expression manipulation, and gene sequence comparison to elucidate the genetic basis for pelvic reduction in stickleback fish. The authors determined that regulatory changes in the gene *Pitx1* are responsible for variation in pelvic size in sticklebacks and confirmed that a similar genetic mechanism underlies pelvic reduction in manatees, indicating parallel genetic origins of this phenotype across vertebrates (Shapiro *et al.* 2006). Complementary to quantitative genetics, genome-wide sequence comparisons and association studies have provided insight to broader patterns of evolution, including which genetic mechanisms are shared among taxa and the age of the common ancestor in which the mechanism was established (see Shubin and colleagues' (1997, 2002) study of appendage patterning or Fraser and colleagues' (2009) study of jaw and teeth modularity).

The domestic dog, *Canis familiaris*, presents an excellent opportunity to identify and study connections between genes and morphology (Galibert and André 2008). Since its domestication from the gray wolf, *C. lupus*, approximately 15,000 years ago (Savolainen *et al.* 2002; Pang *et al.* 2009), the dog has been the subject of intense selection for various functional and aesthetic forms (Coppinger and Schneider 1995; Sampson and Binns 2006). The result is an amazing range of morphologies and behaviors spanning hundreds of modern breeds, each representing a closed gene pool (American Kennel Club, 2006; Wayne and Ostrander 2007). The sequencing of the canine genome in 2005 by Lindblad-Toh and colleagues enabled researchers to explore genetic relationships within breeds more closely. An important finding from this work has been that restrictive breeding histories have led to smaller effective population sizes for and greater genetic drift within breeds, producing a combination of high genetic homogeneity within each breed and high genetic heterogeneity between breeds (Parker *et al.* 2004; Lindblad-Toh *et al.* 2005). This distribution of genetic variation within and between breeds, combined with the extreme degree of phenotypic variation characterizing different breeds, creates an ideal scenario for the mapping of the phenotype to genotype.

In particular, the domestic dog has drawn attention as a model for human genetic disease mapping (Ostrander and Giniger 1997; Shearin and Ostrander 2010), as it shares over three hundred genetic diseases with humans (Patterson 2000), a similarity long recognized in the veterinary medical community (Patterson *et al.* 1982). Over half of these diseases segregate to specific breeds (Patterson 2000), aiding in the design of mapping studies that utilize quantitative trait loci (QTL) (reviewed by Sutter and Ostrander 2004; Karlsson and Lindblad-Toh 2008), linkage disequilibrium (reviewed by Hyun *et al.* 2003), and genome-wide association approaches (Karlsson and Lindblad-Toh 2008). Despite the large focus on disease, the most noteworthy studies of genotype-phenotype relationships in dogs to date have addressed the genetic basis for morphological variation. Recently researchers have identified the primary genetic source of variation in simple traits such as coat color (Cadieu *et al.* 2009) and body size (Sutter *et al.* 2007).

Sutter and colleagues' 2007 investigation of body size across dog breeds is an especially good example of the utility of the dog as a model organism for connecting genes and morphology. Similar to the approach of Shapiro and colleagues' (2004, 2006) stickleback study, this investigation began at the population level, examining the association between size and relatedness in a pedigreed population of Portuguese Water Dogs. The QTL identified in this single breed analysis implicated the gene *IGF1*, which encodes insulin-like growth factor 1 and is known from studies of body size in mice and humans. Instead of next performing a series of genetic crosses to isolate the phenotype in interest as the stickleback group did, Sutter and colleagues utilized the variation created by centuries of dog breeding by exploring single nucleotide polymorphism (SNP) variation at this locus in a sample of over forty breeds representing the extremes of body size in the dog. Interestingly, they found that the presence of only a single *IGF1* SNP haplotype separates small breeds from their large counterparts.

1.2 The brachycephalic dog phenotype

The *IGF1* sequence variant identified by Sutter *et al.* (2007) in small dogs is associated with a fairly straightforward, easily quantifiable phenotype: body size. Cranial shape presents a more complex phenotype that has been quantified using myriad approaches (reviewed with respect to the dog cranium later in this chapter). One of the greatest dimensions of variation in the dog cranium is the relative length of the face. In fact, variation in this regard in dog breeds exceeds that across all the wild canids (Wayne 1984, 1986; Drake and Klingenberg 2010). Naturally, dog breeds have been categorized to reflect these differences. For example, in *Miller's Anatomy of the Dog*, Evans (1993) recognizes three forms: dolichocephalic, or long, narrow-headed breeds; brachycephalic, or short, wide-headed breeds; and mesaticephalic, or intermediate breeds (Figures 1.1-1.4).

Evans (1993) contrasts dolichocephalic and brachycephalic breeds using several skeletal indices. Following Stockard (1941), who demonstrated that indices better distinguish these two groups than individual linear measurements (but did not actually use the terms dolicho- or brachycephalic), Evans (1993) uses skull index (skull width multiplied by a factor of one hundred, divided by skull length) to divide breeds into one group or another. Unfortunately, as Koch and colleagues (2003) point out, there is no consensus on which criteria to use for categorization, as several German authors use the ratio of cranial length to skull length (e.g., Nickel *et al.* 1984; Brehm *et al.* 1985), while Regodon *et al.* (1993) use the angle between the

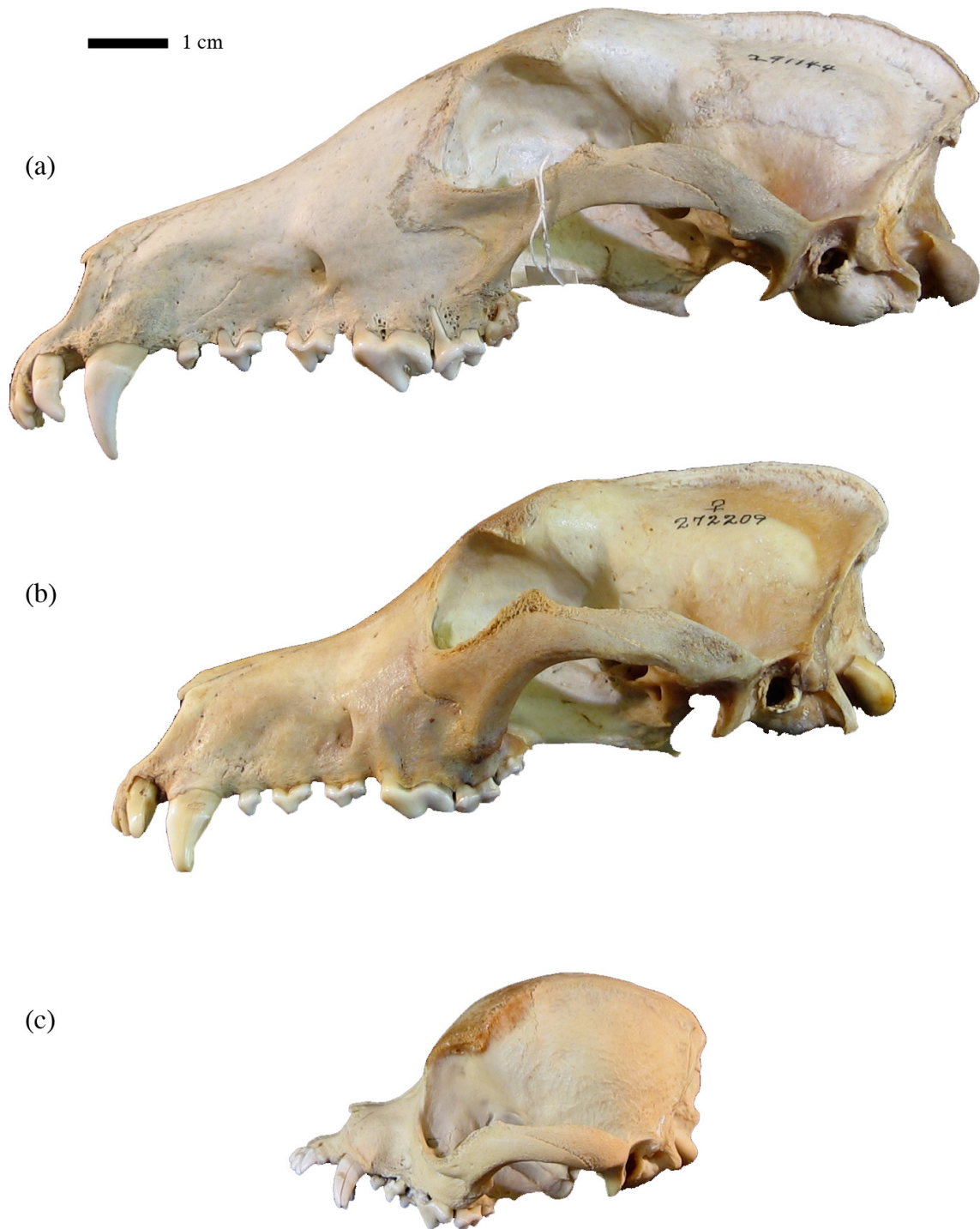


Figure 1.1 Lateral view of: (a) a dolichocephalic Borzoi; (b) a mesaticephalic German Shepherd Dog; and (c) a brachycephalic Pug.

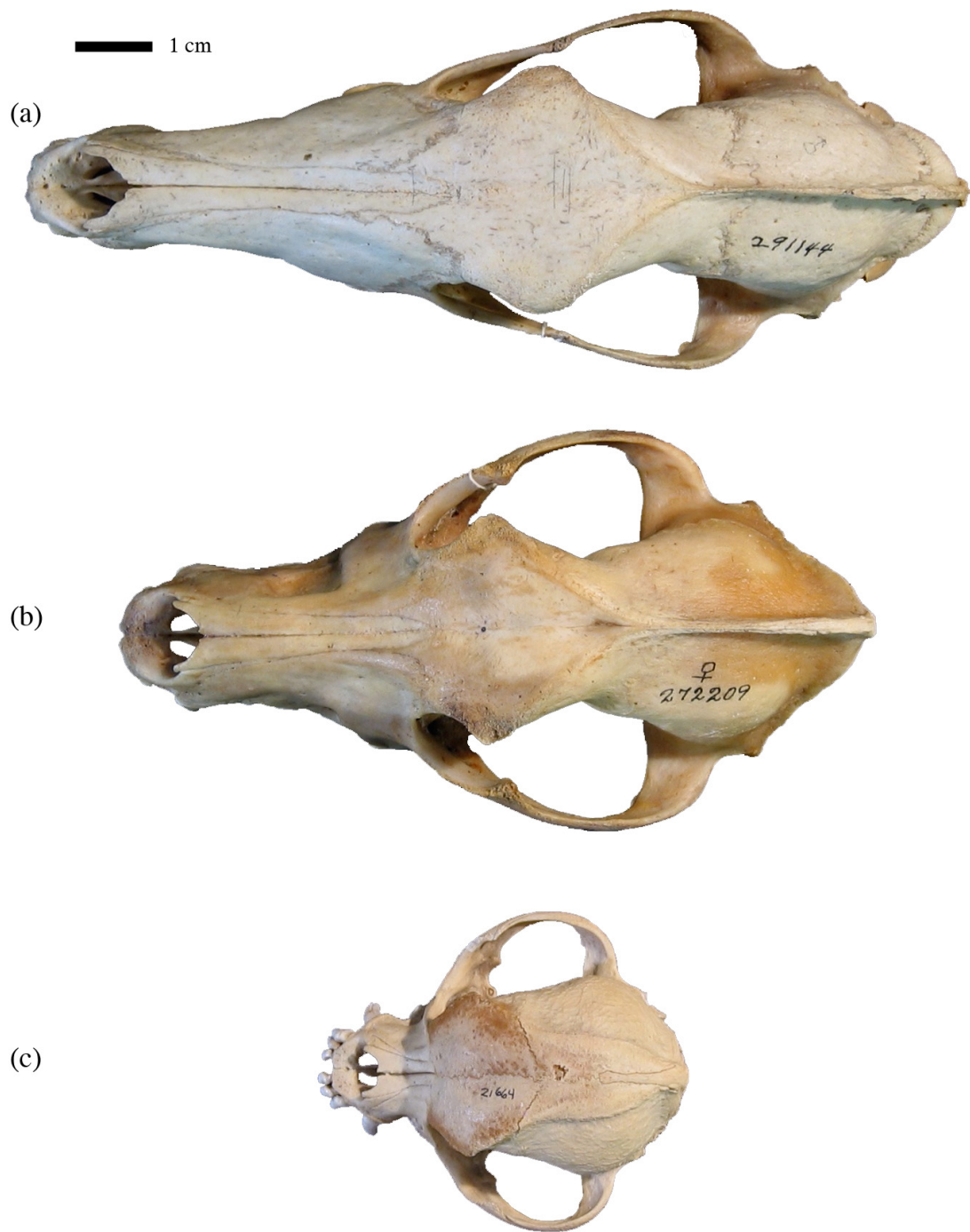


Figure 1.2 Dorsal view of: (a) a dolichocephalic Borzoi; (b) a mesaticephalic German Shepherd Dog; and (c) a brachycephalic Pug.

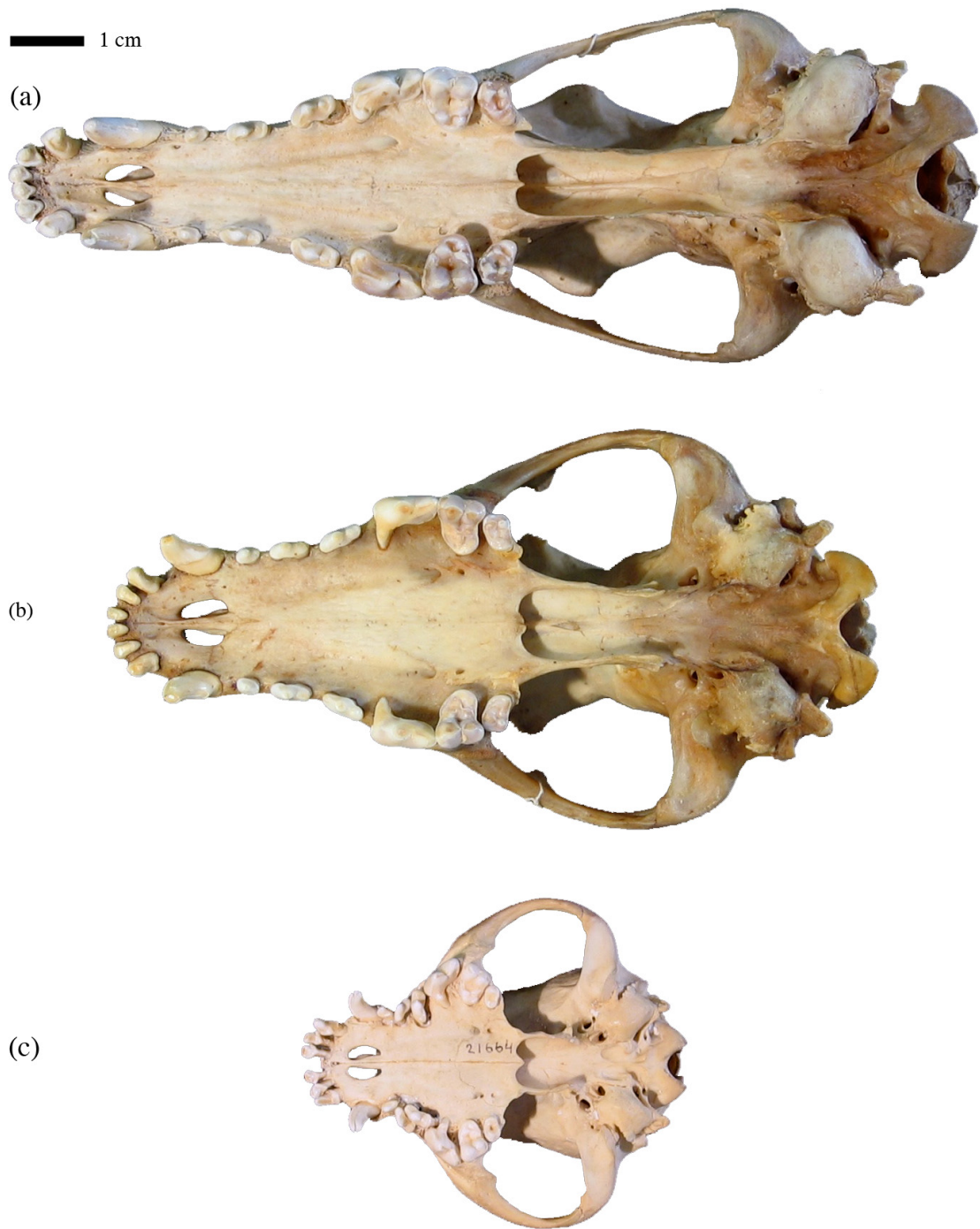


Figure 1.3 Ventral view of: (a) a dolichocephalic Borzoi; (b) a mesaticephalic German Shepherd Dog; and (c) a brachycephalic Pug.

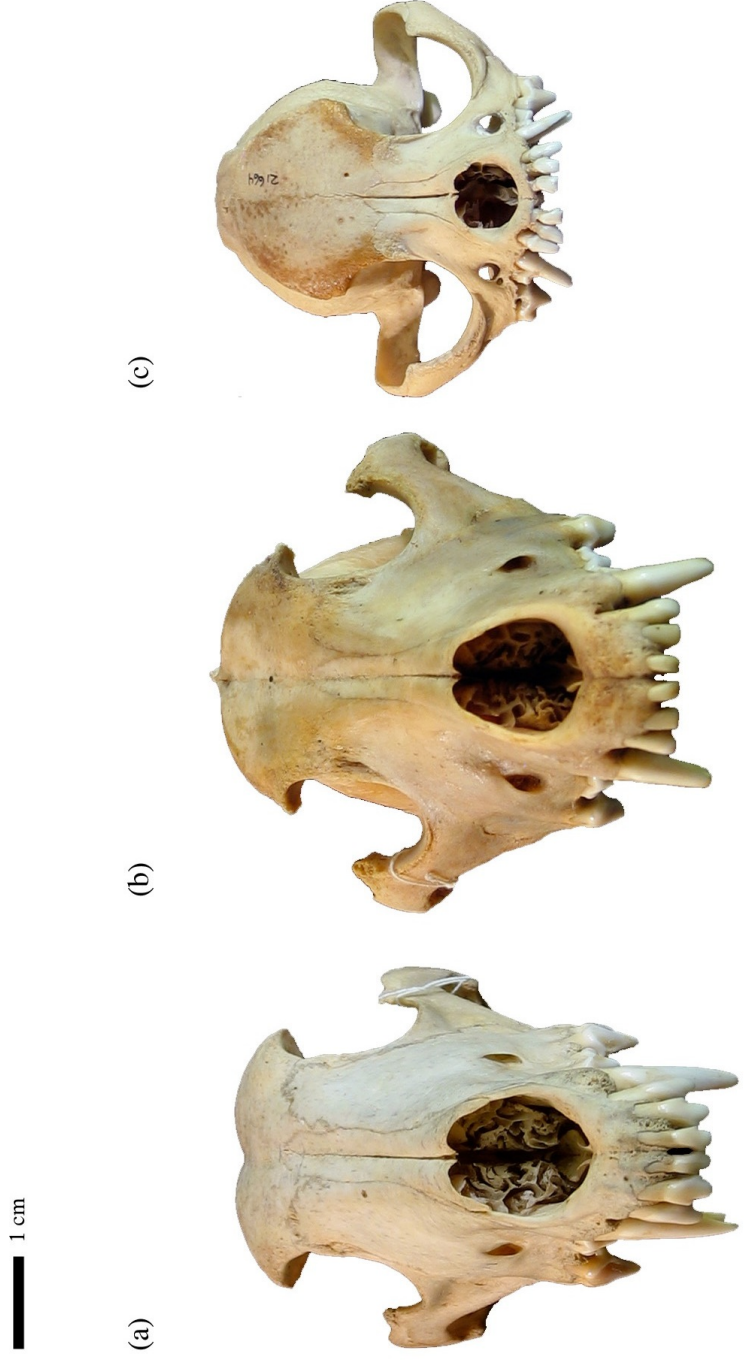


Figure 1.4 Anterior view of: (a) a dolichocephalic Borzoi; (b) a mesaticephalic German Shepherd Dog; and (c) a brachycephalic Pug.

base of the skull and the face. The term “brachycephalic” is also used outside of purely morphological descriptions to refer to a specific medical syndrome in veterinary medicine, “brachycephalic airway syndrome,” which is prevalent in brachycephalic breeds (Koch *et al.* 2003; Nöller *et al.* 2008).

One of the results of this terminological ambiguity is that studies examining the genetic basis for the brachycephalic phenotype are inconsistent with regard to which criteria are used to designate affected breeds. For example, Bannasch and colleagues (2010) cite Stockard’s (1941) categorization approach in their across-breed mapping study, while Haworth *et al.* (2001a,b, 2007) and Hünemeier *et al.* (2009) simply use a qualitative description of short- and wide-faced dogs as the basis for their selection of breeds to study. In each of these cases, an actual quantification of cranial shape is missing from the association study; instead, variation at the genetic level is associated with a particular breed that has been qualitatively assigned a phenotype. This may be misleading if, in fact, brachycephaly varies significantly between breeds. The degree of facial shortening and widening varies among brachycephalic breeds, as do the angles of the midface and palate (Figure 1.2). In other words, a morphological distinction between different brachycephalic breeds could also suggest an accompanying genetic distinction.

One reason to consider this possibility is that brachycephalic dogs are not isolated to one subset of closely related breeds. In one of the most sophisticated genetic analyses of breed relationships to date, vonHoldt and colleagues (2010) surveyed over 48,000 SNPs in dogs and gray wolves and found that modern breeds cluster largely in concordance with the functional groupings used by dog breeders and kennel clubs. In their tree depicting genetic relationships between breeds, the authors showed that brachycephalic breeds exist in two relatively distant groupings: breeds such as the Chihuahua, Pekingese, and Pug fall into the toy dog group, whereas breeds such as the Boxer, Bulldog, French Bulldog, and Bull Terrier belong to the Mastiff-like dog group.

A second reason to consider a distinction between the genetic bases for brachycephaly in different dog breeds comes from our understanding of craniofacial developmental genetics. Modification of development links variation at the genetic level to the generation of new, complex phenotypes (Atchley and Hall 1991). Lovejoy and colleagues (1999) and Hlusko (2004) have advocated the incorporation of developmental information in the definition of phenotypic traits, arguing that many of the morphological character definitions used in phylogenetic analyses assume an independent, particulate inheritance that is not supported by the developmental genetic literature. Unfortunately, developmental genetic resources for the dog are limited (Ruvinsky 2001) and an assessment of brachycephaly in a developmental genetic context requires insight from a separate model organism. In this case, the mouse (specifically the house mouse, *Mus musculus*, the ubiquitous laboratory mouse) is the best resource for studying mammalian craniofacial development and gene expression (Johnston and Bronksy 1991; Ignelzi *et al.* 1995; Sharpe 1999; Trainor 2005), and provides several examples of different developmental genetic pathways to a brachycephalic phenotype (see below).

By rendering a gene completely or partially inoperative, knockout studies enable researchers to identify which elements, if any, of the developing skull are influenced by that gene. More importantly, the phenotypes produced by these generated mutants provide a clue as to how modification of the gene’s function may modify the element(s) of the skull. A review of mouse developmental genetics presents several craniofacial phenotypes that approximate the variation seen across dog breeds. Each case provides a distinct genetic pathway to a brachycephalic mouse phenotype that may parallel the modification seen in brachycephalic dog

breeds. For example, Dixon and colleagues (2006) have described an anteroposteriorly shortened skull in germ line-generated haploinsufficient mice for the gene *Tcofl*, for which autosomal dominant mutations in the human homologous gene *TCOF1* cause Treacher Collins syndrome (characterized by hypoplasia of the facial bones). *Tcofl*^{+/-} neonate mice exhibit reduced head size and a shortened fronto-nasal complex that is dished at the midface. Additionally, the premaxillae, maxillae, and palatines are shortened and misshaped, and the maxillary and palatine shelves are displaced by a midline cleft. The authors attribute this collective hypoplasia to a deficiency of cranial neural crest cells.

Null mutations of two other genes, *Msx1*, which produces defects in frontal bone development in mice (Satokata and Maas, 1994), and *Msx2*, for which null mutants have reduced frontal primordium (Ishii *et al.*, 2003), work together to regulate cranial neural crest cell differentiation during frontal bone formation (Han *et al.*, 2007). Newborn mutant mouse skulls exhibit a gradient of frontal bone defects, ranging from mild in *Msx1*^{-/-} null mutants to severe in *Msx1*^{-/-};*Msx2*^{+/-} double knockout mutants. In the latter, a dorsal midline gap between the two frontal bones creates a shortened phenotype, altering the position and angle of the nasal bones (Han *et al.*, 2007). The end result resembles the shortened face of the *Tcofl* mutants; however, in this case, the overall phenotype is achieved by direct modification of the frontal bone only, which in turn affects the shape of the entire fronto-nasal complex.

The genetics of craniosynostosis—the premature fusion of sutures in the skull vault—present a third mechanism for craniofacial shortening. Eswarakumar *et al.* (2002, 2004) studied the role of the *Fgf* signaling pathway as it applies to the craniosynostosis disorder Crouzon syndrome. Mutations in the gene *Fgfr2c* produce severe shortening in the facial region, paired with coronal sutures that are fused on both sides of the skull. These sutures typically remain open during the lifespan of the mouse, as seen in wild type mice. Fusion of the coronal sutures limits the length of the developing frontal and nasal bones, shortening and ventrally angling the face. Here, modification of the gene *Fgfr2c* provides a mechanism for facial shortening that is distinct from the previous two examples.

It is possible that every brachycephalic dog breed achieves this phenotype by the same means, using the same genetic pathway. However, the effects of *Tcofl*, *Msx1* and *Msx2*, and *Fgfr2c* in mice collectively indicate that there are multiple genetic pathways that can be modified to produce similar craniofacial phenotypes (Dixon *et al.* 2006; Han *et al.* 2007; Eswarakumar *et al.* 2002, 2004).

1.3 Research questions

This dissertation addresses the genetic basis for the brachycephalic phenotype in the domestic dog. The success of canine genetic association studies to date can largely be attributed to the increasingly powerful mapping resources that have been generated from the sequenced dog genome and the inherent structure of that genome (Karlsson and Lindblad-Toh 2008; also reviewed below in this chapter). Equally important, however, is a thorough, quantitative characterization of the phenotype in question. This is especially imperative for complex phenotypes such as cranial shape. An understanding of which cranial elements are modified in terms of their shape to produce a brachycephalic dog cranium and how such modifications vary by breed is essential for any future genetic association study and is the main focus of this dissertation.

I use a geometric morphometric approach to quantify the differences in cranial shape separating the ancestral gray wolf from modern dog breeds representing dolichocephalic, mesaticephalic, and brachycephalic forms. Geometric morphometrics (GM) is a powerful descriptive tool for comparing biological shapes (Richtsmeier *et al.* 2002), in this case represented by three-dimensional landmark coordinates describing the cranial morphology of museum specimens (for a more detailed explanation of GM and materials used in this study, see Chapter 2). By visualizing the patterns of shape differences that characterize relevant dog breeds, I will address the following questions:

(1) **Are there significant distinctions in the patterns of shape differences between the crania of various brachycephalic breeds and the ancestral gray wolf cranium?** GM analysis of craniofacial shape provides an opportunity to contrast dog breeds relative to the gray wolf. It is important to note here that no modern breed evolved directly from the gray wolf, let alone modern gray wolves like the ones used in this study (see Chapter 2). Hence, the goal of presenting side-by-side comparisons of the shape deformation required to transform a wolf cranium into the crania of various dog breeds is not to describe evolutionary processes but to identify what differences characterize breed-specific brachycephaly.

Hypothesis 1: Distinct craniofacial forms corresponding to specific breeds or groups of breeds exist within the larger brachycephalic category.

(2) **Do any distinctions in patterns of shape differences correspond to genetic relationships between breeds?** Any similarities or differences between brachycephalic breeds can be evaluated in the context of the breed phylogeny constructed by vonHoldt and colleagues (2010).

Hypothesis 2: The toy dog and Mastiff-like dog groups represent separate, distinct brachycephalic forms.

(3) **Are these patterns of shape differences comparable to genetic pathways identified in mouse developmental genetic studies?** It is not necessary to introduce new mouse data to address this question. Instead, I draw from the substantial mouse developmental genetic literature to assess the results of the GM analysis. This strategy has been proposed by Hallgrímsson and colleagues (2004), who studied craniofacial variability and modularity in the macaque. The authors outlined an approach in which the screening of mouse mutant models can be used to identify gene effects, which can then be applied to understanding the developmental basis of morphological variation in organisms for which such developmental investigations are less tractable (i.e., primates, dogs). The practicality of this approach has been bolstered by the assembly of a mouse gene–phenotype network by Espinosa and Hancock (2011), based on publicly available gene knockout phenotype data. Three hypotheses are tested using this strategy, corresponding to the multiple mouse genetic pathways identified above.

Hypothesis 3A: Modification of the gene *Tcof1* has provided a mechanism for brachycephaly in dogs via coordinated shortening of both the frontal and nasal bones.

Hypothesis 3B: Modification of the genes *Msx1* and *Msx2* has provided a mechanism for brachycephaly in dogs via shortening of the frontal bones only, which in turn displaces the nasal bones.

Hypothesis 3C: Modification of the gene *Fgfr2c* has provided a mechanism for brachycephaly in dogs via altered sutures in the skull vault, resulting in shortening and angling of both the frontal and nasal bones.

1.4 Dissertation overview

Here I summarize the organization of this dissertation, in which I present the materials and methods that I utilized to address the above research questions, as well as the results of the GM analyses and discussions relevant to the test of each hypothesis.

In the remainder of this first chapter, I review the origin of the domestic dog, including the domestication process from the gray wolf and both the archaeological and genetic evidence for the location and date of this domestication event. Also in this chapter, I review previous studies of dog cranial morphology, with a particular focus on studies that address variation in craniofacial length. Next, I review studies of genetic inheritance preceding the publication of the dog genome sequence. After a brief discussion of the genetic structure of the dog, I move on to review genetic association studies that have examined canine cranial morphology.

Chapter Two provides an explanation of the GM methods used in this dissertation, as well as an overview of the skeletal material utilized and museum collections accessed. First, I list the specimens studied, supplemented by collections data available for my sample, and I explain the rationale for the species and breeds I have chosen to examine. Next, I provide a brief historical background of GM, followed by a description and justification of the set of three-dimensional landmarks collected and the technology implemented in the process. I also assess the error associated with my data collection technique and discuss error assessment in GM studies generally. Finally, I describe the analyses I undertook to contrast the craniofacial morphology of the gray wolf and select dog breeds.

I present the results of the gray wolf and dog breed GM analyses in the third chapter. I begin with an assessment of overall variation in both species, using principal component analysis to identify the greatest dimensions of shape variation for both groups. Next, I address research questions (1) and (2) by comparing the shape differences between the average gray wolf cranium and the average crania of select brachycephalic, dolichocephalic, and mesaticephalic breeds. Patterns of brachycephaly are contrasted and discussed in the context of known genetic relationships between breeds.

Before discussing the gray wolf–dog breed GM analyses in the context of mouse developmental genetics, I begin chapter four with a review of vertebrate craniofacial development. After a general review of craniofacial developmental genetics I then focus on the four candidate genes introduced earlier—*Tcof1*, *Msx1*, *Msx2*, and *Fgfr2c*—summarizing our understanding of their role in craniofacial morphogenesis in mice, humans, and other vertebrates. To address research question (3), I then compare the cranial shape differences that exist between the gray wolf cranium and brachycephalic breed crania to those that exist between wild type and mutant mice for each case of altered candidate gene expression.

1.5 Origin of the domestic dog

The comparisons of cranial shape between the gray wolf and domestic dog breeds undertaken in this dissertation rely on the well-documented relationship between the two species, namely, that the former is the wild progenitor of the latter. However, this relationship has not always been as clearly understood as it is today. For example, in *The Variation of Animals and Plants Under Domestication*, Darwin's (1868) discussion of the domestic dog focused on whether the variety of domestic breeds had descended from one or multiple wild species. Darwin identified the gray wolf as a likely candidate but also reviewed theories that the jackal or an unknown extinct species may have been the single progenitor, or that several species, both extinct and extant, may have given rise to the many different domestic breeds. This latter concept was based largely on the resemblance across the world between local dog breeds and distinct wild species from those areas (Darwin 1859, 1868). Despite lacking the resources to truly resolve the argument, Darwin did comment that dogs had clearly been bred to have different forms and behaviors in order to better function under different conditions, citing, for example, the webbed feet of the aquatic Newfoundland breed. In remarking that "man [had] thusly closely imitate[d] Natural Selection," Darwin (1868, p. 42) hinted at the actual course of artificial selection that produced the numerous modern breeds from a single ancestor, the gray wolf.

Since the time of Darwin, convincing arguments based on morphology (e.g., Miller 1912, 1920) and behavior (e.g., Scott, 1968) have identified the gray wolf and rejected the jackal as the most likely ancestor, while the most persuasive evidence has come from mitochondrial DNA (mtDNA) analysis (Vila *et al.* 1997, 1999a). However, the details of the domestication event, including its evolutionary circumstances, timing, and location, remain subjects of active investigation that are constantly being informed by new archaeological discoveries and advances in molecular techniques (e.g., Ovodov *et al.* 2011 and vonHoldt *et al.* 2010, respectively). Because these questions have motivated many of the genetic and morphological studies of the domestic dog relevant to my own investigation of the genetic basis of craniofacial breed variation, I review the current understanding of the relationship between ancestor and descendant below.

1.5.1 Domestication

1.5.1.A Evolutionary scenarios

The interaction between humans and wolves that led to the beginning of domestication has been discussed by many authors, all of whom agree that as humans transitioned from a nomadic hunter-gatherer lifestyle to a more stable mode of life centering around village settlements during the Neolithic, an association based on food resources began between the two species (Scott 1968; Clutton-Brock 1977, 1992; Morey 1994; Driscoll *et al.* 2009). Wolves scavenging for food from villages drew the attention of humans, for their utility both as protectors of the settlement (e.g., Driscoll 2009) and as aides in the hunt (Clutton-Brock 1977). Schleidt and Shalter (2003) have gone so far as to suggest that herd-following wolves introduced pastoralism to humans following the most recent ice age. Additionally, given the long history of the practice in southern East Asia, Pang *et al.* (2009) raise the point that the dog may have been

domesticated as a food resource. These interactions led to humans taking in wolf pups as pets (Coppinger and Schneider 1995) and eventually exerting control over their mating, at which point Driscoll and colleagues (2009) argue, the wolf technically became a dog—that is, when it became the subject of artificial selection.

It is important to note that these scenarios do not involve humans intentionally seeking out the wild wolf as a target of domestication. Morey (1994) points out that scenarios based on human intentions are nearly impossible to test and argues for an evolutionary perspective that treats humans and wolves as equally invested participants in the domestication process. Similarly, Schleidt and Shalter (2003) hold that the domestication event is a story of co-evolution. Although the history of dog breeding is one of artificial selection, the relationship between the wolf and humans is one originally characterized by natural selection (Scott 1968; Driscoll *et al.* 2009). Specifically, the wolf, like most wild animals that have since been domesticated, possesses a number of behavioral and social traits that make it pre-adapted to domestication: large, gregarious group structure; strong motivation for companionship; capacity for dominance-subordination relationships; cooperative hunting approach; and omnivorous diet (Scott 1968; Fox 1971; Clutton-Brock 1977, 1992, 1995; Coppinger and Schneider 1995; Morey 1994; Driscoll 2009). Driscoll and colleagues (2009) describe a chronology in which less-fearful wolves initiated contact with human settlements for food, after which this founder group, now tied to human camps, was differentiated from other wolves due to natural selection and genetic drift. According to Clutton-Brock (1992, 1995), the domestication of the wolf consisted of both a biological component—this reproductive isolation from the wild population—and a cultural component—the incorporation into human society.

1.5.1.B Selection for behavior

Entering the new environment of human company required several important behavioral and physiological adaptations in the wolf (Clutton-Brock 1995). As Scott (1968) points out, the wolf already possessed an important trait for domestication: a period of primary socialization early in life, during which emotional attachments to inter- and intra-specific individuals are formed. In dogs, this process has been modified such that the normal fear response to strangers exhibited by wolves develops less rapidly (Scott 1968; Clutton-Brock 1995). Hemmer (1990) describes this modification as a suppression of the dog's perception of its environment, wherein the fear response is diminished and tolerance to stress is increased.

Perhaps the greatest opportunity to better understand the selection process that brought about this change has come from the long-running breeding experiment on fur farm silver foxes (*Vulpes vulpes*) initiated by the late geneticist Dmitry Belyaev (Trut 1999; Trut *et al.* 2009). Belyaev and colleagues have bred over fifty years' worth of generations of foxes selecting for only one trait: tameability, as measured by behavioral tests that gauge tolerance towards humans (Trut 1999; Trut *et al.* 2009). Behaviorally, foxes selected for tameability displayed a delay in the development of the fear response and, after only half-a-dozen generations, sought out human contact and affection (Trut *et al.* 2009). The experiment is noteworthy for the physiological and morphological traits that also emerged in successive generations of tame foxes, including many of the same features that distinguish dogs from wolves. For example, tame foxes reach sexual maturity earlier, have larger litters, and experience longer breeding seasons than their wild counterparts (Trut 1999). Foxes under selection also frequently exhibit loss of pigment in coat

color, floppy ears, curly tails, shorter limbs, malocclusion of the lower jaw, and a decrease in cranial height and width, as well as shorter and wider snouts (Trut 1999, 2001; Trut *et al.* 1991, 2004, 2009). In addition, sexual dimorphism decreases in the tame fox population, as evidenced by the feminization of male skulls (Trut 1999; Trut *et al.* 1991, 2004).

Trut and colleagues have monitored the activity of the hypothalamic-pituitary adrenal axis, which regulates the hormones involved in stress response, and have found that the levels of plasma glucocorticoids were significantly lower in the tame animals, suggesting that the genes controlling these hormones were the target of selection for tameability (Trut *et al.* 2004, 2009). Examination of neurotransmitter systems in the foxes revealed similar results: higher levels of serotonin, which inhibits aggressiveness, were observed in tame foxes (Trut *et al.* 2009). Belyaev recognized that selection for tameability had profoundly affected the timing of the development of behavior, and as a corollary, the timing of the development of morphology. His interpretation was that selection for behavior had destabilized development to produce an increase in phenotypic variation (Belyaev 1979; Trut *et al.* 2009). Trut and colleagues (2004, 2009) have proposed that this occurred via epigenetic modification due to neurohormonal changes, from which the alteration of expression in only a small number of genes in the brain produced many regulatory downstream effects.

This proposal of linkage between morphological and behavioral traits selected for during domestication is supported by very recent analysis of the dog genome. VonHoldt and colleagues (2010) searched for genomic regions containing adaptive substitutions reflecting positive selection early in the domestication process based on high fixation index (F_{ST}), and found the highest signals near genes associated with memory formation and the sensitization of behavior (as indicated by studies in mice and humans), as well as near the gene for Williams-Beuren syndrome, a human neurodevelopmental disorder characterized by extreme sociability.

In contrast to Hemmer's (1990) view that selection during domestication targeted genetic control over sensitivity to the environment, Trut *et al.* (2004) argue that the targets of selection were genes governing the rate of behavioral development, resulting in new variation that has given breeders the freedom to simultaneously increase sensitivity in some areas while decreasing it in others. Comparison of adult behavior patterns in wolves and dogs reveals no fundamental differences in organization: every pattern of wolf behavior is also seen in dogs. However, these patterns in dogs differ in their frequency such that the response threshold is increased or decreased, their composition such that components are reordered or omitted, and their motivation (Scott 1968; Fox 1971; Hare *et al.* 2002). For example, Beagles and Wire Fox Terriers share the same pattern of antagonistic behavior as the wolf, but in the former, this pattern is rarely exhibited due to selection for diminished aggression, while in the latter, selection for sensitivity to attack has produced much more aggressive dogs (Scott 1968). Similarly, in their study of behavior in working dogs, Coppinger and colleagues (1987; Coppinger and Schneider 1995) note that the onset of predatory motor patterns varies during development in dogs and that the frequency of the display of these patterns has been targeted in the selection of herding and guard breeds.

1.5.1.C Characteristics of domestication

The morphology separating dogs from the wolf closely follows the new fox forms that emerged in Belyaev's breeding experiment (Trut *et al.* 2009). Dogs, like the tame foxes, are not

limited to a single breeding season and typically have two annual estrum, compared to one in the wolf (Fox 1971). Dogs also reach sexual maturity six to eighteen months earlier than the wolf (Morey 1994). Dogs are generally smaller than wolves on average, a relationship that is observed across most domestic animals with respect to their wild ancestors (Zeuner 1963; Clutton-Brock 1992; Driscoll *et al.* 2009). Similar to the foxes, dogs have floppy ears and characteristically hold their tails erect and curled, the latter due to a change in the shape of their tail vertebrae. Dogs exhibit a straighter and shorter back than wolves, and, when viewed in cross-section, the dog's chest is barrel-shaped, not keeled like that of the wolf, collectively distinguishing the gait of the two animals (Zeuner 1963).

The effects of domestication on the skull of domestic dogs have been well documented, with considerable attention paid to the differences in cranial proportions across small and large dogs compared to similarly sized wolves and other wild canids (e.g., Lumer 1940; Weidenreich 1941; Epstein 1971; Wayne 1986; Morey 1992; Drake 2004, 2011). I review these detailed studies of canine skull allometry and growth in section 1.6. Here, I describe the more general trends in skull morphology distinguishing dogs from wolves that have been applied to the interpretation of the archaeological record (reviewed in the next section) and, by extension, studies of early domestication. It is important to note that the traits described below apply to a generalized dog skull: because one of the key features separating dogs and wolves is an increased variability in cranial proportions in the former, some breeds exhibit the opposite trend than that described (Zeuner 1963; Lawrence and Bossert 1967). For example, compared to the wolf, shortening and broadening of the face relative to the neurocranium is characteristic of most domestic dogs (Zeuner 1963; Epstein 1971; Nowak 1979; Olsen 1985; Benecke 1987; Clutton-Brock and Jewell 1993; Clutton-Brock 1995), however, among modern breeds there do exist extremes in the opposite direction (e.g., the long, narrow face of the borzoi).

Dogs differ from wolves in cranial capacity: dogs have smaller brains relative to the size of their bodies (Lumer 1940; Weidenreich 1941; Epstein 1971; Clutton-Brock 1992; Clutton-Brock & Jewell 1993; Hemmer 1990). Klatt (1921, 1927) observed that while the frontal section of the brain is relatively larger in dogs than in wolves and the parietal portion is of equivalent size, the caudal part of the brain is reduced dorso-ventrally and posteriorly. These changes in brain conformation result in a more steeply ascending frontal portion and descending occipital portion of the neurocranium (Epstein 1971). The neurocranium of the dog is also broader at the base (de Serres 1835; Nowak 1979).

The shape of the dog cranium is characterized in lateral view by the “stop,” a disruption of the continuous slope of the nasal and frontal bones that connects the face and neurocranium in wolves. In dogs, the anterior part of the neurocranium is raised while the insertion of the facial bones is lower, exaggerating the change in angle at mid-face (de Serres 1835; Zeuner 1963; Lawrence and Bossert 1967; Clutton-Brock and Jewell 1993; Clutton-Brock 1995). The enlargement of the frontal sinuses contributes to this feature in large dogs (Studer 1901; Zeuner 1963; Lawrence and Bossert 1967; Epstein 1971), while in small dogs, relatively greater neurocranial height produces a steep upward curve in profile at the posterior end of the nasals (Epstein 1971). The extreme dwarf breeds exhibit greatly reduced maxillae and bulging foreheads, such that there is an incurvation at the nasal bridge (Weidenreich 1941).

Due to the presence of the stop, the orbits are positioned more vertically in dogs (Epstein 1971). Expansion of the frontal bones due to increased sinus development (Studer 1901) alters the position of the post-orbital processes and the shape of the orbits (Dahr 1942; Hauck 1950). As a result, the orbits have a more obtuse orbital angle and the eyes are directed more forward in

dogs than in wolves (Reynolds 1909; Iljin 1941; Zeuner, 1963; Epstein 1971; Nowak 1979; Benecke 1987; Clutton-Brock and Jewell 1993; Clutton-Brock 1995). The angle of the attachment of the zygomatic process of the maxilla, typically acute in wolves, is closer to a right angle or obtuse in dogs (Schäme 1922; Iljin 1941). Domestication has also altered the shape of the auditory bullae in dogs: they are relatively smaller, irregularly shaped (Noack 1916; Iljin, 1941; Harrison 1973; Nowak 1979), and flattened (Miller 1912; Lawrence and Bossert 1967; Clutton-Brock and Jewell 1993; Clutton-Brock 1995).

Dogs have a more omnivorous diet than wolves and correspondingly use their teeth differently (see below), a consequence of which is decreased development of cranial superstructures for the attachment of muscles for mastication, such as the temporal ridges and sagittal crest (de Serres 1835; Zeuner 1963; Epstein 1971; Nowak 1979). The sagittal crest of dogs is more rounded than in wolves, curving ventrally at the posterior tip (Lawrence and Bossert 1967). Another result of their omnivorous diet is that the lower jaw of the dog is narrower and shorter than that of the wolf (Zeuner 1963). The dog mandible is also more curved than the wolf mandible: in dogs, the lower jaw is deeper along the middle of the horizontal ramus, resulting in a more convex inferior margin (de Serres 1835; Epstein 1971; Nowak 1979; Olsen 1985; Clutton-Brock and Jewell 1993). The coronal process of the mandible is more slender and concave at its posterior edge in dogs than in wolves (Clutton-Brock and Jewell 1993; Clutton-Brock 1995), with the exception of the Tibetan wolf *C. lupus chanco* (Olsen 1985).

The evolutionary shortening of the mandible and maxilla occurred at a faster rate than the reduction of the dentition, as evidenced by the crowded tooth rows of the earliest domestic dogs (Benecke 1987; Clutton-Brock 1995; but see also section 1.5.2). Although many dogs display tooth crowding due to reduction in jaw length, the posterior margin of the palate extends beyond or within the plane of the second upper molar in dogs, while the opposite is observed in wolves (Allen 1920; Iljin 1941; Lawrence and Bossert 1967; Nowak 1979). The teeth of modern dogs are smaller than those of the earliest dogs, and frequently large gaps between teeth can be observed (Miller 1912; Zeuner 1963; Nowak 1979; Olsen 1985; Clutton-Brock 1995). Lawrence and Bossert (1967) found the second upper molar in particular to be relatively smaller in dogs. The length of the upper carnassial (P⁴) differentiates the two species as well: it is longer than the combined length of the two upper molars in wolves, but shorter in dogs (Zeuner 1963).

As mentioned with regard to the stop, the crania of dwarf breeds (e.g., the Chihuahua or Pekingese) often represent extreme exaggerations of these traits. In these dogs, the bulging neurocranium projects outwards at both the frontals and occipital and is characterized by patent sutures and fontanelles, while the postorbital processes and superstructures like the temporal ridges are reduced to faintly raised surfaces and lines (Epstein 1971). The dentition of dwarf breeds is particularly altered: the length of the palate is reduced, and the degree of overlap and rotation of teeth increases (Clutton-Brock and Jewell 1993). The whole tooth row is shifted posteriorly so that the molar row is positioned beneath the orbit and the frontal portion of the braincase. In these extreme cases, the size of crowns and roots decreases, and the number of premolars and molars is often reduced (Epstein 1971).

Sexual dimorphism is relatively low in canids relative to other carnivorans (Ewer 1973): measurements of skull size (Jolicœur 1959, 1974; Okarma and Buchalczyk 1993; Milenkovic *et al.* 2010) and tooth size (Dayan *et al.* 1992) indicate that *C. lupus* males are on average 3-8% larger than females. Domestication has reduced sexual dimorphism further in dogs, similar to the trend observed in crania of farm minks (Lynch and Hayden 1995) and foxes (Trut *et al.* 2004). As such, size is not as reliable an indicator of sex for the dog, although the basioccipital

surface of the cranium (The and Trough 1976; Trough *et al.* 1977) and cranial capacity (Regodon *et al.* 1991) have been applied successfully to sex identification in a limited range of breeds.

1.5.2 Archaeology

The characteristics of domestication outlined above differentiate the skull of the domestic dog from the wolf, and have been used as taxonomic identifiers for skulls comprising the archaeological record. Olsen (1985) has argued that the determination of canid species must utilize multiple characters to be effective, a direction followed by the numerous discriminant function analyses of canid subfossil material undertaken in the last twenty-five years (e.g., Benecke 1987; Germonpré *et al.* 2012). Several problems arise in the differentiation of dog from wolf in the archaeological record, however, including the fragmentary state of many skulls that precludes utilizing all of the characters presented above (Benecke 1987). Further, the distinction between dog and wolf becomes more subtle the farther back in time (and the closer to the original domestication event) to which specimens date (Olsen 1985). A more complete picture of the state of domestication is provided by additional cultural and/or molecular data, such as the burial of a puppy in close association with a human dated to 12,000 years before present (BP) in Israel (Davis and Valla 1978) or the bone fragment dating to 9,000 BP in Texas identified as a dog based on ancient mtDNA (Tito *et al.* 2011). In most cases, however, these additional data are not present, and prehistoric dogs are diagnosed as such based on their relative cranial and dental size, snout length, and degree of tooth crowding.

The archaeological record provides information not only on the timing and location of the transition from wild wolf to domestic dog, but also on the history of cranial variation within the dog, that is, the first appearance of breed-specific shapes. At the beginning of the twentieth century, Studer (1901) classified the prehistoric dogs of Europe based on their cranial morphology, designating two major groups: the palaeartic dogs and the southern dogs. Studer (1906) linked the two by what he believed to be the earliest European dog, *Canis familiaris poutiatini*, the type specimen of which came from the Russian Neolithic (Epstein 1971). *C. f. poutiatini* exhibits a medium-sized, generalized dog cranium, in contrast to the variety of forms described by Studer (1901) for the palaeartic dogs. Within this group, based on specimens known from Swiss lake-dwelling sites spanning the Neolithic, Studer (1901) recognized: *C. f. palustris*, a small dog with a rounded neurocranium and well-defined stop; *C. f. inostranzevi*, a large, powerfully built dog with a well-developed sagittal crest and broad forehead; *C. f. leineri*, a slender dog with a long cranium and absent stop; *C. f. intermedius*, a medium-sized dog exhibiting well-developed frontal sinuses, a shorter rostrum, and a high forehead and neurocranium; and *C. f. matris optimae*, a large dog with a flat cranium (Epstein 1971). Studer (1901) saw each palaeartic dog as the predecessor of modern dog groups: small Terriers were derived from *C. f. palustris*, Mastiffs from *C. f. inostranzevi*, Greyhounds from *C. f. leineri*, hounds from *C. f. intermedius*, and Sheepdogs from *C. f. matris optimae*.

Studer's (1901, 1906) southern dog group included dingoes and pariah dogs from Africa and Asia, which he incorrectly believed to be derivative of dingoes (Epstein 1971). The legitimacy of Studer's (1901) classification of palaeartic dogs and their descendants was questioned—first by Klatt (1913), who attributed the cranial differences between *C. f. palustris* and *matris optimae* solely to their difference in body size, and later by Wagner (1929) and Dahr (1942), who came to a similar conclusion regarding the differences between *C. f. palustris*,

intermedius, and *matris optima*. However, at the very least, Studer's (1901) study demonstrates substantial size variation and the presence of at least three cranial forms (the *palustris-intermedius-matris optima* type, the *inostranzevi* Mastiff type, and the *leineri* Greyhound type) in dogs in Europe by the late Neolithic.

A more complete picture of the dog fossil record, not only in Europe (e.g., reviewed by Benecke 1987) but across the world (e.g., reviewed by Epstein 1971; Olsen 1985) has emerged with subsequent discoveries and improved dating techniques. Today, Mesolithic dogs are known from across Eurasia. In western Europe, small-sized dogs have been assigned the following dates: in Spain, c. 19,000 BP at Erralla (Vigne 2005; Germonpré *et al.* 2012); in Germany, c. 16,799-13,800 BP at Kniegrotte, c. 15,770-13,957 BP at Teufelsbrücke and Oelknitz (Musil 2000), and c. 14,708-13,874 BP at Oberkassel (Nobis 1979; Benecke 1987); in France, c. 15,500-13,500 BP at Montespan, c. 14,999-14,055 BP at Le Closeau, and c. 12,952-12,451 BP at Pont d'Ambon (Pionnier-Capitan *et al.* 2011), and c. 12,027-11,311 BP at Saint-Thibaud-de-Coux (Chaix 2000); in Switzerland, c. 15,000-14,000 BP at Hauterive-Champréveyres (Morel and Müller 1997); in England, c. 9,488 BP at Star Carr (Degerbøl 1961; Harcourt 1974; Clutton-Brock and Noe-Nygaard 1990); and in Portugal, c. 8,000 BP at Muge (Detry and Cardoso 2010).

Both Germonpré *et al.* (2012) and Pionnier-Capitan *et al.* (2011) contrast these small western European dogs with larger dogs known from eastern European sites. For example, two skulls from dogs the size of large northern wolves, but with shorter rostra and palates, are dated to c. 16,945-16,190 BP at the site of Eliseevichi I on the Russian Plain (Sablin and Khlopachev 2002). Similar dogs dating to c. 14,700-14,300 BP and c. 8,000 BP are known from Mezin in Ukraine (Pidoplichko 1969; Olsen 1985; Benecke 1987; Germonpré *et al.* 2009) and Vlasac, in Serbia, respectively (Bökönyi 1975).

Early dogs from the Near East are more intermediate in size, but still smaller than the modern wolves known from the area (Turnbull and Reed 1974). Dogs dating to c. 16,810-6,970 BP and c. 11,700 BP have been discovered at the Israeli sites Hayonim Terrace and Ein Mallaha (Davis and Valla 1978; Tchernov and Valla 1997), while a single dog jaw dating to c. 14,400-13,350 BP has been found at Palegawra Cave in Iraq (Turnbull and Reed 1974). Later dogs are also known from c. 10,800 BP at Mount Carmel and c. 10,500 BP at Jericho Tell in Palestine (Garrod and Bate 1937; Clutton-Brock 1962, 1979).

Olsen (1985) describes three sites in eastern Siberia that represent some of the oldest dated dogs in Asia: Afontova Gora II, dated at c. 20,900 BP; Ushki I, c. 10,760-10,360 BP; and Ust'-Belaia, c. 9,000 BP (see also: Olsen and Olsen 1977). In China, dog bones have been dated to c. 7,560-7,160 BP at the early agricultural site Dadiwan (Barton *et al.* 2009) and to c. 7,335-7,235 BP at the contemporary site Cishan (Olsen 1985).

The origin of New World dogs has long been a focus of archaeologists, prompting such comprehensive works as Allen's (1920) categorization of prehistoric N. American dogs. For many years, mandibles of a considerable size range featuring crowded teeth from Jaguar Cave in Idaho were thought to be the oldest evidence for domestic dogs in the New World, dated to c. 11,580-10,370 BP (Lawrence 1967, 1968). However, more recent dating places the site at c. 3,220-940 BP (Gowlett *et al.* 1987; Clutton-Brock 1988; Clutton-Brock and Noe-Nygaard 1990), precluding our knowledge of size variation in the earliest New World dogs. Tito and colleagues (2011) have procured evidence for the presence of domestic dogs in N. America as far back as c. 9,260 BP by extracting and genotyping DNA from an occipital condyle fragment found in a human paleofecal sample from Hinds Cave in Texas; however, this discovery offers no information on the morphology of this early dog.

In the last five years, the oldest dogs thus far have been recovered from sites in Europe and Siberia, dating to 33,000-26,000 BP, collectively. Given that, prior to these discoveries, no dog remains were dated to older than approximately 20,000 BP (Afontova Gora II, which, according to Olsen (1985), is unsubstantiated as the specimens have not been locatable since their initial description in the seventies), these new findings bear importance for studying dog domestication before and during the Last Glacial Maximum (LGM). Germonpré and colleagues (2009, 2012) have described dogs dating to c. 32,130-31,670 BP from Goyet Cave in Belgium and c. 27,000-26,000 BP from Předmostí in the Czech Republic. Jaws from Předmostí exhibit tooth crowding; however, the crania from both sites were primarily identified as dogs based on the relative dimensions of their snouts. When compared alongside prehistoric dog and fossil wolf specimens from other Eurasian sites in discriminant function analyses, both the Belgian and Czech specimens align with dogs and are distinct from wolves in their facial morphology (Germonpré *et al.* 2012).

Older yet are the complete skull and mandibles of a dog found at Razboinichya Cave in the Altai Mountains of southern Siberia described by Ovodov and colleagues (2011). The weighted average of accelerator mass spectrometry ¹⁴C dates taken from the mandibles places the dog at c. 33,500-33,000 BP. The Razboinichya dog exhibits a clear stop and a short, broad snout within the range of the Eliseevichi I dogs. Although the length of the upper fourth molar is shorter than the combined length of the two upper molars, supporting the identification as dog, the length of the lower second molar falls within the range of prehistoric wolves and the teeth are not crowded. The authors interpret this mixture of dog-like skull traits and wolf-like dental traits as an indicator of the specimen's incipient status, and postulate that this dog represents a lineage of early domestication that did not survive the LGM and which included the dogs from Goyet Cave (Ovodov *et al.* 2011).

In contrast to the criteria widely accepted during the last century (Benecke 1987), Ovodov *et al.* (2011) and Germonpré *et al.* (2012) do not infer domestic dog status from crowding in the dentition. The authors note that tooth crowding is occasionally observed in wild wolves (Dolgov and Rossolimo 1964; Buchalczyk *et al.* 1981; Andersone and Ozoliņš 2000) and may represent cases of dog introgression (Koler-Matznick 2002), limiting its usefulness as a taxonomic identifier. Comparison of these early dog crania and contemporary wolf crania does reveal distinguishing differences in snout length and width (Germonpré *et al.* 2009, 2012; Ovodov *et al.* 2011) however, demonstrating that the earliest domesticated dogs had modified facial morphologies. The geographical variation that followed during the Mesolithic (Germonpré *et al.* 2012; Pionnier-Capitan *et al.* 2011) and the incipient breed types of the Neolithic (Studer 1901, 1906) depict an overall pattern of increasing morphological diversity within the domestic dog over time. By the time of the Roman Empire, systematic breeding had begun, as evidenced by the writing of Columella in 1 AD (Clutton-Brock and Jewell 1993) and the distinctly brachy- and dolichocephalic dog crania present at Pompei in 79 AD (Zedda *et al.* 2006).

1.5.3 Molecular studies

The study of prehistoric dogs from Goyet Cave by Germonpré *et al.* (2009) is significant not only for the early date assigned to the fossils, but also for the analysis of ancient mitochondrial DNA (mtDNA) employed by the authors. mtDNA was extracted from six

specimens from Paleolithic Belgian sites, and sequences from the mitochondrial control region were compared to those known for modern dog breeds and global wolf populations. Interestingly, the haplotypes exhibited by the Belgian canids were found to be unique, not corresponding to any modern dog breed or wolf population, indicating that these specimens represent an ancient wolf lineage that has since been lost (Germonpré *et al.* 2009). While this finding agrees with the interpretation made by Ovodov *et al.* (2011)—that these dogs represent a lineage that did not survive the LGM—the discrepancy between osteological and genetic data highlights a larger issue: the descriptions of the archaeological record and the molecular work focusing on the origin of the domestic dog are not always easily reconciled.

Because of the difficulty in distinguishing the earliest dogs from wolves based on morphology (Olsen 1985), researchers have relied more heavily on molecular studies to identify the timing, location, and number of domestication events involved in the origin of the dog. Beginning with investigations of karyology and serology, molecular research also provided the first unequivocal evidence for the wolf as the ancestor of all dogs. I review this work below, including extensive explorations of mtDNA and nuclear DNA variation in the dog and its closest relatives.

1.5.3.A Karyology and serology

Minouchi (1928) was the first to correctly describe the chromosome formula of the dog ($2n = 78$), and in so doing, observed that the number of chromosomes does not vary by breed. This conclusion, arrived at by later karyological work as well (e.g., Gustavsson 1964; Borgaonker 1968; Selden *et al.* 1975), was early evidence for a common ancestry of all dogs. Similarly, concurrent research on blood proteins identified little breed-specific variation (Braend 1966; Clark *et al.* 1975; Simonsen 1976); however, variation in the activity of several enzymes was found to correspond to broader groupings of breeds, confirming the lineages described by Studer (1901) (Leone and Anthony 1966; Tanabe *et al.* 1974). The status of the dingo as a dog, and not the descendent of a different wild canid, was also established by serological work at this time (Clark *et al.* 1975; Shaughnessy *et al.* 1975).

Comparisons of blood proteins between the dog and other canids (reviewed by Simonsen 1976) provided the first molecular evidence of the close relationship between the dog and the wolf, eliminating the more divergent jackal as a possible ancestor (Vriesendorp 1972; Simonsen 1976; Wayne and O'Brien 1987; Lorenzini and Fico 1995). A study of chromosome morphology across the Canidae family also identified the wolf as the closest ancestor (Wayne *et al.* 1987a,b).

1.5.3.B Mitochondrial DNA

Due to its short length and rapid evolution, mtDNA has provided tremendous insight to the recent evolution of wolves and dogs (Vilà *et al.* 1999a; Bardeleben *et al.* 2005). Comparisons of sequence divergence within the mtDNA control region have consistently shown that the smallest divergence exists between the dog and the wolf and that the genetic distance between the two species is of the same magnitude as the distance between wolf subspecies (Wayne *et al.* 1992; Wayne 1993; Lan and Shi 1996; Tsuda *et al.* 1997; Vilà *et al.* 1997; Koop *et*

al. 2000; Arnason *et al.* 2007). High genetic diversity in the dog mtDNA control region indicates a large, genetically diverse founding population (Vilà *et al.* 1999b; Angleby and Savolainen 2005). Furthermore, this diversity is not partitioned by breed (Okumura *et al.* 1996; Vilà *et al.* 1997). Collectively, these features, as well as the overlap of dog and wolf haplotypes in each of the four major mtDNA clades identified, suggest multiple centers of domestication and extensive early interbreeding (Tsuda *et al.* 1997; Vilà *et al.* 1997; Verginelli *et al.* 2005).

The distribution of mtDNA haplotypes shows that hybridization was common among dogs and eastern European wolves (Randi *et al.* 2000) and analysis of both mtDNA and major histocompatibility complex (MHC) alleles indicates preferential backcrossing between male wolves and female dogs (Vilà *et al.* 2005) (but see Gotelli *et al.* (1994) for evidence of the opposite trend between dogs and Ethiopian wolves, based on microsatellite data).

The origin of New World dogs has also been addressed by mtDNA research, with conflicting results. Vilà and colleagues (1999a) found the sequence of the rare, historically old Mexican Xoloitzcuintli breed to be identical to those found in breeds from the Old World. In contrast, Koop *et al.* (2000) discovered two distinct and rare mtDNA lineages in North American indigenous dogs, nearly identical to a rare wolf haplotype from the same region. Leonard *et al.* (2002) provide the most compelling evidence for a common Old World origin in their analysis of ancient mtDNA extracted from Central and South American dogs predating the arrival of Columbus. In this study, all of the ancient American dogs clustered within the four previously defined Old World clades, denoting a shared origin from Eurasian wolves (Leonard *et al.* 2002).

A more specific location within Eurasia for the domestication of dogs has been proposed by Savolainen *et al.* (2002), who found the greatest mtDNA control region variation in East Asia. Boyko *et al.* (2009) have challenged this finding based on Savolainen and colleagues' (2002) disproportionate use of East Asian village dogs in their study. Boyko *et al.* (2009) showed that similar levels of mtDNA diversity exist in both African and East Asian village dogs, citing the potential bias of over-representation of the latter group. This issue has been addressed further by whole mtDNA genome and nuclear DNA studies (see below).

Several dates for the domestication of dogs have been proposed based on mtDNA control region sequence divergence. Okumura *et al.* (1996) applied evolutionary rates estimated from human mtDNA studies to the deepest branchpoints of their dog phylogeny to reach a range of 76,799-120,930 BP for the dog mtDNA common ancestor. However, their study did not include mtDNA from any wild canids and therefore lacked an appropriate outgroup for calibration. Vilà *et al.* (1997) used the sequence divergence of the wolf and coyote, and evidence from the fossil record that these two species diverged one million years ago, to estimate that the dog originated 135,000 BP. Using the same calibration and substitution rate as Vilà and colleagues (1997), Savolainen *et al.* (2002) estimated the age of the oldest dog mtDNA clade based on the mean pairwise distance between East Asian sequences, arriving at a range of approximately 15,000-40,000 BP. More recently, Li *et al.* (2008) used a similar approach to estimate that the ancient Tibetan Mastiff breed was the first dog to diverge from the wolf at 58,000 BP, followed by other domestic dogs at 42,000 BP.

Pang and colleagues (2009) have added considerable resolution to the matters of diversity, timing, and location in the domestication of the dog by examining variation across the entire mitochondrial genome (sequenced by Kim *et al.* in 1998). Their study confirms the findings of earlier control region work that identified the wolf as the ancestor of the dog, as well as the dog's high mtDNA genetic diversity. Importantly, the authors found distinct substructure in the previously identified clades, wherein a complete set of ten subclades was only observed in

an area south of the Yangtze River in China, abbreviated as ASY. From this area of maximum diversity, a gradient extends westward across Eurasia to Europe, where the lowest amount of diversity exists. In response to the concerns of Boyko and colleagues (2009), Pang *et al.* (2009) explain that while a large amount of diversity exists among African village dogs, this diversity is similar to that observed elsewhere in the west and remains lower than the maximum found in the ASY.

Although wolves were included in their study, Pang *et al.* (2009) focused on intraspecific variation in the dog, explaining that, due to the eradication of the wolf in much of its historical range (see Wayne *et al.* 1992; Vilà *et al.* 1999b), it is impossible to recreate the diversity of the wolf at the time of domestication. From the similar proportions of the major dog clades represented in different parts of the Old World, the authors inferred a single origin in time and space. The time to the most recent common ancestor of these clades was estimated using a time range of 1.5-4.5 Ma for the wolf-coyote split as calibration, resulting in a range of 5,400-16,300 BP or earlier (Pang *et al.* 2009).

1.5.3.C Nuclear DNA

Two studies of microsatellite variation in Mexican wolves provide the earliest nuclear DNA evidence for the close relationship between dogs and wolves within the Canidae (García-Moreno *et al.* 1996; Hedrick *et al.* 1997). More recently, Bardeleben and colleagues (2005) used DNA from six nuclear loci to reconstruct the phylogeny of twenty-three canids, but could not resolve the relationship between the dog, coyote, and jackal, relative to the wolf, without incorporating mtDNA data.

Utilizing the extensive genetic marker resources developed since the sequencing of the dog genome (Lindblad-Toh *et al.* 2005; see section 1.7), the SNP analysis of vonHoldt and colleagues (2010) revealed the highest amount of haplotype sharing between dogs and Middle Eastern wolves, leading the authors to cite that region as the primary source of genetic diversity for the dog. Unlike the pattern observed in mtDNA analyses (e.g., Savolainen *et al.* 2002; Pang *et al.* 2009), East Asian wolves were found to be a major source of nuclear DNA diversity only for a small number of ancient Asian breeds. Within dogs, the authors noted no consistent relationship between genetic diversity and geography, reflecting possible significant variation in the demographic history of breeds across the world following domestication. Rather, genetic variation corresponds largely to phenotypic and functional breed groupings, including the following clusters: ancient and Spitz breeds, toy dogs, Spaniels, scent hounds, working dogs, Mastiff-like dogs, small Terriers, Retrievers, herding dogs, and sight hounds (vonHoldt *et al.* 2010).

Most recently, Larson *et al.* (2012) used a similarly sized set of SNPs to examine relationships between over 1,250 individuals representing thirty-five breeds, focusing specifically on “ancient” breeds that are basal to the larger clade containing most modern breeds. Drawing upon the histories of these breeds, the authors explain that their position outside the main clade likely does not represent a close approximation of the earliest domesticated dogs, but, rather, reflects their isolation from the recent admixture that characterizes most breed evolution prior to the last 150 years. Larson and colleagues (2012) reject genetic distinctiveness as a proxy for ancient heritage, citing several historical examples of bottlenecks and introgressions that indicate that these breeds have long since become disconnected from their ancestral populations.

The authors also cite the existence of shared identical mutations for specific phenotypes, such as hairlessness, dermoid sinuses, and foreshortened limbs (see section 1.7.3), across wide geographic ranges as an indication of repeated instances of global diversification and homogenization during dog evolution, highlighting the difficulty of resolving the early history of domestication.

The common origin of all dog breeds from the wolf and the genetic divergence between morphologically distinct groups of modern breeds form the basis of the analysis of cranial shape variation across breeds presented in this dissertation. Having established the relationship between the ancestral gray wolf and its diverse dog breed descendants, I now focus on preceding studies of cranial morphological variation in the dog.

1.6 Craniofacial variation in the domestic dog

Below I review previous work on craniofacial variation in the domestic dog with respect to archaeology, as an expression of cranial metrics and indices, and in relation to allometry, growth, and biomechanics.

1.6.1 With respect to archaeology

As mentioned above, the earliest studies of dog cranial morphology were aimed at understanding the relationship between modern dogs and their ancient ancestor, best exemplified by Studer's work (1901, 1906). The palaeartic dog forms described by Studer (1901, 1906) were further delineated by Noack (1916), who attributed their common ancestry to the Indian wolf, and Marchelewski (1930a), who concluded that only the *C. f. leineri*/Greyhound group was morphologically distinct from the others. Schäme (1922) recognized two ancestral forms distinct in facial type: the broad skull and short snout of the "decumanides" type, represented by the Great Dane, and the long, narrow skull of the "veltrides" type, represented by the German Shepherd Dog. Götze and Dornheim (1926) described a continuous range of variation between these two pure types in which most modern skulls would fall. This dichotomy of an elongated, narrow skull, as seen in Greyhounds, and a shortened, broad skull, as seen in Mastiffs, was also arrived at through studies of archaeological breed variation by Werth (1944) and Baumann and Huber (1946).

1.6.2 As an expression of cranial metrics and indices

Ancestral designations have since been replaced by more descriptive terms for classifying dog breeds based on cranial shape. Brachycephalic breeds have been distinguished from mesaticephalic and dolichocephalic breeds based on skull index, palatal index, upper facial index, snout index (Stockard 1941), facial length and height, cranial length-height index, frontal position index (Wyrośt and Kucharczyk 1967), braincase-face length index, braincase index (Brehm *et al.* 1985), palate width-nasal length index, the ratio of face to skull length (Lignereux *et al.* 1991, 1992), and skull index (Onar *et al.* 2001; Kupczynska *et al.* 2008).

1.6.2.A The Hirnstammbasis

Huber (1952; Lüps and Huber 1969a) attempted to standardize quantitative measurements of brachycephaly by introducing the Hirnstammbasis as a reference measurement for skull size. Measured as the length of the chord from the anterior border of the foramen magnum to the boundary of the pterygoid and palatine bones, the Hirnstammbasis scales independently of facial length, enabling clearer comparison across breeds of facial proportions (Lüps 1974). Relative to this measure of skull size, Lüps and Huber (1968; Huber and Lüps 1968) described snout shortening and skull widening in the Bulldog but only a narrowing in skull width in the Borzoi—relative to the Hirnstammbasis, the face of this breed is not extended. Furthermore, a separation of width and length was observed in the skull of the Chow Chow, which exhibits a disproportionately wide skull, but no facial shortening (Huber and Lüps 1970). The authors noted that in relation to the Hirnstammbasis, variation in ventral snout shape is achieved via disproportionate shortening/lengthening of the palatine and maxillary bones (Lüps and Huber 1969b). Additionally, this variation is independent of skull width across breeds, suggesting that the terms brachy-, mesati-, and dolichocephalic do not sufficiently describe the range of cranial shapes observed in dogs (Lüps 1974). Using the Hirnstammbasis as a reference, Nussbaumer (1985) has shown that within a single breed (the St. Bernard) both brachy- and dolichocephalic forms can be observed, further highlighting the difficulty in assigning breeds to one of these categories.

1.6.2.B Facial angle

Nussbaumer (1982) also addressed the elevation/declination of the face relative to the cranial base, using the relationship between praebasial (between the plane of the clivus and the sphenoid) and praellar (between the Hirnstammbasis and hard palate) angles to classify breeds as klinorhynchic (declined face) or aiorrhynchic (elevated face). Although all brachycephalic skulls studied were aiorrhynchic, aiorrhynchity was observed independently of brachycephaly, indicating that the former does not necessarily lead to the latter. Regodon and colleagues (1993) examined only craniofacial angle (measured between the basioccipital bone and hard palate) and found a statistically significant relationship with breed type, wherein larger angles correspond to dolichocephalic dogs.

1.6.2.C Other anatomical traits

Researchers have also examined covariation between craniofacial shape and various other anatomical traits. For example, Poplin (1976) found no correlation between dental formula (i.e., anomalous number of cheek teeth) or dental size and skull elongation. On the other hand, Kupczynska *et al.* (2009) observed a reduced dental formula in brachycephalic breeds (less than 5% of brachycephalic dogs studied exhibited a full dentition). Brachycephalic dogs tend to be missing an upper premolar and both a lower premolar and molar (M₃). Additionally, Hofmann-Apollo's (2009) comparison of mesati- and brachycephalic dogs demonstrated a higher degree of occlusal asymmetry in the latter group.

Kupczynska and colleagues (2005) also investigated frontal sinus morphology in brachy-, mesasti-, and dolichocephalic breeds, concluding that three independent, fully developed sinuses on both sides of the cranium can be observed only in the latter two groups. McGreevy *et al.* (2004) found eye radii to correlate with skull dimensions, as well as the distribution of retinal ganglion cells with nose length. The latter relationship may be attributed to the more frontally oriented eyes observed in shorter-snouted skulls (McGreevy *et al.* 2004). Lastly, a correlation analysis of skull and long bone indices performed by Alpak *et al.* (2004) indicates that long bones decrease in size as skulls trend toward brachycephaly.

1.6.3 In relation to size (static allometry)

1.6.3.A Body size

Klatt (1913) recognized that across the wide range of size variation in dogs, the proportion of face to neurocranium varies as well: the neurocranium makes a larger relative contribution to the total length of the skull in small dogs compared to large dogs. The relatively smaller neurocranium and larger masticatory muscles of a large dog necessitate the development of large frontal sinuses and a prominent sagittal crest (Klatt 1927). Wagner (1929) arrived at a similar allometric relationship and developed a new typology of crania that consists of two groups: one including mesati- to dolichocephalic breeds, such as the Dachshund, Sheepdog and Greyhound, and another including more brachycephalic breeds, such as the Great Dane and Bulldog. Lumer (1940) further divided this typology into six groups, ranging from the least allometry in the Terrier tribe to the most in the Pug and Bulldog tribes. In addition to the two distinct patterns of snout length relative to body size observed by Wagner (1929), Lumer (1940) described different degrees of negative allometry for mandible length as well as for occipital, palatal, and zygomatic widths.

Huber (1948) proposed that two independent processes determine snout shape in the dog: body size and disproportionate growth of the dorsal and ventral parts of the snout. In contrast, in his study of both domestic dogs and wild canids, Wayne (1984, 1986) found palatal length and facial length to be isometric, attributing the short face of small dogs to negative allometry of the basicranium. This pattern was found to be consistent across wild and domestic canids, whereas the allometries of skull width and dental length only overlap between wolf-sized dogs and wild canids. As a result, small dogs have relatively wider skulls and longer teeth than similarly sized wild species and the reverse is true for large dogs (Wayne 1984, 1986, 2001). From a sample that also included prehistoric dogs, Morey (1992) detected the same tight scaling of cranial length dimensions across *Canis* and unique cranial width allometry within dogs.

Utilizing an historical collection of St. Bernard skulls spanning the last 120 years, Drake and Klingenberg (2008) examined whether cranial shape change over time within the breed could be attributed to static allometry. However, dorsal shifting of the nasal and frontal bones and broadening of the snout over time could not be linked to size variation.

1.6.3.B Brain size

The static allometry of cranial shape has also been studied with respect to brain size. As mentioned above, over the course of domestication, the size of the brain relative to the body has decreased in dogs (Klatt 1921). In addition to this general size decrease, the brain scales with body size differently in dogs compared to wolves: at intermediate body sizes, the relationship to brain size is comparable in dogs and wolves; however, small dogs have relatively larger brains than similarly sized wolves, while the reverse is true for large dogs (Klatt 1912, 1955a; Klatt and Vorsteher 1923).

Weidenreich (1941) attributed the extreme morphology of dwarf breeds to this phenomenon. Due to the relatively larger brain observed in such breeds, the cranial cavity is greatly expanded such that it comprises most of the frontal bone, extending as far anteriorly and ventrally as nasion. As a result, there is a shortage of bony material to complete the braincase, producing very thin walls with patent sutures and fontanelles (Weidenreich 1941; Seiferle 1966). Weidenreich (1941) described this enlargement of the neurocranium as occurring at the expense of the face, which is shortened and lowered, while the palate and dental arch are shortened and widened. Weidenreich (1941) saw a continuous line of dog forms from the small dwarf type to the larger wolf-size type, wherein all intermediate stages of skull shape as determined by brain size exist.

This view was criticized by Stark (1962) and Rosenberg (1966), among others, for ignoring the independence of dwarfism and brachycephaly. Stockhaus (1962, 1965) compared cranial capacity and craniofacial morphology across breeds, but observed both short, broad skulls and long, narrow skulls at similar brain sizes. Seiferle (1966) observed breed-specific variation in brain length and shape: the ratio of brain length and width to total skull length and width increases with brachycephaly, nearing two-thirds in the French Bulldog. Consistent with Weidenreich (1941), the author (1966) found the short, rounded cranium of this breed to reflect the nearly spherical shape of its brain, which bulges anteriorly and laterally. However, Seiferle (1966) went on to make the distinction between the thick bony roof of the neurocranium maintained by medium-sized brachycephalic breeds like the French Bulldog and the paper-thin roof and side walls exhibited by smaller, dwarf forms.

1.6.4 In relation to growth (ontogenetic allometry)

1.6.4.A Ontogeny

Comparisons of craniofacial development across dog breeds and between wild and domestic canids gained a new dimension with the incorporation of developmental information. Contributions to the understanding of dog cranial ontogeny have included accounts of both embryonic and postnatal growth. Olmstead (1911) described the development of the elements of the neurocranium from a series of sections through the head of a dog embryo; however it is not clear which embryonic stage the sections represent, nor which breed was examined. Schliemann (1966) performed a more extensive analysis of six Whippet embryos spanning three growth stages. From this work, cranial shape change over embryonic development can be summarized as an extension of the endocranium and a relative increase in the length of the nasal capsule, paired with a decrease in the declination of the jaws.

A trend observed during embryonic growth that also characterizes postnatal growth is the change in ratio of the face to the neurocranium (Schliemann 1966). Schmitt (1903) described this as the primary shape change over postnatal development and explained the relative growth of the face in terms of the role of the frontal bone. In newborn dogs, this bone primarily serves as the anterior wall of the braincase (in a manner comparable to the arrangement observed in adult dwarf dogs by Weidenreich (1941)), whereas by ten weeks of growth, only the posterior portion of the bone participates in this function while the rest encompasses the face. Schmitt (1903) formed these observations based on three stages from newborn to one year of age in several breeds, in contrast to Becker (1923), who studied thirty different age groups within the German Shepherd Dog. This expansive series of crania demonstrates that relative growth in length exceeds growth in width (also observed by Onar and Günes 2003 in a separate series of German Shepherd puppies). Becker (1923) described the effect of this transformation on the neurocranium as a stretching of a bubble shape into a pear shape.

Becker (1923) also emphasized the area of the nasal-frontal suture which, in profile, is buckled in newborn dogs, but then becomes an unbroken slope as the face extends until finally becoming incurved again as the frontal sinuses develop, forming the “stop” as the final skull shape is achieved. At that point, the roof of the braincase has flattened and the temporal region has become constricted. The strongest growth having occurred in the earliest weeks of life, these final modifications are complete by approximately nine months of age (Sommer 1931).

Herre and Stephan (1955) described the postnatal growth of the brain in the dog, citing the period around birth as the time of greatest change to brain size and morphology. These changes include elongation, particularly of the frontal lobe, and a rostral shift of the olfactory bulb. Hennet and Harvey (1992) addressed the development of the upper jaw, which grows rostrally from the incisive-maxillary suture and caudally from the palate-maxillary suture. The authors noted that the contribution of the palatal bone to the total length of the upper jaw decreases with age, while the contributions of the premaxillary and maxillary bones increases.

Researchers have also compared the cranial development of disparate breeds in an attempt to understand the timing of breed-specific characteristics. Piltz (1951) compared Bulldog and Whippet ontogenies and attributed the greatest differences in development between the two to the influence of the brain, masticatory muscles, and eyes. The broader skull of the Bulldog was explained as a secondary effect of lengthwise restriction of the growing brain, following a reduction in longitudinal growth of the skull base. Rosenberg (1966) made a similar comparison of growth in the Pekingese and the Whippet, but focused on change in the angle between the bases of the neurocranium and the face. In newborn puppies of both breeds, this angle begins in a state of klinorhynchy, which is diminished over time due to elevation of the base of the face. The Whippet remains klinorhynchic as an adult, while the elevation continues further in the Pekingese to a state of airohynchy.

1.6.4.B Heterochrony

From studies of cranial ontogeny it became clear that adult small dogs resemble juvenile large dogs (Epstein 1971). Earlier researchers, such as Bolk (1926), asserted that heterochronic processes shape cranial variation in dogs, particularly neoteny, wherein the rate of shape change over ontogeny is retarded relative to the rate of size change (Gould 1977). Hilzheimer (1926) described the crania of small dogs as arrested in growth at roughly the point in which large dog

crania shed their deciduous teeth. Arrest in cranial growth was also applied to medium and large dogs, all representing a continuum of intermediate growth stages. For Hilzheimer (1926), the reverse trend exists in the Greyhound, whose long face represents growth beyond the normal termination in large dogs.

Hilzheimer's (1926) broad application of neoteny to all small dogs was criticized by Klatt (1927) and Sommer (1931), who maintained that this trend was not consistent across all breeds. Dechambre (1949) also opposed Hilzheimer's (1926) view, rejecting the conclusion that the similarity between the globular skull of a young dog and that of a dwarf dog is due to the persistence of the juvenile form in the latter. Dechambre (1949) held that this same character could develop under independent influences, as it appears to varying degrees within adults of a single breed (the author referred to the bulging heads of Pinschers, specifically). Dechambre (1949) further criticized Hilzheimer for the use of the ratio of basal skull length to face length to highlight the similarity between an adult Pekingese and newborn German Shepherd Dog—this ratio reflects similarity in length, but not the drastically different morphologies of the face.

This point was also the focus of Stark (1962) and Rosenberg (1966), who similarly rejected a neotenic explanation for craniofacial variation. Stark (1962) observed that changes in the size of the whole body are not necessarily followed by changes in the proportions of the individual parts of the skull: in dogs of any size, combinations of both short faces with broad skulls and long faces with narrow skulls can be seen. Rosenberg (1966) concluded that different growth patterns of the face, typified by the Whippet and Pekingese, are inherited independently of body size.

Wayne (1984, 1986, 2001) compared the pattern of ontogenetic allometry to static (adult) allometry within dogs and found them to be fairly similar, from which the author proposed a causal relationship between ontogeny and breed diversity. Within the ontogenetic sequence of an individual dog skull, much of the diversity of adult dog skulls can be observed. Wayne (1984, 1986, 2001) also studied the static allometry of wild canids, but here the similarity to dog ontogenetic allometry is less pronounced. Specifically, domestic puppy skulls do not resemble the skulls of adult small wild canids. The author concluded that the morphologies of small wild canids, particularly the fox-like canid group, do not appear in domestic dogs of any size or at any stage of growth because of the absence of such forms in dog ontogeny. This limitation in variability may be related to the fact that gestation time varies across wild canids, for whom neonate size increases with gestation time, but is fixed across dog breeds (dogs share the same gestation time as the gray wolf: 60-63 days), despite variation in neonate size between breeds (Wayne 1984, 1986, 2001).

Drake (2004) continued this examination of heterochrony between the dog and its ancestor the wolf by comparing three hypotheses: first, that dog crania represent ontogenetic allometry (i.e., small breeds resemble juvenile wolves and large breeds resemble adult wolves); second, that ancestral linkage between shape and size has been dissociated in dog crania (i.e., breeds may resemble stages of wolf ontogeny without being the same size); or third, that dog crania are neomorphic (i.e., breeds do not correspond to any stage of wolf ontogeny). Drake (2004) found cranial shape to vary inconsistently with cranial size, highlighted by the small Pekingese and large Bulldog, and rejected the first hypothesis for most breeds. Breeds of different sizes, including the Chow Chow, Greyhound, Borzoi, and German Shepherd, were identified as isomorphic (shaped like an adult wolf) or even in some cases peramorphic (shaped like an overdeveloped wolf). Breeds that suggested neoteny, or pedomorphic breeds, include the Chihuahua, Newfoundland, Bulldog, and French Bulldog. Of these, the Chihuahua was the

only breed to exhibit proportioned dwarfism: it has a juvenile wolf-looking skull that matches its juvenile wolf size. A more sophisticated analysis of shape identified a neomorphic trend related to face length, wherein mesati- and brachycephalic dogs have dorsally tilted palates and dolichocephalic dogs have ventrally-tilted palates (Drake 2011).

The argument for neoteny with respect to the wolf has also been addressed in terms of behavior by Coppinger and Schneider (1995). Parallel to the appearance of juvenile wolf morphologies in domestic dog breeds, the authors note that the development of fully adult wolf functional motor sequences is retarded in dogs, resulting in a mixture of neonatal and adult behavior that has been selected for and exploited in order to train dogs for novel behaviors. The inheritance of cranial traits linked to selection for behavior, size, and other functional traits is the subject of the studies reviewed in the following section.

1.6.5 In relation to morphological integration

Recently, the diversity of craniofacial morphology across dog breeds has been quantified using geometric morphometric techniques for analyzing shape. Drake and Klingenberg (2010) performed a principal component analysis (PCA) of shape variation in a sample of over 600 dogs representing 108 breeds in order to identify patterns of covariation that may reflect the independence of two highly integrated portions of the skull: the face and the neurocranium. The first three principal components (PCs) produced by their analysis account for 71.8% of the total shape variation and correspond to three distinct dimensions of breed variation: PC1 represents the range of shapes between brachycephaly and dolichocephaly; PC2 contrasts long skulls with neurocrania positioned posterior to the face and short, broad skulls with neurocrania raised dorsally above the rostrum; and PC3 opposes relatively large, broad faces with smaller, anteriorly tapered muzzles. In accord with the large amount of variation covered by these PCs, particularly PC1, which accounts for 63%, Drake and Klingenberg (2010) observed tight integration of the entire skull. The authors also detected some separation of the face and neurocranium, especially in relation to differences between breeds with short versus long skulls, however, covariation within these two regions was only slightly stronger than covariation between them.

1.7 The genetic basis for craniofacial variation in the domestic dog

1.7.1 Studies of inheritance

Concurrent with studies that sought to find correlations between craniofacial shape and other parameters such as body size, ontogeny, or integration, were investigations of how craniofacial shape was transmitted from one generation to the next. Work in this area included crosses between dog and wolf (Iljin 1941) and within and between dog breeds (reviewed from the perspective of dog breeding by Whitney (1948) and Burns and Fraser (1952)).

Iljin (1941) studied the segregation of three skull characters in a cross between a German Shepherd Dog and a wolf. Orbital angle, maxillary zygomatic process shape, and bullae size and shape were all observed as intermediate between dog and wolf forms in F1 hybrids, while distinct segregation of dog and wolf forms were observed in F2. From this relatively simple

pattern, Iljin (1941) concluded that these traits are inherited in a Mendelian fashion through only a few genes.

Within dogs, the recessive or dominant nature of individual, breed-specific traits was explored for several cranial phenotypes. For example, Grüneberg and Lea (1940) and Phillips (1945) studied shortened mandibles in Dachshunds and Cocker Spaniels, respectively, and found this trait to be recessive and independent of the length of the maxilla. Hauck (1941) found the downward angle of the Bull Terrier face to also be recessive. Recessive traits that tend to be lethal were analyzed by Pullig (1952), who studied patent sutures and cleft palate in Cocker Spaniels, and Fox (1964), who examined otocephaly (and accompanying agnathia) in Beagles.

The inheritance of brachycephaly has also been documented, beginning with Wriedt (1929), who crossed a Pekingese and Dachshund and found the skull shape of the former to be partially dominant. Marchelewski (1930b) contrasted the inheritance of long, narrow faces with smooth profiles and short, wide faces with concave profiles within the English Pointer. The narrow face type was found to be dominant in relation to the broad face within this breed, prompting the author to extrapolate that brachycephaly in Bulldogs and Pugs may also be recessive.

The scale of the studies described thus far is dwarfed by the extensive series of crosses performed by the geneticists Stockard and Klatt. Stockard (1941) was concerned with the inheritance of cranial indices that distinguish brachycephalic breeds from dolichocephalic breeds, which he monitored in a variety of hybrids between the two types of breed. Stockard (1941) made sure to capture the full range of brachycephalic forms in the crosses, including the Boston Terrier, French Bulldog, English Bulldog, Brussels Griffon, and Pekingese. Each brachycephalic breed was crossed with the Dachshund, except for the English Bulldog, which was crossed with the German Shepherd Dog and Basset Hound, and the Pekingese, which was also crossed with the Saluki. The results of the majority of the crosses are exemplified by the Boston Terrier–Dachshund cross, in which F1 and F2 hybrids display a combination of parental traits, backcrosses onto the dolichocephalic parent produce hybrids similar to that parent, and backcrosses onto the brachycephalic parent produce wide variations in hybrid skull morphology. For example, both the wide zygomatic arches and pronounced stop of the Boston Terrier and the long face and strong dentition of the Dachshund were observed in combination in the same F1 individual. Hybrids with intermediate forms were typically found to more closely resemble the dolichocephalic parent, which, combined with the results of the backcrosses, led Stockard (1941) to conclude that the genetic factors producing dolichocephaly were more dominant than those for brachycephaly. However, the fact that many F1 hybrids exhibit short, heavy skulls suggests that brachycephaly is genetically complex, influenced by both recessive and dominant factors.

Not every brachycephalic breed presented identical patterns of inheritance in Stockard's (1941) crosses. For example, face shortening and mandible shortening were found to be fairly independent in the English Bulldog, but not the Brussels Griffon. The English Bulldog was further contrasted with the Pekingese, whose reduced face barely protrudes from underneath its bulging forehead. Based on these observations Stockard (1941) proposed an independent origin of the European Bulldog brachycephalic type and the Pekingese brachycephalic type.

In contrast to Stockard (1941), Klatt (1941, 1942, 1943, 1944) focused on only one brachycephalic breed, the English Bulldog, which was crossed repeatedly with the Greyhound. The results of these crosses were similar to Stockard's (1941), in that the F1 hybrid crania were intermediate: nearer to the Greyhound in form, but heavily built and broad like a Bulldog. The segregation of Bulldog features in F2 and F3 hybrids appeared to Klatt (1955b) to be a

contradiction, wherein on one hand the recombinations of these traits suggest a mosaic of independent single genes, while on the other the recognizable suite of these traits displayed by purebreds suggests strong linkage. However, when considering the existence of a continuum of brachycephalism between extreme breeds, Klatt (1950, 1958) arrived at a similar interpretation as Stockard (1941), agreeing that brachycephaly in non-Bulldog breeds may represent different developmental mechanisms involving different genes or differences in the timing of gene expression.

1.7.2 The genome of the domestic dog

The sequencing and mapping of the dog genome has enabled researchers to move beyond the breeding experiments of Stockard and Klatt to actual comparisons of the genetic material between breeds. The publication of the dog genome by Lindblad-Toh and colleagues in 2005 was the culmination of decades of chromosomal mapping (reviewed by Breen and Thomas 2006) and accumulation of genetic markers (see, for example, Zajc *et al.* 1997; Kirkness *et al.* 2003; Clark *et al.* 2004; and Parker *et al.* 2004). Several key features of the structure of the dog genome and its patterning across breeds were established at this time, namely that linkage disequilibrium (LD) is extensive (e.g., several megabases) within breeds but limited (e.g., tens of kilobases) across breeds. Lindblad-Toh *et al.* (2005) explained that this pattern reflects two main bottlenecks: the early domestication of dogs, and the more recent creation of distinct breeds (see also a more detailed discussion of LD by Gray *et al.* 2009).

Comparison of genomic variation across breeds has also demonstrated that breeds are genetically distinct. Utilizing ninety-six genetically unlinked microsatellite markers, Parker *et al.* (2004) were able to correctly assign 99% of over 400 dogs to their respective eighty-five breeds. Broader genetic relationships between breeds were identified in a cluster analysis based on genetic distances between dogs from the same dataset: four distinct groups were observed, including mastiff, herding, and modern European breed groups, and a group of ancient breeds from various continents (Parker *et al.* 2004; Wayne and Ostrander 2007). The work of vonHoldt and colleagues (2010) mentioned earlier added much more resolution to these relationships, demonstrating that historical functional/phenotypic groups are genetically distinct as well. This pattern of genetic relationships is particularly useful for comparing phenotypes that vary across these groups (e.g., brachycephaly).

1.7.3 Studies of genetic association

Aided by the unique structure of LD within breeds and the genetic relationships between breeds, mapping genetic variation across breeds has become a powerful tool. Boyko *et al.* (2010) presented one of the most comprehensive high density maps of genetic variation in the dog, based on 60,968 SNPs from more than 900 dogs from eighty breeds. This map was then used to assess the genetic architecture underlying over fifty complex traits, including body size and external dimensions, and cranial and dental size. Interestingly, the majority of variation in these traits is explained by only a small number of quantitative trait loci (often between two and six). The authors explain that this simple architecture likely reflects the preference of breeders for single point mutations that can be exploited in a variety of genetic backgrounds, combined

with rapid genetic drift between isolated breeds. A fortunate consequence of these circumstances is the efficient mapping of the regions of the genome underlying phenotypic variation (Boyko *et al.* 2010).

Following the development of such sophisticated mapping resources for the dog, associations between genetic variation and morphological variation have been reported for a wide variety of phenotypes, including: coat color (Berryere *et al.* 2005; Cadieu *et al.* 2009; Candille *et al.* 2007; Hédan *et al.* 2006; Karlsson *et al.* 2007; Kerns *et al.* 2003, 2004, 2007; Phillipp *et al.* 2005; Pollinger *et al.* 2005; Schmutz *et al.* 2002, 2003; van Hagen *et al.* 2004), skin wrinkling (Akey *et al.* 2010), hairlessness (Drögemüller *et al.* 2008), dermoid sinus development (Karlsson *et al.* 2007; Salmon Hillbertz & Andersson 2006; Salmon Hillbertz *et al.* 2007), pelvis and limb bone dimensions (Carrier *et al.* 2005; Chase *et al.* 2002, 2004, 2005a, 2009; Kemp *et al.* 2005; Kharlamova *et al.* 2007), body size (Chase *et al.* 2005b; Lark *et al.* 2006; Sutter *et al.* 2007, 2008), tail length (Haworth *et al.* 2001c), chondrodysplasia (Parker *et al.* 2009), and achondroplasia (Pollinger *et al.* 2005).

Association studies of craniofacial variation number fewer but have yielded insightful results. Haworth and colleagues (2001a,b, 2007) characterized three canine candidate genes and performed a survey of variation at these loci across a limited sample of morphologically diverse breeds (sample sizes ranged from four to thirteen dogs). The sequence of the homeobox gene *MSX2*, which is expressed in developing craniofacial structures in mice, was found to be highly conserved across breeds, with no contribution to diversity in face shape (Haworth *et al.* 2001a). No association was found for the canine gene *Fgf8* either, despite this signaling molecule's role in craniofacial patterning during embryonic development in mice (Haworth *et al.* 2007). The dog homolog of the Treacher Collins Syndrome gene *TCOF1*, on the other hand, presented a sequence variant between breeds corresponding to brachycephaly (Haworth *et al.* 2001b). However, Hünemeier *et al.* (2009) performed a similar analysis of *TCOF1* in a much larger sample of dogs ($n = 95$) and did not find a statistical difference in the frequency of the sequence variant in dolicho-, mesati-, or brachycephalic dogs.

Taking a different approach than the candidate gene route taken by Haworth and colleagues (2001a,b, 2007), Bannasch *et al.* (2010) undertook an across-breed mapping strategy to identify chromosomal locations associated with brachycephaly. From a panel of 96 affected dogs and 187 controls (i.e., dolichocephalic), the authors identified an association with the 31 Kb region on canine chromosome one containing the gene *THBS2*. Thrombospondin, the protein encoded by this gene, is expressed in bone and cartilage during development, and mouse mutants with reduced expression exhibit mild brachygnathism and other craniofacial abnormalities (Bannasch *et al.* 2010).

Fondon and Garner (2004, 2007) have pursued an alternative source of genetic variation to the point mutations discussed above. The authors examined length variation in tandemly repeated sequences within coding regions of developmental candidate genes, and compared such polymorphisms to craniofacial variation across breeds. A correlation between total allele length in the gene *Runx2* and the degree of klinorhynchism and midface length was observed for a large panel of dogs. Allele length in *Runx2*, whose inactivation in humans causes cleidocranial dysplasia, was further investigated in the Bull Terrier, a breed that has exhibited an increasing trend of klinorhynchism over the past century. DNA extracted from a Bull Terrier dating to 1931 displayed a shorter *Runx2* repeat allele than modern representatives of the breed, supporting Fondon and Garner's (2004) assertion that incremental changes in repeat length have led to incremental changes in craniofacial shape. The correlation between tandem repeat length and

both *Runx2* transcriptional activity and facial length has also been demonstrated across the order Carnivora (Sears *et al.* 2007).

Chapter 2: Materials and methods

2.1 Materials

This dissertation examines craniofacial shape variation in two species: the gray wolf, *Canis lupus* and the domestic dog, *Canis familiaris*. Below I summarize the samples of each species used in this study, which are tabulated in Appendices One and Two.

2.1.1 *Canis lupus*

Gray wolf crania were obtained from the collections of the University of Alaska Museum of the North in Fairbanks. The state of Alaska is divided into twenty-six game management units (GMUs), eleven of which are represented by gray wolf specimens examined in this study (Figure 2.1). The eleven GMUs sampled cover the majority of the state, extending from the northern coast along the Arctic Ocean to the eastern Canadian border. The only areas of Alaska not represented by these GMUs are the southernmost coastal regions along the Gulf of Alaska and the western coast. Alaskan gray wolves were chosen for this study for two reasons. First, among collections for which it was practical to visit for approximately two weeks of data collection, these wolves represent the closest geographical approximation to East Asian wolves, from which domestic dogs were most likely derived (according to mtDNA data: see Chapter 1 and Pang *et al.* 2009). Second, given the tremendous population decline of the gray wolf over the last several hundred years, Alaska and Northern Canada (as well as Northern Russia and China) are the only regions in which one can find large, contiguous wolf populations similar to those that existed across Eurasia and North America at the time of domestication (Wayne *et al.* 1992; Vila *et al.* 1999b).

A total of 120 adult crania, including sixty-one females and fifty-nine males, were examined. Adult status was determined based primarily on the fusion of the spheno-occipital suture and the extent of ossification of cranial sutures (Milenkovic *et al.* 2010), and to a lesser degree on dental wear (Gipson *et al.* 2000). Collection identification numbers and the sex of individual specimens are described in Appendix One.

2.1.2 *Canis familiaris*

Multiple collections were accessed in order to compile a large sample of domestic dog crania: the Natural History Museum of Bern (NHMB) in Bern, Switzerland; the Museum of Vertebrate Zoology (MVZ) at the University of California Berkeley in Berkeley, California; the Yale Peabody Museum of Natural History (YPM) in New Haven, Connecticut; the Harvard Museum of Comparative Zoology (MCZ) in Cambridge, Massachusetts; the American Museum of Natural History (AMNH) in New York, New York; the National Museum of Natural History (NMNH) in Washington, D.C.; the Royal Ontario Museum (ROM) in Toronto, Canada; the Los Angeles County Museum of Natural History (LACM) in Los Angeles, California; the California Academy of Science (CAS) in San Francisco, California; and the private collection of Ray Bandar (RB), also in San Francisco, California. The large majority of crania examined come

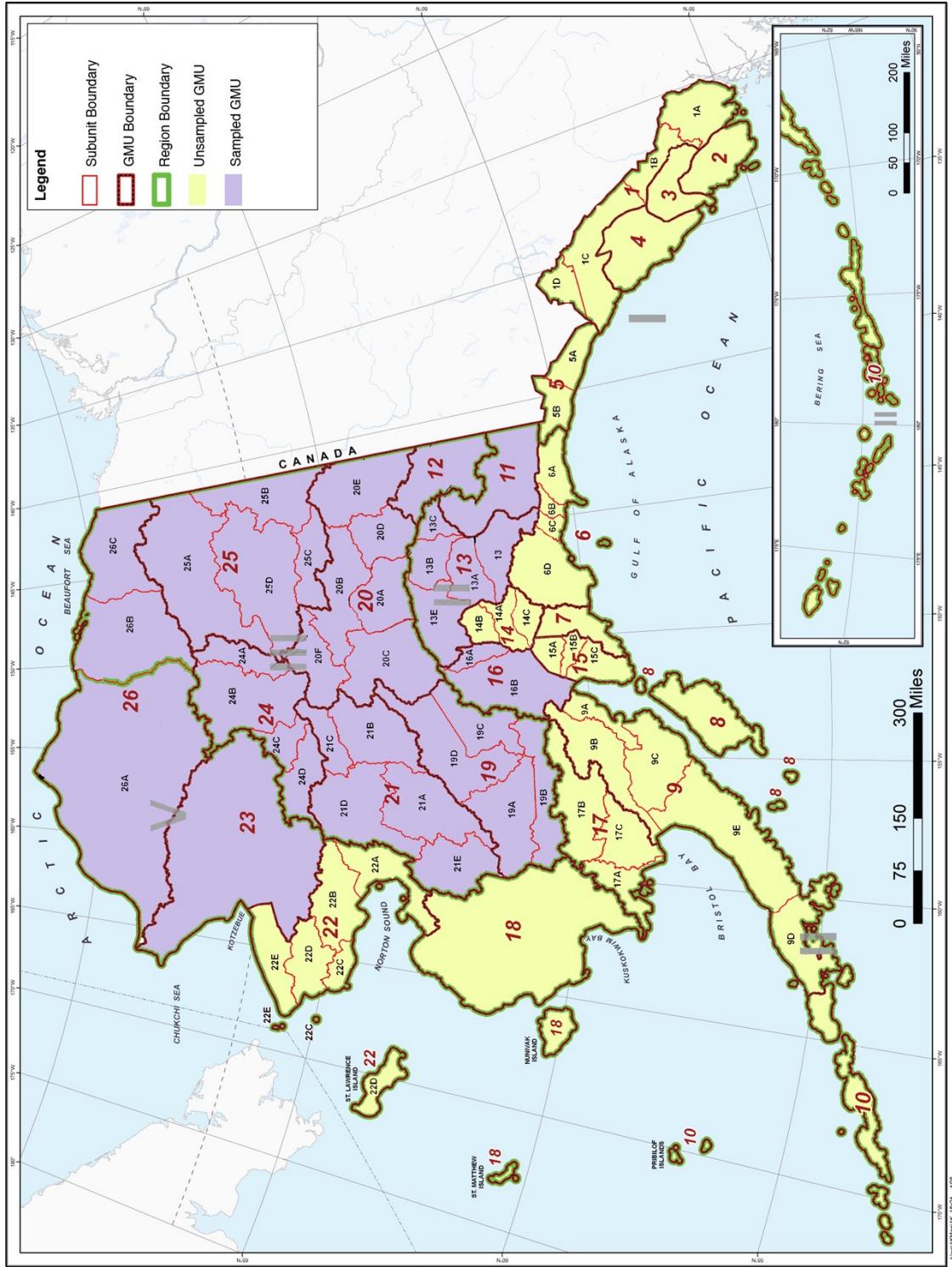


Figure 2.1 Alaskan game management units (GMUs) included in the *Canis lupus* sample. Modified from www.adfg.alaskagov.

from the NHMB, which houses the Albert Heim Foundation for Canine Research, a collection of over 2,500 dog specimens spanning from the time of Théophile Studer (former head of zoology at the museum) to the present.

A total of 527 adult dogs, representing sixty-nine breeds, were studied. Only dogs for which the breed had been identified by the collector were included. Adult status was assessed using the same criteria used with wolves; however, this process was complicated by several factors. Given the fact that it is characteristic for the cranial sutures of many small breeds to never completely fuse (and to be accompanied by large fontanels in extreme cases), the fusion of the sphenoccipital suture was the only suture informative across all breeds. Sample sizes permitting, observation of size and shape variation within breeds was extremely helpful for age assessment. Because the individual diet and lifestyle of domestic dogs vary substantially more than in members of the wild wolf species, dental wear was also much less informative for determining the age of dogs.

A list of all domestic dog specimens, including the collection of origin, collection identification number, breed, and sex (when available) are presented in Appendix Two. Breed selection for the study sample was conducted in two ways. First, given the relative ease of accessing the major domestic natural history collections, and in an effort to sample as much of the range of across-breed cranial variation as possible, every dog for which breed had been identified from every collection (excluding the NHMB) was included. Second, in order to properly capture within-breed variation for breeds representative of the three cranial types (dolicho-, meso-, and brachycephalic), sample size was maximized for fifteen focus breeds that met these requirements, drawing largely from the extensive collections at the NHMB.

Dolichocephalic focus breeds include the Borzoi ($n = 45$), the Collie ($n = 45$), and the Greyhound ($n = 26$). Mesocephalic breeds are represented by the Chow Chow ($n = 28$), the German Shepherd Dog ($n = 22$), the Great Dane ($n = 23$), the Irish Wolfhound ($n = 25$), and the Newfoundland ($n = 17$). Lastly, brachycephalic breeds of focus include the Boxer ($n = 60$), the Bull Terrier ($n = 25$), the English Bulldog ($n = 21$; hereafter referred to simply as the 'Bulldog'), the Chihuahua ($n = 18$), the French Bulldog ($n = 17$), the Pekingese ($n = 15$), and the Pug ($n = 14$). Importantly, the sampling of brachycephalic focus breeds includes representatives from the genetically distinct Toy Dog (Chihuahua, Pekingese, Pug) and Mastiff-like Dog (Boxer, Bull Terrier, Bulldog, French Bulldog) groups (vonHoldt *et al.* 2010).

Additionally, focus breeds were chosen to capture the size range within each category. Among dolichocephalic breeds, the Borzoi is one of the largest, measuring twenty-six to twenty-eight inches at the withers (a size measurement taken on dogs that are standing with erect heads, from the ground to the most dorsal point of the scapulae), while the Greyhound is roughly two-thirds this size and the Collie is intermediate. The largest focus breeds are the mesocephalic Great Dane and Irish Wolfhound, both measuring thirty to thirty-two inches at the withers. At the smaller end of the mesocephalic size spectrum is the Chow at seventeen to twenty inches, with the German Shepherd and Newfoundland falling in between. The greatest range of size exists within the brachycephalic group, starting with the large Boxer at twenty-one to twenty-five inches, followed by the Bulldog, Bull Terrier, and French Bulldog. At the small end are the toy dogs: the Pug, Pekingese, and the smallest, the Chihuahua, which can be as small as six inches at the withers (all measurements reported are taken from the breed standards described by the American Kennel Club 2006).

Details for the fifteen focus breeds are summarized in Table 2.1 and lateral, dorsal, ventral, and anterior views of their crania are presented in Figures 2.2–2.5, respectively.

Table 2.1 Focus breeds

Category	Breed	Sample size
Dolichocephalic	Borzoi	45
	Collie	45
	Greyhound	26
Mesaticephalic	Chow Chow	28
	German Shepherd Dog	22
	Great Dane	23
	Irish Wolfhound	25
	Newfoundland	17
Brachycephalic	Boxer*	60
	Bull Terrier*	25
	Bulldog*	21
	Chihuahua†	18
	French Bulldog*	17
	Pekingese†	15
	Pug†	14

* Mastiff-like breeds

† Toy dog breeds

2.2 Methods

2.2.1 Introduction to geometric morphometrics

2.2.1.A Early origins of geometric morphometrics approaches

Fred L. Bookstein describes morphometrics as “the empirical fusion of geometry and biology,” or more specifically as the integration of data from two sources: “geometric location and biologic homology” (1982, p. 451). The work of Bookstein beginning in the late 1970s contributed to the rise of the field of geometric morphometrics, as described by Richtsmeier *et al.* (2002); however the fundamental idea of examining biological forms in the context of geometry can be traced back much earlier to the work of D’Arcy Thompson. In his 1917 book, *On Growth and Form* (1961), Thompson introduced his method of “Cartesian transformation,” with the purpose of expressing differences between biological forms as coordinate transformations. Thompson depicted biological forms overlaid with grids and the differences between forms as deformations of those grids based on the corresponding coordinates of biological landmarks. While these grid transformations elegantly illustrated form change in geometrical terms, Thompson did not indicate a means for quantification or statistical analysis of this change (Bookstein 1977, 1986), which was remedied by Bookstein (1978, 1982) some sixty years later in the form of his biorthogonal grid analysis method. This method, later modified into

- 1 cm



Borzoi



Collie



Greyhound



Irish Wolfhound



German Shepherd Dog



Great Dane



Newfoundland



Chow Chow



Boxer



Bulldog



Bull Terrier



French Bulldog



Pug



Pekingese



Chihuahua

Figure 2.2 Lateral views of dolichocephalic (green), mesaticephalic (red), Mastiff-like brachycephalic (blue), and toy dog brachycephalic (black) focus breeds.

■ 1 cm

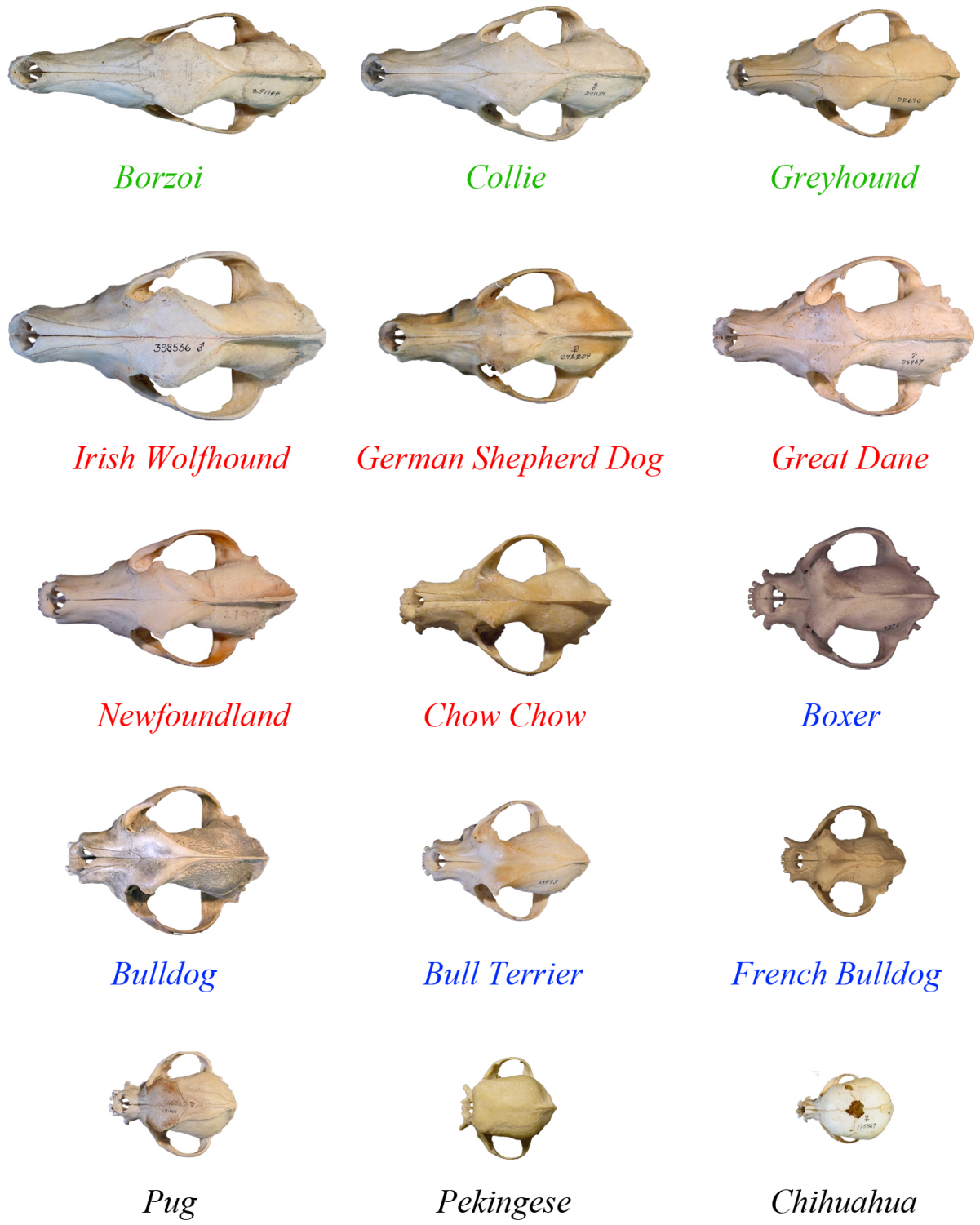


Figure 2.3 Dorsal views of dolichocephalic (green), mesaticephalic (red), Mastiff-like brachycephalic (blue), and toy dog brachycephalic (black) focus breeds.

■ 1 cm



Borzoi



Collie



Greyhound



Irish Wolfhound



German Shepherd Dog



Great Dane



Newfoundland



Chow Chow



Boxer



Bulldog



Bull Terrier



French Bulldog



Pug



Pekingese



Chihuahua

Figure 2.4 Ventral views of dolichocephalic (green), mesaticephalic (red), Mastiff-like brachycephalic (blue), and toy dog brachycephalic (black) focus breeds.

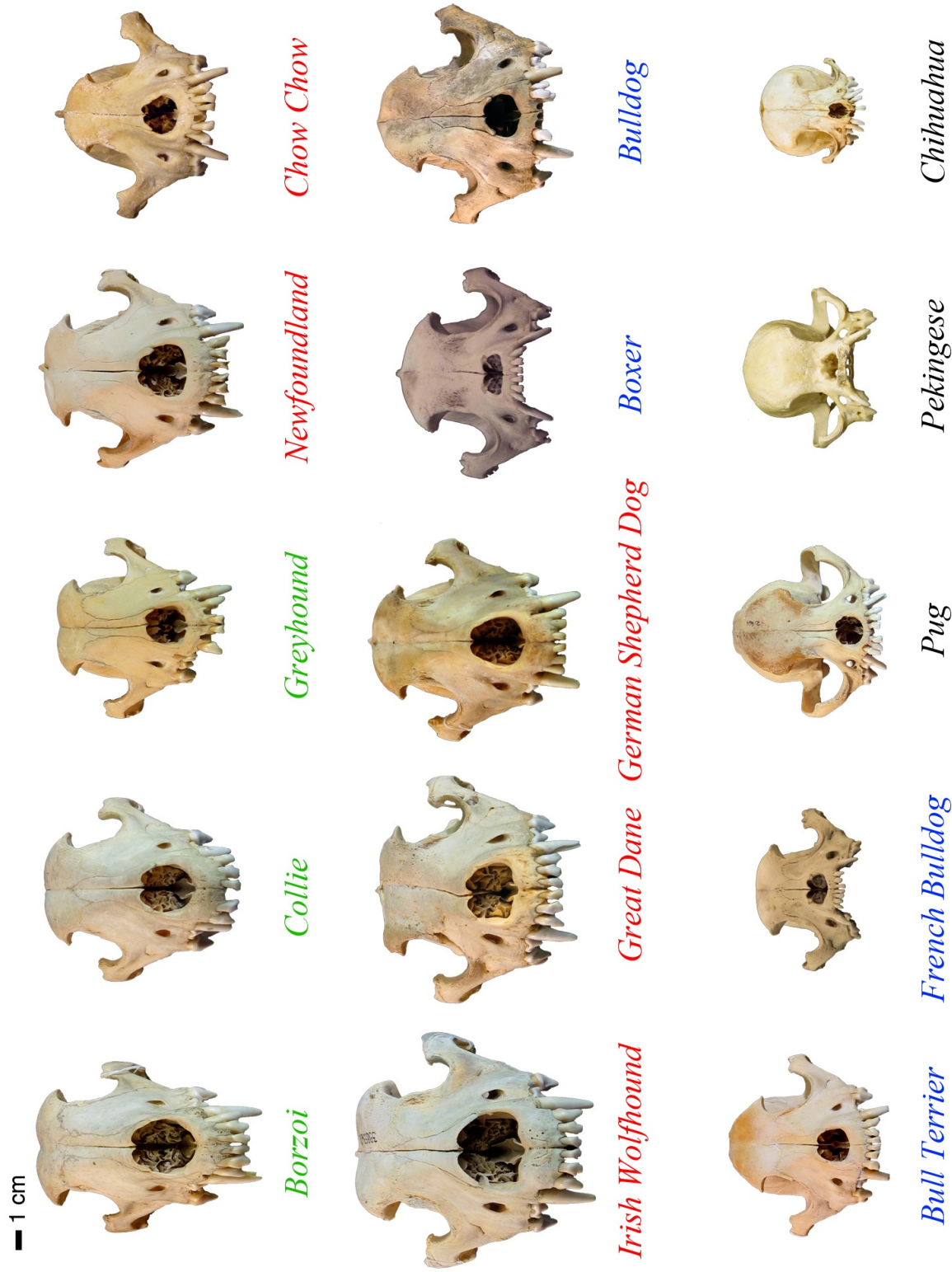


Figure 2.5 Anterior views of dolichocephalic (green), mesaticephalic (red), Mastiff-like brachycephalic (blue), and toy dog brachycephalic (black) focus breeds.

the “tensor approach,” paved the way for the expansion of deformation techniques within the field of geometric morphometrics, followed shortly by Cheverud and colleagues’ (1983) implementation of finite-element scaling analysis (FESA) and Bookstein’s (1989) own thin-plate spline (TPS) method.

An equally important contribution to morphometrics comes from the 1905 work of Franz Boas. While Thompson’s transformation grids are the foundation upon which subsequent deformation methods have been built, Boas introduced the idea of superimposition as a means of identifying form difference (Boas 1905; Cole 1996). Boas criticized aligning skulls for comparison based on two arbitrarily chosen points, as is commonly done when skulls are placed in the Frankfurt Horizontal. Instead, he argued that a superimposition that minimizes the sum of the squared distances between all pairs of homologous points is ideal. His student Eleanor Phelps (1932) continued to study the process of superimposition via the method of least differences, in which she demonstrated that the natural variation specific to one landmark was spread to other landmarks in the minimization process—an issue that has reemerged in debates regarding the consistency and validity of superimposition methods (e.g., Richtsmeier *et al.* 2002). Phelps also suggested that form difference could be measured using the Euclidean distances between landmarks (Phelps 1932; Cole 1996), foretelling another popular morphometrics approach of the present, Euclidean distance matrix analysis (EDMA) (Lele 1991, 1993).

The range of morphometric approaches presently in use can be broken down into several categories. The early work by Thompson, Boas, and Phelps discussed above contributed to the development of landmark-based morphometrics techniques. Landmark-based studies implement either coordinate-based or coordinate-free approaches and the validity of the former group, which includes superimposition and deformation methods, has been questioned by proponents of EDMA, the most commonly applied coordinate-free method (Richtsmeier *et al.* 2002). In addition there exist non-landmark-based morphometrics techniques that focus on the outlines or curves of biological forms, best represented by eigenshape and Fourier analyses. Below I outline the basic premises of these various techniques, provide examples of the range of biological questions of form to which they have been applied, and review some of the controversy that has arisen regarding their limitations and biases. This discussion provides context for the specific geometric morphometric methods used in this dissertation, which are described in the subsequent section.

2.2.1.B Landmark-based methods

Landmark-based morphometric comparisons of form depend on point-to-point mapping based on homology between forms. Bookstein (1986, 1991) clarifies the type of homology referred to by morphometrics, citing the difference between the biological and biometrical definitions of homology: instead of relating parts to parts, homology in morphometrics is a mapping function that relates points to points. Zelditch and colleagues (2004) elaborate on the subject by describing mapping of corresponding points based on a very restricted sense of correspondence—that is, the corresponding points must be “the same anatomical locus” (2004, p. 25). These anatomical loci are referred to as landmarks.

Bookstein originally categorized landmarks as being either “anatomical” or “extremal” (1978), but later expanded his typology to include three classes. Landmarks fall into “types”

depending upon how they can be defined. Type I landmarks, originally termed anatomical landmarks, are defined by the discrete intersection of three structures—structures not involved in that intersection are not required in the definition (Bookstein 1991; Zelditch *et al.* 2004). Examples of Type I landmarks include the intersection of the coronal and sagittal sutures on the cranium, also known as bregma, or the intersection of the internasal suture and the superior margin of the nasal aperture, also known as rhinion. Extremal landmarks were renamed as Type III landmarks and are defined by their extreme location relative to another point or structure (Bookstein 1991). An example of a Type III landmark is the highest ectocranial point on the midline of a skull placed in the Frankfurt Horizontal, also known as vertex. Type II landmarks are intermediates between these two disparate categories—landmarks defined purely by anatomy and landmarks that are measurement-based. These include the tips of extruding processes and the deepest points of grooves (Bookstein 1991). An example is the tip of the coronoid process of the mandible, or coronion.

Zelditch and colleagues (2004) outline several criteria for the choice of landmarks in geometric morphometric studies. The first criterion is homology in terms of anatomical location, followed by consistency of relative position, which refers to overall topology between forms. The authors provide the example of a foramen that is present in only some of the taxa being compared as an extreme difference in landmark topology. Equally important is coverage of form, or whether the landmarks being considered adequately represent the overall form being compared. The last criterion presented is repeatability, which reflects how easily landmarks can be located both on a specimen over repeated trials and across multiple specimens. The authors point out that some landmarks may be difficult to locate only in one dimension, resulting in error that is biased in one particular dimension and hence may lead to false positives during the detection of patterns of form difference. Type III landmarks, which are not easily defined with regard to some local structure, often do not satisfy this criteria and the authors caution their use. In a test of data capture repeatability from three-dimensional surfaces reconstructed with computed tomography (CT) scans, Valeri and workers (1998) demonstrated that although measurement error was higher for Type III “fuzzy” landmarks, it still fell within an acceptable range and justified inclusion in studies of the craniofacial skeleton. The study of Valeri *et al.* (1998) addresses an important question: to what extent is it acceptable to forego one criterion for the sake of satisfying another? Valeri and colleagues (1998) argue that including fuzzy landmarks, such as the center of the left frontal boss, adds coverage to an area of the skull typically disproportionately lacking in landmarks. A model for balancing the demands of conflicting criteria is presented in the authors’ measurement of the error associated with questionable landmarks (I will return to the subject of landmark error in a later section). Zelditch *et al.* (2004) propose a final criterion of coplanarity, which applies only to data taken from two-dimensional representations of three-dimensional forms.

2.2.1.B.i Coordinate-based approaches

Landmarks are recorded as x , y , and z coordinates in all landmark-based studies (or simply x and y in two-dimensional cases); however the subsequent transformations made upon these coordinate values vary by method. Coordinate-free methods do not alter these original values, calculating only the Euclidean distances between them for comparison. Euclidean distance matrix analysis follows this pattern and is summarized later. Coordinate-based methods

include superimposition and deformation, which both require manipulation of landmark coordinate values for form comparison (Richtsmeier *et al.* 2002). I discuss both types of method below.

2.2.1.B.i.a Superimposition: Generalized Procrustes analysis

Sneath (1967) pursued D'Arcy Thompson's transformation grid concept by applying the geological technique of trend-surface analysis to the displacement of landmarks between two superimposed forms. Bookstein (1986) explains that Sneath's (1967) goal was to express the difference in forms numerically via the coefficients of the polynomial trends fitted to the displacements in the x and y dimensions. This final analytical portion of Sneath's method, in which form difference is treated like the contoured surface of a geological map, was not as important to the imminent field of geometric morphometrics as was his method of registration for the two forms being compared. Sneath sought the same 'best fit' as Boas (1905) for his comparison of form, achieved by the processes of centering the forms onto one another (translation), reducing them to the same size (scaling), facing them in the same direction (reflection) and finally rotating them. The least-squares criterion used by Sneath (1967) to ensure that these processes converge on the best fit between forms remains the basis of the most popular means of superimposition, Procrustes analysis, at its simplest level.

Gower (1975) generalized Sneath's pair-wise comparison so that multiple forms could be translated, scaled, reflected and rotated simultaneously. Gower minimized the sum-of-squares between clusters of homologous landmarks and their centroid, an extension of the previous method that only dealt with pairs of landmarks. Siegel and Benson (1982) recognized that in the least squares method a large amount of variation associated with one or several landmarks is minimized to achieve the best fit at all landmarks, potentially obscuring true shape differences. As a robust alternative the authors developed a resistant-fit utilizing the repeated median algorithm, which prevents changed regions between forms from influencing the fit of unchanged regions. A comparison of four primate skulls after Sneath (1967) using both least squares and repeated median resistant-fit by Siegel and Benson (1982) suggested different allometric relationships and demonstrated that the different superimposition methods identify different patterns of form change. Specifically, the resistant fit method is better able to show differences between two forms when the difference is isolated to one region represented by a few landmarks (Rohlf & Slice 1990).

Procrustes superimposition received further revision by Rohlf and Slice (1990) in their generalization of both least squares and resistant-fit. The authors generalize the resistant-fit analysis by combining an initial least squares alignment and a final resistant-fit alignment to a mean consensus object (this combined approach has become the most widely accepted and commonly used superimposition technique, referred to simply as generalized Procrustes analysis, or GPA). Following the suggestion of Goodall and Green (1986) that the detection of uniform shape change be included in mapping strategies, Rohlf and Slice (1990) also expand their generalized approach to include affine transformations, which help identify subtler, local changes.

Rohlf and Slice (1990) also expanded upon the previous methods of visualization utilized by Sneath (1967), Siegel and Benson (1982) and Goodall and Green (1986), which relied on the depiction of residual vectors at each reference landmark of a plotted configuration. Rohlf and

Slice (1990) presented each fitted landmark as a scatter plot in two dimensions, corresponding to the first and second principal component axes of variation relative to the reference landmarks. A similar representation was presented using the eigenvectors and eigenvalues of the within-landmark variance-covariance matrix to construct constant frequency ellipses around each landmark. Groups within the total sample can be compared on the basis of the centroid of that group's residuals about each landmark. Rohlf and Slice (1990) applied these visualization methods to mosquito wing form and provided instructions for using them to detect patterns of directionality and magnitude of change. GPA was extended to three-dimensional data by Slice (1996), including affine resistant fitting and visualization using residual plots in a manner similar to two-dimensional analyses.

GPA has been applied to cranial morphology extensively, particularly in the field of physical anthropology. Some of the earliest examples include O'Higgins and Jones' (1998) superimposition of facial landmarks taken from skulls of the mangabey *Cercocebus torquatus*, and Lockwood and colleagues' (2002) quantification of temporal bone morphology across great apes and humans. Havarti (2003) also examined temporal bone morphology using GPA, including both fossil Neanderthal and humans specimens. Singleton (2002) used GPA as a taxonomic tool, applying principal component, canonical variate, and regression analyses to landmark data representing variation across the Cercopithecinae. Frost and colleagues (2003) applied a similar set of multivariate tests to data generated from GPA of cranial landmarks of papionins.

GPA has been utilized in studies of canids as well. *Canis lupus* has been included in surveys of morphological integration in Carnivora and Mammalia by Goswami (2006a and b, respectively). Covariance matrices based on the superimposition of three-dimensional cranial landmarks indicated that patterns of integration are correlated with phylogenetic distance within carnivorans and marsupials (Goswami 2006a), and that when viewed across all therians, the separation of an anterior oral-nasal, a basicranial, and a molar module is conserved (Goswami 2006b). Wroe and Milne (2007) also compared skull shape in a large sample of carnivorans, including *C. lupus*, and marsupials. Their principal component analysis of GPA data demonstrated that brain size and bite force are correlated with different patterns of constraint on skull shape for the two groups.

Milenkovic and colleagues (2010) used principal component analysis of superimposed landmark data to contrast the cranial morphology of two populations of gray wolves in Serbia. Elevation of the snout and sagittal crest, as well as dorsal flexion of the face, distinguish the Dinaric-Balkan wolf from the Carpathian wolf. Drake and Klingenberg (2010) superimposed configurations of cranial landmarks for wolves and other wild canids in comparison to domestic dogs, also using principal component analysis to compare and contrast the greatest dimensions of shape variation within each group. The amount of variation within dogs was found to exceed that in wild canids, being more comparable to that seen across all of Carnivora. Furthermore, the shape space occupied by dogs extends outside of that occupied by other canids and includes novel cranial shapes relative to the rest of Carnivora.

Drake and Klingenberg (2008) have also used GPA to study shape variation within a single breed of dog, the St. Bernard, over 120 years of its history. A multivariate regression of superimposed shape coordinates on time demonstrated that the nose has shifted upward and posteriorly, while the palate and maxillae have become more dorsally inclined over time in the St. Bernard, independent of size changes. Hofmann-Apollo (2009) performed a multivariate analysis of GPA data to quantify differences in asymmetry and malocclusion between

brachycephalic and mesaticephalic dog breeds and found higher variability in the anterior region of the jaws in the former group. Most recently, Drake (2011) tested for patterns of heterochrony in dog breeds relative to the ontogeny of the gray wolf, for which the author compared shape variation in the whole cranium, and separately in the neurocranium and face, across a sample of adult dogs and an ontogenetic series of wolves. The hypothesis that dogs represent paedomorphic wolves was rejected and instead a novel pattern of shape variation was presented in which brachycephalic and mesaticephalic breeds exhibit dorsally tilted palates and dolichocephalic breeds present ventrally tilted palates.

2.2.1.B.i.b Superimposition: Two-point and edge-matching registration

Bookstein (1991) provides a simpler alternative to Procrustes superimposition in the form of two-point registration, which standardizes the distance between two arbitrarily chosen landmarks and uses only these two points to align forms. Richtsmeier *et al.* (2002) trace a similar practice back to the roentgenographic cephalometry work of Broadbent and colleagues (1975), in which a specific edge was used to align forms. Bookstein's (1991) method was developed for the unique case of a single triangle of three landmarks, beyond which the quality of the fit becomes greatly dependent on the magnitude and direction of variation around the two points chosen for registration. In a separate context, Bookstein (1982, 1991) looked at the examination of landmarks in sets of three, comprising multiple overlapping triangles; he referred to this as the simplest form of the finite-element deformation description, discussed in the next section.

2.2.1.B.i.c Deformation: Finite-element scaling analysis

The biorthogonal grid analysis presented by Bookstein (1978) quantified Thompson's (1961) Cartesian transformation approach by utilizing a grid that expresses the direction of greatest and least rates of change between forms along principal axes. Originally applied to single comparisons of two forms, the biorthogonal grid analysis was generalized into the tensor method (Bookstein 1982) to calculate average transformations for populations of similar deformations. Both methods require that the form be represented by a configuration of landmarks that are then analyzed in groups of three, forming the vertices of many overlapping triangles. The deformation of each triangle onto its counterpart is represented by the axes of greatest and least percent change, which can be graphically depicted in the interior of the triangle at a ninety degree angle. In the tensor method group differences in deformation are quantified as the greatest and least differences in these axes (Bookstein 1982).

Cheverud *et al.* (1983) introduced a new form of deformation analysis applicable to three dimensions based on the scaling method proposed by Lew and Lewis (1977) and Lewis and colleagues (1980), which they adapted from the field of engineering. In their generalization of finite-element scaling analysis (FESA) Cheverud and colleagues (1983) also credit Niklas (1977) for introducing the method into the study of growth and form. The work of all these authors shares the common approach of approximating continuous deformation by finite elements, similar to Bookstein's (1982) decomposition of form into triangles of homologous landmarks. The spatial relationship of the landmarks comprising the nodes of each element are used to

determine shape functions, which allow mapping of all mathematically homologous points within the reference and deformed elements (Cheverud *et al.* 1983; Richtsmeier *et al.* 2002). Cheverud and colleagues (1983) demonstrated that these shape functions could be used to determine the three-dimensional coordinates of both the nodal and nonnodal points of the deformed object following transformation. Transformations can be graphically represented by placing an arbitrary coordinate system on the reference object that is then used to plot the transformed coordinates of the homologous nodal and nonnodal points. The authors applied FESA to a population of rhesus macaque skulls, for which they were able to define a mean cranium form and measure the variation in local shape changes around this mean in terms of the strain and stretch of individual elements.

Although a coordinate system is required for the method of visualization proposed by Cheverud *et al.* (1983), special registration or orientation is not required for quantification of the change in form. This advantage is shared by Bookstein's biorthogonal grid technique (1978), however FESA has the additional advantages of three-dimensional application and the potential to generate hypothetical transformations based on prescribed functions of homology (Cheverud *et al.* 1983). Richtsmeier *et al.* (1992) identify the greatest assets of FESA as its ability to identify form difference at the local level of specific elements and the specific directions of the strain for those elements. However, they argue that this latter advantage is lost during statistical analysis of within- and between-group variation, which requires adoption of the optimal dimensions of the mean reference relative to each target and hence cannot account for the unique dimensions optimal for each individual.

Cheverud and colleagues (1991) applied FESA to the mouse mandible in a quantitative genetics context to explore the genetic variation for mandibular size and shape. Their results indicated a pattern of morphological integration that corresponds to the developmental and functional history of the mandible. This work was followed by a comparison of mandible shape between mice and rats that also utilized FESA and quantitative genetics in an effort to characterize which morphogenetic components contributed to the differentiation in form between species (Atchley *et al.* 1992). Isometric size scaling, mesenchymal condensation differentiation and muscle hypertrophy were all identified as factors.

Diewert and Lozanoff (1993) used finite element modeling to capture shape change from photographs of midsagittal sections of the face and palate of human embryos between stages 15 to 19. Increases in size in the face and cranium during growth were associated with specific shape changes, including a decrease in the posterior angle of the cranium, an increase in the orofacial angle and a superior rotation of the forebrain and midbrain toward the hindbrain. Takeshita and colleagues (2001) also studied the human craniofacial complex, analyzing growth in subjects four to eighteen years old. Over this time period the authors observed the greatest change in the maxillary complex, followed by the mandible, and the least change in the upper face and cranial base.

A functional perspective was taken by Preuschoft and Witzel (2005) in their construction of finite-element models to recreate the loading of external muscles and bite forces in fossil synapsids and extant mammals. The forms of models iteratively loaded and modified by removing low stress elements were compared with real skulls and were found to be very similar in stress flow. The majority of morphological difference between fossil synapsids and extant mammals was attributed to braincase size, while a protective function for the postorbital bar was rejected.

2.2.1.B.i.d Deformation: Thin-plate spline

Bookstein (1989) introduced another deformation technique called the thin-plate spline (TPS), which is invariant under translation or rotation. Originally advanced in the field of approximations theory, TPS uses an interpolation function in a similar fashion to FESA to map homologous points between forms (Richtsmeier *et al.* 1992). Algebraically, the name for this function comes from the idea of a thin steel plate that conforms to a surface beneath it in the (x, y) -plane based on a two-dimensional generalization of the one-dimensional cubic spline function (Bookstein 1989). Whereas FESA minimizes the strain between the reference and target objects on an element-by-element basis, the splined mapping function of TPS minimizes the bending energy required to deform the surface of the entire object. This deformation can be decomposed into both affine and non-affine (Richtsmeier *et al.* 1992). For the non-affine, or non-uniform changes, Bookstein (1989) developed the concept of “principal warps”, which are the eigenvectors of the bending-energy matrix and “represent features of deformation at distinct geometrical scales” (p. 569). Principal warps correspond to successively higher levels of bending energy and the higher the bending energy term, the smaller the physical scale at which the deformation is occurring, i.e., the more local the change.

Bookstein (1989) used TPS to quantify deformation across eight craniofacial landmarks in normal and Apert Syndrome affected humans. Form difference was expressed in terms of four deformation features, including a general affine term and three localized deformations, defined in terms of the magnitude and direction of the affected anatomical landmarks. While Bookstein’s example analysis (1989) was limited to two dimensions, he did propose the algebraic means of extending the TPS function to three-dimensional data, which has since been performed using several different means of visualization. Ahlström (1996), for example, drew the total warp that expressed sexual dimorphism in their sample of medieval human crania as vectors on a two-dimensional plot, while Gunz (2001) depicted a three-dimensional configuration of the cranial landmarks studied intersected periodically with curtains of grid points showing the deformation at those intervals.

Recently, Rosas and Bastir (2002) analyzed patterns of allometry and sexual dimorphism in the lateral profiles of human adult skulls with TPS. The authors observed an allometric trend in the proportions of the neurocranium and viscerocranium and identified sex-specific variation in the nasopharyngeal space and at muscle attachment sites. TPS has also been utilized by Rosas and colleagues (2008) to explore dental malocclusion in African, Asian and European populations. Canonical variates analysis revealed two significant axes of discrimination and the authors concluded that the geographic groups studied could be differentiated based on basicranial orientation and posterior cranial base length. TPS has frequently been applied to the study of malocclusion (e.g., Franchi *et al.* 2007), but recently Kieser and colleagues (2007) also examined the dentition using TPS, but in the context of forensic science. The authors performed principal components analysis on TPS-decomposed coordinates of the incisal surfaces of the anterior dentition and were able to show that individuals differ both in terms of relative tooth position and arch shape.

2.2.1.B.ii Coordinate-free approaches: Euclidean distance matrix analysis

A discussion of coordinate-free geometric morphometric approaches begins with the issue of registration, recognized as problematic beginning with Boas (1905), who cited the arbitrary nature of the two-point registration system employed in the use of the Frankfurt horizontal. Despite the development of registration methods that utilize information from all landmarks in a configuration (e.g., Sneath 1967), Lele (1991) pointed out that the methodology was still flawed because the different “loss functions” used to minimize distances between landmarks gave different superimpositions. In other words, arbitrary choice of loss function leads to inconsistent superimpositions and inconsistent tests of hypotheses on form difference.

Richtsmeier and colleagues (2002) explain that the inherent problem with all superimposition approaches is their arbitrary selection of a coordinate system for analysis. Registration is helpful in terms of visualizing the difference between two forms, however it requires parameters that are unknown. The authors cite the statistical model used by Goodall (1991), among other authors, to express the relationship between individuals and a mean form. This model, expressed as

$$X_i = (M + E_i)\Gamma_i + t_i$$

where X_i is the landmark coordinate matrix of the i th specimen, M is the mean form, E_i is the error or the variation related to each specimen, Γ_i is the rotation, and t_i is the translation, includes two parameters, rotation and translation, which are unique for each specimen and cannot be estimated. The presence of these nuisance parameters precludes estimation of the mean, M , or the variance covariance matrix E_i . Richtsmeier and colleagues (2002) argue that these nuisance parameters are unimportant and that analyses of form should only focus on M and E_i . This follows the reasoning of Lele (1991), who defines form as “that characteristic which remains invariant under translation, rotation, and reflection of the object” (p. 410). Lele (1991) expands upon this definition to characterize all the possible matrices of landmark coordinates obtainable via rotation, reflection or translation of a given landmark coordinate matrix as an “orbit,” which allows coordinate data to be studied in a coordinate-free “maximal invariant” space. Lele’s (1991) Euclidean distance matrix analysis (EDMA) takes these theoretical considerations into account, following the author’s invariant definition of form.

EDMA utilizes a matrix of all possible distances between pairs of landmarks that is invariant under translation, rotation and reflection, called a form matrix (Lele 1991). The form matrix corresponds to the orbit defined by the form and can be used to define a mean form matrix for a sample of forms, from which comparisons between forms can be based on ratios, absolute differences, or some other metric of the linear distances (Lele 1993; Richtsmeier *et al.* 2002). Lele (1991) acknowledges that depending on the number of landmarks, the form matrix can become very large and redundant, complicating interpretation, and recommends focusing on the landmark pairings that exhibit the extreme cases of small and large ratios. Another difficulty with EDM is graphical representation. Compared to the superimpositions and deformation grids, which can display both the magnitude and direction of affine and non-affine form difference, EDM does not provide a readily accessible means of visualization. Richtsmeier and colleagues (2002) present one strategy in showing only the linear distances that are more than five percent different from the mean and then further distinguishing distances by color or line weight to correspond to the magnitude of change.

Richtsmeier and Lele (1990, 1993) first applied EDM to studies of growth patterns. Using landmarks located on lateral cephalometric radiographs, the authors identified differences

between normal postnatal growth patterns and those of Crouzon syndrome individuals (Richtsmeier and Lele 1990). Growth matrices were also used to study the sexual dimorphism of facial growth in *Macaca fascicularis*, where the authors were able to localize growth differences to the anterior snout and palate, a result of the sexually dimorphic canines in this species (Richtsmeier and Lele 1993).

Hlusko (2002) used EDMA for cross-sectional and occlusal landmarks of the first and second mandibular molars of three hominoid taxa and identified two distinct patterns of metameric variation: one for humans and another for chimpanzees and gorillas. Variation in fossil hominid molars from Sterkfontein, South Africa, was compared to these patterns and found to resemble that observed in the African great apes. Ackermann (2005) also compared humans and great apes, focusing on the craniofacial complex. Covariation patterns were compared to theoretical integration matrices to test hypotheses on morphological integration through ontogeny. The author identified a common integration pattern through ontogeny across hominoids and several differences in magnitude and covariance that may underlie the differences between human and great ape cranial form. Richtsmeier and colleagues (2006) addressed the subject of integration at the level of the neurocranium and the brain. A variation on EDMA that focuses on the differences between the elements of two covariance matrices was applied to landmark data taken from both brain MR images and head CT images. The authors showed strong integration between the skull and brain in both normal growth patterns and those seen in individuals with isolated craniosynostosis, however, the differences in growth pattern were found not to be local to the suture affected by craniosynostosis.

Drake (2004) used Euclidean distances to represent cranial shape variation in the author's first analysis of heterochronic patterns and processes in wolves and domestic dogs (see also Drake 2011, described with respect to GPA above). The evolution of most dog breeds could not be described by heterochronic processes, although several breeds were found to be paedomorphic. Common principal components and shared correlation matrix structure analyses were also used to investigate developmental integration. In comparing wolves to domestic dogs, Drake (2004) found that the ancestral pattern of developmental integration does not predict domestic dog integration.

2.2.1.C Non-landmark-based methods

The categories of landmarks listed earlier reveal several of the shortcomings of landmark-based studies, most importantly, that certain aspects of biological forms are not reliably represented by discrete points in two- or three-dimensional space. One limitation of landmark data is that they do not include information regarding the spaces, curves, or surfaces between them. Additionally, the location and number of landmarks used often corresponds to the density of biological features and may result in overrepresentation of some areas and underrepresentation of others (Richtsmeier *et al.* 2002). Bookstein's (1991) landmark typology and the selection criterion proposed by Zelditch and colleagues (2004) illustrate the compromises that must be made to represent biological form using landmarks. To avoid such problems, the non-landmark-based method of Fourier analysis was borrowed from geological studies of particle shape (e.g., Ehrlich and Weinberg 1970). Eigenshape analysis, which uses a series of orthogonal shape functions, instead of the harmonic functions of Fourier analysis, has also been developed for the analysis of outline data (Lohmann 1983). I discuss both of these approaches below.

2.2.1.C.i Eigenshape and Fourier analyses

Lu (1965) was one of the earliest to recognize that the natural curves of biological forms could be mathematically represented using periodic functions of the Fourier series. Lu applied a harmonic analysis using three-cycled Fourier equations to the study of the human face in frontal and profile views using the midpoint of the distance between the two fronto-zygomatic sutures as a point of origin. Harmonic functions were fit to profile and frontal outline curves divided into sub-intervals by forty points and the coefficients of these functions were compared across groups to assess form difference. The technique received further attention in the field of geology, where it was used to characterize sand grain shape (Ehrlich and Weinberg 1970), and invertebrate paleontology, in which Anstey and Delmet (1973) analyzed fossil bryozoan shape and Kaesler and Waters (1972) described ostracods, for example.

Despite its popularity, researchers were faced with several limitations of conventional Fourier analysis. One problem was that the intervals of the curve being fit all had to be of the same length, in correspondence to the interval of the harmonic series. Additionally, complex shape outlines that curve back on themselves would require multivalued functions, deemed computationally too complex at the time (Lestrel 1989). In response, the parametric approach developed by Kuhl and Giardina (1982) was adopted, called elliptical Fourier analysis. Instead of fitting the original two-dimensional form with Fourier functions, the x and y coordinate values of data points comprising a polygon that approximates the original outline are separately projected against a third variable, time, and it is these two new functions that are fit by Fourier functions (Kuhl and Giardina 1982; Lestrel 1989). The separate harmonics plot as ellipses and sum to the original polygonal approximation. Elliptical Fourier analysis replaced the conventional method on account of its ability to vary division length over an interval and remain single-valued, no matter the complexity of the outline (Ferson *et al.* 1985; Lestrel 1989).

Contemporary with the refinement of Fourier analysis was the introduction of eigenshape analysis, another method of mathematically representing shape outlines. Lohmann (1983) introduced the technique, which utilizes a shape function originally proposed by Zahn and Roskies (1972) as an alternative to radial Fourier analysis (Lohmann 1983; MacLeod 1999). Zahn and Roskies' (1972) shape function $\phi^*(l)$ "represents a shape as the net angular bend at each step around an outline" (Lohmann 1983, p. 668). Shapes are matched using either homologous points on the outline or by mutual rotation to positions of maximum correlation, allowing subsequent comparison of shape functions. An eigenfunction analysis of the correlations between shapes produces a set of orthogonal shape functions, or "eigenshape functions," that are the fewest shapes needed to represent the majority of the variation between shapes (Lohmann 1983). Lohmann (1983) applied this technique to a cross-latitudinal sample of a planktonic foraminifer, for which only two eigenshape functions were required to represent seventy-four percent of the observed shape variation.

Both eigenshape and Fourier analyses were met with criticism from the proponents of landmark-based morphometrics, an already significant community by the mid 1980s. Bookstein and colleagues (1982) claimed that Fourier analysis inadequately described biological form because it lacked the homology underlying landmark-based methods. Additionally, the authors questioned the biological meaning of Fourier coefficients, citing them as uninterpretable. Ehrlich and colleagues (1983) responded by demonstrating that the orientation of the second harmonic function of their analysis of fossil foraminifera remained in a consistent orientation relative to the spiral side keel homologous across shell outlines. Read and Lestrel (1986) also

defended Fourier analysis, citing its utility in cases where the space or boundary between homologous points is of greater biological interest than the points themselves. The authors raised the important point that neither approach—landmark or outline—may be universally superior over the other, but rather the nature of the biological form dictates which is the most appropriate representation. The shape alteration between forms that undergo radial growth is one example of form difference better studied under Fourier analysis presented by Read and Lestrel (1986).

Despite the acknowledgement made by some that each approach had its separate value (e.g., Read and Lestrel 1986), proponents of landmark-based work continued to emphasize both Fourier and eigenshape analyses' problematic inattention to homology (e.g., Bookstein 1991). MacLeod (1999) sought to join the divided camps of landmark- and outline-based researchers by generalizing and extending eigenshape analysis to include both types of data. Besides the landmark used as starting point for the shape function, MacLeod's (1999) extended eigenshape analysis utilized additional landmarks located both on the outline and internal or external to the form to constrain the outline sequence of coordinate points. The minimum number of coordinate points required to accurately represent each segment were determined using a tolerance criterion, allowing the study of open curves as well. This feature of extended eigenshape analysis differentially weights the outline segments based on their complexity. MacLeod (1999) also extended eigenshape analysis to three dimensions, in which paired angles are used to represent the angular directions to succeeding points.

Recently both Fourier and eigenshape analysis have been applied to the symphyseal shape of the mandible in hominoids, a morphology that presents few reliable landmarks along its irregular outline. Daegling and Jungers (2000) approached the symphysis using elliptical Fourier analysis. Cross-sectional contours of mandibular symphyseal shapes taken from CT scans were digitized and characterized by the first fifteen harmonics of the elliptical Fourier series. Within-sex species differences were found only in the gorilla and it was concluded that taxa could be sorted using symphyseal shape. However, a discriminant function test revealed large room for error and the authors cautioned that this approach was still limited.

Sherwood and colleagues (2005) addressed shape variation in the symphyseal shapes of the same group of apes, but added humans and used eigenshape analysis. The first eigenshape was explained as largely representative of the functional adaptation at the midline to counteract masticatory stress. The authors concluded that eigenshape analysis was effective for taxonomic identification of the four species. Results of a discriminant function analysis showed that the eigenshape analysis had a lower error than Daegling and Jungers' (2000) Fourier analysis.

2.2.1.C.ii Geodesic distance analysis

Recently, Joshi and colleagues (2011) introduced a new landmark-free approach to quantifying shape variation entitled 'geodesic distance analysis,' or GDA. GDA was designed specifically for continuous curves that are not easily represented by landmarks. The technique uses continuous angle functions of parameterized curves to represent the boundaries of biological objects, which is similar to Fourier analysis, but diverges in its use of arc lengths to represent the angle function, as opposed to Fourier descriptors. To date this method has only been demonstrated on hadrosaurid dinosaur teeth and pubes and the outline of the foraminifer *Globorotalia truncatulinoides* (Joshi *et al.* 2011).

2.2.1.D Rationale for the geometric morphometric techniques applied in this study

As discussed above, an important critique of popular coordinate-based superimposition and deformation techniques accompanied the introduction of the coordinate-free alternative EDMA (Lele 1991, 1993; Richtsmeier *et al.* 1992, 2002). Specifically, proponents of EDMA fault the arbitrary nature of the loss functions used in superimposition methods. Despite the fact the deformation methods such as FESA and TPS avoid superimposition, there remains an arbitrary element in these approaches as well. Authors such as Lele (1991) and Richtsmeier and colleagues (2002) criticize these two main forms of deformation for their dependence on the functions that map the relative locations of points in the reference to the target—a homology function in the case of FESA and the minimal bending-energy function of TPS. In other words, just as superimpositions change depending on the criterion used, so do deformations based on the interpolation function used.

Richtsmeier and workers (2002) tested each of these methods against one another by comparing analyses of an artificial data set, for which the true changes in form are known. Three types of form change were scrutinized: the shift of two landmarks in an area high in landmark density, the shift of two landmarks in an area low in landmark density, and an unequal shift of all landmarks away from the center of the form. In the first case, GPA yielded an accurate illustration of which landmarks were different between forms, while FESA and TPS depicted accurate change with regard to the two landmarks that had actually moved, but also suggested that nearby landmarks were also shifting. EDMA correctly associated change with the two landmarks that had actually shifted, showing that all the notably different distances shared one of these two landmarks as a common endpoint. For the low-density landmark shift in the second situation, GPA accurately recorded the landmark shifts, and, as in the previous comparison, deformation identified areas of form change in addition to the actual changed landmarks. EDMA was the most accurate, yielding similarly correct results as in the previous comparison. In the final comparison, in which every landmark was shifted out and away from the center of the form to varying degrees, GPA captured the overall shift, but was more accurate with respect to landmarks in high landmark density regions than in low landmark density regions. FESA did not show that all landmarks were moving in the correct direction and also gave conflicting results depending on the different functions employed. EDMA and TPS deformation correctly identified the overall change across areas of both high and low landmark density.

The comparisons performed by Richtsmeier *et al.* (2002) highlight the effect of landmark density on superimposition: the lower the density of landmarks (i.e., the worse the coverage of landmarks for the anatomical region in question), the more pronounced are the effects of the arbitrary functions under criticism. Lawing and Polly (2010) explain that, as a result, in the case of superimposition, an *a priori* model of shape variation for the morphology being studied is required to determine which landmarks are more variable than others. Hence, the practical difference between superimposition and EDMA lies in the ability to detect overall variation in shape versus localized shape variation at individual landmarks, respectively (Lawing and Polly 2010). This difference can be overcome by careful selection of a set of landmarks that provide dense, adequate coverage of the morphology.

Taking these factors into consideration, this study utilizes GPA (Rohlf and Slice 1990) to superimpose a set of landmarks that densely cover the canid craniofacial complex (see below for further description of the landmarks collected). Two factors contributed to the decision to use GPA over EDMA. First, EDMA lacks the powerful tools of visualization that are available for

GPA (Richtsemeier *et al.* 2002; Lawing and Polly 2010), an important consideration for this study, which focuses heavily on qualitative differences in shape change between the wolf and dog breeds. Second, the limited number of studies to date that have examined shape variation in the crania of dogs and wolves all use GPA (e.g., Drake and Klingenberg 2008, 2010; Milenkovic *et al.* 2010; Drake 2011; see above). Therefore, implementation of the same method of shape quantification will facilitate a comparison of results between this study and previous work.

2.2.2 Data collection

A total of seventy three-dimensional landmarks were collected from each wolf and dog cranium. Numbered landmarks are illustrated in dorsal and ventral views of a generalized dog skull in Figure 2.6 and defined in Appendix Three. Originally, a preliminary set of eighty-eight landmarks was designed for data collection, however, assessment of the error associated with each landmark demonstrated that a large subset could not be collected without substantial error. These landmarks included points on the sagittal crest and points posterior to each tooth. In the case of the former, the standard deviation exceeded 2.0 millimeters (mm) along the anteroposterior (y) axis, and for the latter, the standard deviation exceeded 1.5 mm along the mediolateral (x) axis. The error assessment technique implemented in this study and the error associated with the landmarks used in shape analyses are described below in Section 2.2.4.B.

Crania were positioned and stabilized with plasticine clay such that landmarks could be collected from two orientations: dorsal (thirty-six landmarks) and ventral (thirty-four landmarks). Given the large amount of variation in facial length, width, and breadth, landmarks were selected for maximal coverage of this region, adding additional landmarks along the midline of the nasal and frontal bones to the set established by Drake (2004, 2011; Drake and Klingenberg 2008, 2010).

The two most commonly employed three-dimensional data capturing techniques include digitizers and laser scanners. The three-dimensional coordinates of each landmark are collected with a stylus from the actual surface of the specimen in the case of the former, while the latter generates a computer model from which landmarks are collected on-screen. Based on repeated trials of data collection from human crania, Sholts and colleagues (2011) have demonstrated that coordinate measurements taken with a digitizer have lower overall standard deviations than those taken from a scanner-generated model (0.79 and 1.05 mm, respectively).

A three-dimensional digitizer was chosen for this study based on its greater precision and the advantage of being able to locate landmarks using both tactile and visual means (Sholts *et al.* 2011). Three-dimensional landmark coordinates were collected using a MicroScribe G2X digitizer, which has a demonstrated accuracy of up to 0.38 mm (eMicroScribe, Amherst, Virginia). Each cranium was digitized twice so as to have a back-up in the case that an error was made during the digitization process (e.g., a skipped landmark or misplaced reference landmark for joining the dorsal and ventral datasets—see below).

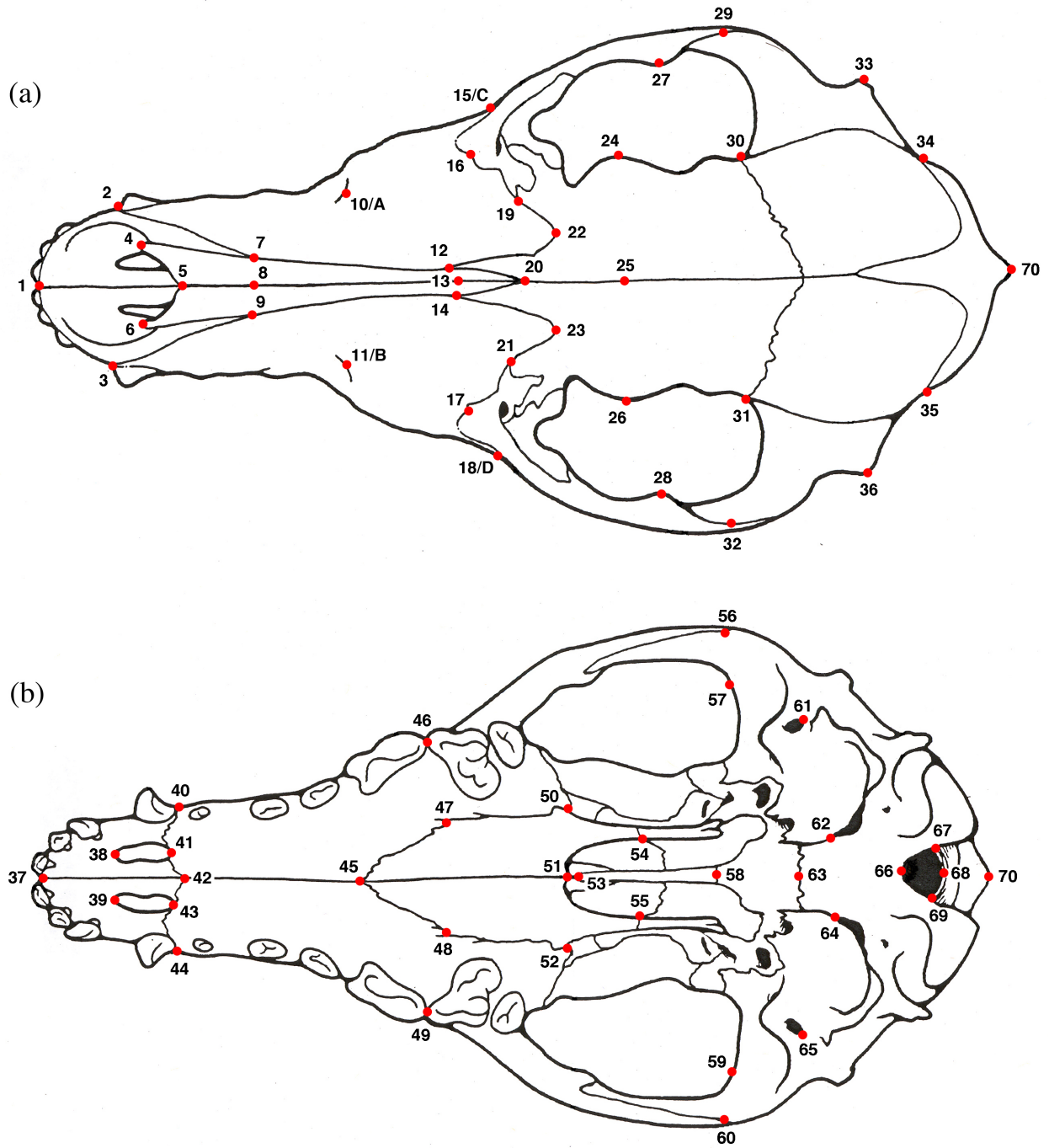


Figure 2.6 Seventy landmarks collected from (a) dorsal and (b) ventral cranial orientations. Note the four reference landmarks (A–D) utilized for joining the dorsal and ventral datasets.

2.2.3 Data formatting

Dorsal and ventral datasets were joined to create one comprehensive dataset for the entire cranium using the least squares fitting program DVLR (Raaum 2006), which required the collection of four reference points in both orientations (see Figure 2.6 and Appendix Three).

Missing or undetectable landmarks (due to damage, missing teeth, or obliterated sutures) precluded the use of crania only in cases where these points fell on the midline or comprised a complete bilateral pair. In cases where only one of two points comprising a bilateral pair could not be collected, the missing data was overcome by reflecting the coordinate of its antimere across the midline. Reflections were carried out in R using a geometric function designed by Julien Claude (2008).

2.2.4 Measurement error

2.2.4.A Error assessment in geometric morphometric studies

Just as the precision of linear measurements has been a central issue in traditional morphometrics, so has the precision of landmark identification in geometric morphometrics. The same sources of variation need to be taken into account (i.e., inter- and intra-observer), however, the nature of landmarks, specifically which class they belong to, create an additional challenge for error assessment. Because Type I landmarks are defined using discrete anatomy while Type III landmarks rely on extremes, a typical configuration of landmarks will include some points that can be more precisely identified than others. Furthermore, Sholts *et al.* (2011) have shown that precision for landmark types varies between digitization techniques: three-dimensional digitizers yield the most precise data for Type I landmarks, while computer models created by three-dimensional laser scanners are better for Type III landmarks. von Cramon-Taubedal and colleagues (2007) recently reviewed three commonly used error assessment techniques and arrived at a composite method that allows for landmark-by-landmark assessment and applies to all types of landmarks. I summarize the three techniques reviewed and the composite technique developed by the authors below.

The first approach examined by von Cramon-Taubedal *et al.* (2007) uses a registration method to superimpose trial configurations of landmarks. O'Higgins and Jones (1998) submitted five repeat sets of coordinate data from two test specimens to GPA and subsequent principal component analysis to gauge their precision error relative to the variability of their total sample of 49 mangabey faces. Lockwood and colleagues (2002) used GPA in a similar fashion to assess intra-observer error across three repeated trials of a sub-sample of the humans and chimpanzees observed in their study of temporal bone morphology. von Cramon-Taubedal and workers (2007) criticized the registration method because it randomly distributes landmark error across the configuration in an effort to minimize the overall error. In other words, residual variation around imprecise landmarks is lowered while the variation around very precise landmarks is raised, resulting in a phenomenon called the "Pinocchio effect," (Chapman 1990). von Cramon-Taubedal *et al.* (2007) provided a clear example of the Pinocchio effect in the form of a case study in which simple foam cubes were digitized repeatedly, changing only the position of one landmark between trials. Registration using GPA correctly depicted variation around the one changed landmark, however it also showed variation around the other landmarks, for which no

change had actually occurred. The case study demonstrated that one error-prone landmark affects the entire configuration, making error assessments based on the entire configuration misleading.

The second approach reviewed was utilized by Singleton (2002) in her study of cranial shape variation in the Old World monkey tribe Papionini. This method uses the Euclidean distance between a 3D landmark and the centroid of the specimen, a distance called the centroid radius. Landmark deviations were calculated relative to the observer landmark mean for each of the three observers, allowing for landmark-by-landmark assessment of observer precision. According to von Cramon-Taubedal and colleagues (2007), the problems with this method lie in the centroid radius, which is appropriate for assessing error for landmarks that are collinear with the original centroid vector but underestimates error in any other orientation. Additionally, error is dependent upon the absolute distance between individual landmarks and the centroid, resulting in high relative error for landmarks that lie close to the centroid and vice versa.

The last method, put forward by Corner and colleagues (1992) avoids the problems associated with registration by employing repeated digitizations while keeping the digitizer and specimen in a fixed orientation. Standard deviations of landmark coordinates are calculated for the x , y , and z values, enabling detection of axis-specific patterns of error. von Cramon-Taubedal and workers (2007) criticized this method for limiting the digitization process and introduced an alternative that incorporates components of this method and the registration method, allowing freedom of movement of the specimen between trials. The revised method requires the selection of three intrinsically low-variance reference landmarks from the total configuration. The measurement variance due to inter- and intra-observer effects is calculated for the reference landmarks following the methods of Corner *et al.* (1992), from which a single variance value is chosen to represent the error associated with all three landmarks. Next, non-reference landmarks can be chosen and digitized multiple times with multiple observers and the configurations from the repeat trials are superimposed using only the three reference landmarks. Measurement variance can be assessed on an individual landmark basis by calculating the mean landmark standard deviation from GPA (von Cramon-Taubedal *et al.* 2007).

The compromise suggested by von Cramon-Taubedal and colleagues (2007) addresses many of the problems of earlier error assessment approaches, but more importantly it provides a model for an important beginning step in any morphometrics study. These techniques allow for identification of not only landmarks with high associated error, but also patterns of error that might reveal subtle problems in the data collection process. The majority of morphometrics papers do not include an assessment of the precision of the landmarks chosen or an exploration of measurement-biasing factors. The information garnered from error assessment can be used to plan subsequent data collection, as Corner *et al.* (1992) pointed out, suggesting that problematic landmarks be digitized an additional two to three times.

Error assessment in non-landmark-based studies is a more complicated issue that can be at least partially addressed using von Cramon-Taubedal and colleagues' (2007) approach for landmarks incorporated into outline data to bound homologous segments following MacLeod's (1999) extended eigenshape analysis. The development of precision analysis for outlines must take into account the nature of the outline acquisition, which has varied considerably across studies, from computer-based recognition of pixel brightness in digital images (Ferson *et al.* 1985) to digitized putty molds (Sherwood *et al.* 2005). Currently this is an area that requires further attention.

2.2.4.B Error assessment for canid crania digitization

Maintaining a fixed orientation for both the digitizer and specimen during error assessment presented no difficulty, therefore the method proposed by Corner *et al.* (1992) was adopted for this study. A single male gray wolf specimen not included in the actual dataset was digitized twenty times, first in dorsal orientation and then in ventral orientation, without moving the specimen or MicroScribe between trials. The average standard deviation across all axes and all landmarks was 0.442 mm. The mediolateral (x) axis had the highest average standard deviation across all landmarks (0.585 mm), the anteroposterior axis (y) was intermediate (0.447 mm), and the dorsoventral (z) axis had the lowest (0.294 mm). Standard deviations for coordinate values for the three axes for all seventy landmarks from the gray wolf trials are presented in Appendix Four.

2.2.5 MorphoJ analyses

GPA and all subsequent statistical analyses were carried out using the integrated geometric morphometric software package MorphoJ (Klingenberg 2011). First, a separate superimposition was performed for each taxon, from which taxon-specific covariance matrices were generated. Next, the major axes of shape variation for the gray wolf and domestic dog were identified in principal component analyses based on the decomposition of each taxon-specific covariance matrix. Two types of graphical output produced by MorphoJ were used to compare variation between the two species: scatter plots of principal component scores and shape deformations associated with principal components. For the latter, shape change was visualized as the difference between extreme shapes along the principal component axis using the relative magnitude and direction of vectors originating from landmarks to illustrate change from the mean shape.

Next, specific comparisons were made between the gray wolf and the fifteen focus breeds. Separate superimpositions and covariance matrices were performed and generated, respectively, for the fifteen breeds. Pairwise discriminant function analyses were then executed between the gray wolf and each breed, in order to visualize the shape differences relative to the ancestral form that characterize each breed, and also between breeds, in order to assess the similarity of breed forms. Shape differences were visualized similarly to principal components, but instead of contrasting vector graphs of extreme shapes along a principal component axis, graphs of the mean gray wolf shape were contrasted graphs of mean breed shapes.

Shape differences were quantified using two different statistics output by the discriminant function analyses: Procrustes distance, the length of the arc representing the shortest distance between two “pre-shapes” across the surface of a hypersphere prior to superimposition (Zelditch *et al.* 2004), and Mahalanobis distance. Statistically significant Procrustes distances were identified using both a parametric T-test and a permutation test. In the latter test, for each pairwise comparison, the two groups were resampled without replacement from a combined dataset of both groups and the Procrustes distance was calculated between the two resampled groups. This calculation was repeated for 1,000 permutation sets to determine the probability that the observed distances could have arisen from a random sampling of the combined dataset (Zelditch *et al.* 2004).

Chapter 3: Craniofacial Shape Differences between Domestic Dog Breeds and the Gray Wolf

3.1 Introduction

This chapter addresses whether there are significant distinctions in the patterns of shape differences between the crania of various brachycephalic breeds and the ancestral wolf cranium, and whether such distinctions in patterns of shape differences correspond to genetic relationships among breeds. Geometric morphometric analysis of craniofacial shape was utilized to perform side-by-side comparisons of the shape deformation required to transform a wolf cranium into the crania of various dog breeds. These comparisons form the basis for testing *Hypothesis 1*—that distinct craniofacial forms corresponding to specific breeds or groups of breeds exist within the larger brachycephalic category. Similarities or differences between brachycephalic breeds were next evaluated in the context of the breed phylogeny constructed by vonHoldt *et al.* (2010) to test *Hypothesis 2*—that the toy dog and Mastiff-like dog groups represent separate, distinct brachycephalic forms. A description of the principal components of variation for the wolf and dog samples is presented first.

3.2 Principal component analyses

Here I describe and discuss the results of principal component analyses of the shape variation captured by the Procrustes superimposition of the landmark data collected for both the wolf and the domestic dog. I focus on patterns of variation between the two taxa and between breeds (principal component scores are listed in Table 3.1).

3.2.1 *Canis lupus*

The first principal component (PC) of shape variation in the cranium of *C. lupus* explains 12.79% of the total variance and represents differences in mediolateral width at the zygomatic arches and differences in the angles of the rostrum and the occipital bone, relative to the ventral surface of the cranium (Figures 3.1 and 3.2). At one end of the PC1 axis are crania with wider, more rostrally positioned zygomatic arches and more dorsally angled rostra and occipitals. In these crania, the face is more concave in lateral view largely due to extension of the premaxillae caudally along the premaxilla-nasal suture and extension of the frontals rostrally between the nasals and maxillae. This phenomenon is combined with nasals that are shortened rostrally. The caudal surface of the occipital is also positioned such that the angle between this surface and the ventral base of the cranium is less obtuse in lateral view. In other words, seen in profile, these crania angle dorsally at the rostral and caudal extremes. Crania shaped toward the other extreme lie at the opposite end of the PC1 axis: the ventral surface is a straighter angle, the nasals are less concave and the zygomatic arches do not extend as far laterally.

PC2 accounts for nearly as much variation (10.18%) and represents differences in the nasal region very similar to those seen in PC1, but without any other coordinated variation in the rest of the cranium (Figures 3.1 and 3.2). In PC1, the extension of the premaxillae caudally and frontals rostrally was coupled with rostral shortening of the nasals and differences in the width of

Table 3.1 Principal component (PC) scores

Taxa	% Variance Explained				
	PC1	PC2	PC3	PC4	PCs 1-4:
<i>Canis lupus</i>	12.79	10.18	7.87	6.67	37.51
Taxa	PC1	PC2	PC3	PCs 1-3:	
<i>C. familiaris</i>	75.64	6.36	4.11	86.11	
Breed	PC1	PC2	PC3	PCs 1-3:	
Borzoï	32.17	11.93	8.7	52.8	
Boxer	21.83	11.76	8.32	41.91	
Bull Terrier	60.93	11.88	5.68	78.49	
Bulldog	52.91	8.74	6.67	68.32	
Chihuahua	53.19	14.44	6.81	74.44	
Chow Chow	29.72	10.79	9.68	50.19	
Collie	39.06	9.42	6.8	55.28	
French Bulldog	18.78	14.48	13.14	46.4	
German Shepherd Dog	18.81	13.63	10.86	43.3	
Great Dane	28.41	12.15	9.37	49.93	
Greyhound	28.1	11.03	9.78	48.91	
Irish Wolfhound	18.79	14.79	9.8	43.38	
Newfoundland	24.54	17.44	11.36	53.34	
Pekingese	36.78	19.97	9.69	66.44	
Pug	48.83	12.49	8.03	69.35	

the cranium and the angle of the ventral surface. Variation in the cranium in PC2 is isolated to the face. At one extreme of the PC2 axis are crania in which the caudal extent of the premaxillae and rostral extent of the frontals come close to meeting midway along the nasals. At the other extreme, there is greater separation between these bones along the rostrocaudal axis, with the maxillae bordering the nasals laterally for most of their length. Unlike the trend seen in PC1, these differences are not accompanied by substantial differences in the length or angle of the nasals.

The third principal component explains 7.87% of the total shape variation and, like PCs 1 and 2, represents differences primarily in the facial region (Figures 3.1 and 3.2). Here, the caudal extent of the premaxillae varies in the same direction as the rostral extent of the frontals. In crania at one end of the PC3 axis, the caudal extent of the premaxillae is dramatically shifted rostrally. So is the rostral extent of the frontals, but to a lesser degree. The slope of the frontals is decreased with this rostral extension, producing a flatter forehead. The nasals are also slightly elongated rostrally and these crania are narrower overall. At the opposite end of the PC3 axis, the reverse pattern produces wider crania with a slightly shorter rostrum and more domed forehead.

PC4 accounts for only 6.67% of the total variation and again represents isolated differences in the caudal extent of the premaxillae, as well as in the position of the junction of

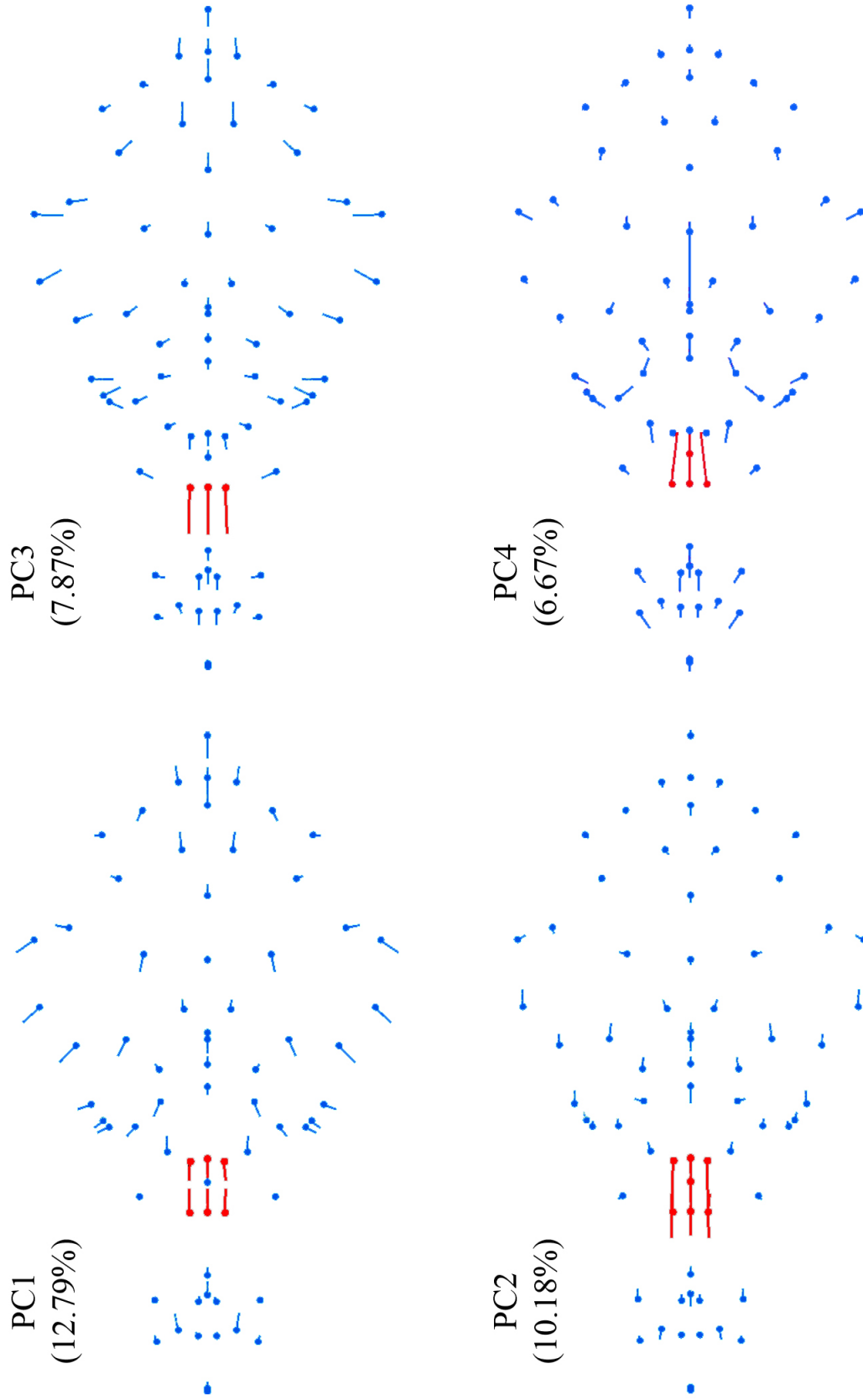


Figure 3.1 Dorsal view of the shape deformations associated with the first four principal components of variation in the gray wolf cranium. Vectors on landmarks indicate deformation relative to the mean shape in one direction along the principal component axis. Specific regions of the cranium exhibiting variation of note are highlighted in red (see text for explanation).

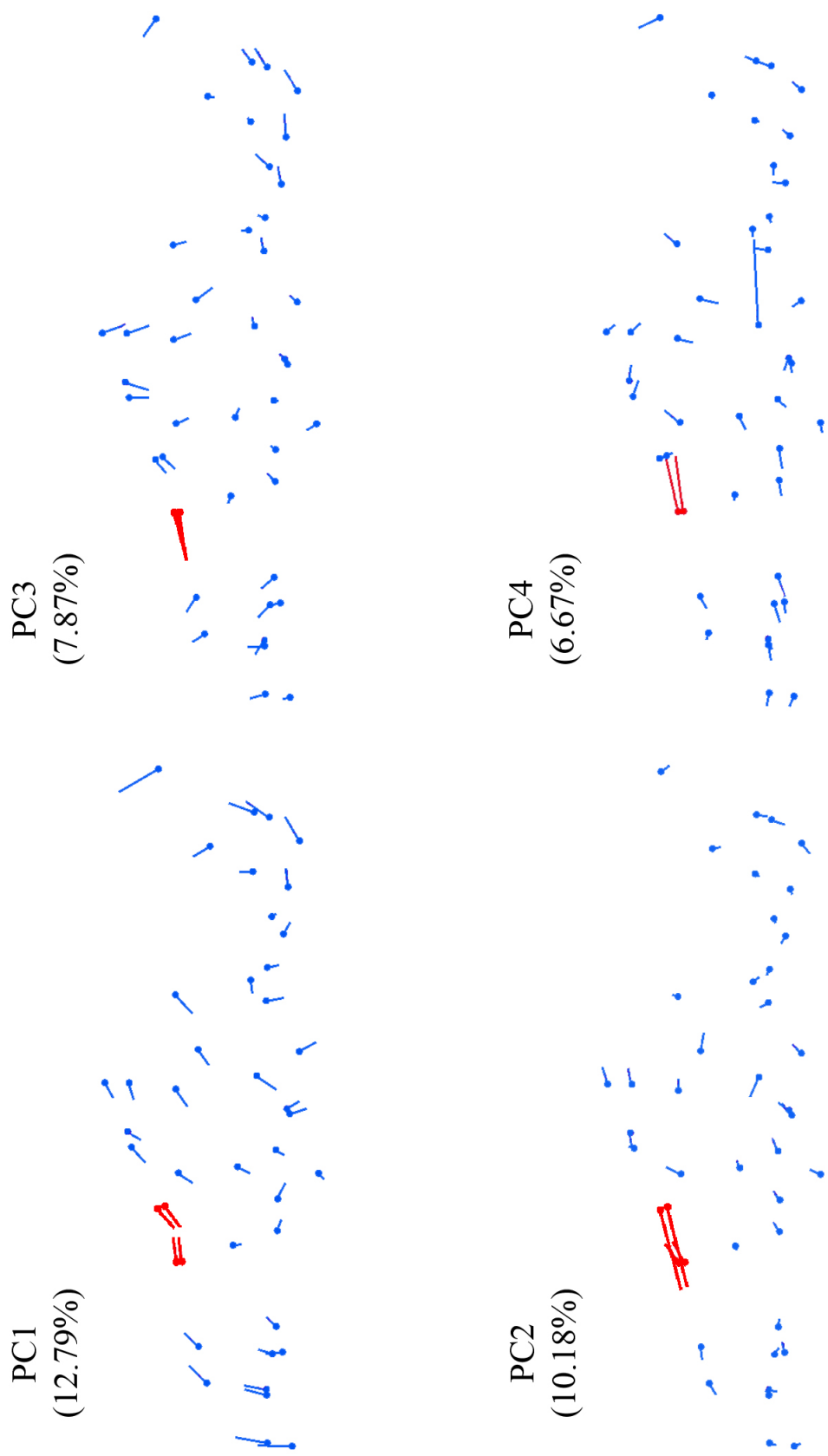


Figure 3.2 Lateral view of the shape deformations associated with the first four principal components of variation in the gray wolf cranium. Vectors on landmarks indicate deformation relative to the mean shape in one direction along the principal component axis. Specific regions of the cranium exhibiting variation of note are highlighted in red (see text for explanation).

the presphenoid and vomer along the midline of the ventral surface of the cranium (Figures 3.1 and 3.2). At one extreme, crania have dramatically caudally extended premaxillae, coupled with a caudal shift of the caudal extent of the vomer. For this PC, variation in the extent of the caudal premaxillae is independent of the position of the rostral frontals, which remain relatively static.

Combined, PCs 1 through 4 account for 37.51% of the total shape variation. These first four principal components of shape variation for the gray wolf cranium primarily describe the relationship between the bones of the face—specifically, their contribution to its length and angle along the rostrocaudal axis. Although each PC describes differences in the same bones, the independence of these bones relative to one another in the described patterns sets each PC apart. In PC1, there is coordinated variation in the contribution to the bony face of the premaxillae, nasals, and frontals. This variation is also associated with differences in the width of the zygomatic arches and the angle of the ventral cranial surface. Similarly, in PC3, variation in the bones of the face is associated with cranial width. PCs 2 and 4 represent variation isolated only in the face (with the exception of movement of the vomer-presphenoid contact in PC4), with varying involvement of the premaxillae, nasal, and frontal bones.

In other words, the majority of variation in the gray wolf cranium is localized in the degree to which the premaxillae and frontals extend along the lateral sides of the nasals. That these crania exhibit four PCs accounting for similar portions of the total variation (i.e., 12.79, 10.18, 7.87, and 6.67) suggests that although variation in this dimension may account for almost 40% of the total variation overall, this variation can become manifest in several ways—e.g., coupled with overall variation in width and concavity, but also independent of any other substantial variation in cranial shape.

It is also worth noting that none of the first four PCs represent sexually dimorphic variation. Plots of the data along the first two PC axes do not reveal any indication of separation by sex (Figure 3.3). Furthermore, the shape of the scatter of data in each plot is fairly uniform, without the presence of any obvious outliers.

3.2.2 *Canis familiaris*

In contrast to PC1 for the sample of gray wolves, PC1 for shape variation in the pooled sample of domestic dogs accounts for a much larger portion of the total variation—roughly three-quarters (75.64%). This PC describes variation in the overall dimensions of the cranium along a dolicocephalic-brachycephalic continuum: at one extreme are crania with wider, shorter faces and taller, more domed braincases. At the other are crania with longer, narrower faces and more flat braincases, exemplified by the Pug and Borzoi, respectively (Figure 3.4). A plot of all dogs along the PC1 axis, in which breeds are color-coded to follow the group designations used by vonHoldt and colleagues (2010), illustrates the separation of traditionally recognized dolicocephalic breeds at one end and brachycephalic breeds at the other (Figure 3.5).

The dolicocephalic end of the axis includes sight hounds and herding dogs, such as the long-faced Borzoi, Collie, and Greyhound. At the brachycephalic end are many of the toy dogs, including the Pekingese and Pug. Also at this extreme are some members of the Mastiff-like dog group, which includes the brachycephalic Boxer, Bulldog, Bull Terrier, and French Bulldog. However, this group also includes the Mastiff, Great Dane, and St. Bernard. These fall closer to the center of the axis among the other mesaticephalic breeds. The shape variation described in

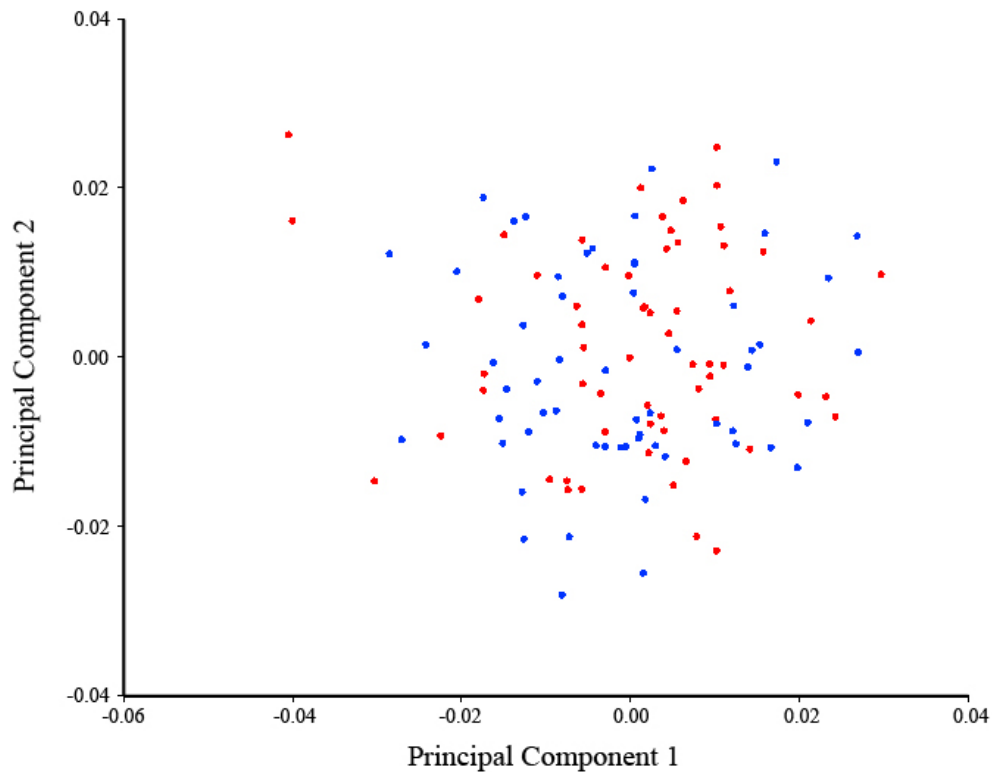


Figure 3.3 Plot of gray wolf specimens along principal component axes 1 and 2. Females are depicted in red and males are depicted in blue.

PC1 and the separation of breeds along this axis are consistent with the findings of Drake and Klingenberg (2010).

Relative to mesaticephalic crania at the midpoint of the PC1 axis, brachycephalic crania display faces that are shorter relative to the braincase at both ends of the rostrum (Figure 3.4). In other words, the maxillae are positioned more rostrally relative to their attachment to the zygomatics and frontals, and the premaxillae and nasals are reduced rostrally. The premaxillae, maxillae, and nasals are all reduced in rostrocaudal length. However, this reduction in length is accompanied by a mediolateral expansion. The maxillae are also extended higher dorsally and the caudal extent of the nasals is raised rostrocaudally, creating a concave, dished face in lateral view. The frontals are also more prominent, particularly at the stop.

The second PC accounts for considerably less of the total variation (6.36%) and describes shape differences largely in the height and width of the face, independent of shape change in the braincase (Figure 3.6). Here, crania with dorsally raised faces and narrower, more tapered rostra are contrasted with crania that exhibit a wider, flatter snout. There is very little separation between breeds along this axis at the dolichocephalic end of the PC1 axis. Instead, PC2 separates toy dogs from Mastiff-like and working dogs towards the brachycephalic end of PC1. PC2 highlights the greater variation within brachycephalic breeds compared to dolichocephalic breeds. Whereas the sight and herding hounds vary little in the width and height of their long

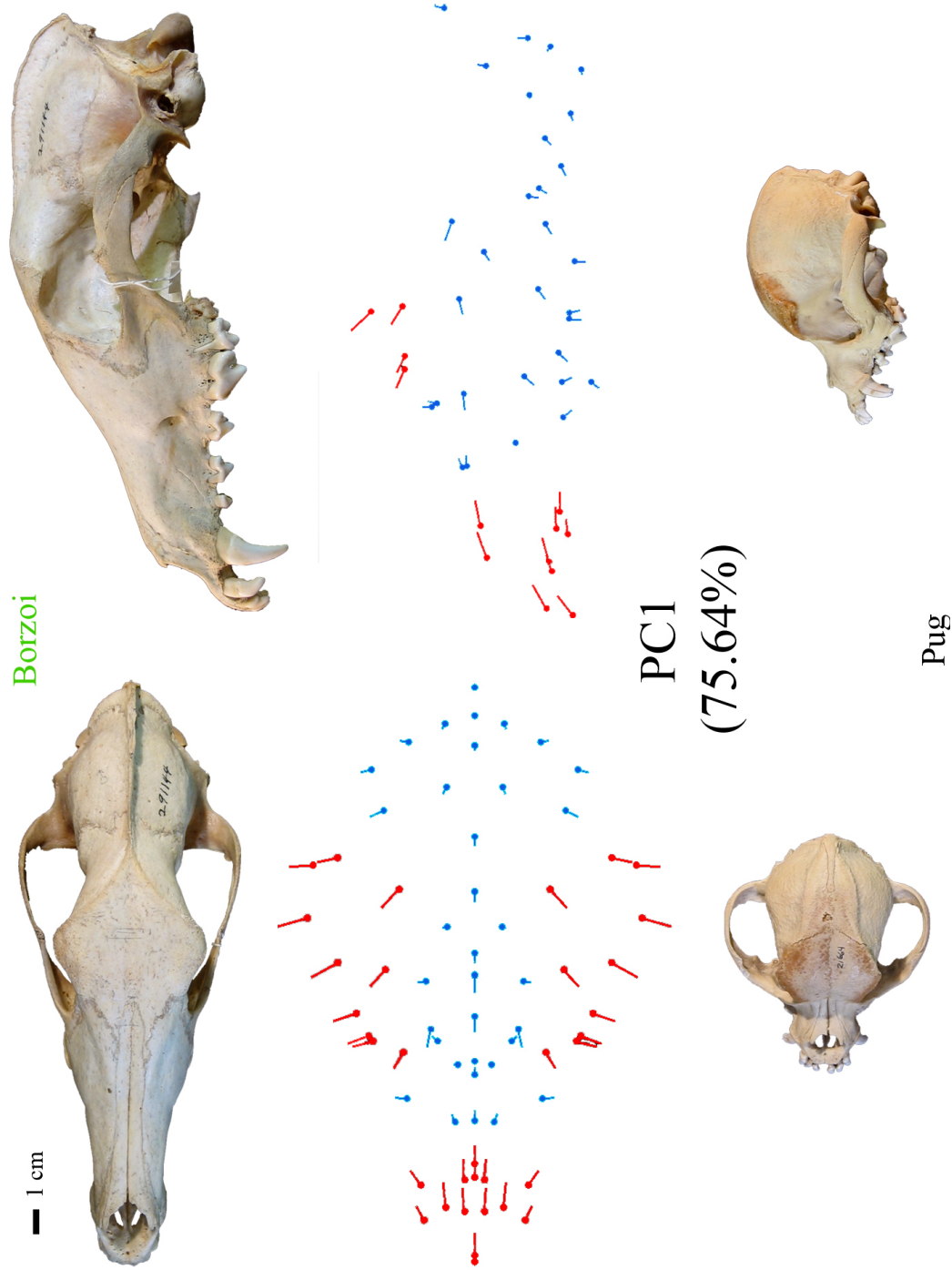


Figure 3.4 Shape deformations associated with the first principal component of variation in the domestic dog cranium, as exemplified by the dolichocephalic (green) Borzoi and the toy dog brachycephalic (black) Pug. Vectors on landmarks indicate deformation relative to the mean shape in one direction along the principal component axis. Specific regions of the cranium exhibiting variation of note are highlighted in red (see text for explanation).

faces, these are important dimensions of distinction between the different types of short-faced dogs.

In the toy dog crania occupying one end of PC2, the nasals and frontals are positioned more rostro-dorsally, but in contrast to PC1, this phenomenon occurs closer to the beginning of the rostrum so that the concavity of the face is more rostral. The caudal extent of the premaxillae and the rostral extent of the frontals are reduced rostrally as part of this trend.

The rostrum is narrower primarily due to narrower premaxillae and maxillae, with very little difference in the width of the nasals. This feature suggests that PC2 is largely driven by the extreme morphology of the Chihuahuas included in the sample. Compared to Mastiff-like dogs, the rostra of Chihuahuas are much narrower relative to the width of the braincase, and although the Chihuahua falls on the brachycephalic end of the PC1 axis, this feature is not as extreme for the breed compared to the other toy dogs and does not involve as much concave dishing of the face at the nasals (Figure 3.6).

PC3 accounts for only 4.11% of the total shape variation and represents variation in the dorsoventral angle of the rostrum relative to the braincase. As in the case of PC2, shape differences described by this PC are localized to the rostrum and can be attributed to the large effect of one extreme breed morphology, the Bull Terrier. This breed is characterized by an especially ventrally angled snout, and Nussbaumer (1982) and Fondon and Garner (2004) have described the exaggeration of this trait over the last several decades of breeding. Examination of the scatterplot for this PC axis reveals very little scatter of data along the axis, with the exception of a subset of the Mastiff-like dogs (the Bull Terriers) that drive the trend. Opposite the Bull Terriers are several brachycephalic toy dogs for which rostral shortening also includes slight dorsal angling.

Compared to the PC analysis performed by Drake and Klingenberg (2010), there is an inconsistency between our second and third PCs: their PC2 contrasts long crania that have lower-positioned braincases with broader crania that have braincases positioned above the rostrum, and their PC3 matches large-faced crania against crania that have a relatively larger braincase. These inconsistencies are most likely related to the sample composition of the two studies. The eighteen Chihuahuas and twenty-five Bull Terriers in my study may outnumber those measured by Drake and Klingenberg (2010), driving the trends in shape within the total sample that produce PCs 2 and 3, respectively. Additionally, differences in the variation detected between the two studies can also be attributed to differences in the numbers of landmarks collected (70 in my study compared to their 50) and their location (I was not confident in placing landmarks on the dorsal surface at sutures obliterated by the presence of a sagittal crest and did not use such landmarks, for example). Combined, PCs 1 through 3 account for 86.11% of the total variation, which is higher than the 71.8% reported by Drake and Klingenberg (2010).

3.2.3 Comparison of *C. lupus* and *C. familiaris*

Most of the variation in the cranium of the gray wolf described by PCA occurs in the face, particularly the relative contributions of the premaxillae, nasals, and frontals (Figures 3.1 and 3.2). Although this does not translate into variation in the length or width of the face relative to the braincase, or variation in the angle or height of the face, it is worth noting that the same bones exhibit the greatest variation in domestic dogs. Next, I describe the PCs of shape variation for individual focus breeds, grouped by skull type (PC1s are illustrated in Figures 3.7-3.14 and

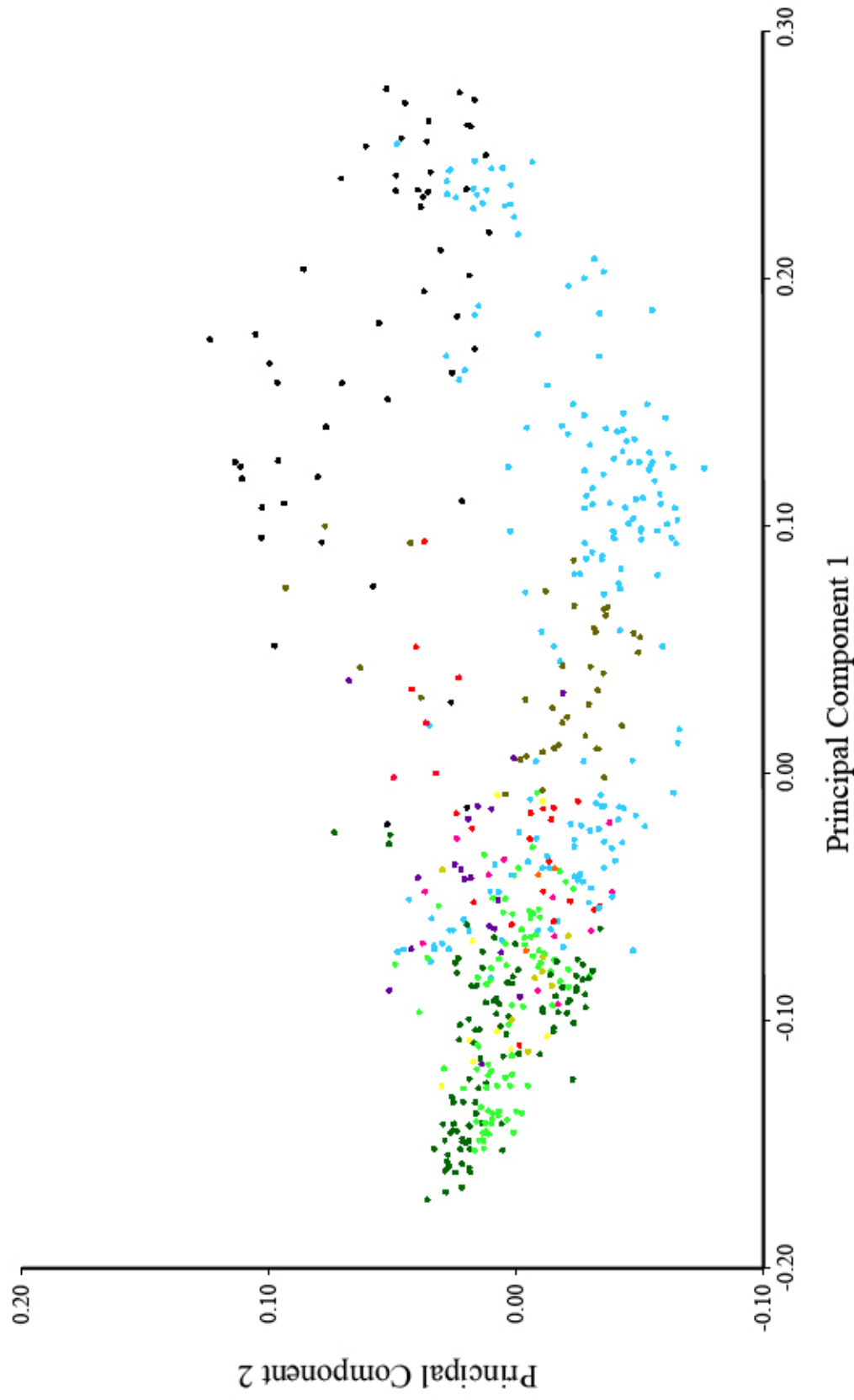


Figure 3.5 Plot of domestic dog specimens along principal component axes 1 and 2. Breeds are color-coded following the color scheme implemented by vonHoldt *et al.* (2010), wherein dark brown = ancient breeds; yellow= Spitz breeds; black = toy dogs; red = Spaniels; pink = scent hounds; light brown = working dogs; light blue = Mastiff-like dogs; purple = small terriers; orange = retrievers; light green = herding dogs; and dark green = sight hounds.

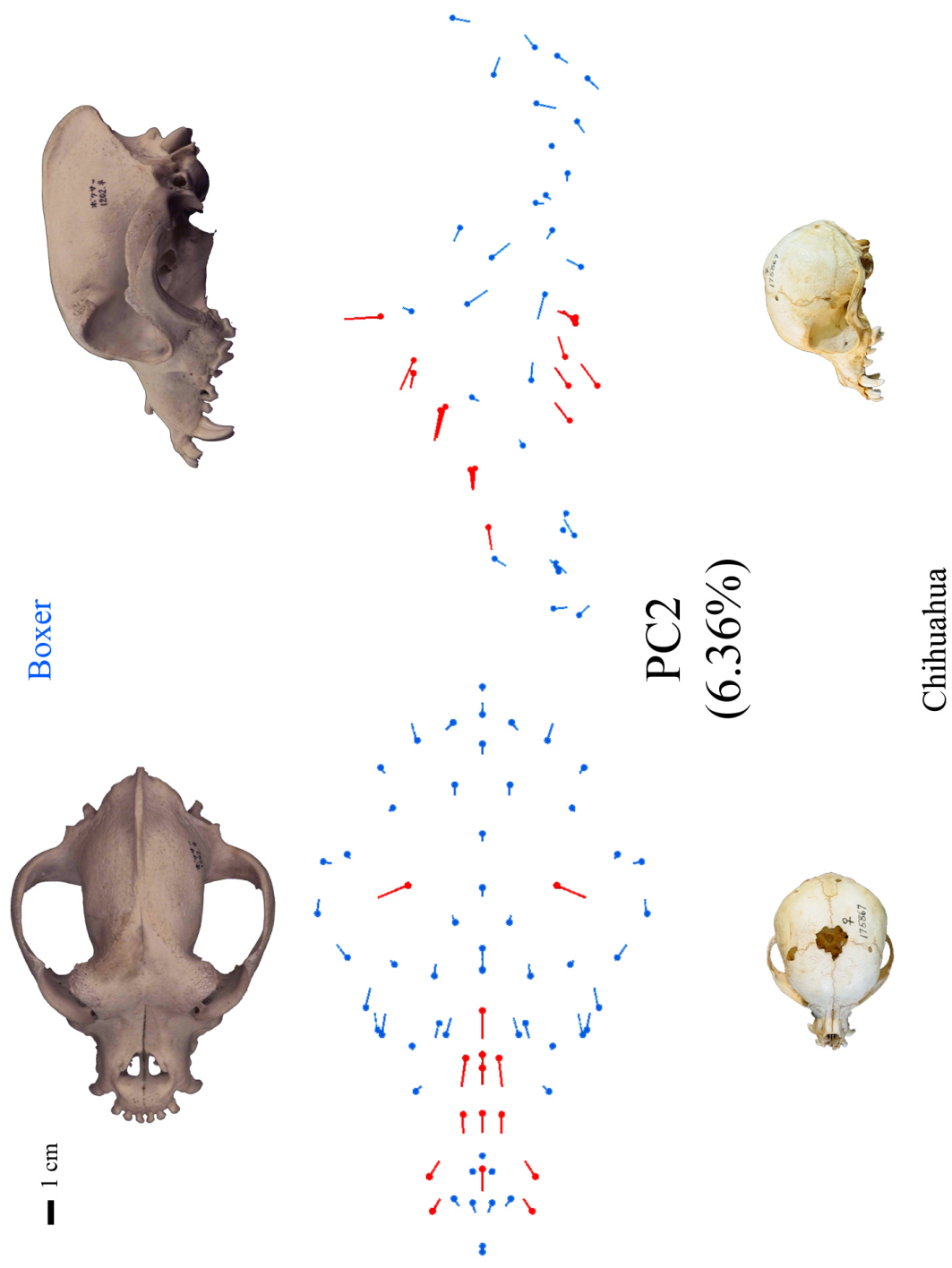


Figure 3.6 Shape deformations associated with the second principal component of variation in the domestic dog cranium, as exemplified by the Mastiff-like brachycephalic (blue) Boxer and the toy dog brachycephalic (black) Pug. Vectors on landmarks indicate deformation relative to the mean shape in one direction along the principal component axis. Specific regions of the cranium exhibiting variation of note are highlighted in red

PC2s are illustrated in Figures A.1-A.8 in Appendix Five). No breed exhibits PCs identical to those seen in the wolf. However, for the most part, the greatest amount of variation exists in the face and involves these same bones.

3.2.4 Dolichocephalic breeds

The Borzoi, Collie, and Greyhound share first PCs that include substantial variation in the width of the cranium, accounting for 32.17%, 39.06%, and 28.1% of their total variation, respectively (Figures 3.7 and 3.8). Width differences are displayed in the mediolateral projection of the zygomatic arches and their attachment to the maxillae, whereas the width of the rostrum and braincase remains relatively static. Wide Borzoi and Collie crania also exhibit rostrally shortened nasals, but this feature is compounded by rostral extension of the frontal bones in the Greyhound. In all three breeds, increased width at the zygomatic arches is also associated with a more dorsally angled rostrum.

3.2.5 Mesaticephalic breeds

The Chow Chow and Newfoundland exhibit similar PC1s, accounting for 29.72% and 24.54% of their total variation, respectively (Figures 3.9 and 3.10). In both breeds, PC1 describes a relationship between cranial width and the contribution of the premaxillae and frontals to the face: at one end of the axis are wide crania in which the caudal extent of the premaxillae and the rostral extent of the frontals are positioned more caudally and the rostral nasals are reduced, collectively producing a shorter rostrum with a dorso-caudally shifted forehead. Great Danes and Irish Wolfhounds display a similar rostral shift in the frontals in wide crania in their first PC (28.41%, 18.79%, respectively). However, the associated differences of the nasals and premaxillae and subsequently short rostrum observed in the Chow Chow and Newfoundland are absent.

The German Shepherd Dog presents a unique PC1 (18.81%) in which variation is almost completely confined to the rostral extent of the frontals. At one extreme are slightly narrow and elongated crania with dramatically rostral frontal bones. At the other, the opposite is seen, with frontal bones barely extending rostrally past the caudal extent of the nasals.

3.2.6 Brachycephalic breeds

Short-faced breeds from the toy and Mastiff-like dog groups exhibit the greatest similarity between PCs of shape variation. PC1 describes rostro-caudal length of the nasals and premaxillae, as well as the angle of the nasals and frontals in the Boxer (21.83% of the variation explained), Bulldog (52.91%), Chihuahua (53.19%), Pekingese (36.78%), and Pug (48.83%) (Figures 3.11 and 3.12). Crania with shorter, more steeply angled faces are also wider at the zygomatic arches in these breeds. Short rostra are achieved by rostral reduction of the nasals and rostrocaudal shortening of the premaxillae. In these crania, the rostral portion of the frontals is positioned more rostro-dorsally to bring the angle of the face even closer to 90 degrees. Similarity across lower PCs is not exhibited in short-faced dogs, although several breeds vary in

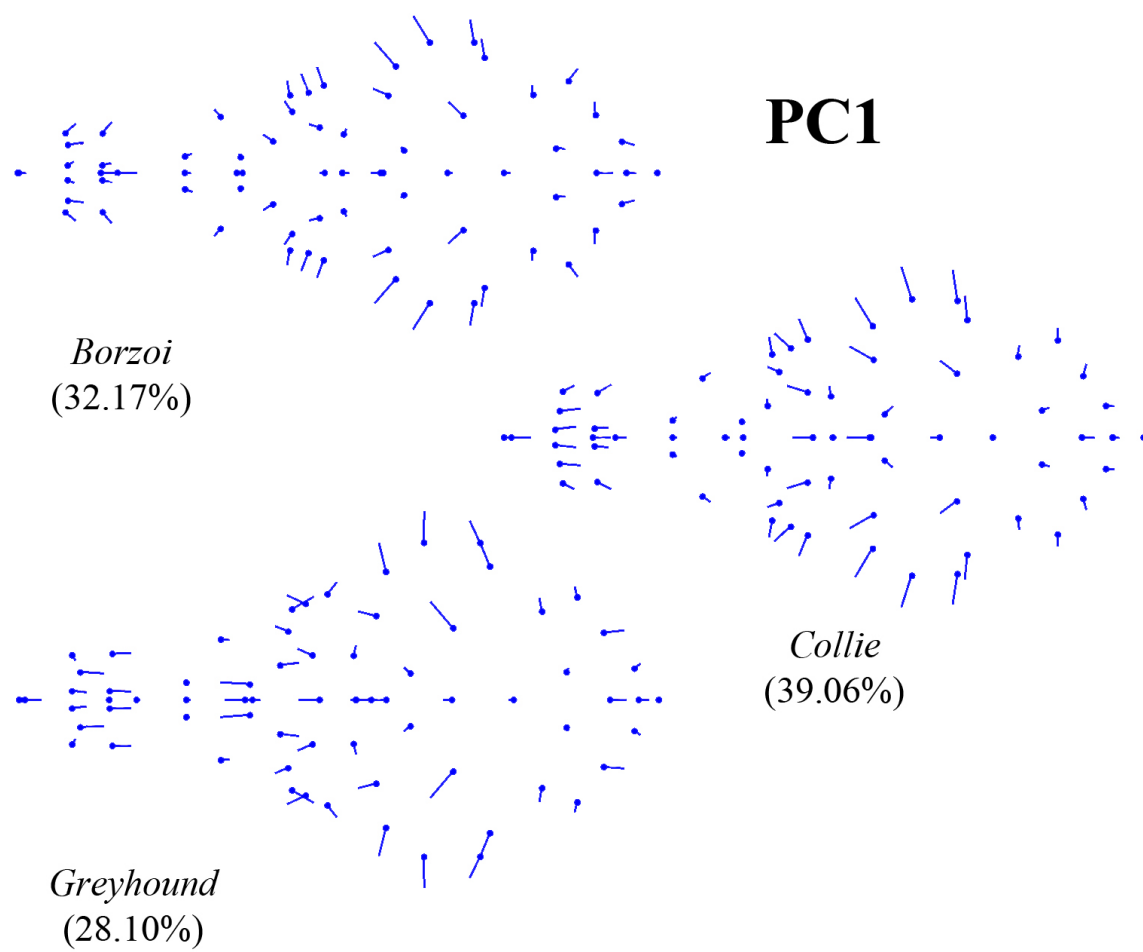


Figure 3.7 Dorsal view of the shape deformations associated with the first principal component of variation in dolichocephalic breed crania. Vectors on landmarks indicate deformation relative to the mean shape in one direction along the principal component axis.

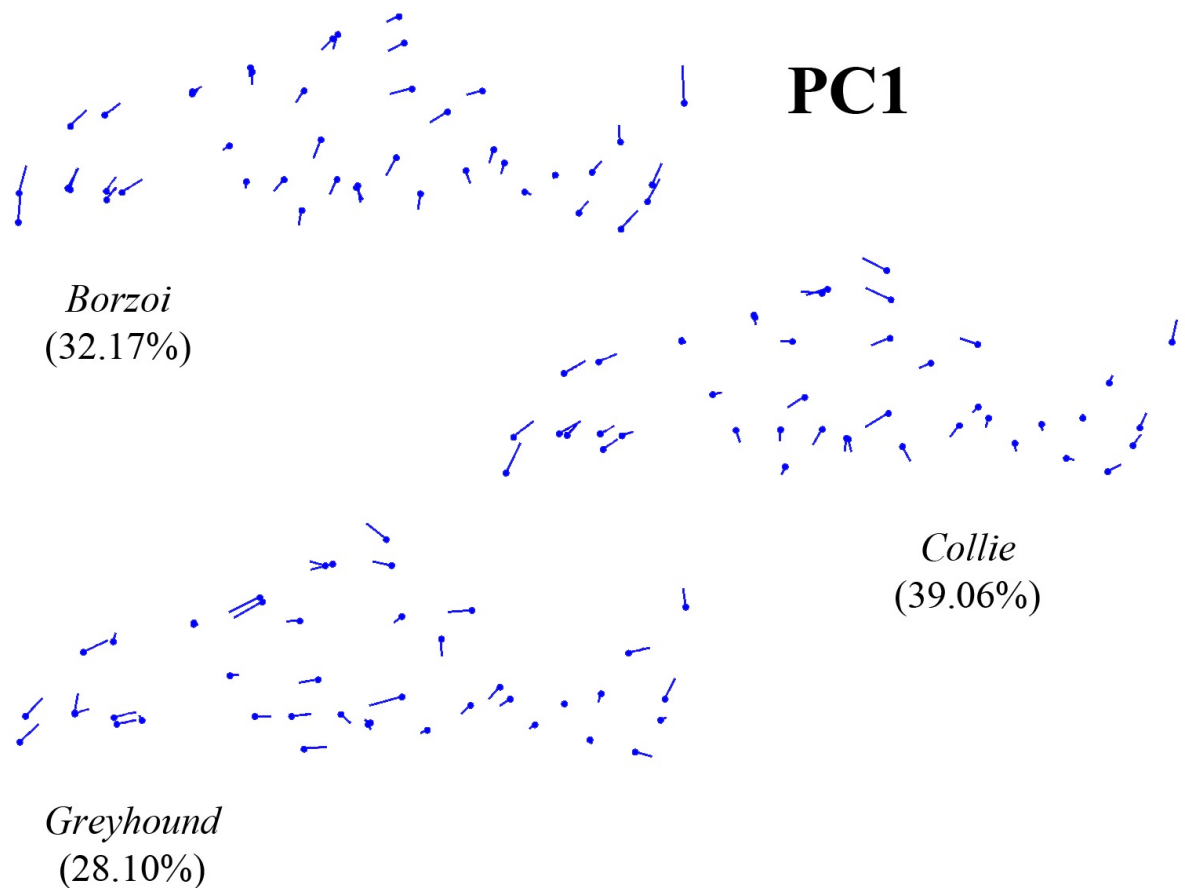


Figure 3.8 Lateral view of the shape deformations associated with the first principal component of variation in dolichocephalic breed crania. Vectors on landmarks indicate deformation relative to the mean shape in one direction along the principal component axis.

the mediolateral and dorsoventral position of the zygomatic attachment to the maxillae and frontals. Variation in the height and prominence of the stop exists as well.

Unique to this group are the Bull Terrier and French Bulldog (Figures 3.13 and 3.14, respectively). The PCs of shape variation for the Bull Terrier describe the angle of the rostrum with respect to the ventral braincase (PC1 explains 60.93% of the variation). In the Bull Terrier, this trait has become more exaggerated over time (Nussbaumer, 1982; Fondon and Garner, 2004), so it is not surprising that this should be the largest source of variation in a sample of dogs drawn from over several decades. PCs for the French Bulldog describe differences in the convexity of the forehead, mediolateral width of the facial bones, and rostral projection of the incisive alveolar bone (PC1: 18.78%, PC2: 14.48%). This breed exhibits an interesting pattern of variation in the width of the rostrum: on both the PC1 and PC2 axes, narrow maxillae are

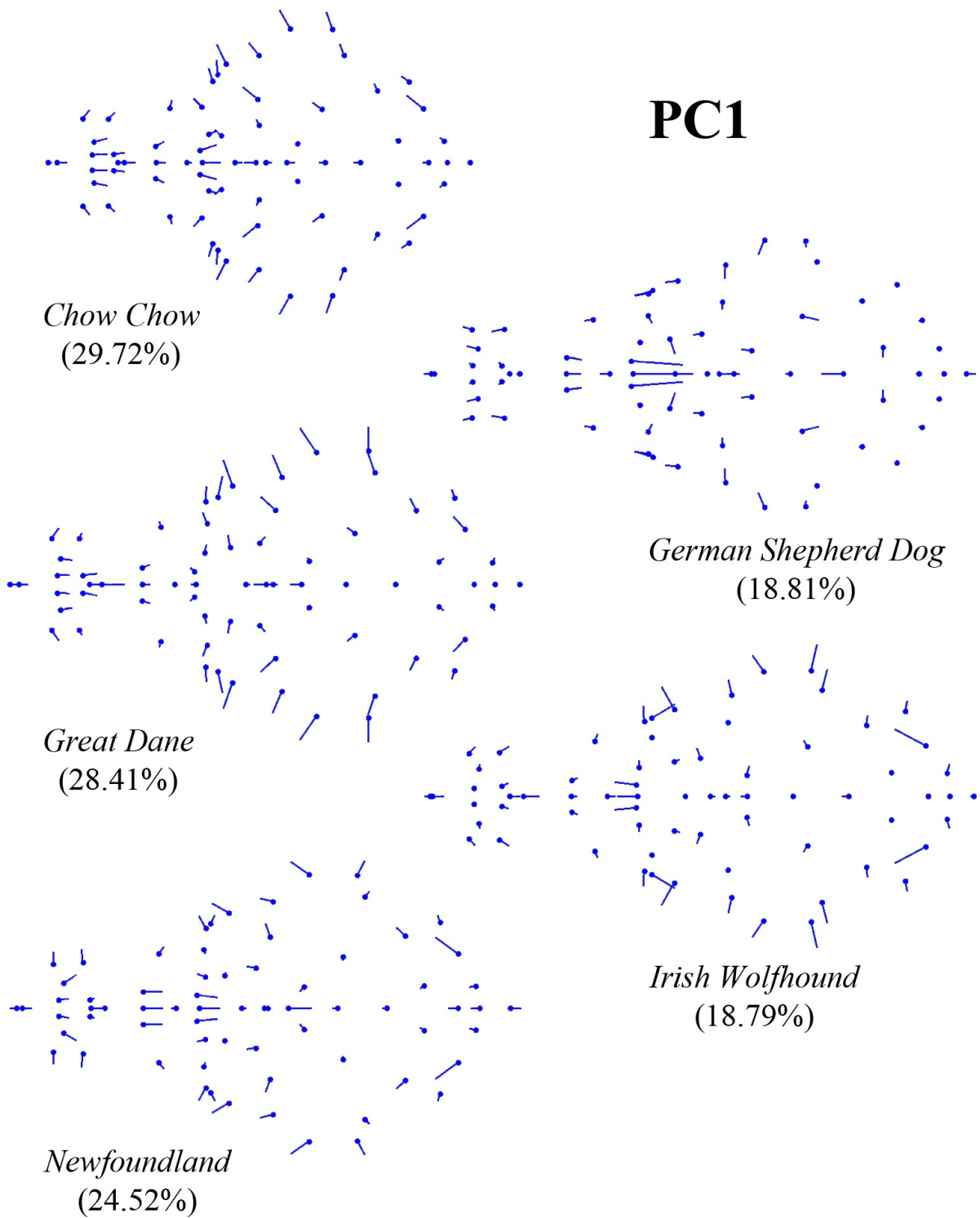


Figure 3.9 Dorsal view of the shape deformations associated with the first principal component of variation in mesaticephalic breed crania. Vectors on landmarks indicate deformation relative to the mean shape in one direction along the principal component axis.

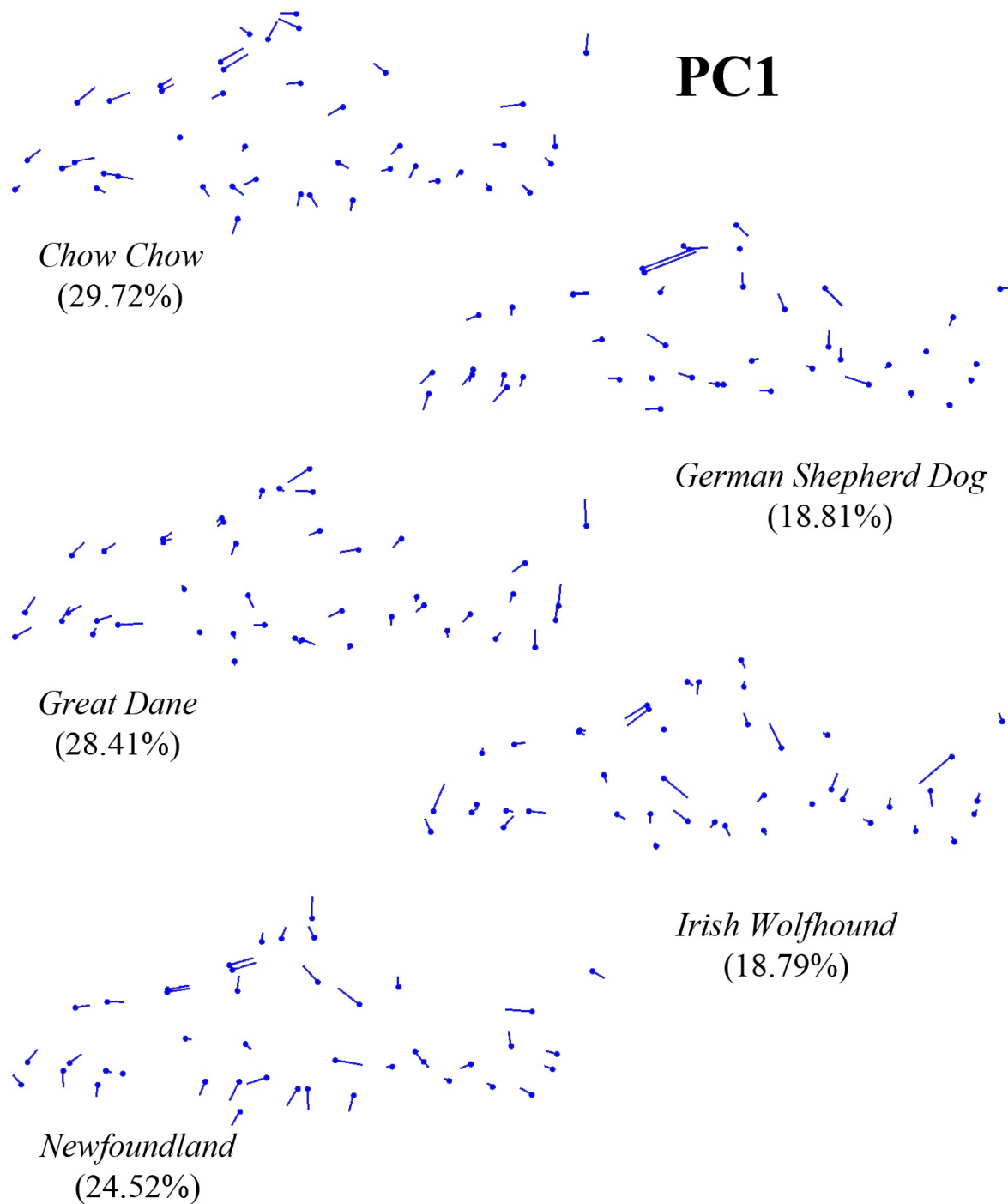


Figure 3.10 Lateral view of the shape deformations associated with the first principal component of variation in mesaticephalic breed crania. Vectors on landmarks indicate deformation relative to the mean shape in one direction along the principal component axis.

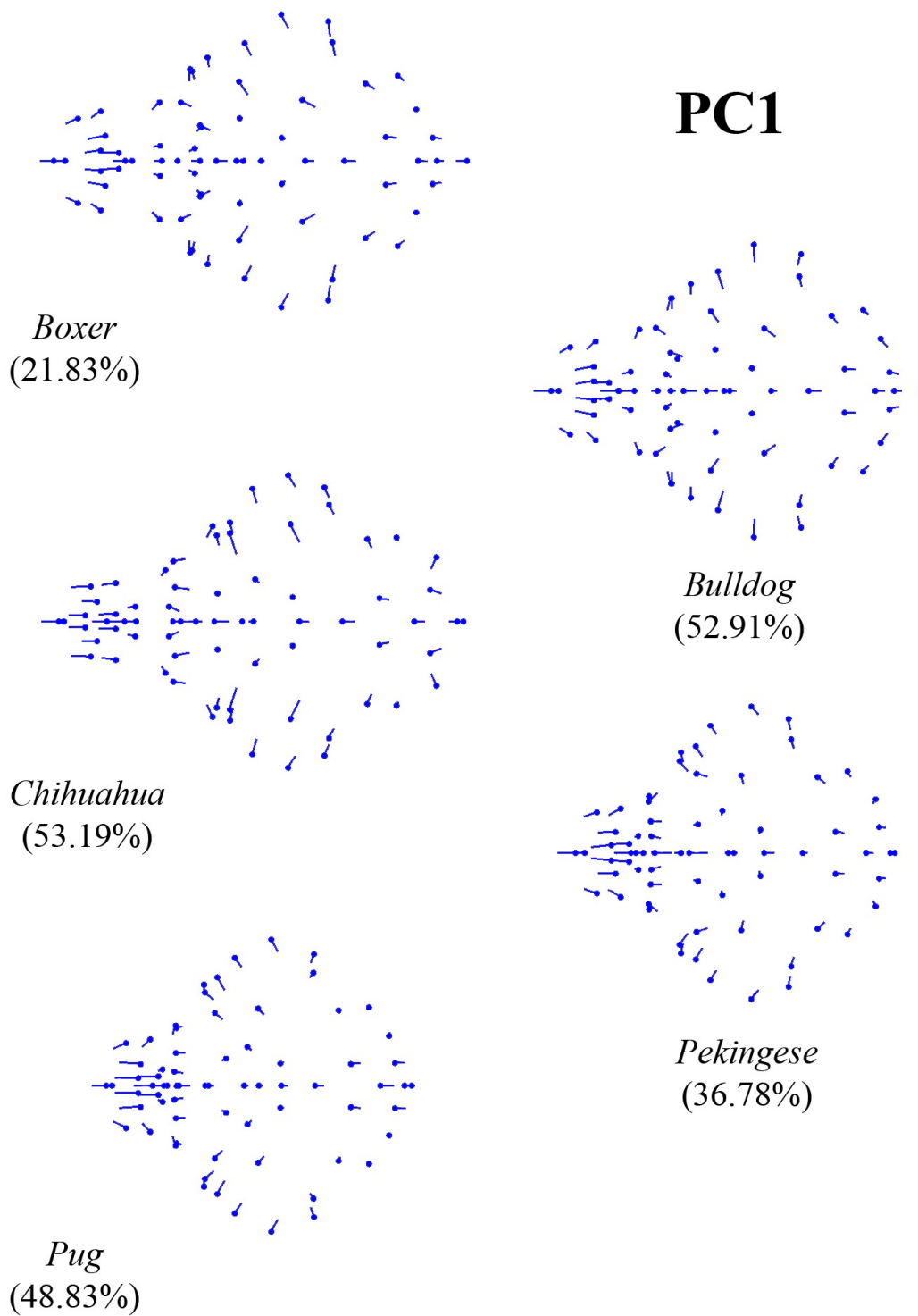


Figure 3.11 Dorsal view of the shape deformations associated with the first principal component of variation in brachycephalic breed crania. Vectors on landmarks indicate deformation relative to the mean shape in one direction along the principal component axis.

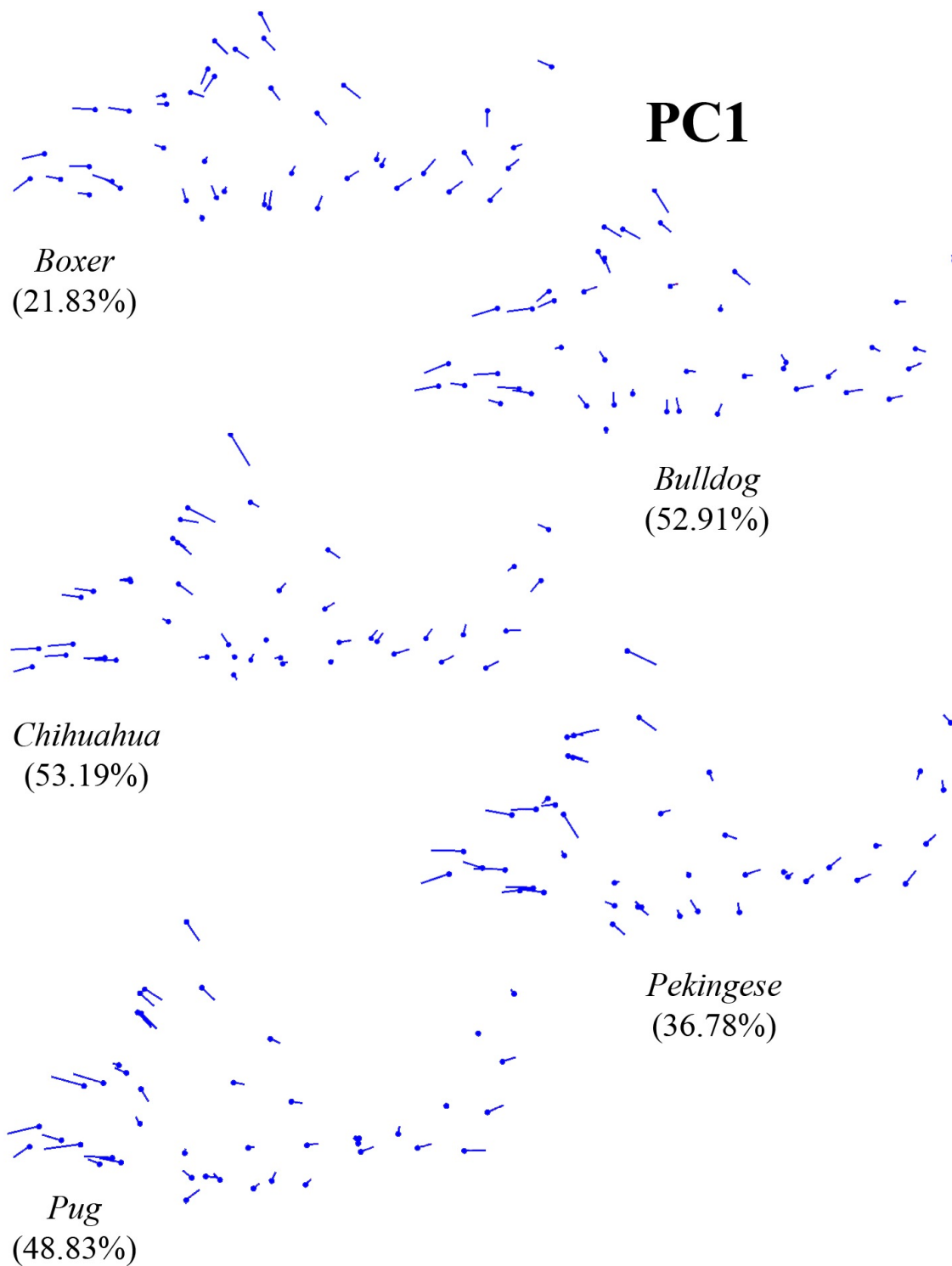


Figure 3.12

Lateral view of the shape deformations associated with the first principal component of variation in brachycephalic breed crania. Vectors on landmarks indicate deformation relative to the mean shape in one direction along the principal component axis.

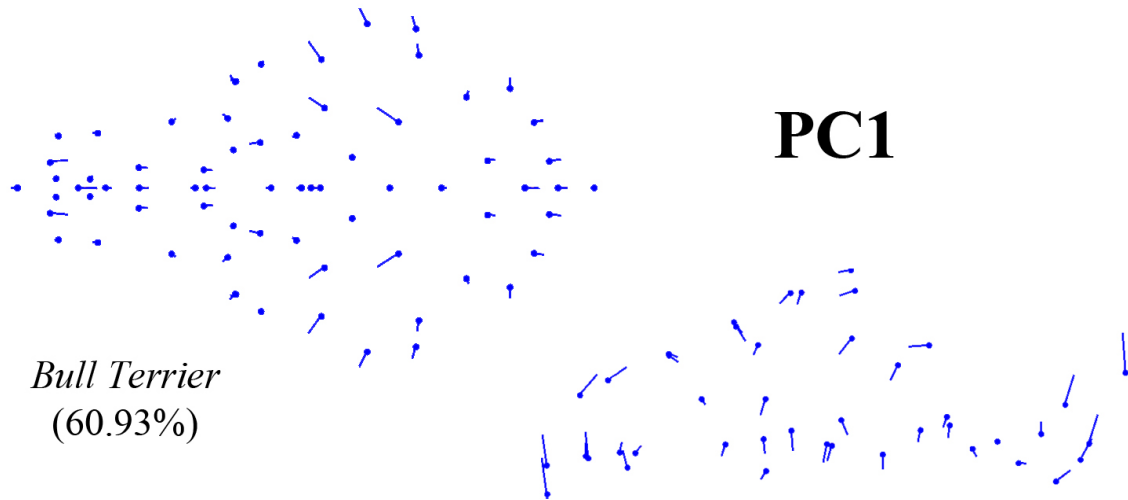


Figure 3.13 Shape deformations associated with the first principal component of variation in the Bull Terrier cranium. Vectors on landmarks indicate deformation relative to the mean shape in one direction along the principal component axis.



Figure 3.14 Shape deformations associated with the first principal component of variation in the French Bulldog cranium. Vectors on landmarks indicate deformation relative to the mean shape in one direction along the principal component axis.

paired with wider nasals in overall narrower rostra at one extreme, and wide maxillae with narrow nasals comprise overall wider rostra at the other. Increased width is coupled with a shortened, more convex facial profile in PC1, but with a less prominent, more concave fronto-nasal region in PC2. Variation in facial width of this nature is not observed in any of the first three PCs of the other brachycephalic breeds.

None of the first three PCs for any breed separate individuals by sex, at least for individuals for which sex is known.

3.3 Discriminant function Analyses

The shape differences between the average gray wolf cranium and the average crania of the fifteen focus breeds are described below. Figure 3.15 illustrates the relationship between the shape of the Borzoi cranium and the wolf cranium, and is representative of dolichocephalic breeds in general. Figure 3.16 depicts cranial shape differences between the German Shepherd Dog and the wolf, and is representative of mesaticephalic breeds in general. The brachycephalic Pug, Chihuahua, Boxer, and Bull Terrier are contrasted with the wolf in Figures 3.17, 3.18, 3.19, and 3.20, respectively. Additional comparisons between the wolf and focus breeds from each category are presented in Appendix Six, Figures A.9-A.17. As mentioned earlier, these comparisons illustrate the shape differences between the crania of modern breeds and the modern wolf in order to identify distinctions in breed-specific morphology. Although these differences provide insight into the evolutionary changes that have led from the historical gray wolf ancestor to modern breeds, they are distinct from the latter.

Discriminant function analysis in MorphoJ (Klingenberg 2011) produces several measures of disparity, including Procrustes distance, which describes the similarity of the shapes being superimposed—in this case, the shapes of the average wolf cranium and the average focus breed cranium. Procrustes distances are presented in Table 3.2. Other measures of disparity obtained in the analyses include Mahalanobis distance and the T-squared statistic, which are summarized for each pair-wise comparison in Appendix Seven.

3.3.1 Dolichocephalic breed differences from the gray wolf

The average Borzoi and Collie crania are nearly identical in their shape difference from the average wolf cranium (Figures 3.15 and A.9, respectively). Compared to the wolf, the crania of these two breeds are much narrower and tapering: the zygomatic arches do not project as far from the braincase laterally and the maxillae are narrower both at the attachment of the zygomatics and at the tip of the rostrum. The rostrum is longer relative to the size of the braincase in the Borzoi and the Collie. This difference in length involves rostral extension of the frontal bones, increase in the total length of the nasals, and translation of the premaxillae rostrally along the lengthened nasals. When observed in profile, there is a ventral angle to the rostra of the longer Borzoi and Collie crania, meaning the rostral premaxillae extends further rostro-ventrally and the forehead and nasals form a more convex arc than in the wolf cranium. The rostral extent of the frontals is not shifted rostro-dorsally in the Collie, making the profile of the face closer to a straight line than in the Borzoi.

Table 3.2 Procrustes distances (d) for pairwise discriminant function analyses of average cranial shapes for domestic dog breeds and the gray wolf. Statistically significant distances ($P < 0.0001$) identified from the parametric T-test are indicated in **bold**. All distances are statistically significant ($P < 0.0001$) according to the permutation test (1,000 runs) except for the one marked with an asterisk (*). Patterns of statistical significance are discussed in section 3.4.1. Breed abbreviations are explained in Appendix Two.

	BLT	BOR	BOX	BUL	CHI	CHO	COL	FRB	GRD	GRY	GSD	IRW	NEW	PEK	PUG
WOLF	0.1004	0.1045	0.1781	0.2163	0.212	0.1056	0.0807	0.3024	0.0489	0.0564	0.0475	0.0572	0.051	0.2889	0.3034
BLT	x	0.1263	0.1779	0.2	0.198	0.123	0.1117	0.2789	0.0956	0.0979	0.0918	0.1083	0.0937	0.2792	0.289
BOR		x	0.2625	0.2963	0.2726	0.1939	0.0394	0.3784	0.1223	0.0666	0.0844	0.0791	0.133	0.3669	0.3803
BOX			x	0.0579	0.1398	0.092	0.2403	0.1488	0.1525	0.2073	0.1901	0.2046	0.14	0.1443	0.1565
BUL				x	0.1347	0.1263	0.2751	0.0998	0.191	0.2417	0.2267	0.2426	0.1785	0.114	0.1184
CHI					x	0.1497	0.2547	0.1647	0.1977	0.2188	0.2154	0.2362	0.1848	0.1271	0.1437
CHO						x	0.1689	0.2109	0.0857	0.1353	0.1197	0.1377	0.0725	0.2009	0.2139
COL							x	0.3588	0.0976	0.0492	0.0582	0.0556	0.1071	0.3462	0.3597
FRB								x	0.2791	0.3239	0.3128	0.3299	0.2666	0.0852	0.0676
GRD									x	0.0716	0.0508	0.0618	0.0257	0.2681	0.2816
GRY										x	0.0391	0.0533	0.0786	0.3094	0.3235
GSD											x	0.0357	0.057	0.2997	0.3137
IRW												x	0.0711	0.3173	0.3312
NEW													x	0.2552	0.2687
PEK														x	0.0414*
PUG															x



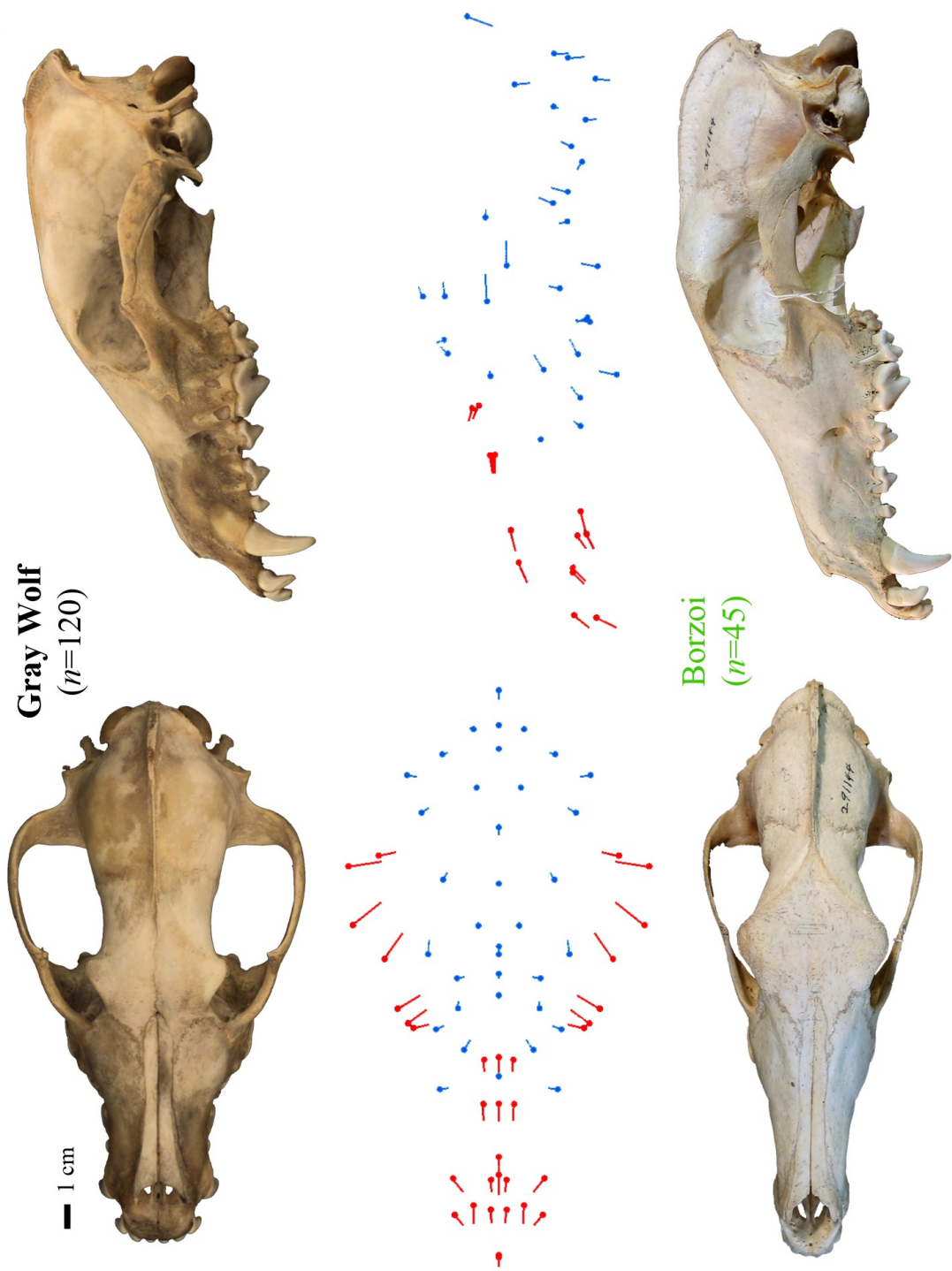


Figure 3.15 Shape deformations based on discriminant function analysis of the average gray wolf cranium and the average Borzoi cranium. Vectors on landmarks indicate deformation relative to the gray wolf cranium in the direction of the Borzoi cranium.

The Greyhound shares the narrow zygomatic arches and maxillae observed in the Borzoi and Collie. However, its rostrum is not significantly longer compared to that of the wolf (Figure A.10). The nasals are slightly longer in the Greyhound cranium than in the wolf cranium, but not to the same degree as in the Borzoi and Collie. The nasals and premaxillae of the Greyhound are slightly longer rostrally and the caudal extent of the premaxillae is positioned rostrally with them, but the shape of the frontal bone is fairly static.

The Procrustes distance of 0.0564 between the Greyhound and gray wolf is relatively short, whereas the Collie and Borzoi are farther from the wolf (0.0807 and 0.1045, respectively). The Borzoi exhibits the most extreme dolicocephaly among the breeds examined here, and is as distant in shape from the gray wolf as is the Chow Chow, the most divergent of the mesaticephalic breeds studied (see below).

3.3.1 Mesaticephalic breed differences from the gray wolf

The average German Shepherd Dog and Irish Wolfhound cranial shapes differ only slightly from the average wolf cranial shape (Figures 3.16 and A.11 respectively). Crania of these two breeds are narrower at the zygomatic arches compared to the crania of wolves. The caudal extent of the premaxillae is more rostral and the rostral extent of the frontals is more caudal in the dog crania. The angle of the nasals and frontals is steeper in the German Shepherd Dogs and Irish Wolfhounds as a result.

The average cranial shapes of the Newfoundland and Great Dane exhibit an increase in mediolateral width at the caudal palate and at the maxillary attachment of the zygomatic compared to the average cranial shape of the wolf (Figures A.12 and A.13, respectively). The Chow Chow shares this difference, but is also wider than the wolf along the whole length of the rostrum and at the zygomatic arches (Figure A.14). Similar to the German Shepherd Dog and Irish Wolfhound, the Newfoundland, Great Dane, and Chow Chow's average cranial shapes display caudally shorter premaxillae and rostrally shorter frontals. However, the crania of these three breeds also have nasals that are reduced in rostral length. The frontals are raised more dorsally, creating a facial angle steeper than that of the wolf or German Shepherd Dog and Irish Wolfhound. The average cranium is shorter in these three breeds, in particular for the Chow Chow, with the widest, steepest face of the group.

Procrustes distances between average cranial shapes of mesaticephalic breeds and the average wolf cranial shape range from the lowest among all breed-wolf comparisons of 0.0475 for the German Shepherd Dog to 0.1056 for the Chow Chow. The Chow Chow is the only member of the group that demonstrates any substantial departure from the average wolf cranial shape: it has a shorter, wider, and steeper face than the wolf, achieved by broader maxillae, shorter nasals, and angled frontals. The Procrustes distance between wolf and Chow Chow (0.1056) is approximately twice the distance between wolf and Great Dane (0.0489), German Shepherd Dog (0.0475), Irish Wolfhound (0.0572), or Newfoundland (0.051).

3.3.3 Brachycephalic breed differences from the gray wolf

The patterns of shape differences between the gray wolf and the brachycephalic Pug, Pekingese, and French Bulldog breeds are very similar (Figures 3.17, A.15, and A.16,

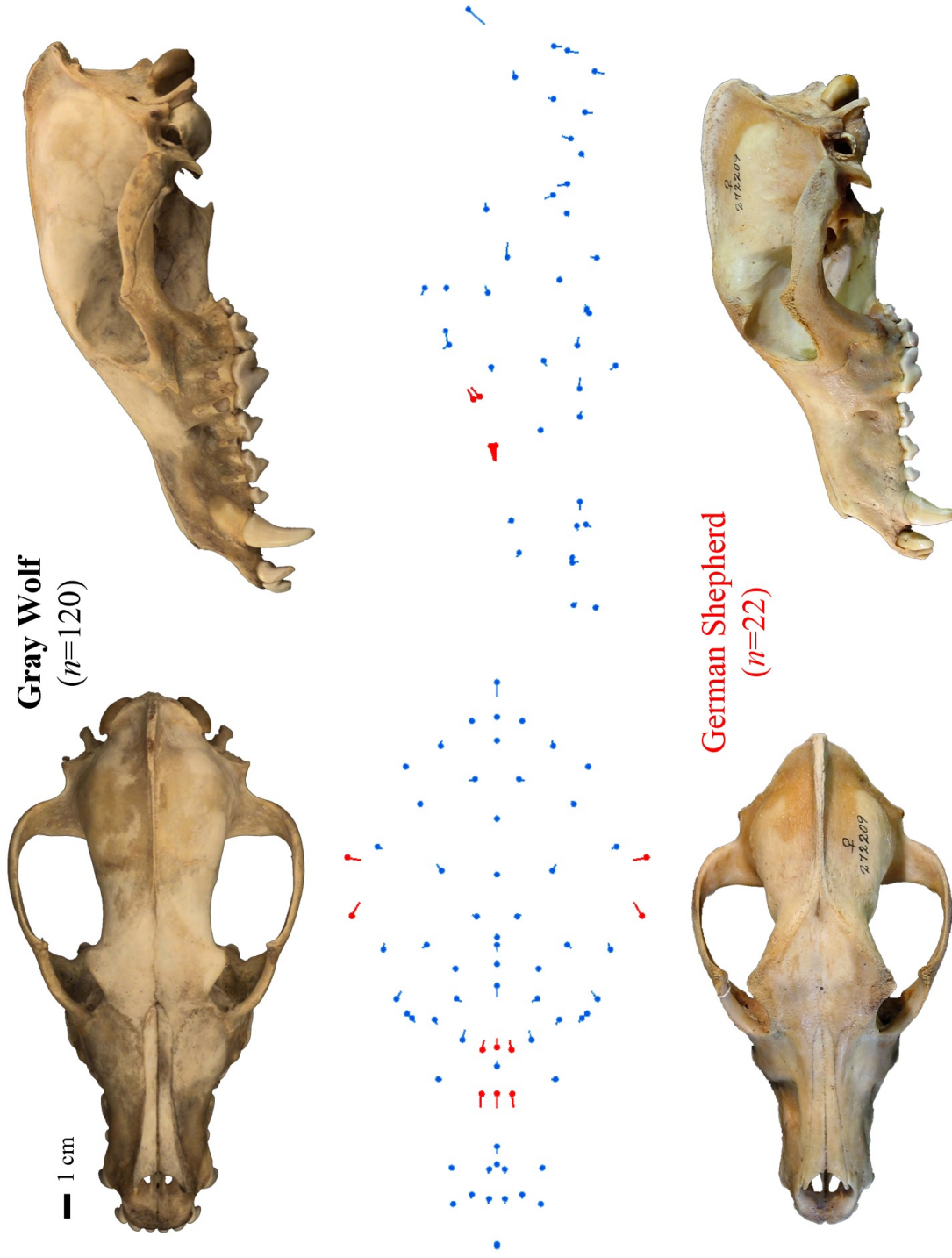


Figure 3.16 Shape deformations based on discriminant function analysis of the average gray wolf cranium and the average German Shepherd Dog cranium. Vectors on landmarks indicate deformation relative to the gray wolf cranium in the direction of the German Shepherd Dog cranium.

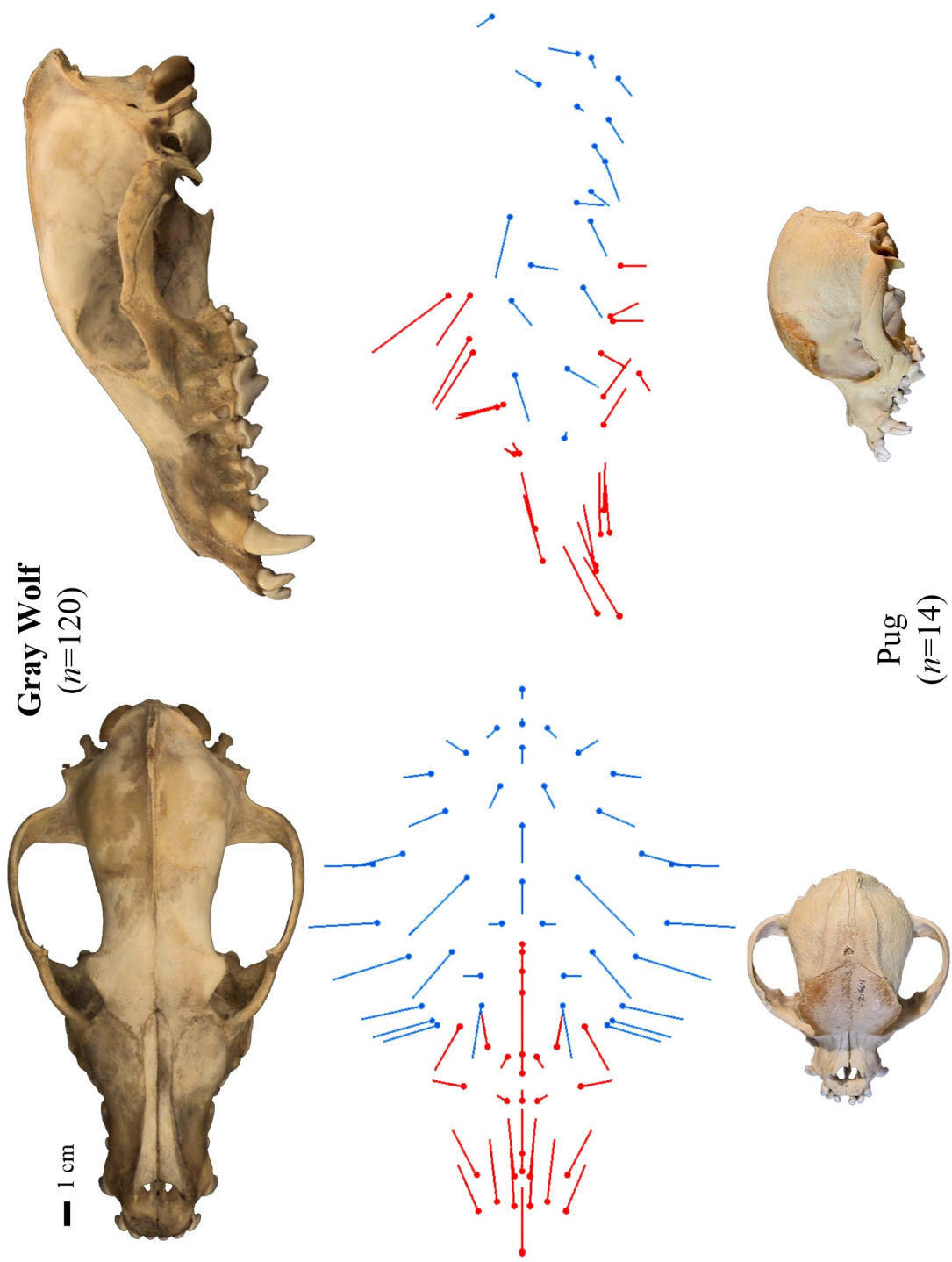


Figure 3.17 Shape deformations based on discriminant function analysis of the average gray wolf cranium and the average Pug cranium. Vectors on landmarks indicate deformation relative to the gray wolf cranium in the direction of the Pug cranium.

respectively). These comparisons result in the greatest Procrustes distances in shape: 0.2889 between the Pekingese and wolf, 0.3024 between the French Bulldog and wolf, and 0.3034 between the Pug and wolf. This extreme pattern is characterized by an overall reduction in the length of the face that includes a substantially shorter rostral half of the nasals and a nearly forty-five degree rostro-dorsally angled caudal half. The resulting nasal bones curve inward at the stop as well as turn inward at their medial border along the midline. The premaxillae are reduced in length proportionally and the frontals are positioned forward to achieve a high, domed forehead. The end of the rostrum is much more blunt and broad: all the incisors now lie alongside one another in a near straight line instead of in an arc as at the tip of the wolf rostrum. The greatest mediolateral widening of the rostrum occurs caudal to the canines: here, the truncated maxillae abruptly broaden out laterally to the zygomatic arches, which are much wider relative to the width of braincase in these brachycephalic breeds.

In contrast to the bony palate of the average gray wolf cranium, the palates of the average Pug, Pekingese, and French Bulldog crania include much less contribution from the maxillae and more contribution from the premaxillae and palatine bones. The shape of the palate is compressed rostrocaudally and expanded mediolaterally. It is also curved dorsally rostral to the first molars. The Chihuahua lacks this difference from the wolf: the ventral surface of its skull is similar to the wolf in being closer to a flat plane (Figure 3.18). With this exception, the Chihuahua differs from the wolf very much in the same pattern as the Pug, Pekingese, and French Bulldog, although at a smaller Procrustes distance (0.212). This breed displays similarly shorter nasals but less angling of the frontals, resulting in an equally short face but less domed of a forehead than other breeds. The rostrum of the Chihuahua tapers more than those of the more extreme brachycephalic breeds.

The pattern of shape difference from the wolf described for the Pug, Pekingese, and French Bulldog is preserved in the larger brachycephalic Boxer and Bulldog breeds (Figures 3.19 and A.17 respectively). The largest difference between the large and small brachycephalic breeds in terms of divergence from the wolf cranial shape is the magnitude of the shape differences described above. This matches the corresponding Procrustes distances between the wolf and Boxer and the wolf and Bulldog. These are high (0.1781 and 0.2163, respectively), but not as high as the distances for the toy size brachycephalic breeds. There is relatively less difference in nasal length and facial width in the Boxer and Bulldog. In these two breeds, the rostral extent of the frontals is reduced, not extended, and the dishing of the face is less extreme and occurs more caudally along the length of the nasals, closer to the frontals than the premaxillae. The same dorsal tilt of the rostrum is displayed in both large and small brachycephalic breeds.

The ventral tilt of the rostrum characterizing the Bull Terrier breed sets it apart from all other brachycephalic breeds (Figure 3.20). Although the nasals are slightly reduced in length, the rostro-caudally short face relative to the braincase is more a product of the extreme angling of the face than of the reduction of any facial bones. Similar to the dolicocephalic Borzoi, this angling produces the opposite of a dished face: a sloping face with little change in angle from the tip of the rostrum to the frontals. The Bull Terrier cranium differs little in relative width from the wolf cranium and overall has a Procrustes distance from the wolf of 0.1004, comparable to the distance between the wolf and the Borzoi or Chow Chow.

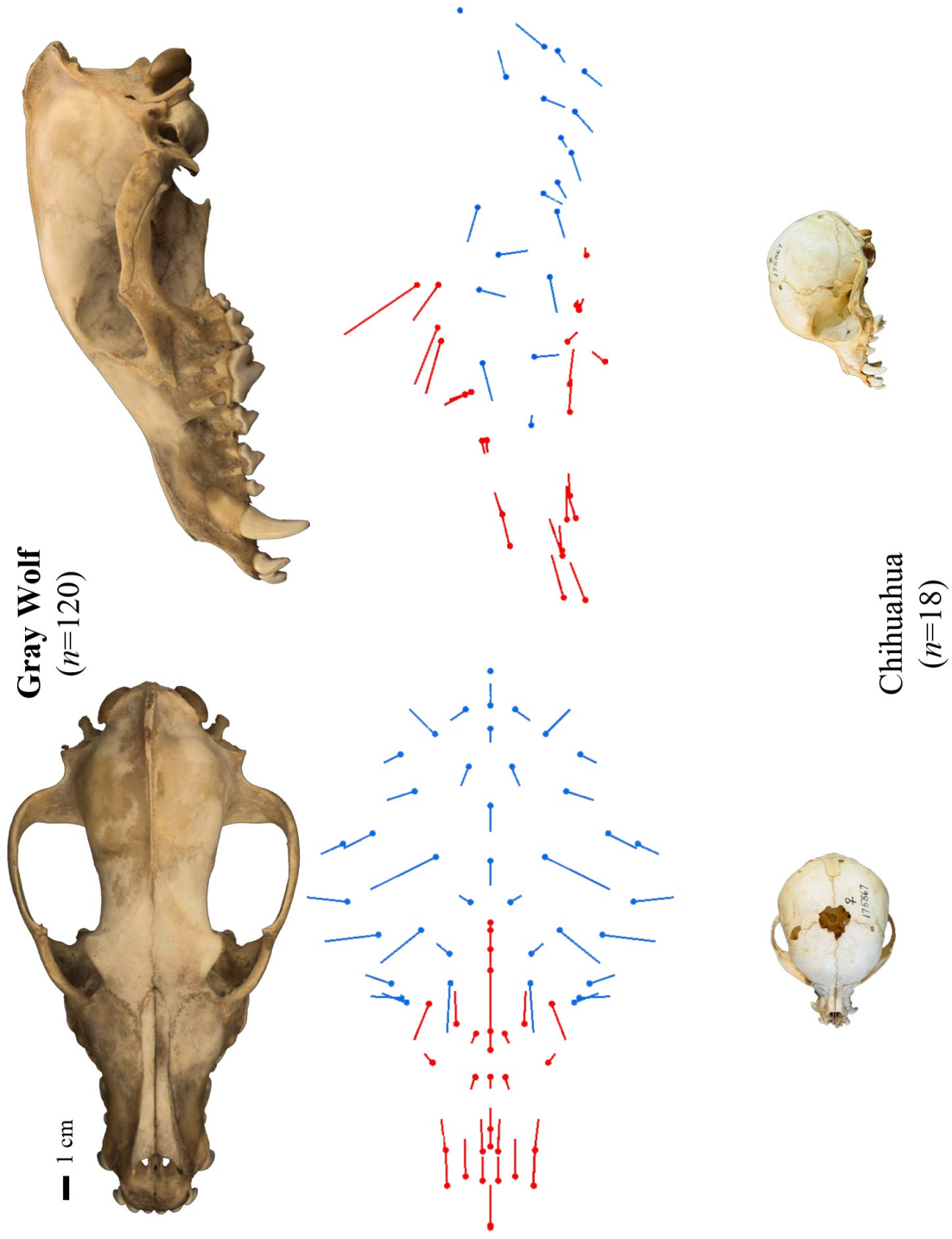


Figure 3.18 Shape deformations based on discriminant function analysis of the average gray wolf cranium and the average Chihuahua cranium. Vectors on landmarks indicate deformation relative to the gray wolf cranium in the direction of the Chihuahua cranium.

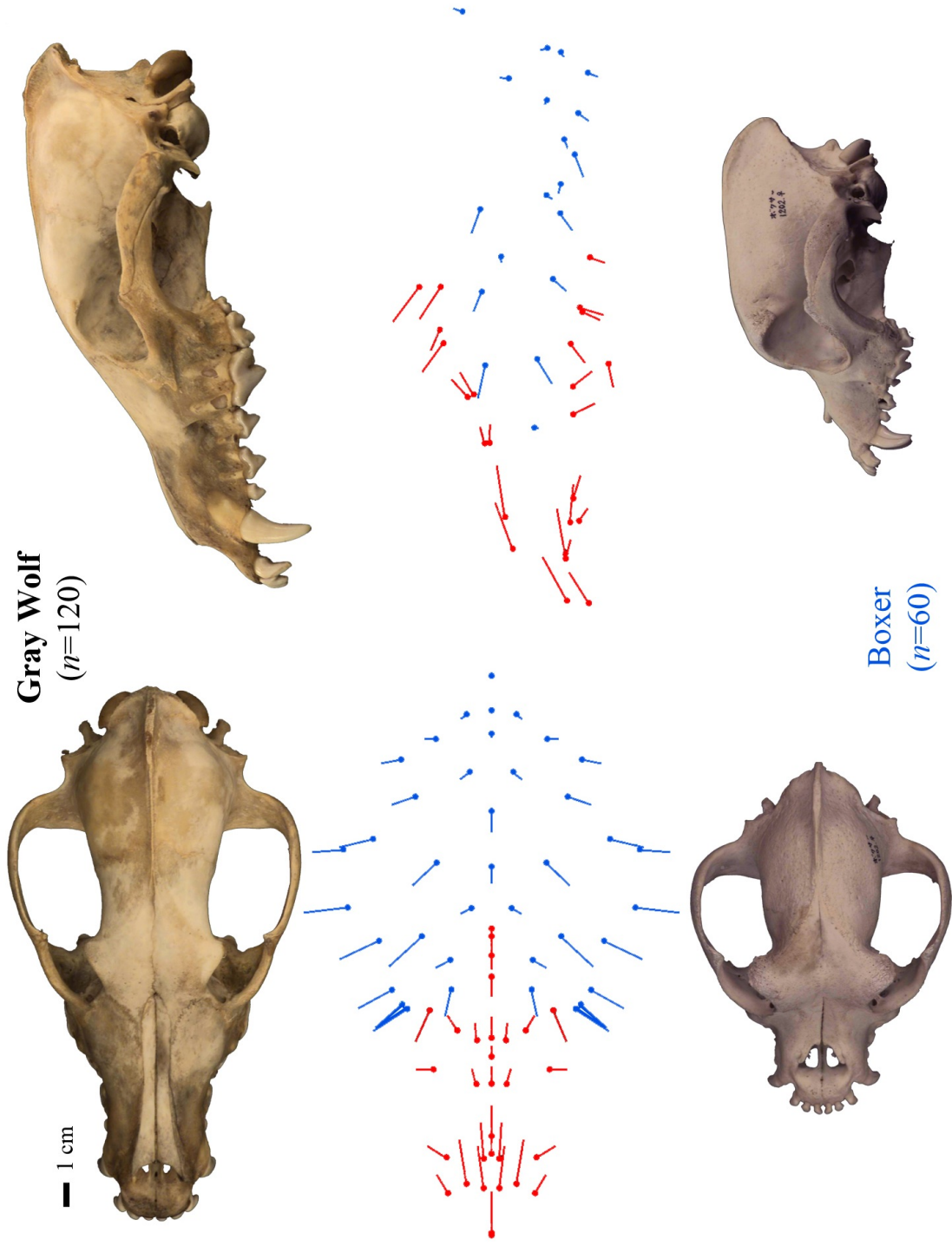


Figure 3.15 Shape deformations based on discriminant function analysis of the average gray wolf cranium and the average Boxer cranium. Vectors on landmarks indicate deformation relative to the gray wolf cranium in the direction of the Boxer cranium.

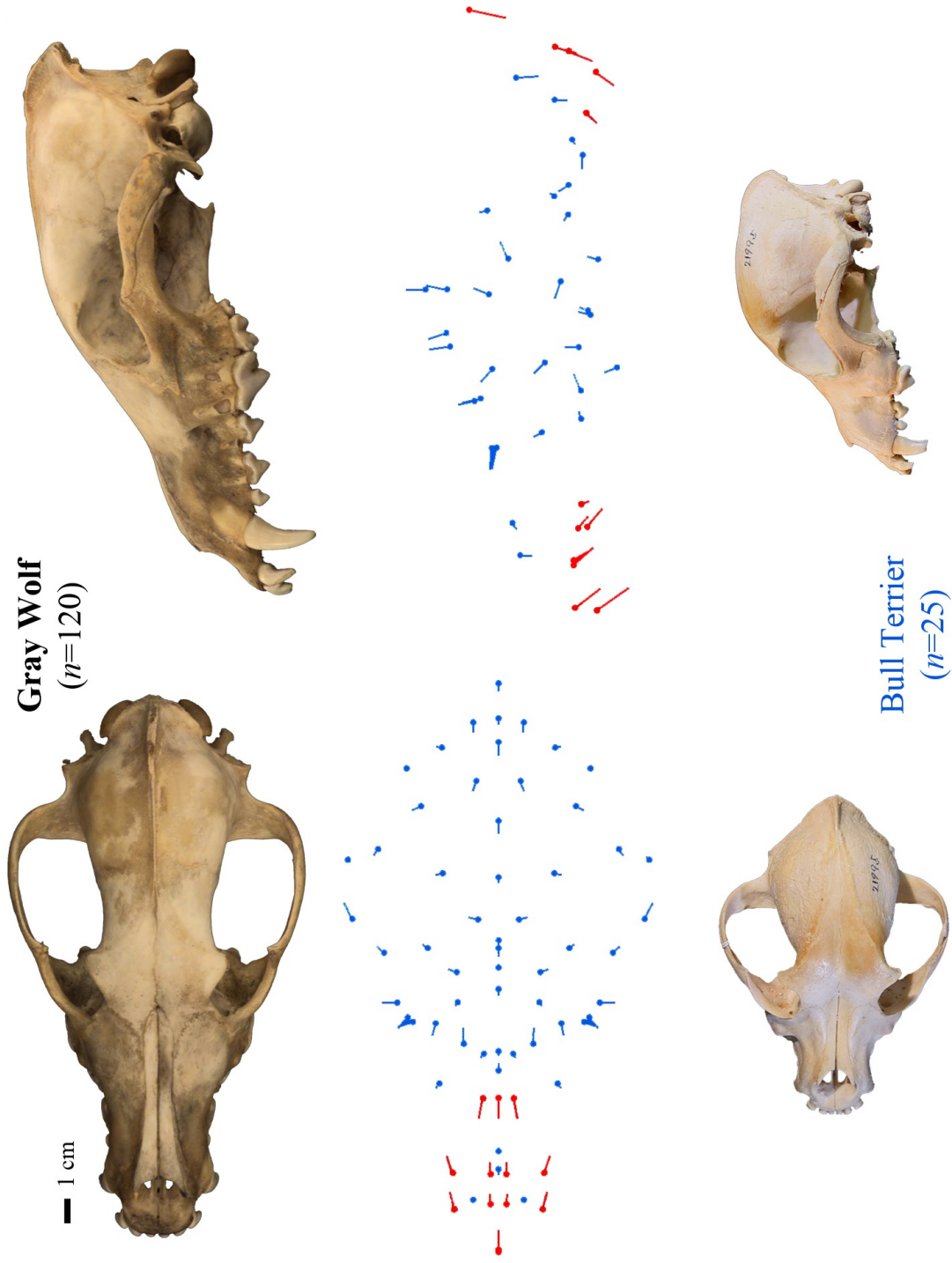


Figure 3.20 Shape deformations based on discriminant function analysis of the average gray wolf cranium and the average Bull Terrier cranium. Vectors on landmarks indicate deformation relative to the gray wolf cranium in the direction of the Bull Terrier cranium.

3.4 Discussion

3.4.1 Differences between brachycephalic breeds

The shape differences and Procrustes distances that separate brachycephalic dog breeds from the gray wolf demonstrate three patterns. The first distinct pattern corresponds to the large brachycephalic Mastiff-like dogs studied: the Boxer and the Bulldog. Represented by the Boxer in Figures 3.21 and 3.22, this pattern consists of moderately rostro-dorsally positioned frontals and caudally translated and reduced nasals, combined with shortened, dorsally tilted rostral-most elements of the snout. The shorter rostra of these breeds are also proportionately wider. This pattern can be contrasted with that of the smaller Mastiff-like and toy brachycephalic breeds studied: the Pug, the Pekingese, and the French Bulldog. Represented by the Pug in Figures 3.21 and 3.22, this second pattern includes the same shortened rostral-most snout elements, but to a greater degree, resulting in an even greater reduction in the relative length of the face. The main difference compared to the Boxer pattern is that in the Pug, the nasals exhibit the same extreme rostro-dorsal expansion as the frontals. Instead of being pushed back caudally as in the Boxer, these bones are curved dorsally to create a nearly 90-degree angle when viewed in profile.

Lastly, the shape difference between the average crania of the wolf and the Chihuahua presents a third brachycephalic pattern (seen in the center row of Figures 3.21 and 3.22). Here the reduction of the rostral snout bones is not combined with an increase in snout width, nor is the rostral snout angled dorsally—the plane of the palate is the same as in the wolf. The rostro-dorsal expansion of the frontals exceeds that observed in the Boxer pattern, and although it is closer to the Pug pattern in this regard, it lacks the accompanying deformation of the nasals. In the Chihuahua pattern, the nasals are more uniformly positioned rostro-dorsally along their anteroposterior length, creating a less dramatic stop.

Based on these qualitative differences in shape differences between wolf and breed, it is difficult to reject *Hypothesis 1*—that distinct craniofacial forms corresponding to specific breeds or groups of breeds exist within the larger brachycephalic category. A Boxer pattern, characterizing larger brachycephalic breeds; a Pug pattern, characterizing small brachycephalic breeds; and a Chihuahua pattern, unique relative to both large and small brachycephalic breeds, are each clearly discernable.

The Procrustes distance separating breeds provides a quantitative test of *Hypothesis 1*. The Procrustes distance between the gray wolf and the fifteen focus breeds ranges from 0.0475, for the wolf-German Shepherd Dog comparison, to 0.3034, for the wolf-Pug comparison (Table 3.2). Most mesaticephalic breed crania have a Procrustes distance near 0.05 from the gray wolf cranium, whereas the distance is closer to 0.1 for dolicocephalic breeds and for the Chow Chow and Bull Terrier. Brachycephalic breed crania are the farthest in Procrustes distance from the gray wolf cranium, beginning with the Boxer at 0.1781. Smaller brachycephalic breeds have crania even more disparate from the wolf, with distances all over 0.2. Given the large sample size for the gray wolf ($n=120$), the parametric T-test for each wolf-breed comparison yielded a statistically significant Procrustes distance ($P<0.0001$) (Table 3.2).

Due to smaller sample sizes for breeds (n ranges from 14-60), the parametric T-tests for all breed-breed comparisons yielded non-significant Procrustes distances (see Table 3.2). The permutation test, which does not assume that the data are normally distributed and which is amenable to small sample sizes (Zelditch *et al.* 2004), indicated statistically significant

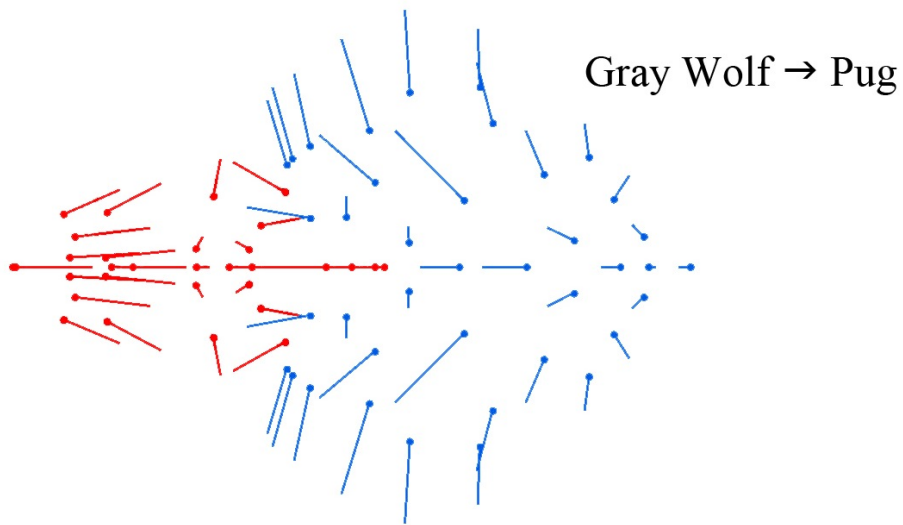
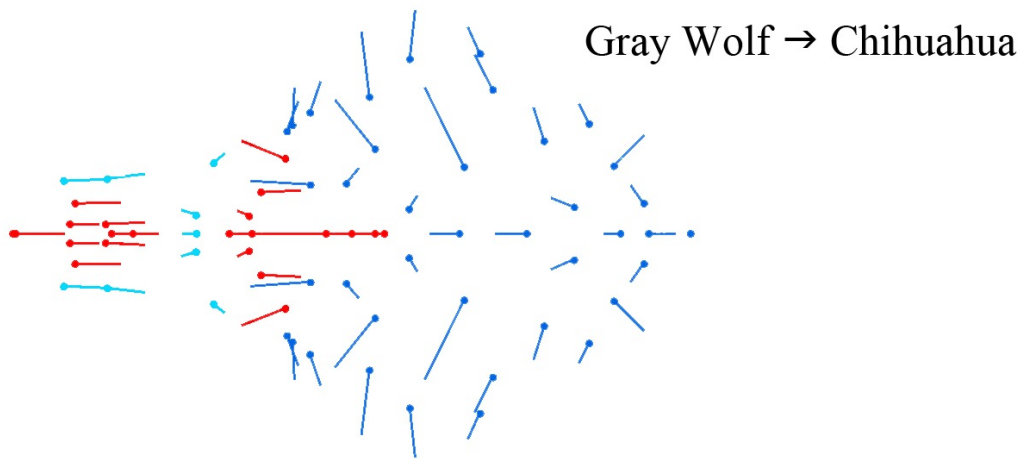
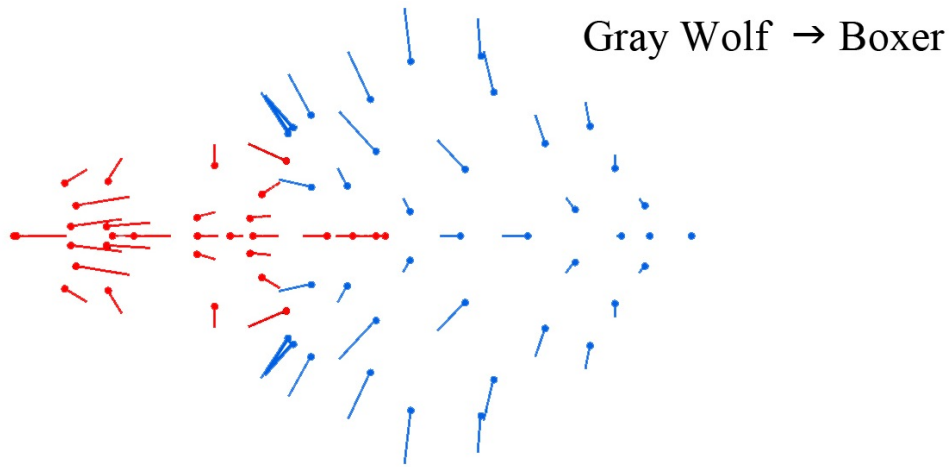
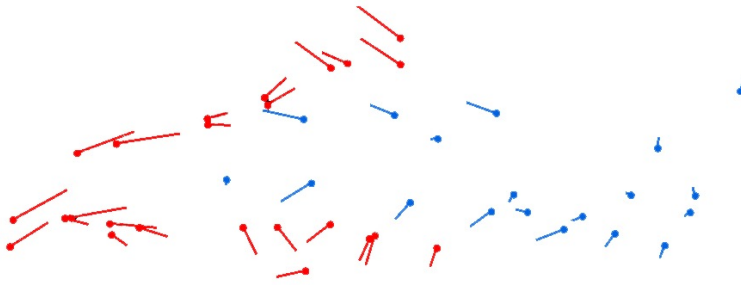


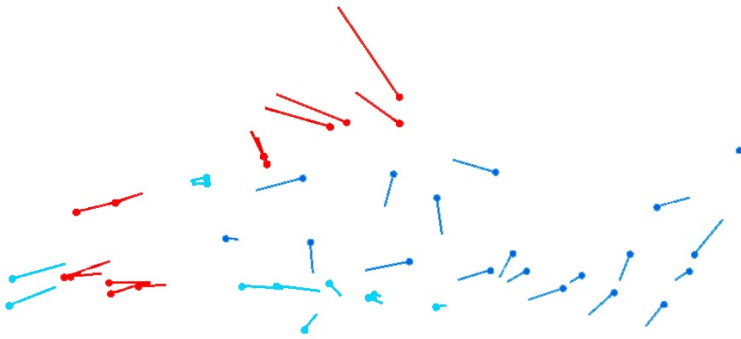
Figure 3.21

Dorsal view of shape deformations corresponding to different forms of brachycephaly. Face-shortening vectors are highlighted in red, with the vectors that characterize the unique Chihuahua form in light blue.

Gray Wolf → Boxer



Gray Wolf → Chihuahua



Gray Wolf → Pug

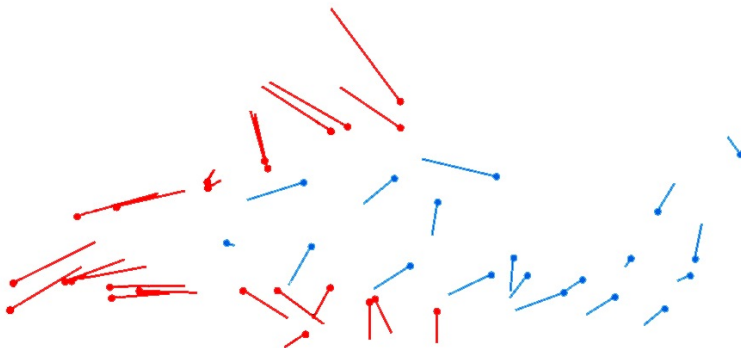


Figure 3.22 Lateral view of shape deformations corresponding to different forms of brachycephaly. Face-shortening vectors are highlighted in red, with the vectors that characterize the unique Chihuahua form in light blue.

Procrustes distances ($P < 0.0001$) for all breed-breed comparisons, with the exception of the Pug-Pekingese analysis. Therefore, based on the more reliable permutation test, the cranial shapes of all but two breeds are distinct from each other. By examining the relative differences in Procrustes distance between breeds, a pattern of distinction emerges that is similar to the qualitative interpretation based on the morphology above.

The average crania of dolichocephalic breeds are all very close to each other, with Procrustes distances ranging from 0.0394 to 0.0666. Greater distances exist between mesaticephalic breed crania, in which Procrustes distances range from 0.0257 to 0.1377. The largest Procrustes distances within this group are attributable to the cranium of the Chow Chow, which stands apart due to its wide rostrum. Procrustes distances within brachycephalic breeds range from 0.0414 to 0.289. However, the largest distances involve the Bull Terrier, whose uniquely angled rostrum is described above. Removing the Bull Terrier from discussion, the most disparate brachycephalic crania belong to the Chihuahua and French Bulldog (0.1647). The average Chihuahua cranium has a Procrustes distance of at least 0.1271 from all other brachycephalic breeds. A similar distance exists between the crania of large brachycephalic breeds (the Boxer and Bulldog) and small brachycephalic breeds (the Pug, Pekingese, and French Bulldog). Brachycephalic breeds within these size categories are more similar: the average Boxer and Bulldog crania are separated by a Procrustes distance of 0.0579; the Pekingese and Pug by 0.0414; and the French Bulldog from the Pekingese and Pug by 0.0852 and 0.0676, respectively.

To summarize, comparison of the Procrustes distances separating the average crania of brachycephalic dog breeds indicates that within this group of dogs, three clusters of more similarly shaped crania exist: the Boxer and Bulldog; the Pug, Pekingese, and French Bulldog; and the Chihuahua. These groupings correspond to the qualitative differences observed between brachycephalic dog breeds based on the shape differences described above. Thus, both the qualitative and quantitative descriptors of shape differences between breeds generated by the discriminant function analyses support the rejection of the null hypothesis that all brachycephalic breeds share a single cranial shape relative to the gray wolf.

3.4.2 The genetic relationship between brachycephalic breeds

Having established that distinct forms of brachycephaly characterize different dog breeds, the next question is, do these shape differences correspond to genetic differences between breeds? To address this question, and more specifically *Hypothesis 2*, it is necessary to examine the current understanding of genetic relationships between modern dog breeds. The large-scale study of nuclear DNA variation across dog breeds by vonHoldt *et al.* (2010) provides the best resolution of breed relationships to date. Figure 3.23 illustrates a simplified schematic of the neighbor-joining tree produced by vonHoldt and colleagues (2010) including only the breeds studied in this dissertation. Genetic groupings largely correspond to the functional breed groupings used by the American Kennel Club (2006), differentiating the following groups of breeds: ancient and Spitz breeds, working dogs, toy dogs, scent hounds, Spaniels, herding dogs, sight hounds, retrievers, small terriers, and Mastiff-like dogs.

Mapping brachycephaly onto the tree of vonHoldt and colleagues (2010) distinguishes two sets of occurrences: the Chihuahua, Pekingese, Pug, and Griffon Bruxellois within the toy dog group; and the Bull Terrier, Boston Terrier, Boxer, Bulldog, and French Bulldog in the

Mastiff-like dog group. Therefore, *Hypothesis 2* predicts that the toy dog and Mastiff-like dog groups represent separate, distinct brachycephalic forms. In the preceding section, distinct brachycephalic forms were described for three groups of breeds: small brachycephalic breeds, including the Pug, Pekingese and French Bulldog; large brachycephalic breeds, including the Boxer and Bulldog; and the Chihuahua. These groups do not match the genetic groupings of toy and Mastiff-like dogs—forms are shared across the two groups (e.g., the Pug, Pekingese, and French Bulldog) and multiple forms exist within a single group (e.g., the Boxer and Bulldog versus the French Bulldog in the Mastiff-like dog group, or the Pug and Pekingese versus the Chihuahua in the toy group). As a result, the null of hypothesis 2—that differences in brachycephaly do not correspond to genetic relationships between breeds—cannot be rejected.

Brachycephaly appears to vary by the size of the breed, not the functional/genetic group to which the breed belongs. This contrast parallels the findings of Stockard (1941), who observed different patterns of inheritance for the Bulldog and the Pekingese in crosses with mesaticephalic breeds. These results led Stockard (1941) to conclude that these two types of brachycephaly have independent origins, a concept also recognized by Klatt (1950) regarding differences in brachycephaly between Bulldog and non-Bulldog breeds. It is possible that different genetic mechanisms have been exploited during selection for short faces in the Bulldog and the Pekingese, as proposed by Klatt (1950). However, the genetic relationships among breeds described by vonHoldt *et al.* (2010) and the evidence for numerous shared identical mutations for specific phenotypes across breeds cited by Larson *et al.* (2012) suggest that this is likely not the case.

For example, in the case of the closely related Bulldog and French Bulldog, the most parsimonious explanation for their morphologies may be that the two breeds share a mutation for brachycephaly that is identical by descent, but that the facial shape of the French Bulldog has been further modified during selection for decreased size. Bannasch *et al.* (2010) explain that although brachycephaly was originally selected in dogs used for fighting, the resemblance of brachycephalic dog crania to the crania of human infants may have also been an important basis for selection. New dog breeds are typically created by the crossing of pre-existing breeds that exhibit traits that the breeder wishes to combine. Therefore, it is not difficult to imagine scenarios in which the mutation for brachycephaly was incorporated into small breeds, or the reverse, in which the mutation for small size was incorporated into breeds that already exhibited brachycephaly, depending upon the motivation of the breeder. If this has been the case, the Pug/Pekingese/French Bulldog and the Boxer/Bulldog brachycephalic forms share the same genetic basis for brachycephaly, but presentation of this trait has been affected by the decreased size of the former group.

The short face of the Chihuahua, in contrast, may represent a separate genetic mechanism for brachycephaly. Although grouped with the Pug and the Pekingese in the toy dog category, the Chihuahua is distinct in that no increase in width or dorsal tilt accompany the shorter face of this breed. Of the breeds studied by Drake (2004, 2011), the Chihuahua presented the only example of proportioned dwarfism of cranial shape. Unlike other small breeds, the Chihuahua displays a cranium similar to that of a juvenile wolf the same size. The short face of this breed tapers rostrally, which is different from the broad, short faces of other brachycephalic breeds, but similar to the face of a small, juvenile wolf. Therefore, selection for a paedomorphic cranium has most likely produced the short face of the Chihuahua, and may represent a separate genetic mechanism than that involved in the short faces of the other brachycephalic breeds discussed above.

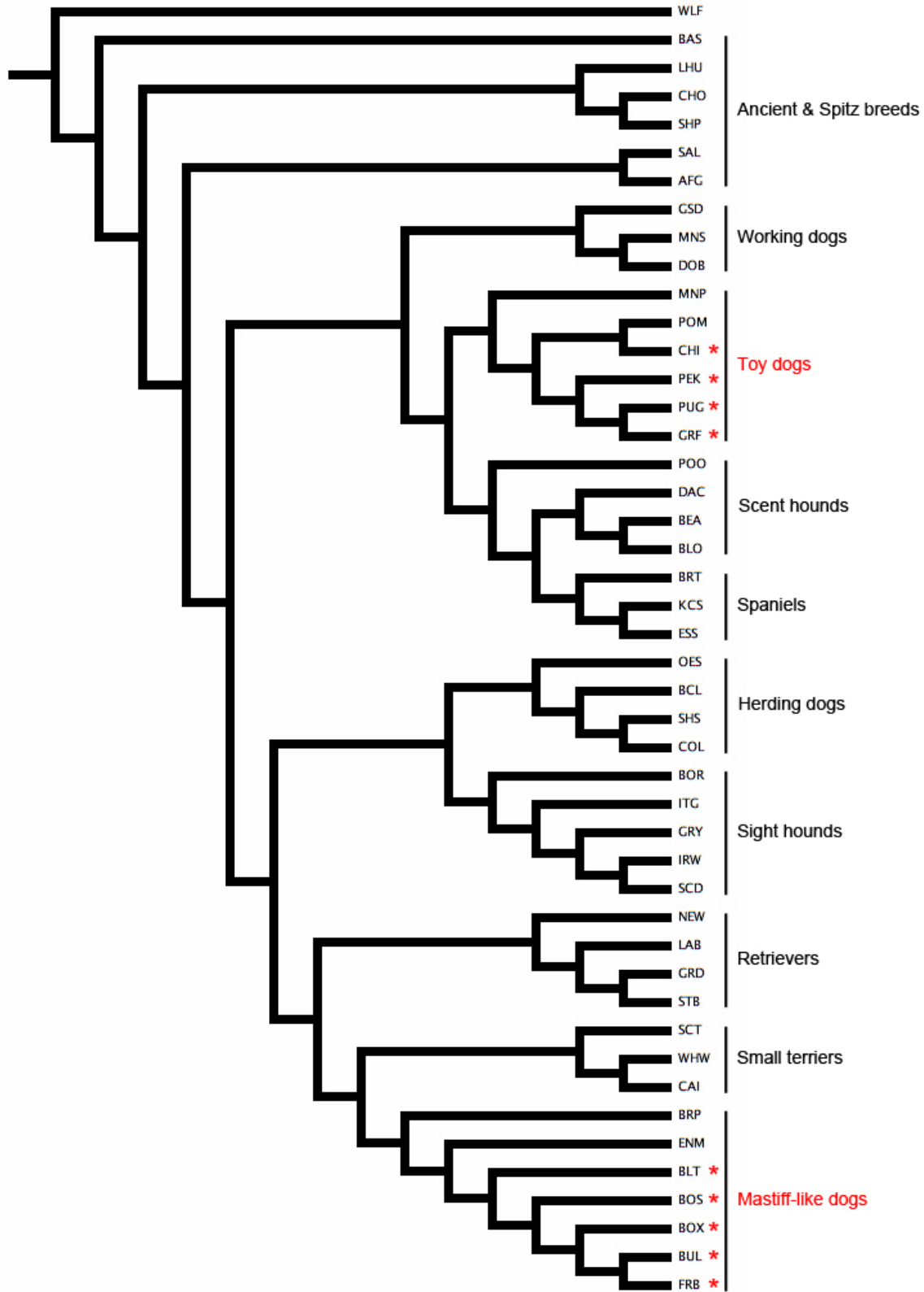


Figure 3.23 Cladogram depicting the genetic relationships between the dog breeds included in this study, after vonHoldt *et al.* (2010). Red asterisks mark occurrences of brachycephaly. Breed abbreviations are explained in Appendix Two.

As Larson *et al.* (2012) explain, the complex history of admixture and the creation of modern breeds within the last 150 years have made it difficult to resolve the relationships between breeds. Similarly, the history of selection for specific traits and combinations of traits across various breeds is not well understood. However, the resolving power of genetic data for the dog stands only to increase as larger and more comprehensive datasets are combined with more rapid sequencing techniques. In the meantime, insight into the genetic basis for brachycephaly in different dog breeds can be gained from studies of developmental genetics. Patterns of craniofacial shape in mouse mutants provide an opportunity to identify specific genes whose altered expression generates brachycephaly similar to that observed in dogs. In the next chapter, three such candidate genes are discussed in the context of the morphological results presented here.

Chapter 4: Candidate Genes for Canine Brachycephaly

4.1 Introduction

Having established the distinct patterns of craniofacial shape differences that exist between the gray wolf and brachycephalic dog breeds in the previous chapter, I now examine potential genetic mechanisms for generating these phenotypes. In Chapter 1, I described three such mechanisms that have been identified in studies of craniofacial developmental genetics in mice (see Dixon *et al.* 2006, Han *et al.* 2007, and Eswarakumar *et al.* 2002, 2004). In this chapter, I address my third and final research question—whether the patterns of shape differences that distinguish the wolf from brachycephalic dogs are comparable to genetic pathways identified in mouse mutants—by testing three hypotheses based on these mechanisms:

Hypothesis 3A: Modification of the gene *Tcof1* has provided a mechanism for brachycephalism in dogs via coordinated shortening of both the frontal and nasal bones.

Hypothesis 3B: Modification of the genes *Msx1* and *Msx2* has provided a mechanism for brachycephalism in dogs via shortening of the frontal bones only, which in turn displaces the nasal bones.

Hypothesis 3C: Modification of the gene *Fgfr2c* has provided a mechanism for brachycephalism in dogs via altered sutures in the skull vault, resulting in shortening and angling of both the frontal and nasal bones.

Before I compare the observed patterns of shape differences between the dog and the wolf with the mouse mutant phenotypes associated with each mechanism, I present a brief overview of vertebrate craniofacial development. In this review, I focus on the genes that regulate patterning and bone formation during cranial embryonic development in order to provide a broader context for the subsequent discussion of the specific genetic pathways described in each hypothesis.

4.2 Development of the vertebrate head

The vertebrate head is a complex structure comprised of the skull, nervous system, sensory organs, and muscles, each with its own distinct embryonic origin. Furthermore, the skull, a unique innovation of vertebrates, is also a composite structure that can be decomposed into elements with separate embryonic and phylogenetic origins. The integrated patterning and growth of these elements during embryonic development is guided by a complicated network of gene regulation, our understanding of which has been aided tremendously by gene expression studies in model organisms such as the mouse, chicken, zebrafish, and frog (see reviews by Murray 2011, Jheon and Schneider 2009, Yelick and Schilling 2002, and Morvan-Dubois *et al.* 2008, respectively), as well as studies of human genetic skeletal disorders (see, for example, review by Wilkie and Morriss-Kay 2001).

4.2.1 Evolutionary origins of the components of the skull

The skull can be divided into three main components: the chondrocranium, which functions to support the brain and sensory organs; the splanchnocranium, which originally served as a support for the gill arches of early aquatic vertebrates, and which contributes to the jaws, hyoid, and inner ear bones of later vertebrates; and the dermatocranium, which forms the superficial sides and roof of the skull (Kardong 1995; Hildebrand and Goslow 2001). Of these three, the splanchnocranium is the most ancient structure, having evolved to support the gill pouches of early chordates. In its simplest form, the splanchnocranium exists as a series of cartilage rods that support each gill bar, or branchial arch, in jawless vertebrates. The evolution of jaws involved the co-option of the first branchial arch cartilage for upper and lower jaw elements, and the second arch cartilage for hyoid formation (Kardong 1995; Hildebrand and Goslow 2001; Morriss-Kay 2001). In mammals, derivatives of the first arch have evolved to serve a different function, forming the malleus and incus bones of the inner ear and the greater wings of the sphenoid bone, whereas derivatives of the second arch form the stapes bone of the inner ear and the majority of the hyoid (Kardong 1995).

With the exception of lampreys, hagfish, and cartilaginous fishes, the elements of the vertebrate splanchnocranium undergo endochondral ossification, whereby a cartilage template is replaced by bone (see also section 4.2.4). Similarly, the chondrocranium, which evolved as a series of fused cartilages flanking the nerve cord and sensory capsules, remains unossified in cartilaginous fish, but undergoes endochondral ossification in most other vertebrates (Kardong 1995; Hildebrand and Goslow 2001; Morris-Kay 2001). In mammals, ossification of the chondrocranium contributes the turbinate bones, occipital bone, ethmoid bone, sphenoid bone (with the exception of the greater wings—see above), and the petrous portion of the temporal bone, including the mastoid process (Kardong 1995; Hildebrand and Goslow 2001).

Lastly, the dermatocranium component of the skull originated from the protective bony head armor of early fishes, an extreme example of which are the ostracoderm fishes of the Devonian and Ordovician, whose entire bodies were covered with such armor (Kardong 1995; Morris-Kay 2001). The evolution of the dermatocranium involved the sinking inward of this armor from the integument (Kardong 1995). As a result, the dermal bones that comprise this component of the skull ossify directly from the dermal mesenchyme without a cartilage precursor, a process that is known as intramembranous ossification (Morris-Kay 2001). In amniotes, bones of the dermatocranium comprise most of the braincase and lower jaw, including the facial, orbital, temporal, vault, palatal, and mandibular series of bones (Kardong 1995). A trend of tetrapod evolution has been the simplification of the skull through the loss of many bones in these series, such that in mammals, the elements of the dermatocranium are reduced to the premaxillary, maxillary, nasal, lacrimal, frontal, parietal, vomer, palatine, and pterygoid bones, as well as the non-petrous portion of the temporal bone (Kardong 1995; Hildebrand and Goslow 2001).

4.2.2 Embryonic tissue origins of the components of the skull

During early embryonic development, the process of gastrulation converts the multicellular blastula to the gastrula, in which distinct tissue types, or germ layers, first differentiate. These include the ectoderm on the outside of the gastrula, the endoderm on the

inside of the gastrocoel cavity, and the mesoderm, which lines the cavities between the ectoderm and endoderm (Gilbert 2000; Hildebrand and Goslow 2001). Concurrent with the formation of the germ layers, the process of neurulation induces a thickening of the ectoderm known as the neural plate. The longitudinal margins of the neural plate then fold inward to fuse at the midline, creating the hollow neural tube, a precursor of the brain and spinal cord (Gilbert 2000; Hildebrand and Goslow 2001). From the region between the dorsal neural tube and the overlying ectoderm, a fourth cell type arises that is distinct from ectoderm, endoderm, or mesoderm: the neural crest (Trainor *et al.* 2003; Szabo-Rogers *et al.* 2010). Together, these four types of cells give way to the tissues of the vertebrate head: the epidermis, nervous system, and sense organs are derived from the ectoderm; the lining of the pharynx and associated glands are derived from the endoderm; the muscles and epithelial cells of the head are derived from the mesoderm; and the majority of the craniofacial skeleton is derived from the neural crest (Szabo-Rogers *et al.* 2010).

Both mesoderm and neural crest cells contribute to the undifferentiated mesenchyme of the head that gives way to cartilage and bone (Szabo-Rogers *et al.* 2010). In the chondrocranium, the anterior cartilage flanking the notochord, as well as the nasal and otic capsule cartilages, is formed from neural crest–derived mesenchyme, whereas the remaining cartilages are formed from mesoderm-derived mesenchyme (Kardong 1995). The splanchnocranium is entirely neural crest–derived (Kardong 1995; Morriss-Kay 2001). Similarly, the frontonasal and mandible mesenchymes that give way to the dermal bones of the face and jaws are derived from the neural crest. However, the dermal bones of the skull vault are not entirely neural crest–derived. The frontal bone, squamosal portion of the temporal bone, and the sutural membrane between the parietal bones arise from the neural crest, but the parietal and interparietal bones arise from the mesoderm (Morriss-Kay 2001).

These relationships highlight the importance of neural crest cells for the formation of the craniofacial skeleton. Szabo-Rogers and colleagues (2010) outline the key events of craniofacial development: the induction of the neural crest at the dorsal neural tube, the migration of neural crest cells into the presumptive face, the proliferation of neural crest cells to form facial prominences, the fusion of these prominences to set up the ultimate form of the face, and the shaping of the face via directional growth of the skeleton. Variation in craniofacial morphology arises from modification of these developmental processes. The hypotheses tested in this chapter each propose a distinct developmental modification, based on changes in genetic regulation. The genetic regulation of craniofacial development and the formation of bone are reviewed in the subsequent sections in order to provide a context for discussion of the specific modifications proposed by each hypothesis.

4.2.3 Genetic regulation of embryonic craniofacial development

The primary genes and transcription factors involved in the key events of mouse craniofacial development are reviewed below. This review is intended to provide only a very basic overview of regulation and is by no means comprehensive. For more detailed reviews, see Knecht and Bronner-Fraser (2002) and Sauka-Spengler and Bronner-Fraser (2008) (neural crest induction), Minoux and Rijli (2010) (neural crest migration), Creuzet *et al.* (2005) (neural crest patterning), and Nie *et al.* (2006a,b) (specific families of growth factors).

4.2.3.A Neural crest induction

The induction of neural crest cells occurs at the interface between the non-neural ectoderm and the neural tube, with contributions from both tissues (Trainor *et al.* 2003). Three signaling pathways intersect at this location and are essential for induction: the bone morphogenetic protein (BMP) group, the fibroblast growth factor (FGF) group, and the Wnt network of proteins (“Wnt” is a portmanteau of the names of the *Drosophila* gene *wingless* and its vertebrate homologue, *integrated*) (Gilbert 2000; Knecht and Bronner-Fraser 2002; Trainor *et al.* 2003). BMPs secreted by the ectoderm induce neural crest formation under the regulation of Delta-Notch signaling (Knecht and Bronner-Fraser 2002; Trainor *et al.* 2003). An important step in this process is the transition of neural crest from epithelial cells to mesenchymal cells, which is achieved via the repression of cell adhesion molecules by the genes *Slug* and *Snail* (Trainor 2005). BMP signaling functions in this delamination process by inducing the expression of the *Slug* (Trainor *et al.* 2003). The influence of BMPs on induction requires Wnt and FGF signaling as well, both from the ectoderm and the paraxial mesoderm, although studies of *Wnt* gene expression suggest a larger role in neural crest proliferation than induction (Knecht and Bronner-Fraser 2002; Trainor *et al.* 2003; Trainor 2005).

4.2.3.B Neural crest migration

Cranial neural crest cells originate in three populations along the developing nervous system and subsequently migrate to populate different components of the face. Neural crest cells from the forebrain and rostral midbrain migrate to the frontonasal and periocular regions; caudal midbrain neural crest cells migrate to the maxillary portion of the first branchial arch; and hindbrain cells, divided into seven distinct compartments called rhombomeres, migrate to the first three branchial arches, giving way to the dental mesenchyme and the mandible (Trainor 2005).

The specific pathway along which a neural crest cell migrates is not an intrinsic property of that cell. Rather, it is regulated by morphogens from the surrounding tissues (Trainor *et al.* 2003; Trainor 2005). BMPs secreted in the neural tube regulate the expression of *rhoB* and synthesis of cadherin proteins. These, in turn, modify cell adhesion and allow migration (Trainor 2005). FGFs expressed in the branchial arches create permissive areas for neural crest cell migration via chemo-attraction (Trainor 2005). Synthesis of retinoic acid is also required for proper migration (Trainor 2005).

Migration of hindbrain neural crest cells from the appropriate rhombomeres to specific branchial arch destinations is regulated by signals from the surrounding tissues. *ErbB4* enzyme from the mesenchyme adjacent to the rhombomeres, *Twist1* transcription factor from the pharyngeal mesenchyme, and T-box 1 protein from the mesoderm at the core of the pharyngeal arches jointly maintain migratory pathways from only the even-numbered rhombomeres (Trainor 2005; Minoux and Rijli 2010). The formation of distinct pathways separated by neural crest-free zones facilitates the population of each branchial arch with neural crest cells from the appropriate rhombomere.

4.2.3.C Patterning of the facial prominences

The spatial arrangement and differentiation of neural crest cells once they have migrated to their final destination is a complex process involving different genetic mechanisms for each component of the craniofacial skeleton. The developing skull vault is differentiated from the rest of the frontonasal region by epigenetic-mediated repression of the gene *orthodenticle homolog 2* (*Otx2*), normally expressed in the forebrain-derived neural crest cells that populate this part of the head (Minoux and Rijli 2010). Further patterning of the facial primordia is regulated by endodermal signaling via the Sonic hedgehog homolog (Shh) protein (Sazbo-Rogers *et al.* 2010). The condensation of neural crest cells in the location of future facial prominences is likely guided by Shh induction of an unknown factor in the ectoderm (Sazbo-Rogers *et al.* 2010).

The patterning of hindbrain-derived neural crest cells in the branchial arches follows two different inter-arch homeobox gene codes: anteroposterior identity is determined by *homeobox A* (*Hoxa*) genes, and dorsoventral identity by *distal-less homeobox* (*Dlx*) genes (Minoux and Rijli 2010). Neural crest cells in the first branchial arch exhibit a Hox-free patterning program that is then modified in a nested combinatorial manner in subsequent arches: *Hoxa2* expression in the second arch is a selector of hyoid fate, and *Hoxa3* and *Hoxa2* together pattern the third and fourth arches. Therefore the expression of Hox genes is crucial for development of structures posterior to the jaws and face along the embryonic anteroposterior axis (Creuzet *et al.* 2005; Minoux and Rijli 2010). Jaw and facial development occurs through repression of Hox genes by Fgf8-mediated signaling in the first branchial arch and special AT-rich sequence binding protein (SATB2) in the frontonasal process (Minoux and Rijli 2010).

Overlapping expression of *Dlx* genes in the branchial arches establishes the dorsoventral identity of subsequent skeletal elements. *Dlx1* and *Dlx2* are expressed throughout, *Dlx5* and *Dlx6* are expressed more ventrally, and *Dlx3* and *Dlx4* are only expressed at the ventralmost portion of each arch. In the first arch, *Dlx1/2* expression extends across both the maxillary and mandibular processes, while *Dlx5/6* expression is confined to the mandible. *Dlx3/4* expression is seen in only the ventral tip of the mandible (Minoux and Rijli 2010). This *Dlx* patterning program is established by differential sensitivity to Shh in the dorsal and ventral portions of the arch prior to neural crest cell migration, and is mediated by endothelin signaling in post-migratory cells (Sazbo-Rogers *et al.* 2010).

4.2.3.D Outgrowth of the face

Condensations of neural crest cells in the face establish the following facial prominences/processes: the midline frontonasal mass, paired medial and lateral nasal processes, paired maxillary prominences, and paired mandibular processes. The frontonasal mass and medial nasal processes fuse to form the midface, forehead, dorsal rostrum, and primary palate; the lateral nasal processes and maxillary prominences fuse to form the lateral rostrum; and the mandibular process becomes the lower jaw (Sazbo-Rogers *et al.* 2010). Fusion of the maxillary prominences with the lateral and medial nasal processes forms the upper lip, and midline fusion of the medial nasal processes forms the nasal septum. Subsequently, the secondary palate develops via fusion of the palatal shelf outgrowths of the maxillary prominences (Sazbo-Rogers *et al.* 2010).

These growth processes are regulated by signals from both the adjacent ectoderm and endoderm. Hedgehog (Hh) protein from the foregut endoderm, as well as the neuroectoderm and facial ectoderm, stimulates the formation of the upper face (Szabo-Rogers *et al.* 2010). Shh in particular plays a role in the three-dimensional growth and position of the upper jaw. In the superficial facial ectoderm, the interface between *Fgf8*- and *Shh*-expression domains establishes a signaling center known as the frontonasal ectodermal zone (FEZ), which is located at the tips of the medial nasal prominences in mice (Minoux and Rijli 2010; Szabo-Rogers *et al.* 2010).

The size and orientation of the FEZ varies across vertebrates, and it has been proposed that modification of the organization of the FEZ may contribute to craniofacial morphological diversity (Minoux and Rijli 2010). Studies of avian embryonic development have contributed significantly to our understanding of the effects of FEZ modification: as a result of differences in the regions of proliferation determined by the FEZ, the narrow pointed beak of the chicken is formed by maximal growth at the center of the frontonasal mass, whereas the broad beak of the duck grows from across the entire mediolateral extent of the frontonasal mass (Wu *et al.* 2004, 2006; Szabo-Rogers *et al.* 2010). Similarly, beak curvature is correlated with FEZ position and differential regions of proliferation (Wu *et al.* 2006; Szabo-Rogers *et al.* 2010). Furthermore, in finches, frontonasal mesenchymal *Bmp4* expression is linked to the regulation of beak length and calcium-dependent calmodulin signaling is associated with beak length (Abzhanov *et al.* 2004, 2006; Szabo-Rogers *et al.* 2010). In mice, Wnt and FGF signaling also regulate the regional proliferation that leads to facial outgrowth (Szabo-Rogers *et al.* 2010).

4.2.4 Genetic regulation of skeletogenesis

The transformation of undifferentiated mesenchymal tissue into bone occurs either directly via intramembranous ossification, or indirectly through a cartilage precursor via endochondral ossification (White, 2000; Hildebrand and Goslow 2001). In both processes, mesenchymal cells first differentiate into osteochondroprogenitor cells, regulated by the transcription factor Sex determining region Y-box 9 (Sox9) (Karsenty 2008; Karsenty *et al.* 2009). Subsequently, progenitor cells are differentiated into either chondrocytes, which form cartilage, or osteoblasts, which form bone. For more detailed accounts of these processes, see Goldring *et al.* (2006) (chondrocyte differentiation), as well as Ducy *et al.* (2000), Yamaguchi *et al.* (2000), and Chen *et al.* (2012) (osteoblast differentiation).

Chondrogenesis, or cartilage formation, occurs in two steps: the differentiation of mesenchymal condensations into nonhypertrophic chondrocytes, and the subsequent differentiation into hypertrophic chondrocytes. The first differentiation event is marked by a change in the composition of the extracellular matrix produced by these cells from type I collagen to type II collagen (Karsenty *et al.* 2009). Sox9, with the aid of closely related Sox5 and Sox6, controls the proliferation of nonhypertrophic chondrocytes by regulating the expression of genes involved in the production of type II collagen and aggrecan (Karsenty 2008; Karsenty *et al.* 2009). Peripheral mesenchymal cells that do not undergo this differentiation continue to produce type I collagen and form the perichondrium, which influences later stages of chondrogenesis (Karsenty *et al.* 2009).

Nonhypertrophic chondrocytes are kept in a resting proliferating state by inhibition of the cell cycle progression, which is maintained by FGF signaling with the perichondrium (Karsenty *et al.* 2009). The transcription factor runt-related 2 (Runx2) inactivates FGF signaling, allowing

the cells to exit the cell cycle, hypertrophy, and begin producing type X collagen (Karsenty 2008; Karsenty *et al.* 2009). These conditions favor mineralization of the extracellular matrix and the vascular invasion of cells of the osteoblast lineage, which fill the cartilage mold and replace it with a bone matrix of type I collagen (Karsenty *et al.* 2009).

In the case of intramembranous ossification, osteochondroprogenitor cells differentiate directly into osteoblasts under the regulation of the transcription factors Runx2 and Osterix (*Osx*) (Karsenty 2008). Runx2, the earliest determinant of osteoblast differentiation, promotes the synthesis of osteocalcin, an osteoblast-specific hormone, under the regulation of several other transcription factors. Inhibitors include: Twist-1, whose transient coexpression with Runx2 affects the timing of osteogenesis; signal transducer and activator of transcription 1 (*Stat1*); and Scnrr3 (*Shn3*). Enhancers include: muscle segment homeobox homolog 2 (*MSX2*), which functions upstream of Runx2; bagpipe homeobox gene 1 homolog (*Bapx1*); and *SATB2* (Karsenty 2008; Karsenty *et al.* 2009). *Osx* acts downstream of Runx2, where it interacts with nuclear factor of activated T cells 1 (*Nfatc1*) to begin type I collagen production (Karsenty 2008).

Osteoblast differentiation is further regulated by the secretion of Indian hedgehog (*Ihh*), FGFs, Wnt proteins, and LDL receptor-related protein 5 (*LRP5*) (Karsenty *et al.* 2009; Marie 2012). *LRP5* is not expressed in osteoblasts, but instead, through secretion in the duodenum, regulates the expression of the enzyme that biosynthesizes serotonin, an inhibitor of osteoblast proliferation (Karsenty *et al.* 2009). Proliferation is also affected by the hormone leptin, which acts through the sympathetic nervous system to decrease bone formation and increase bone resorption.

Lastly, Activating transcription factor 4 (*ATF4*) acts at a later stage of differentiation to activate *Osteocalcin*, leading to type I collagen production (Karsenty *et al.* 2009). This factor also enhances expression of a gene coding for the differentiation of osteoclasts, the cell type responsible for the resorption of bone (White 2000; Karsenty 2008; Karsenty *et al.* 2009). Regulators of *ATF4*, including the activator Ribosomal S6 kinase 2 (*Rsk2*) and the inhibitor Neurofibromatosis 1 (*NF1*), play important roles in bone remodeling (Karsenty 2008).

4.3 Candidate genes for brachycephaly based on mouse models

Our understanding of how the abovementioned genes and transcription factors function together to direct craniofacial development is largely informed by studying the effects of perturbations to this system. From a genetic perspective, these defects are essential to characterization of normal development, whereas from a morphological perspective, they supply valuable insight as to how phenotypic diversity may arise. In the case of craniofacial variation across domestic dog breeds, mouse genetic mutants that approximate canine brachycephaly provide such information.

The mouse mutant phenotypes of three sets of genes in particular stand out as possible analogs of brachycephalic dogs: *Tcof1*, *Msx1* and *Msx2*, and *Fgfr2c*. The human homologs of these genes are also each linked to congenital cranial malformations. Mutations in *TCOF1* are associated with Treacher Collins syndrome (TCS, OMIM number 154500), an autosomal dominant syndrome characterized by cleft palate and hypoplasia of the facial bones, particularly the zygomatic complex and the mandible (Sakai and Trainor 2009; Trainor *et al.* 2009; Masotti *et al.* 2009; Beygo *et al.* 2011). Mutations in *MSX2* are associated with two autosomal dominant

disorders: parietal foramina-1 (PFM1, OMIM number 168500), which is characterized by persistent calvarial foramina (Satokata *et al.* 2000; Ishii *et al.* 2003), and isolated craniosynostosis type 2 (OMIM number 604757), wherein the sutures of the calvarial bones fuse prematurely (Ishii *et al.* 2003). Craniosynostosis also occurs as part of Crouzon syndrome (OMIM number 123500), an autosomal dominant syndrome caused by mutations in the gene encoding for FGFR2 (Galvin *et al.* 1996; Mangasarian *et al.* 1997; Mahnsukhani *et al.* 2000; Eswarakumar *et al.* 2004; Park *et al.* 2012).

Below, I describe the roles of the murine genes *Tcofl*, *Msx1* and *Msx2*, and *Fgfr2c* in craniofacial development and the mutant phenotypes produced by alteration of their expression. I then compare these cranial phenotypes to the shape differences characterizing brachycephalic dog breed crania from the “wild-type” wolf cranium, and evaluate each gene’s potential as a mechanism for brachycephaly in dogs.

4.3.1 *Tcofl*

4.3.1.A The role of *Tcofl* in neural crest cell generation and proliferation

The expression of *Tcofl* in neuroepithelial cells is required for the generation and proliferation of neural crest cells that migrate to form the craniofacial mesenchyme (Dixon *et al.* 2006; Sakai and Trainor 2009). *Tcofl* encodes a phosphoprotein called treacle, which is localized to the nucleolus of the cell (Marsh *et al.* 1998). In the nucleolus, treacle plays an important role in ribosome biogenesis, where it binds to Upstream binding factor (UBF) to form a complex with Promoter selectivity factor (SL1) that participates in RNA polymerase 1 activity (Dixon *et al.* 2006; Jones *et al.* 2008). Furthermore, Dixon and colleagues (2006) have shown that this process occurs downstream of BMP and Wnt signaling, but upstream of Snail1 expression, all of which regulate the cell cycle of neural crest cells during induction. Therefore, a functional role for treacle in generating mature ribosomes during the cell cycle progression of neural crest cells has been proposed (Dixon *et al.* 2006; Sakai and Trainor 2009).

In mouse models carrying a germ-line mutation in one allele of *Tcofl* (notated as *Tcofl*^{+/-}), insufficient ribosome biogenesis arrests the cell cycle, leading to neuroepithelial apoptosis and the reduced proliferation of neural crest cells (Dixon *et al.* 2000, 2006). Jones *et al.* (2008) have shown that the cause of this reduction is activation of the Tumor protein 53 (p53)–dependent apoptotic pathway in the absence of *Tcofl* expression (Sakai and Trainor 2009). As a result, *Tcofl*^{+/-} mice exhibit a thinner neural plate and approximately 22% fewer migrating cranial neural crest cells than wild-type mice (measured as a proportion of the total number of craniofacial mesenchyme cells) (Dixon *et al.* 2006).

4.3.1.B The craniofacial phenotype of *Tcofl* haploinsufficiency

As a result of the reduction in neural crest cells in the craniofacial mesenchyme, the skeletal elements formed from these mesenchymal condensations are underdeveloped. *Tcofl*^{+/-} neonates have smaller, more domed heads that are shortened along the anteroposterior axis (Dixon *et al.* 2000, 2006). Whole-mount skeletal analysis at E17.5 indicates that relative to wild-type crania, *Tcofl*^{+/-} crania exhibit a domed cranial vault, underdeveloped and abnormally

shaped nasals and frontals, truncated premaxillae, maxillae, and palatines, a shortened mandible, and underdeveloped temporals (Dixon *et al.* 2000, 2006). Of particular interest is the severe frontonasal hypoplasia, which produces a short-faced phenotype in which a nearly-90 degree angle exists between the reduced nasals and domed frontals (Dixon *et al.* 2006; Sakai and Trainor 2009; Trainor *et al.* 2009).

4.3.1.C *Tcofl* as a candidate gene for canine brachycephaly

The third research question presented in this study asks whether the patterns of shape differences between the gray wolf and brachycephalic dogs are comparable to phenotypes produced by genetic pathways identified in mouse developmental genetic studies. The first of three hypotheses proposed to address this question, Hypothesis 3A, posits that modification of the gene *Tcofl* has provided a mechanism for brachycephalism in dogs via coordinated shortening of both the frontal and nasal bones. The craniofacial hypoplasia of *Tcofl*^{+/-} mouse mutants affects the development of both bones, creating a short face phenotype comparable to canine brachycephaly (Dixon *et al.* 2006).

Before evaluating this hypothesis further, it is necessary to review the shape differences that characterize the three groups of brachycephalic dogs described in Chapter 3. Relative to the gray wolf, large Mastiff-like brachycephalic breeds (e.g., the Boxer and Bulldog) exhibit rostro-dorsally positioned frontals, caudally translated and reduced nasals, and shorter, wider rostra that are tilted at the dorsal-most elements. Smaller Mastiff-like and toy brachycephalic breeds (e.g., the Pug, Pekingese, and French Bulldog) differ from the gray wolf in terms of the same shortened rostra, but to a greater degree. These breeds display a rostro-dorsal expansion of the nasals similar to that of the frontals that is not seen in larger Mastiff-like breeds, creating a dorsal curvature and stop angled close to 90 degrees. Lastly, the Chihuahua exhibits a third brachycephalic pattern of shape difference from the wolf in which reduction in the length of the rostral bones is not combined with an increase in snout width. Also absent from this pattern is a dorsal tilt of the snout. Furthermore, unlike the small Mastiff-like and toy breeds, the Chihuahua displays uniformly angled nasal bones that do not create a dramatic stop at the midface.

In comparing these three patterns to the phenotype of *Tcofl* haploinsufficient mice, overall similarities are undeniable. The alterations in frontal and nasal bone morphology in the mouse mutants produce a dished face and domed forehead that parallels the facial bone arrangement in the Pug/Pekingese/French Bulldog brachycephalic pattern. In these breeds, a short frontal bone bulges rostro-dorsally above short nasal bones that curve dorsally at their caudal end. This feature does not appear in the Boxer/Bulldog or Chihuahua patterns, making them less similar to the *Tcofl* mouse mutant phenotype.

In conclusion, given the similarity between *Tcofl*^{+/-} mutants and brachycephaly in the Pug, Pekingese, and French Bulldog, the hypothesis that this short face phenotype is achieved via the coordinated shortening of the frontal and nasal bones, due to modification of *Tcofl*, cannot be rejected for this group of breeds. This mechanism does not appear to operate in the Boxer and Bulldog or the Chihuahua, which, despite exhibiting both shortened frontal and nasal bones, do not display the same extreme midfacial stop phenotype observed in the Pug, Pekingese, French Bulldog, and *Tcofl* mutant mice.

Dixon and Dixon (2004) have shown that the penetrance and severity of the *Tcofl*^{+/-} phenotype vary depending upon the genetic background of the mice in which the mutation is

generated. Some strains of mice in which *Tcofl* is modified exhibit the full range of cranial defects, while others present malformations of the skull vault but not the nasal region. This suggests that the genetic background of dog breeds may also play a large role in determining phenotypic variability across both breeds and the brachycephalic breed categories identified in this study.

4.3.2 *Msx1* and *Msx2*

4.3.2.A The role of *Msx1* and *Msx2* in frontal bone development

The homeobox genes *Msx1* and *Msx2* transcriptionally regulate cellular proliferation and differentiation at a number of levels during embryonic development (Gilbert 2000; Han *et al.* 2007). In frontal bone development, the transcription factor *Msx1* has been shown to interact with *Dlx5* to regulate differentiation of neural crest–derived mesenchymal cells into osteoblasts (Chung *et al.* 2010). *Msx2* has been shown to cooperate with *Twist* in the regulation of differentiation and proliferation of the same mesenchymal cells (Satokata *et al.* 2000; Ishii *et al.* 2003). The combined activity of *Msx1* and *Msx2* is required for cranial neural crest survival (Ishii *et al.* 2005). Specifically in the frontal bone, the combination of *Msx1* and *Msx2* act upstream of *Runx2* to control osteoblast differentiation (Han *et al.* 2007). However, this activity is specific to the neural crest–derived mesenchyme cell subpopulation: *Msx* genes also act to inhibit BMP signaling activity and subsequent osteoblast differentiation in an ectocranial layer of cells that is not allocated to bone formation (Roybal *et al.* 2010).

Double knockout mice for *Msx1* and *Msx2* (notated as *Msx1*^{-/-};*Msx2*^{+/-}, *Msx1*^{+/-};*Msx2*^{-/-}, and *Msx1*^{-/-};*Msx2*^{-/-} for *Msx1* null mutants in the background *Msx2* haploinsufficiency, *Msx2* null mutants in the background of *Msx1* haploinsufficiency, and double null mutants, respectively) exhibit failure of neural crest–derived mesenchymal frontal bone precursors to differentiate into osteoblasts (Han *et al.* 2007; Roybal *et al.* 2010). This is due to the failure of mesenchymal cells of *Msx1*^{-/-};*Msx2*^{-/-} mutants to express either *Runx2* or *Osx* (Han *et al.* 2007). *Msx1*^{-/-};*Msx2*^{-/-} mutants also exhibit increased BMP signaling in early-migrating neural crest mesenchyme, which drives heterotopic bone formation (Roybal *et al.* 2010).

4.3.2.B The craniofacial phenotype of *Msx1* and *Msx2* null mutants

Relative to wild-type mice, *Msx1*^{-/-} mutants exhibit more rounded frontal bones, distally shortened maxillae and mandibles, and a complete cleft of the secondary palate (Satokata and Maas 1994; Chung *et al.* 2010). *Msx2*^{-/-} mice are characterized by a large frontal foramen due to defective frontal bone ossification (Satokata *et al.* 2000), a trait that is further exaggerated in *Msx2*-*Twist* double mutants (Ishii *et al.* 2003). Double knockouts of *Msx1* and *Msx2* present a range of cranial defects: in both *Msx1*^{-/-};*Msx2*^{+/-} and *Msx1*^{+/-};*Msx2*^{-/-} mutants, the midline frontal foramen observed in *Msx2*^{-/-} mutants is enlarged (Ishii *et al.* 2005; Han *et al.* 2007). This feature is combined with a domed skull vault (more pronounced in *Msx1*^{-/-};*Msx2*^{+/-} mutants) and a reduced rostrum characterized by shortened nasals and maxillae (Han *et al.* 2007). Double knockout mutants also possess ectopic islands of bone that fill the space between the reduced frontal bones anterior to the parietal (Roybal *et al.* 2010). Lastly, *Msx1*^{-/-};*Msx2*^{-/-} mice exhibit no

calvarial ossification—although most of the cranial cartilage persists, the only ossified elements in the cranium include the rudimentary mandible, maxillae, and cranial base (Ishii *et al.* 2005; Han *et al.* 2007).

4.3.2.C *Msx1* and *Msx2* as candidate genes for canine brachycephaly

Hypothesis 3B postulates that modification of the genes *Msx1* and *Msx2* provides a mechanism for brachycephaly in dogs via shortening of the frontal bones only, which in turn displaces the nasal bones. Because these genes only affect the development of frontal bone mesenchyme, it can be assumed that the reduced rostrum and nasals of the mouse mutants are secondary effects. *Msx1*^{-/-};*Msx2*^{-/-} mice lack bony calvaria entirely and are missing most of the other skeletal elements of the skull. However, the null mutations of either *Msx1* or *Msx2* in the haploinsufficient background of the other produce a phenotype in which a large frontal foramen defect is paired with a domed skull and shortened nasals and upper jaws (Han *et al.* 2007).

Msx1^{-/-};*Msx2*^{+/-} and *Msx1*^{+/-};*Msx2*^{-/-} mice do not display a significant curvature of the shortened nasal bones. The presence of the frontal foramen creates a shorter, domed forehead, but the transition from frontals to nasals at the midface is not sharply angled (Han *et al.* 2007). This feature aligns the phenotype closer to the Boxer/Bulldog and Chihuahua forms of brachycephaly than to the Pug/Pekingese/French Bulldog form (reviewed above in section 4.3.1.C). However, the shorter snout of the mutant mice is tilted dorsally at the rostral end, a trait that is observed in the Boxer/Bulldog pattern but not in the Chihuahua (Han *et al.* 2007). As a result, the similarity between the *Msx1*^{-/-};*Msx2*^{+/-} and *Msx1*^{+/-};*Msx2*^{-/-} mutant phenotypes and the form of brachycephaly observed in Boxers and Bulldogs precludes the rejection of Hypothesis 3B.

Similar to the case of *Tcofl* expression, phenotypic variation between single knockout mutants of *Msx1* and *Msx2* and double knockouts of both genes suggests that genetic background plays an important role in this system (Han *et al.* 2007; Roybal *et al.* 2010). Although no brachycephalic dog possesses the midline frontal foramen observed in most *Msx* mouse gene mutants, it is possible that given the right genetic background, a less severe malformation of the frontal bone could still produce the short face phenotype.

4.3.3 *Fgfr2c*

4.3.3.A The role of *Fgfr2c* in osteoblast development and cranial suture fusion

FGF signaling plays an important role in osteogenic cell proliferation and differentiation in the developing skull vault: differential levels of FGF ligand modulate the expression of *Fgfr2* and *Fgfr1* in regions of osteoblast precursor proliferation and differentiation, respectively (Morriss-Kay 2001; Iseki *et al.* 1999). Hence, the receptor protein encoded by *Fgfr2* regulates osteogenic proliferation, whereas *Fgfr1* regulates differentiation (Iseki *et al.* 1999). In this manner, sutural development is controlled by an FGF signaling–regulated balance between proliferation and differentiation (Mai *et al.* 2010).

Of the two major isoforms of *Fgfr2*, *Fgfr2c* is expressed in these mesenchymal condensations (Eswarakumar *et al.* 2002). *Fgfr2c*^{-/-} mice initially experience delayed

ossification in the sphenoid, but during later stages of skeletal growth experience a shift towards differentiation in the balance between proliferation and differentiation. This results in an early stop to growth and premature fusion of the coronal suture (Eswarakumar *et al.* 2002). The introduction of a gain-of-function mutation in *Fgfr2c* similar to that seen in human *FGFR2* Crouzon syndrome mutations increases *Spp1* and *Runx2* expression and proliferation in osteoprogenitor cells, which leads to rapid bone growth and premature suture fusion as well (Eswarakumar *et al.* 2004).

4.3.3.B The craniofacial phenotype of *Fgfr2c* mutants

As mentioned above, both loss- and gain-of-function mutations in *Fgfr2c* lead to craniosynostosis of the coronal suture (Eswarakumar *et al.* 2002, 2004). Paired with this phenotype are a suite of features that include a shortened face and a domed skull. Specifically, the base of the skull is shortened in the sphenoid region, the nasomaxillary region is shortened and down-curved, and the secondary palate is cleft (Eswarakumar *et al.* 2002, 2004, 2006). All mutants exhibit midfacial hypoplasia and alterations in nasal cartilage size and shape (Eswarakumar *et al.* 2002, 2004, 2006; Mai *et al.* 2010).

4.3.3.C *Fgfr2c* as a candidate gene for canine brachycephaly

The third mechanism considered is presented in Hypothesis 3C, which states that modification of *Fgfr2c* contributes to brachycephaly in dogs via altered sutures in the skull vault, resulting in shortening and angling of both the frontal and nasal bones. Unfortunately, it is difficult to determine whether the coronal sutures of brachycephalic dogs fuse earlier than those of mesaticaphalic dogs without the appropriate comparative ontogenetic series. However, a comparison of the morphology resulting from premature suture fusion in mice with the shape of adult brachycephalic dogs may still provide some insight.

As in the cases of *Tcof1* and *Msx1* and *Msx2*, modification of *Fgfr2c* produces a short face phenotype in mice that is characterized by underdevelopment of the facial bones and a domed braincase. However, unlike the phenotypes of these other genes, *Fgfr2c* loss- and gain-of-function mutant crania exhibit both a ventrally angled snout and an anteroposteriorly shortened cranial base (Eswarakumar *et al.* 2002, 2004). All three patterns of canine brachycephaly identified in this study include shortening of the cranial base proportionate to the reduction in facial length (see Figures 3.21 and 3.22). Even so, the brachycephalic form of the Chihuahua does not exhibit the dorsally tilted snout of the Boxer/Bulldog and Pug/Pekingese/French Bulldog forms. Based on these similarities and differences, Hypothesis 3C can be rejected for the latter two forms of canine brachycephaly, but not the Chihuahua form.

4.4 Discussion

The three candidate genes considered in this study represent three distinct mechanisms for producing a brachycephalic phenotype in the mouse. These are achieved by

perturbations/modifications of the genetic regulation of craniofacial development at three different stages. The protein encoded by *Tcofl* is required for neural crest cell generation and proliferation. Inactivation of this gene disrupts this stage of development by inhibiting ribosome biogenesis and the cell cycle progression of neural crest cells, resulting in a brachycephalic face (Dixon *et al.* 2006). In contrast, *Msx1* and *Msx2* are required for the differentiation of neural crest-derived mesenchyme into osteoblasts in the frontal bone. Insufficiency of these genes affects the downstream signaling of *Runx2* and *Osx* activity and osteoblasts fail to differentiate, producing a frontal bone defect that also results in brachycephaly (Han *et al.* 2007). Lastly, *Fgfr2c* regulates the proliferation of osteoprogenitor cells in the skull vault. Modification of this gene to either limit or enhance its function affects cell proliferation negatively or positively, leading to premature coronal suture fusion via either decreased or precocious bone development, respectively (Eswarakumar *et al.* 2002, 2004). Craniosynostosis produced by either mechanism results in a brachycephalic face.

These examples demonstrate that brachycephaly in the mouse can be generated by modifying the processes described in sections 4.2.3 and 4.2.4 at multiple stages: neural crest cell formation at the dorsal neural tube, and both the differentiation and proliferation of osteoprogenitor cells from post-migratory neural crest cells in the mesenchyme of the face. The brachycephalic phenotypes produced by modification of each candidate gene are superficially similar—they each include short facial bones and a domed forehead. However, more subtle differences characterize each phenotype as well. By comparing these different phenotypes with brachycephalic dog crania, the likelihood that the same mechanisms play a role in dog morphological variation can be evaluated.

The hypothesis that modification of *Tcofl* contributes to canine brachycephaly (Hypothesis 3A) could not be rejected for the Pug/Pekingese/French Bulldog group. Both *Tcofl*^{-/-} mutants and representatives of these breeds exhibit a pattern of brachycephaly that features extremely angled nasal bones at the midface, resulting in a pronounced stop in the latter (Dixon *et al.* 2006). From this similarity it can be extrapolated that the shape differences separating these brachycephalic breeds from the gray wolf may be related to differences in neural crest cell development.

The shape differences from the gray wolf that characterize the Boxer/Bulldog brachycephalic pattern may be the result of modified osteogenic differentiation in the frontal bone. The absence of a sharp midface angle and the presence of a dorsally tilted rostral snout are shared features of the short face phenotype of these breeds and *Msx1* and *Msx2* double mutants (Han *et al.* 2007; Roybal *et al.* 2010). As a result, Hypothesis 3B, that modification of *Msx1* and *Msx2* contributes to canine brachycephaly, cannot be rejected for this group.

Finally, *Fgfr2c* mutants exhibit a brachycephalic phenotype in which the snout is angled ventrally (Eswarakumar *et al.* 2002, 2004). The Chihuahua is unique among the brachycephalic breeds studied because it does not have a dorsally tilted snout—instead, the palate lies parallel to the plane of the ventral surface of the skull base, as seen in the gray wolf. Although the angle of the Chihuahua snout does not approach the ventral tilt seen in *Fgfr2c* mouse mutants, the lack of any dorsal angling in either the Chihuahua or the mutants precludes the rejection of Hypothesis 3C. Subsequently, the timing of coronal suture fusion may contribute to brachycephaly in this breed.

It should be made clear that the phenotypic comparisons made in this chapter between mutant mice and brachycephalic dogs address only qualitative similarities or differences in shape. This type of analysis is useful because it identifies patterns of morphological similarity

that are more descriptive than superficial categorical terms such as brachycephalic and non-brachycephalic (e.g., Bannasch *et al.* 2010). Hence, this detailed qualitative comparison functions to direct future comparisons between mice and dogs that are more resource-intensive and quantitative. For example, these qualitative comparisons are informative for choosing which genetic loci to target across domestic dog breeds in a genetic association study.

A more robust test of each hypothesis could also include a quantification of mouse mutant craniofacial morphological variation at the same level of detail as that performed for dogs in this study. The number of detailed quantitative studies of mouse mutant craniofacial morphology to date is limited. However, the work of Perlyn and colleagues (2006) is one example of such a study that is particularly relevant. The authors collected 35 three-dimensional landmarks from cranial MicroCT images of ten wild-type and ten *Fgfr2c* gain-of-function mutant mice, and used EDMA to quantify their shape differences. Further supporting the *Fgfr2c* mutant brachycephalic phenotype described above, the authors observed a statistically different skull shape between wild-type and mutant mice. In the latter, the nasal bones and posterior palate were significantly shorter but the length and width of the premaxilla remained unchanged from the wild-type (Perlyn *et al.* 2006). A direct comparison between GM data from mouse mutants and dogs would be possible only if both datasets share a common set of landmarks based on homologous morphological features.

It is also important to note that the list of potential candidate genes for brachycephaly is not limited to the three gene sets discussed here. These genes were chosen for examination based purely on the similarity between their associated mutant phenotypes and the characterization of brachycephaly presented in Chapter 3. Other candidate genes could be identified based on our knowledge of dog development. For example, Drake's (2004, 2011) analysis of heterochrony in the domestic dog indicated that the Chihuahua exhibits proportioned dwarfism. Sutter *et al.* (2007) identified a single allele variant of the gene *IGF1* that determines small size in dogs. Taking both findings into consideration, it is possible that the *IGF1* pathway may also influence brachycephaly in dogs.

Furthermore, only one type of genetic modification has been discussed thus far: mutations in the protein-coding or regulatory elements of a gene. Phenomena such as the gene-associated tandem repeat expansions and contractions identified by Fondon and Garner (2004, 2007) could have a significant effect on craniofacial variation. Brachycephaly could also be affected by epigenetic interactions between the developing face and brain (see Parsons *et al.* 2011).

Chapter 5: Conclusion

5.1 Research questions

This dissertation has examined the craniofacial morphologies of various brachycephalic dog breeds relative to the gray wolf. The main goal of the study has been to address the relationship between variation in this phenotype and variation at the genetic level, laying the groundwork for future studies of genetic association and cranial skeletal evolution. By using a three-dimensional geometric morphometric approach, I have successfully quantified the craniofacial shape differences between the gray wolf and domestic dog breeds that underlie brachycephaly in the latter. I then integrated these morphological data with evidence from the fields of dog phylogenetics (see Chapters 1 and 3) and mouse developmental genetics (see Chapter 4) to provide insight into the genetic basis of this phenotype. This insight applies to both the genetic mechanisms that have been utilized by dog breeders and that have been the target of natural selection over the course of canid and vertebrate evolution.

Here, I review the three questions posed at the beginning of this study:

(1) Are there significant distinctions in the patterns of shape differences between the crania of various brachycephalic breeds and the ancestral gray wolf?

(2) Do any distinctions in patterns of shape differences correspond to genetic relationships between breeds?

(3) Are these patterns of shape differences comparable to genetic pathways identified in mouse developmental genetic studies?

The results of the geometric morphometric analyses directly address Question 1. The implications of these results in the context of known genetic relationships between dog breeds and in the context of craniofacial developmental genetics in mice address Questions 2 and 3, respectively. I summarize these results and the responses to each research question below. This summary is followed by a brief discussion of their application to future genetic association studies, as well as to the study of the canid fossil record.

5.2 Findings

5.2.1 Response to research question 1

Geometric morphometric analyses indicated that distinct patterns of shape differences relative to the gray wolf do exist between various brachycephalic breeds. This confirmed the hypothesis that distinct craniofacial forms corresponding to specific breeds or groups of breeds exist within the larger brachycephalic category. Three distinct forms of canine brachycephaly were described: a Boxer/Bulldog form, a Pug/Pekingese/French Bulldog form, and a Chihuahua form.

Each form of brachycephaly includes the same superficial pattern of facial shortening relative to the gray wolf. However, the three forms are distinguished by the angle of the rostral snout and midface, as well as the width of the shortened rostrum. Relative to the gray wolf, the Boxer/Bulldog form is characterized by moderately rostro-dorsally positioned frontals and caudally translated and reduced nasals. These features are combined with shortened, dorsally

tilted elements of the rostral snout. The shorter rostrum of this form is also proportionately wider. The Pug/Pekingese/French Bulldog form differs from the gray wolf in a similar way, including the same shortened rostral-most snout elements, but to a greater degree, resulting in an even greater reduction in the relative length of the face. This form is also characterized by extremely angled nasal bones and a pronounced stop.

Lastly, the Chihuahua exhibits reduction of the rostral snout bones without an increase in snout width, relative to the gray wolf. In addition, the rostral snout is not angled dorsally in this form of brachycephaly—the plane of the palate is the same as that found in the wolf—and the nasals are more uniformly positioned rostro-dorsally along their anteroposterior length, creating a less dramatic stop.

5.2.2 Response to research question 2

It was hypothesized that the toy dog and Mastiff-like dog groups represent separate, distinct brachycephalic forms. However, both the Chihuahua form and the Pug/Pekingese/French Bulldog form exist within the toy dog group. In addition, both the Pug/Pekingese/French Bulldog form and Boxer/Bulldog form are represented in the Mastiff-like dog group. As a result, Hypothesis 2 is not supported: the groups of breeds represented by these three distinct forms of brachycephaly do not correspond to the genetic groupings described by vonHoldt *et al.* (2010).

The genetic groupings used to address this hypothesis are based on 5- and 10-SNP haplotypes. However, several of the designations arrived at via genetic distance analysis conflict with the historical breed groupings used by international kennel clubs. For example, the Chihuahua and Pug are genetically assigned to the toy dog group, but have traditionally been included in the ancient dog and Mastiff-like dog groups, respectively (vanHoldt *et al.* 2010). This suggests that breeds with similar origins have diverged to such a great extent from their original common stock that they are now more genetically similar to other breeds that share the same trait for which they have been bred over many generations. The Pug, for example, after being the subject of intense selection for smaller size relative to other Mastiff-like dogs, may now be more genetically similar to other dogs bred for small size. This result would be expected if the same established small dog breed were repeatedly crossbred with different incipient breeds to introduce small size. Similarly, if dogs bred for fighting did not contribute to New World dog lineages, this would explain the lack of Mastiff-like dog features in the brachycephalic Chihuahua.

5.2.3 Response to research question 3

Three genetic pathways involved in mouse craniofacial development were presented as candidates for mechanisms underlying canine brachycephaly. Qualitative comparison of the mutant phenotypes of mice in which these pathways had been altered and craniofacial variation among brachycephalic domestic dog breeds indicated that each candidate gene or set of genes may be associated with one of the three forms of canine brachycephaly.

The gene *Tcofl* is involved in the generation and proliferation of cranial neural crest cells. Partial inactivation of this gene in mice produces a brachycephalic phenotype characterized by a pronounced stop (Dixon *et al.* 2006). Therefore, the hypothesis that

modification of *Tcofl* contributes to canine brachycephaly could not be rejected for the Pug/Pekingese/French Bulldog group.

The genes *Msx1* and *Msx2* regulate osteoblast differentiation in the frontal bone. Double knockout mice are brachycephalic and exhibit a moderate midfacial angle and a dorsally tilted rostral snout (Han *et al.* 2007). Due to the similarities between these mutant mice and the Boxer/Bulldog form, the hypothesis that modification of *Msx1* and *Msx2* contributes to canine brachycephaly could not be rejected for this group.

The FGF signaling gene *Fgfr2c* regulates osteoblast proliferation in the skull vault (Iseki *et al.* 1999). Both loss- and gain-of-function mutations in this gene in mice lead to craniosynostosis and brachycephaly (Eswarakumar *et al.* 2004, 2006). *Fgfr2c* mouse mutants have ventrally angled snouts and are most similar to the Chihuahua form, which does not include the dorsally angled snout that characterizes the other two forms of canine brachycephaly. As a result, the hypothesis that modification of *Fgfr2c* contributes to canine brachycephaly could not be rejected for the Chihuahua.

5.3 Future directions

5.3.1 Genetic association

The results of this study provide a foundation for future work associating genotypic and phenotypic variation in the domestic dog. Association studies to date have had limited success for craniofacial phenotypes (e.g., Haworth *et al.* 2001a,b, 2007), highlighting the need for more detailed quantification of this type of morphological variation. Here, it has been demonstrated that three-dimensional geometric morphometric shape analyses sufficiently meet this requirement. Once quantified, it is also necessary to understand how this variation is patterned across breeds. The analyses in this dissertation have shown that brachycephaly is a complex phenotype that occurs in at least three distinct forms across dog breeds.

Comparison of the three forms of canine brachycephaly with mouse mutant phenotypes has provided resolution at the genetic level as well. The choice of genetic loci to target is an important consideration for association studies. Based on qualitative similarities between brachycephalic dog and mutant mouse morphology, three sets of candidate genes have been identified in this study. These candidate genes provide the basis for more focused studies of genetic association in the future. For example, variation at the *Tcofl* locus must be explored in brachycephalic breeds such as the Pug, Pekingese, and French Bulldog; variation in the *Msx1* and *Msx2* loci in the Boxer and Bulldog; and variants at the *Fgfr2c* locus in the Chihuahua.

5.3.2 The canid fossil record

In domestic dogs, short faces have been artificially selected for by breeders. The motivation underlying this selection has been both functional and aesthetic (Bannasch *et al.* 2010). In fighting dogs, shorter rostra have been selected for stronger bite forces, whereas in toy and companion dogs, this same phenotype has been selected for its resemblance to the face of an infant (Ellis *et al.* 2009; Bannasch *et al.* 2010). Despite the fact that these phenotypes in dogs

are the products of artificial selection, their developmental genetic basis may parallel that of similar naturally occurring phenotypic variation in the Canidae family.

The Canidae consist of three subfamilies: the Hesperocyoninae, the Borophaginae, and the Caninae. The Caninae are the only living representatives of the Canidae and include the gray wolf and the domestic dog described here. Both the Hesperocyoninae and Borophaginae included large, hypercarnivorous canids that evolved parallel cranial and dental features such as a domed forehead, short snout, and massive premolars (Wang and Tedford 2008). These features were most extreme in the extinct Borophagine species *Borophagus secundus* and *Epicyon haydeni*, whose robust crania and jaws approximated those of modern hyenas and were capable of comparable bone-crushing power (Tseng and Wang 2010).

It is possible that in selecting for stronger, heavier crania, the breeders of domestic fighting dogs exploited the same genetic mechanisms that produced the short snouts and domed foreheads of fossil canids under natural selection. A quantitative comparison of the brachycephalic phenotypes of dog breeds derived from dogs bred for fighting and the brachycephalic phenotypes of fossil hypercarnivorous canids will provide insight into this possibility.

A future direction of this dissertation research will be to examine similarities between the patterns of craniofacial morphological variation in extant and extinct canids. Before addressing the extreme morphologies of species such as *Borophagus secundus* or *Epicyon haydeni*, it will be important to characterize variation in a fossil species more closely related to the two members of the Caninae subfamily studied here. The extinct dire wolf, *Canis dirus*, provides an excellent opportunity to do so. *C. dirus*, which is known from the early to late Pleistocene in both North and South America, is characterized by a large robust skull with a broad rostrum and less convex frontal bones, relative to *C. lupus* (Leidy 1858, 1869; Nowak 1979). Importantly, large samples of *C. dirus* crania have been collected from the Rancho La Brea asphalt bed locality in southern California and are accessible from the University of California Museum of Paleontology and the Los Angeles County Museum of Natural History (Merriam, 1906, 1908, 1911, 1912; Woodard and Marcus, 1973; Akersten *et al.* 1983).

Geometric morphometric analysis of craniofacial shape variation in *Canis dirus* and other extinct canids has the potential to identify shared patterns of brachycephaly with modern dog breeds. As a result, insight may be gained into the genetic basis of such morphologies in the fossil record and the course of their natural selection during canid evolution. Due to its unique history of artificial selection and resulting phenotypic diversity, the domestic dog is an exceptionally powerful tool for drawing connections between genotype and phenotype in both extant and extinct taxa.

References

- Abzhanov, A., M. Protas, B. R. Grant, P. R. Grant and C. J. Tabin. 2004. Bmp4 and morphological variation of beaks in Darwin's finches. *Science* **305**: 1462-1465.
- Abzhanov, A., W. P. Kuo, C. Hartmann, B. R. Grant, P. R. Grant and C. J. Tabin. 2006. The calmodulin pathway and evolution of elongated beak morphology in Darwin's finches. *Nature* **442**: 563-567.
- Ackermann, R. R. 2005. Ontogenetic integration of the hominoid face. *J. Hum. Evol.* **48**: 175-197.
- Ahlström, T. 1996. Sexual dimorphism in medieval human crania studied by three-dimensional thin-plate spline analysis. Pp. 415-421 in L. F. Marcus, M. Corti, A. Loy, G. Naylor and D. Slice, eds. *Advances in Morphometrics*. Plenum Press, New York.
- Akersten, W. A., C. A. Chaw and G. T. Jefferson. 1983. Rancho La Brea: status and future. *Paleobiology* **9**(3): 211-217.
- Akey, J. M., A. L. Ruhe, D. T. Akey, A. K. Wong, C. F. Connelly, J. Madeoy, T. J. Nicholas and M. W. Neff. 2010. Tracking footprints of artificial selection in the dog genome. *Proc. Natl. Acad. Sci. U. S. A.* **107**: 1160-1165.
- Allen, G. M. 1920. Dogs of the American aborigines. *Bull. Mus. Comp. Zool.* **63**: 431-517.
- Alpak, H., R. Mutus and V. Onar. 2004. Correlation analysis of the skull and long bone measurements of the dog. *Anat. Anz.* **186**(4): 323-330.
- American Kennel Club. 2006. *The Complete Dog Book. Official Publication of the American Kennel Club*. Ballantine Books, New York.
- Andersons, Ž. and J. Ozoliņš. 2000. Craniometrical characteristics and dental anomalies in wolves *Canis lupus* from Latvia. *Acta Theriol.* **45**: 549-558.
- Angleby, H. and P. Savolainen. 2005. Forensic informativity of domestic dog mtDNA control region sequences. *Forensic Sci. Int.* **154**: 99-110.
- Anstey, R. L. and D. A. Delmet. 1973. Fourier analysis of zooecial shapes in fossil tubular bryozoans. *Geology* **84**: 1753-1764.
- Arnason, U., A. Gullberg, A. Janke and M. Kullberg. 2007. Mitogenomic analyses of caniform relationships. *Mol. Phylogenet. Evol.* **45**: 863-874.
- Atchley, W. R. and B. K. Hall. 1991. A model for development and evolution of complex morphological structures. *Biol. Rev. Camb. Philos. Soc.* **66**: 101-157.

- Atchley, W. R., D. E. Cowley, C. Vogel, and T. McLellan. 1992. Evolutionary divergence, shape change, and genetic correlation structure in the rodent mandible. *Syst. Biol.* **41**(2): 196-221.
- Bannasch, D., A. Young, J. Myers, K. Truvé, P. Dickinson, J. Gregg, R. Davis, E. Bongcam-Rudloff, M. T. Webster, K. Lindblad-Toh, and N. Pederson. 2010. Localization of canine brachycephaly using an across breed mapping approach. *PLoS One* **5**: e9632.
- Bardeleben, C., R. L. Moore and R. K. Wayne. 2005. A molecular phylogeny of the Canidae based on six nuclear loci. *Mol. Phylogenet. Evol.* **37**: 815.
- Barton, L., S. D. Newsome, F.-H. Chen, H. Wang, T. P. Guilderson and R. L. Bettinger. 2009. Agricultural origins and the isotopic identity of domestication in northern China. *Proc. Nat. Acad. Sci. U. S. A.* **106**(14): 5523-5528.
- Baumann, F. and W. Huber. 1946. Über ausgewachsene und juvenile Schädelformen bei verschiedenen Hunderassen. *Arch. Jul-Klaus-Stiftung* **21**: 352-361.
- Becker, A. 1923. Das postembryonale Wachstum des deutschen Schäferhundsschädels. *Arch. F. Naturgesch. A.* **89**(9): 131-197.
- Belyaev, D. K. 1979. Destabilizing selection as a factor in domestication. *J. Hered.* **70**: 301-308.
- Benecke, N. 1987. Studies on early dog remains from northern Europe. *J. Archaeol. Sci.* **14**: 31-49.
- Berryere, T. G., J. A. Kerns, G. S. Barsh and S. M. Schmutz. 2005. Association of an Agouti allele with fawn or sable coat color in domestic dogs. *Mamm. Genome* **16**: 262-272.
- Beygo, J., K. Buiting, S. Seland, H.-J. Lüdecke, U. Hehr, C. Lich, B. Prager, D. R. Lohmann and D. Wiczorek. 2011. First report of a single exon deletion in *TCOF1* causing Treacher Collins syndrome. *Mol. Syndromol.* **2**: 53-59.
- Boas, F. 1905. The horizontal plane of the skull and general problem of the comparison of variable forms. *Science* **21**(544): 862-863.
- Bökönyi, S. 1975. Vlasac: an early site of dog domestication. Pp. 167-178 in A. T. Clason, ed. *Archaeozoological Studies*. North Holland, Amsterdam.
- Bolk, L. L. 1926. *Das Problem der Menschwerdung*. Gustav Fischer, Jena.
- Bookstein, F. L. 1977. The study of shape transformation since D'Arcy Thompson. *Math. Biosci.* **34**: 177-219.

- Bookstein, F. L. 1978. *The Measurement of Biological Shape and Shape Change*. Springer, Berlin.
- Bookstein, F. L. 1982. Foundations of morphometrics. *Annu. Rev. Ecol. Syst.* **13**: 451-470.
- Bookstein, F. L. 1986. Size and shape spaces for landmark data in two dimensions. *Stat. Sci.* **1**(2): 181-242.
- Bookstein, 1989. Principal warps: thin-plate splines and decomposition of deformations. *IEEE Trans. on Pattern Anal. Mach. Intell.* **2**(6): 567-585.
- Bookstein, F. L. 1991. *Morphometric Tools for Landmark Data*. Cambridge University Press, Cambridge.
- Bookstein, F. L., R. E. Strauss, J. M. Humphries, B. Chernoff, R. L. Elder and G. R. Smith. 1982. A comment upon the uses of Fourier methods in systematics. *Syst. Zool.* **31**(1): 85-92.
- Borgaonkar, D. S., O. S. Elliott, M. Wong and J. P. Scott. 1968. Chromosome study of four breeds of dog. *J. Hered.* **56**: 157-160.
- Boyko, A. R., R. H. Boyko, C. M. Boyko, H. G. Parker, M. Castelhamo, L. Corey, J. D. Degenhardt, A. Auton, M. Hedimbi, R. Kityo, E. A. Ostrander, J. Schoenebeck, R. J. Todhunter, P. Jones and C. D. Bustamante. 2009. Complex population structure in African village dogs and its implication for inferring dog domestication history. *Proc. Natl. Acad. Sci. U. S. A.* **106**: 13903-13908.
- Boyko, A. R., P. Quignon, L. Li, J. J. Schoenebeck, J. D. Degenhardt, K. E. Lohmueller, K. Zahao, A. Brisbin, H. G. Parker, B. M. vonHoldt, M. Cargill, A. Auton, A. Reynolds, A. G. Elkahoun, M. Castelhamo, D. S. Mosher, N. B. Sutter, G. S. Johnson, J. Novembre, M. J. Hubisz, A. Siepel, R. K. Wayne, C. D. Bustamante, E. A. Ostrander. 2010. A simple genetic architecture underlies morphological variation in dogs. *PLoS Biol.* **8**(8): e1000451.
- Braend, M. 1967. Serum transferrin of dogs. *Proceedings of the Xth European Conference on Animal Blood Groups and Biochemical Polymorphisms, Paris* **1966**:319-322.
- Breen, M. and R. Thomas. 2006. Karyotype and chromosomal organization. Pp. 159-178 in E. A. Ostrander, U. Giger and K. Linblad-Toh, eds. *The Dog and its Genome*. Cold Spring Harbor Laboratory Press, Cold Spring Harbor, New York.
- Brehm, H., K. Loeffler and H. Komeyli. 1985. The shapes of the canine skull. *Anat. Histol. Embryol.* **14**(4): 324-331.
- Broadbent, B. S., B. J. Broadbent and W. Golden. 1975. *Bolton standards of dentofacial developmental growth*. Mosby, St Louis.

- Buchalczyk, T., J. Dynowoski and S. Szteyn. 1981. Variations in the number of teeth and asymmetry of the skull in the wolf. *Acta Theriol.* **26**: 23-30.
- Burns, M. and M. N. Fraser. 1966. *Genetics of the Dog*. 2nd edition. Oliver and Boyd, Edinburgh and London.
- Cadiou, E., M. W. Neff, P. Quignon, K. Walsh, K. Chase, H. G. Parker, B. M. vonHoldt, A. Rhue, A. Boyko, A. Byers, A. Wong, D. S. Mosher, A. G. Elkahoun, T. C. Spady, C. André, K. G. Lark, M. Cargill, C. D. Bustamante, R. K. Wayne and E. A. Ostrander. 2009. Coat variation in the domestic dog is governed by variants in three genes. *Science* **326**: 150-153.
- Candille, S. I., C. B. Kaelin, B. M. Cattanach, B. Yu, D. A. Thompson, M. A. Nix, J. A. Kerns, S. M. Schmutz, G. L. Millhuaser and G. S. Barsh. 2007. A β -defensin mutation causes black coat color in domestic dogs. *Science* **318**: 1418-1423.
- Carrier, D. R., K. Chase and K. G. Lark. 2005. Genetics of canid skeletal variation: size and shape of the pelvis. *Genome Res.* **15**: 1825-1830.
- Chaix, L. 2000. A preboreal dog from the Northern Alps (Savoie, France). Pp. 49-59 in S. J. Crockford, ed. *Dogs Through Time: An Archaeological Perspective*. British Archaeological Reports, International Series 889.
- Chapman, R. E. 1990. Conventional Procrustes approaches. Pp. 251-267 in F. J. Rohlf and F. L. Bookstein, eds. *Proceedings of the Michigan Morphometrics Workshop*. University of Michigan Museum of Zoology, Ann Arbor.
- Chase, K., D. R. Carrier, F. R. Adler, T. Jarvik, E. A. Ostrander, T. D. Lorentzen and K. G. Lark. 2002. Genetic basis for systems of skeletal quantitative traits: principal component analysis of the canid skeleton. *Proc. Natl. Acad. Sci. U. S. A.* **99**: 9930-9935.
- Chase, K., D. F. Lawler, F. R. Adler, E. A. Ostrander and K. G. Lark. 2004. Bilaterally asymmetric effects of quantitative trait loci (QTLs): QTLs that affect laxity in the right versus left coxofemoral (hip) joints of the dog (*Canis familiaris*). *Am. J. Med. Genet.* **124A**: 239-247.
- Chase, K., D. F. Lawler, F. R. Adler, D. R. Carrier and K. G. Lark. 2005a. Genetic regulation of osteoarthritis: a QTL regulating cranial and caudal acetabular osteophyte formation in the hip joint of the dog (*Canis familiaris*). *Am. J. Med. Genet.* **135A**: 334-335.
- Chase, K., D. R. Carrier, F. R. Adler, E. A. Ostrander and K. G. Lark. 2005b. Interaction between the X chromosome and an autosome regulates size sexual dimorphism in Portuguese Water Dogs. *Genome Res.* **15**: 1820-1824.

- Chase, K., P. Jones, A. Martin, E. A. Ostrander and K. G. Lark. 2009. Genetic mapping of fixed phenotypes: disease frequency as a breed characteristic. *J. Hered.* **100**(suppl. 1): S37-S41.
- Chen, G., C. Deng and Y.-P. Li. 2012. TGF- β and BMP signaling in osteoblast differentiation and bone formation. *Int. J. Biol. Sci.* **8**: 272-288.
- Cheverud, J. M. 1982. Phenotypic, genetic, and environmental morphological integration in the cranium. *Evolution* **36**(3): 499-516.
- Cheverud, J. M. 1995. Morphological integration in the saddle-back tamarin (*Saguinus fuscicollis*). *Am. Nat.* **145**(1): 63-89.
- Cheverud, J. M. 1996. Quantitative genetic analysis of cranial morphology in the cotton-top (*Saguinus Oedipus*) and saddle-back (*S. fuscicollis*) tamarins. *J. Evol. Biol.* **9**: 5-42.
- Cheverud, J., J. L. Lewis, W. Bachrach and W. D. Lew. 1983. The measurement of form and variation in form: an application of three-dimensional quantitative morphology by finite-element methods. *Am. J. Phys. Anthropol.* **62**: 151-165.
- Cheverud, J. M., S. E. Hartman, J. T. Richtsmeier and W. R. Atchley. 1991. A quantitative genetic analysis of localized morphology in mandibles of inbred mice using finite elements scaling analysis. *J. Craniofac. Genet. Dev. Biol.* **11**(3): 122-137.
- Chung, I.-H., J. Han, J. Iwata and Y. Chai. 2010. *Msx1* and *Dlx5* function synergistically to regulate frontal bone development. *Genesis* **48**: 645-655.
- Clark, L. A., K. L. Tsai, J. M. Steiner, D. A. Williams, T. Guerra, E. A. Ostrander, F. Galibert and K. E. Murphy. 2004. Chromosome-specific microsatellite multiplex sets for linkage studies in the domestic dog. *Genomics* **84**: 550-554.
- Clark, P., G. E. Ryan and A. B. Czappon. 1975. Biochemical markers in the family Canidae. *Aust. J. Zool.* **23**: 411-417.
- Claude, J. 2008. *Morphometrics with R*. Springer, New York.
- Clutton-Brock, J. 1962. Near Eastern canids and the affinities of the Natufian dogs. *Z. Tierzucht. Zuchtungsbiol.* **76**(2/3): 326-333.
- Clutton-Brock, J. 1977. Man-made dogs. *Science* **197**(4311): 1340-1342.
- Clutton-Brock, J. 1979. The mammalian remains from the Jericho Tell. *Proc. Prehistoric Soc.* **45**: 135-157.

- Clutton-Brock, J. 1988. The carnivore remains excavated at Fell's cave in 1970. Pp. 188-195 in J. Hyslop, ed. *Travels and Archaeology in South America by Junius B. Bird*. University of Iowa Press, Iowa City.
- Clutton-Brock, J. 1992. The process of domestication. *Mammal. Rev.* **22**: 79-85.
- Clutton-Brock, J. 1995. Origins of the dog: domestication and early history. Pp. 7-20 in J. Serpell, ed. *The Domestic Dog, its Evolution, Behaviour and Interactions with People*. Cambridge University Press, Cambridge.
- Clutton-Brock, J. and P. Jewell. 1993. Origin and domestication of the dog. Pp. 21-31 in H. E. Evans, ed. *Miller's Anatomy of the Dog*. W. B. Saunders, Philadelphia.
- Clutton-Brock, J. and N. Noe-Nygaard. 1990. New osteological and C-isotope evidence on Mesolithic dogs: companions to hunters and fishers at Star Carr, Seamer Carr and Kongemose. *J. Archaeol. Sci.* **17**: 643-653.
- Cole, T. M. III. 1996. Historical note: early anthropological contributions to "geometric morphometrics." *Am. J. Phys. Anthropol.* **101**: 291-296.
- Coppinger, R. and R. Schneider. 1995. Evolution of working dogs. Pp. 21-47 in J. Serpell, ed. *The Domestic Dog, its Evolution, Behaviour and Interactions with People*. Cambridge University Press, Cambridge.
- Coppinger, R. P., J. Glendinning, E. Torop, C. Mathay, M. Sutherland and C. Smith. 1987. Degree of behavioral neoteny differentiates canid polymorphs. *Ethology* **75**: 89-108.
- Corner, B. D., S. Lele and J. T. Richtsmeier. 1992. Measuring precision of three-dimensional landmark data. *J. Quant. Anthropol.* **3**: 347-359.
- Creuzet, S., G. Couly and N. M. Le Douarin. 2005. Patterning the neural crest derivatives during development of the vertebrate head: insights from avian studies. *J. Anat.* **207**: 447-459.
- Daegling, D. J. and W. L. Jungers. 2000. Elliptical Fourier analysis of symphyseal shape in great ape mandibles. *J. Hum. Evol.* **39**: 107-122.
- Dahr, E. 1942. Über die Variation der Hirnschale bei wilden und zahmen Caniden. *Arkiv För Zoologi Stockholm* 33A (16): 1-56.
- Davis, S. and F. R. Valla. 1978. Evidence for the domestication of the dog 12,000 years ago in the Natufian of Israel. *Nature* **276**: 608-610.
- Darwin, C. 1859. *On the Origin of Species. A Facsimile of the First Edition*. Harvard University Press, Cambridge, Massachusetts.

- Darwin, C. 1868. *The Variation of Animals and Plants Under Domestication. Volume One.* The Johns Hopkins University Press, Baltimore.
- Dayan, T., D. Simberloff, E. Tchernov and Y. Yom-Tov. 1992. Canine carnassials: character displacement in the wolves, jackals and foxes of Israel. *Biol. J. Linn. Soc. Lond.* **45**: 315-331.
- Dechambre, E. 1949. La theorie de la foetalisation et la formation des races de chiens et de porcs. *Mammalia* **13**: 129-137.
- Degerbøl, M. 1961. On a find of a preboreal domestic dog (*Canis familiaris* L.) from Star Carr, Yorkshire, with remarks on other Mesolithic dogs. *Proc. Prehistoric Soc.* **27**: 35-55.
- de Serres, M. 1835. On the distinctive characters of the dog, the wolf, and the fox, as supplied by the skeleton. *Edinburgh New Philosophical Journal* **19**: 244-253.
- Detry, C. and J. L. Cardoso. 2010. On some remains of dog (*Canis familiaris*) from the Mesolithic shell-middens of Muge, Portugal. *J. Archaeol. Sci.* **37**: 2762-2774.
- Diewert, V. M. and S. Lozanoff. 1993. A morphometric analysis of human embryonic craniofacial growth in the median plane during primary palate formation. *J. Craniofac. Genet. Dev. Biol.* **13**(3): 147-161.
- Dixon, J. and M. J. Dixon. 2004. Genetic background has a major effect on the penetrance and severity of craniofacial defects in mice heterozygous for the gene encoding the nucleolar protein treacle. *Dev. Dyn.* **229**: 907-914.
- Dixon, J., C. Brakebusch, R. Fässler and M. J. Dixon. 2000. Increased levels of apoptosis in the pre-fusion neural folds underlie the craniofacial disorder, Treacher Collins syndrome. *Hum. Mol. Genet.* **9**(10): 1473-1480.
- Dixon, J., N. C. Jones, L. L. Sandell, S. M. Jayasinghe, J. Crane, J. P. Rey, M. J. Dixon and P. A. Trainor. 2006. *Tcof1*/Treacle is required for neural crest cell formation and proliferation deficiencies that cause craniofacial abnormalities. *Proc Nat Acad Sci USA* **103**:13403-13408.
- Dolgov, V. A. and O. L. Rossolimo. 1964. Dental abnormalities in *Canis lupus* Linnaeus, 1758. *Acta Theriol.* **8**: 237-244.
- Drake, A. G. 2004. *Evolution and Development of the Skull Morphology of Canids: An investigation of Morphological Integration and Heterochrony.* Ph.D. dissertation, University of Massachusetts Amherst.
- Drake, A. G. 2011. Dispelling dog dogma: an investigation of heterochrony in dogs using 3D geometric morphometric analysis of skull shape. *Evol. Dev.* **13**(2): 204-213.

- Drake, A. G. and C. P. Klingenberg. 2008. The pace of morphological change: historical transformation of skull shape in St. Bernard dogs. *Proc. R. Soc. B* **275**: 71-76.
- Drake, A. G. and C. P. Klingenberg. 2010. Large-scale diversification of skull shape in domestic dogs: disparity and modularity. *Am. Nat.* **175**(3): 289-301.
- Driscoll, C. A., D. W. Macdonald and S. J. O'Brien. 2009. From wild animals to domestic pets, an evolutionary view of domestication. *Proc. Natl. Acad. Sci. U. S. A.* **106**: 9971-9978.
- Drögemüller, C., E. K. Karlsson, M. K. Hytönen, M. Perloski, G. Dolf, K. Sainio, H. Lohi, K. Lindblad-Toh and T. Leeb. 2008. A mutation in hairless dogs implicates FOX13 in ectodermal dysplasia. *Science* **321**: 1462.
- Ducy, P., T. Schinke and G. Karsenty. 2000. The osteoblast: a sophisticated fibroblast under central surveillance. *Science* **289**: 1501-1504.
- Ehrlich, R. and B. Weinberg. 1970. An exact method for characterization of grain shape. *J. Sediment. Petrol.* **40**(1): 205-212.
- Ehrlich, R., R. B. Pharr, Jr. and N. Healy-Williams. 1983. Comments on the validity of Fourier descriptors in systematics: a reply to Bookstein et al. *Syst. Zool.* **32**(2): 202-206.
- Ellis, J. L., J. Thomason, E. Kebreab, K. Zubair and J. France. 2009. Cranial dimensions and forces of biting in the domestic dog. *J. Anat.* **214**: 362-373.
- Epstein, H. 1971. *The Origins of the Domestic Animals of Africa, Vol. 1.* Africana, New York.
- Espinosa, O. and J. M. Hancock. 2011. A gene-phenotype network for the laboratory mouse and its implication for systematic phenotyping. *PLoS ONE* **6**(5): e19693.
- Eswarakumar, V. P., E. Monsonogo-Ornan, M. Pines, I. Antonopoulou, G. M. Morriss-Kay and P. Lonai. 2002. The *IIIc* alternative of *Fgfr2* is a positive regulator of bone formation. *Development* **129**: 3783-3793.
- Eswarakumar, V. P., M. C. Horowitz, R. Locklin, G. M. Morriss-Kay and P. Lonai. 2004. A gain-of-function mutation of *Fgfr2c* demonstrates the roles of this receptor variant in osteogenesis. *Proc. Natl. Acad. Sci. U.S.A.* **101**: 12555-12560.
- Eswarakumar, V. P., F. Özcan, E. D. Lew, J. H. Bae, F. Tomé, C. J. Booth, D. J. Adams, I. Lax and J. Schlessinger. 2006. Attenuation of signaling pathways stimulated by pathologically activated FGF-receptor 2 mutants prevents craniosynostosis. *Proc. Natl. Acad. Sci. U.S.A.* **103**: 18603-18608.
- Evans, H. E. 1993. *Miller's Anatomy of the Dog.* W. B. Saunders, Philadelphia.
- Ewer, R. G. 1973. *The Carnivores.* Cornell University Press, Ithaca, New York.

- Ferson, S., F. J. Rohlf and R. K. Koehn. 1985. Measuring shape variation of two-dimensional outlines. *Syst. Zool.* **34**(1): 59-68.
- Fondon, J. W., III and H. R. Garner. 2004. Molecular origins of rapid and continuous morphological evolution. *Proc. Natl. Acad. Sci. U. S. A.* **101**: 18058-18063.
- Fondon, J. W., III and H. R. Garner. 2007. Detection of length-dependent effects of tandem repeat alleles by 3-D geometric decomposition of craniofacial variation. *Dev Genes Evol.* **217**: 79-85.
- Fox, M. W. 1964. Anatomy of the canine skull in low grade otocephaly. *Canad. J. Comp. Med. Vet. Sci.* **28**: 105-107.
- Fox, M. W. 1971. *Behaviour of Wolves, Dogs and Related Canids*. Jonathan Cape, London.
- Franchi, L., T. Baccetti, F. Stahl and J. A. McNamara, Jr. 2007. Thin-plate spline analysis of craniofacial growth in Class I and Class II subjects. *Angle Orthod.* **77**(4): 595-601.
- Fraser, G. J., C. D. Hulsey, R. F. Bloomquist, K. Uyesugi, N. R. Manley and J. T. Strelman. 2009. An ancient gene network is co-opted for teeth on old and new jaws. *PLoS Biology* **7**(2): e1000031.
- Frost, S. R., L. F. Marcus, F. L. Bookstein, D. P. Reddy and E. Delson. 2003. Cranial allometry, phylogeography, and systematics of large-bodied papionins (Primates: Cercopithecinae) inferred from geometric morphometric analysis of landmark data. *Anat. Rec. A Discov. Mol. Cell. Evol. Biol.* **275A**: 1048-1072.
- Galibert, F. and C. André. 2008. The dog: a powerful model for studying genotype-phenotype relationships. *Comp. Biochem. Physiol. Part D Genomics Proteomics* **3**(1): 67-77.
- Galvin, B. D., K. C. Hart, A. N. Meyer and M. K. Webster. 1996. Constitutive receptor activation by Crouzon syndrome mutations in fibroblast growth factor receptor (FGFR) 2 and FGFR2/New chimeras. *Proc. Natl. Acad. Sci. U.S.A.* **93**: 7894-7899.
- García-Moreno, J., M. D. Matocq, M. S. Roy, E. Geffen and R. K. Wayne. 1996. Relationship and genetic purity of the endangered Mexican wolf based on analysis of microsatellite loci. *Conserv. Biol.* **10**: 376-389.
- Garrod, D. A. E. and D. M. A. Bate. 1937. *The Stone Age at Mount Carmel, Excavations at the Wady-el-Mughara, I*. Oxford University Press, Oxford.
- Germonpré, M., M. V. Sablin, R. E. Stevens, R. E. M. Hedges, M. Hofreiter, M. Stiller and V. R. Després. 2009. Fossil dogs and wolves from Palaeolithic sites in Belgium, the Ukraine and Russia: osteometry, ancient DNA and stable isotopes. *J. Archaeol. Sci.* **36**(2): 473-490.

- Germonpré, M., M. Lázničková-Galetová and M. V. Sablin. 2012. Palaeolithic dog skulls at the Gravettian Předmostí site, the Czech Republic. *J. Archaeol. Sci.* **39**: 184-202.
- Gilbert, S. F. 2000. *Developmental Biology. Sixth Edition.* Sinauer Associates, Inc., Publishers, Sunderland, Massachusetts.
- Gipson, P. S., W. B. Ballard, R. M. Nowack and L. D. Mech. 2000. Accuracy and precision of estimating age of gray wolves by tooth wear. *J. Wildl. Manage.* **64**(3): 752-758.
- Goldring, M. B., K. Tsuchimochi and K. Ijiri. 2006. The control of chondrogenesis. *J. Cell. Biochem.* **97**: 33-44.
- Goodall, C. R. and P. B. Green. 1986. Quantitative analysis of surface growth. *Bot. Gaz.* **147**: 1-15.
- Goodall, C. 1991. Procrustes methods in statistical analysis of shape. *J. R. Stat. Soc. Series B Stat. Methodol.* **53**(2): 285-339.
- Goswami, A. 2006a. Morphological integration in the carnivoran skull. *Evolution* **60**: 169-183.
- Goswami, A. 2006b. Cranial modularity shifts during mammalian evolution. *Am. Nat.* **168**(2): 270-280.
- Götze, R. and F. Dornheim. 1926. Messungen und variationsstatistische Untersuchungen an Haushundschädeln, ein Beitrag zur Abstammungsfrage. *Zeitschrift für Tierzüchtung und Züchtungsbiologie einschließlich Tierernährung* **5**: 75-99.
- Gotteli, D., C. Sillero-Zubiri, G. D. Applebaum, M. S. Roy, D. J. Girman, J. García-Moreno, E. A. Ostrander and R. K. Wayne. 1994. Molecular genetics of the most endangered canid: the Ethiopian wolf, *Canis simensis*. *Mol. Ecol.* **3**: 301-312.
- Gould, S. J. 1977. *Ontogeny and Phylogeny.* Harvard University Press, Cambridge.
- Gower, J. C. 1975. Generalized Procrustes analysis. *Psychometrika* **40**(1): 33-51.
- Gowlett, J. A. J., R. E. M. Hedges, I. A. Law and C. Perry. 1987. Radiocarbon dates from the Oxford AMS System: Archaeometry datelist 5. *Archaeometry* **29**(1): 125-155.
- Gray, M. M., J. M. Granka, C. D. Bustamante, N. B. Sutter, A. R. Boyko, L. Zhu, E. A. Ostrander and R. K. Wayne. 2009. Linkage disequilibrium and demographic history of wild and domestic canids. *Genetics* **181**: 1493-1505.
- Grüneberg, H. and A. J. Lea. 1940. An inherited jaw anomaly in long-haired dachshunds. *J. Genet.* **39**: 285-296.

- Gunz, P. 2001. *Using semilandmarks in three dimensions to model human neurocranial shape*. Masters thesis. University of Vienna, Austria.
- Gustavsson, I. 1964. The chromosomes of the dog. *Hereditas* **51**: 187-189.
- Hallgrímsson, B., K. Willmore, C. Dorval and D. M. L. Cooper. 2004. Craniofacial variability and modularity in macaques and mice. *J. Exp. Zool. (Mol. Dev. Evol.)* **302B**: 207-225.
- Han, J., M. Ishii, P. Bringas Jr., R. L. Maas, R. E. Maxson Jr. and Y. Chai. 2007. Concerted action of *Msx1* and *Msx2* in regulating cranial neural crest cell differentiation during frontal bone development. *Mech Dev* **124**:729-745.
- Harcourt, R. A. 1974. The dog in prehistoric and early historic Britain. *J. Archaeol. Sci.* **1**: 151-175.
- Hare, B., M. Brown, C. Williamson and M. Tomasello. 2002. The domestication of social cognition in dogs. *Science* **298**: 1634-1636.
- Harrison, D. L. 1973. Some comparative features of the skulls of wolves (*Canis lupus*) and pariah dogs (*Canis familiaris* Linn) from the Arabian peninsula and neighboring lands. *Bonn. Zool. Beitr.* **24**: 185-191.
- Hauck, E. 1941. Wie kommt der Winkelkopf zustande? *Wien. tierärztl. Mschr.* **28**: 443-447.
- Hauck, E. 1950. Abstammung Ur- und Frühgeschichte des Haushundes. *Prähistorische Forschungen* **1**: 1-164.
- Havarti, K. 2003. Quantitative analysis of Neanderthal temporal bone morphology using three-dimensional geometric morphometrics. *Am. J. Phys. Anthropol.* **120**: 323-338.
- Haworth, K., M. Breen, M. Binns, D. A. Hopkinson and Y. H. Edwards. 2001a. The canine homeobox gene *MSX2*: sequence, chromosome assignment and genetic analysis in dogs of different breeds. *Anim. Genet.* **32**: 32-36.
- Haworth, K., I. Islam, M. Breen, W. Putt, E. Makrinou, M. Binns, D. Hopkinson and Y. Edwards. 2001b. Canine *TCOF1*; cloning, chromosome assignment and genetic analysis in dogs with different head types. *Mamm. Genome* **12**: 622-629.
- Haworth, K., W. Putt, B. Cattanaach, M. Breen, M. Binns, F. Lingaas and Y. H. Edwards. 2001c. Canine homolog of the T-box transcription factor T; failure of the protein to bind to its DNA target leads to short-tail phenotype. *Mamm. Genome* **12**: 212-218.
- Haworth, K. E., C. Healy, I. M. McGonnell, M. Binns and P. T. Sharpe. 2007. Characterisation of the genomic canine *Fgf8* locus and screen for genetic variants in 4 dogs with different face types. *DNA Seq.* **18**(3): 209-219.

- Hédan, B., S. Corre, C. Hitte, S. Dréano, T. Vilboux, T. Derrien, B. Denis, F. Galibert, M. -D. Galibert and C. André. 2006. Coat colour in dogs: identification of the *Merle* locus in the Australian shepherd breed. *BMC Vet. Res.* **2**: 9.
- Hedrick, P. W., P. S. Miller, E. Geffen and R. Wayne. 1997. Genetic evaluation of the three captive Mexican wolf lineages. *Zoo Biol.* **16**: 47-69.
- Hemmer, H. 1990. *Domestication: The Decline of Environmental Appreciation*. Cambridge University Press, Cambridge.
- Hennet, P. R. and C. E. Harvey. 1992. Craniofacial development and growth in the dog. *J. Vet. Dent.* **9**(2): 11-18.
- Herre, W. and H. Stephan. 1955. Zur postnatalen Morphogenese des Hirnes verschiedener Haushundrassen. *Gegenbaurs Morphol. Jahrb.* **96**: 210-264.
- Hildebrand, M. and G. E. Goslow, Jr. 2001. *Analysis of Vertebrate Structure*. John Wiley & Sons, Inc., New York.
- Hilzheimer, M. 1926. *Natürliche rassengeschichte der haussäugetiere*. W. de Gruyter, Berlin.
- Hlusko, L. J. 2002. Identifying metameric variation in extant hominoid and fossil hominid mandibular molars. *Am J. Phys. Anthropol.* **118**: 86-97.
- Hlusko, L. J. 2004. Integrating the genotype and phenotype in hominid paleontology. *Proc. Nat. Acad. Sci. U. S. A.* **101**(9): 2653-2657.
- Hlusko, L. J., M. -L. Maas and M. C. Mahaney. 2004. Statistical genetics of molar cusp patterning in pedigreed baboons: implications for primate dental development and evolution. *J. Exp. Zool. (Mol. Dev. Evol.)* **302**: 268-283.
- Hofmann-Apollo, F. 2009. *Estudo comparativo da forma do crânio de cães braquicefálicos e mesaticefálicos por meio de técnicas de morfometria geométrica em três dimensões*. Ph.D. dissertation. University of São Paulo, Brazil.
- Huber, W. 1948. Die Beurteilung der Hundeschнауze als genetisches Problem. *Arch. Julius Klaus-Stiftg.* **23**: 486-496.
- Huber, W. 1952. Die Beziehungen zwischen Kopflänge und Schnauzenlänge bei verschiedenen Hunderassen. *Arch. Julius Klaus-Stiftg.* **27**: 211-216.
- Huber, W. and P. Lüps. 1968. Biometrische und entwicklungsmechanische Kennzeichnung der Brachyphalie beim Haushund. *Arch. Julius Klaus-Stiftg.* **43**: 57-65.
- Huber, W. and P. Lüps. 1970. Biometrische analyse der Breitschädeligkeit beim Chow Chow. *Mitt. Naturforsch. Ges. Bern* **27**: 27-35.

- Hünemeier, T., F. M. Salzano and M. C. Bortolini. 2009. *TCOF1/Ser* variant and brachycephaly in dogs. *Anim. Genet.* **40**: 357-358.
- Hyun, C., L. J. Filippich, R. A. Lea, G. Shepherd, I. P. Hughes and L. R. Griffiths. 2003. Prospects for whole genome linkage disequilibrium mapping in domestic dog breeds. *Mamm. Genome* **14**(9): 640-649.
- Ignelzi, M. A., Y.-H. Liu, R. E. Maxson, Jr. and M. L. Snead. 1995. Genetically engineered mice: tools to understand craniofacial development. *Crit. Rev. Oral Biol. Med.* **6**(3): 181-201.
- Iljin, N. A. 1941. Wolf-dog genetics. *J. Genet.* **42**: 359-414.
- Iseki, S., A. O. M. Wilkie and G. M. Morriss-Kay. 1999. *Fgfr1* and *Fgfr2* have distinct differentiation- and proliferation-related roles in the developing mouse skull vault. *Development* **126**: 5611-5620.
- Ishii, M., A. E. Merrill, Y. S. Chan, I. Gitelman, D. P. Rice, H. M. Sucov and R. E. Maxson Jr. 2003. *Msx2* and *Twist* cooperatively control the development of the neural crest-derived skeletogenic mesenchyme of the murine skull vault. *Development* **130**: 6131 – 6142.
- Ishii, M., J. Han, H.-Y. Yen, H. M. Sucov, Y. Chai and R. E. Maxson, Jr. 2005. Combined deficiencies of *Msx1* and *Msx2* cause impaired patterning and survival of the cranial neural crest. *Development* **132**(22): 4937-4950.
- Jheon, A. H. and R. A. Schneider. 2009. The cells that fit the bill: neural rest and the evolution of craniofacial development. *J. Dent. Res.* **88**(1): 12-21.
- Johnston, M. C. and P. T. Bronsky. 1991. Animal models for human craniofacial malformations. *J. Craniofac. Genet. Dev. Biol.* **11**(4): 277-291.
- Jolicoeur, P. 1959. Multivariate geographical variation in the wolf *Canis lupus* L. *Evolution* **13**(3): 283-299.
- Jolicoeur, P. 1974. Sexual dimorphism and geographical distance as factors of skull variation in the wolf *Canis lupus* L. Pp. 54-61 in M. W. Fox, ed. *The Wild Canids: Their Systematics, Behavioral Ecology and Evolution*. Van Nostrand Reinhold, New York.
- Jones, N. C., M. L. Lynn, K. Gaudenz, D. Sakai, K. Aoto, J.-P. Rey, E. F. Glynn, L. Ellington, C. Du, J. Dixon, M. J. Dixon and P. A. Trainor. 2008. Prevention of the neurocristopathy Treacher Collins syndrome through inhibition of p53 function. *Nat. Med.* **14**(2): 125-133.
- Joshi, S. H., A. Prieto-Márquez and W. C. Parker. 2011. A landmark-free method for quantifying biological shape variation. *Biol. J. Linn. Soc. Lond.* **104**: 217-233.

- Kaesler, R. L. and J. A. Waters. 1972. Fourier analysis of the ostracode margin. *Geology* **83**: 1169-1178.
- Kardong, K. 1995. *Vertebrates: Comparative Anatomy, Function, Evolution*. McGraw-Hill Higher Education, Boston, Massachusetts.
- Karlsson, E. K. and K. Lindblad-Toh. 2008. Leader of the pack: gene mapping in dogs and other model organisms. *Nat. Rev. Genet.* **9**: 713-725.
- Karlsson, E. K., I. Baranowska, C. M. Wade, N. H. C. Salmon Hillbertz, M. C. Zody, N. Anderson, T. M. Biagi, N. Patterson, G. R. Pielberg, E. J. Kulbokas III, K. E. Comstock, E. T. Keller, J. P. Mesirov, H. von Euler, O. Kämpe, Å. Hedhammar, E. S. Lander, G. Andersson, L. Andersson and K. Lindblad-Toh. 2007. Efficient mapping of mendelian traits in dogs through genome-wide association. *Nat. Genet.* **39**: 1321-1328.
- Karsenty, G. 2008. Transcriptional control of skeletogenesis. *Annu. Rev. Genomics Hum. Genet.* **9**: 183-196.
- Karsenty, G., H. M. Kronenberg and C. Settembre. 2009. Genetic control of bone formation. *Ann. Rev. Cell Dev. Biol.* **25**: 629-648.
- Kemp, T. J., K. N. Bachus, J. A. Nairn and D. R. Carrier. 2005. Functional trade-offs in the limb bones of dogs selected for running versus fighting. *J. Exp. Biol.* **208**: 3475-3482.
- Kerns, J. A., M. Olivier, G. Lust and G. S. Barsh. 2003. Exclusion of melanocortin-1 receptor (*Mclr*) and *Agouti* as candidates for dominant black in dogs. *J. Hered.* **94**: 75-79.
- Kerns, J. A., J. Newton, T. G. Berryere, E. M. Rubin, J. -F. Cheng, S. M. Schmutz and G. S. Barsh. 2004. Characterization of the dog *Agouti* gene and a *nonagouti* mutation in German Shepherd Dogs. *Mamm. Genome* **15**: 798-808.
- Kerns, J. A., E. J. Cargill, L. A. Clark, S. I. Candille, T. G. Berryere, M. Olivier, G. Lust, R. J. Todhunter, S. M. Schmutz, K. E. Murphy and G. S. Barsh. 2007. Linkage and segregation analysis of black and brindle coat color in domestic dogs. *Genetics* **176**: 1679-1689.
- Kharlamova, A. V., L. N. Trut, D. R. Carrier, K. Chase and K. G. Lark. 2007. Genetic regulation of canine skeletal traits: trade-offs between the hind limbs and forelimbs in the fox and dog. *Integr. Comp. Biol.* **47**(3): 373-381.
- Kieser, J. A., V. Bernal, J. N. Waddell and S. Raju. 2007. The uniqueness of the human anterior dentition: a geometric morphometric analysis. *J. Forensic Sci.* **52**(3): 671-677.
- Kim, K. S., S. E. Lee, H. W. Jong and J. H. Ha. 1998. The complete nucleotide sequence of the domestic dog (*Canis familiaris*) mitochondrial genome. *Mol. Phylogenet. Evol.* **10**: 210-220.

- Kirkness, E. F., V. Bafna, A. L. Halpern, S. Levy, K. Remington, D. B. Rudch, A. L. Delcher, M. Pop, W. Wang, C. M. Fraser and J. C. Venter. 2003. The dog genome: survey sequencing and comparative analysis. *Science* **301**: 1898-1903.
- Klatt, B. 1912. Über Veränderungen der Schädelkapazität in der Domestikation. *Sitzber. Ges. Naturforsch. Freunde Berlin* **1912**(3): 153-179.
- Klatt, B. 1913. Über den Einfluß der Gesamtgröße auf das Schädelbild nebst Bemerkungen über die Vorgeschichte der Haustiere. *Wilhelm Roux Arch. Entwickl. Mech. Org.* **36**: 387-471.
- Klatt, B. 1921. Studien zum Domestikationsproblem: Untersuchungen am Hirn. *Bibliotheca genetica* **2**: 1-180.
- Klatt, B. 1927. Entstehung der Haustiere. *Handbuch der vererbungswissenschaft* **3**: 1-107.
- Klatt, B. 1941. Kreuzungen an extremen Rassetypen des Hundes. I. *Z. Mensch. Vererb. Konstitutionsl.* **25**: 28-93.
- Klatt, B. 1942. Kreuzungen an extremen Rassetypen des Hundes. II. *Z. Mensch. Vererb.-Konstitutionsl.* **26**: 320-356.
- Klatt, B. 1943. Kreuzungen an extremen Rassetypen des Hundes. III. *Z. Mensch. Vererb. Konstitutionsl.* **27**: 283-345.
- Klatt, B. 1944. Kreuzungen an extremen Rassetypen des Hundes. IV. *Z. Mensch. Vererb. Konstitutionsl.* **28**: 113-158.
- Klatt, B. 1950. Craniometrisch-physiognomische Studien an Hunden. *Mitt. Hamburgisch. Zool. Mus. Inst.* **50**: 9-129.
- Klatt, B. 1955a. Noch einmal: Hirngösse und Körpergröße. *Zool. Anz.* **155**: 215-232.
- Klatt, B. 1955b. Reciprocal crosses between dogs of contrasting growth types. *Wilhelm Roux Arch. Entwickl. Mech. Org.* **148**: 1-36.
- Klatt, B. 1958. Die Schädelgestaltung bei reciproken Kreuzungen von Hunden gegensätzlicher Wuchsform. *Z. wiss. Zool.* **161**:1-37.
- Klatt, B. and H. Vorsteher. 1923. Studien zum Domestikationsproblem II. *Bibl. Genetica* **6**: 1-166.
- Klingenberg, C. P. 2011. MorphoJ: an integrated software package for geometric morphometrics. *Molec. Ecol. Resour.* **11**: 353-357.

- Knecht, A. K. and M. Bronner-Fraser. 2002. Induction of the neural crest: a multigene process. *Nat. Rev. Genet.* **3**: 453-461.
- Koch, D. A., S. Arnold, M. Hubler and P. M. Montavon. 2003. Brachycephalic syndrome in dogs. *Compend. Contin. Educ. Vet.* **25**: 48-55.
- Koler-Matznick, J. 2002. The origin of the dog revisited. *Anthrozoös* **15**: 98-118.
- Koop, B. F. M. Burbridge, A. Byun, U. Rink and S. J. Crockford. 2000. Ancient DNA evidence of a separate origin for North American indigenous dogs. Pp. 271-285 in S. J. Crockford, ed. *Dogs Through Time: An Archaeological Perspective*. British Archaeological Reports, Oxford, UK.
- Kuhl, F. P. and C. R. Giardina. 1982. Elliptic Fourier features of a closed contour. *Comput. Graph. Image Process.* **18**: 236-258.
- Kupczynska, M., M. Makowiecka, M. Skibniewski, M. Galanty and I. Bissenik. 2005. Morphology of dog's frontal sinuses. *Med. Weter.* **61**(9): 1011-1014.
- Kupczynska, M., M. Wasowicz, K. Barszcz, P. Poblocki and A. Michalczuk. 2008. Morphometric standards of the heads of living brachycephalic dogs. *Med. Weter.* **64**(5): 702-706.
- Kupczynska, M., K. Barszcz, M. Wasowicz, and A. Wieladek. 2009. Dentition in brachycephalic dogs. *Med. Weter.* **65**(5): 334-339.
- Lan, H. and L. Shi. 1996. The mitochondrial DNA evolution of four species of Canidae. *Dong Wu Xue Bao* **42**: 87-95.
- Lark, K. G., K. Chase and N. B. Sutter. 2006. Genetic architecture of the dog: sexual size dimorphism and functional morphology. *Trends Genet.* **22**: 537-544.
- Larson, G., E. K. Karlsson, A. Perri, M. T. Webster, S. Y. W. Ho, J. Peters, P. W. Stahl, P. J. Piper, F. Lingaas, M. Fredholm, K. E. Comstock, J. F. Modiano, C. Schelling, A. I. Agoulnik, P. A. Leegwater, K. Dobney, J.-D. Vigne, C. Vila, L. Andersson and K. Lindblad-Toh. 2012. Rethinking dog domestication by integrating genetics, archeology, and biogeography. *Proc. Nat. Acad. Sci. U.S.A.* doi: 10.1073/pnas.1203005109.
- Lawing, A. M. and P. D. Polly. 2010. Geometric morphometrics: recent applications to the study of evolution and development. *J. Zool.* **280**: 1-7.
- Lawrence, B. 1967. Early domestic dogs. *Z. Saugetierkd.* **32**: 44-59.
- Lawrence, B. 1968. Antiquity of large dogs in North America. *Tebiwa* **11**(2): 43-49.

- Lawrence, B. and W. H. Bossert. 1967. Multiple character analysis of *Canis lupus, latrans* and *familiaris* with a discussion of the relationships of *Canis niger*. *Amer. Zool.* **7**: 223-232.
- Leamy, L. J., E. J. Routman and J. M. Cheverud. 1999. Quantitative trait loci for early- and late-developing skull characters in mice: a test of the genetic independence model of morphological integration. *Am. Nat.* **153**(2): 201-214.
- Leidy, J. 1858. Notice of remains of extinct Vertebrata, from the valley of the Niobrara River, collected during the exploring expedition of 1857, in Nebraska, under the command of Lieut. G. K. Warren, Top. Eng., by Dr. F. V. Hayden, geologist to the expedition. *Proc. Acad. Nat. Sci. Philadelphia* **1858**: 20-29.
- Leidy, J. 1869. The extinct mammalian fauna of Dakota and Nebraska, including an account of some allied forms from other localities, together with a synopsis of the mammalian remains of North America. *J. Acad. Nat. Sci. Philadelphia* **7**: 1-472.
- Lele, S. 1991. Some comments on coordinate-free and scale-invariant methods in morphometrics. *Am. J. Phys. Anthropol.* **85**: 407-417.
- Lele, S. 1993. Euclidean distance matrix analysis (EDMA): estimation of mean form and mean form difference. *Math. Geol.* **25**(5): 573-602.
- Leonard, J. A., R. K. Wayne, J. Wheeler, R. Valadez, S. Guillén and C. Vilà. 2002. Ancient DNA evidence for Old World origin of New World dogs. *Science* **298**: 1613-1616.
- Leone, C. A. and R. L. Anthony. 1966. Serum esterases among registered breeds of dogs as revealed by immunoelectrophoretic comparisons. *Comp. Biochem. Physiol.* **18**: 359-368.
- Lestrel, P. E. 1989. Method for analyzing complex two-dimensional forms: elliptical Fourier functions. *Am. J. Hum. Biol.* **1**: 149-164.
- Lew, W. and J. Lewis. 1977. An anthropometric scaling method with application to the knee joint. *J. Biomech.* **10**: 171-181.
- Lewis, J., W. Lew and J. Zimmerman. 1980. A nonhomogeneous anthropometric scaling method based on finite element principles. *J. Biomech.* **13**: 815-824.
- Li, Q., Z. Liu, Y. Li, X. Zao, L. Dong, Z. Pan, Y. Sun, N. Li, Y. Xu and Z. Xie. 2008. Origin and phylogenetic analysis of Tibetan Mastiff based on mitochondrial DNA sequence. *J. Genet. Genomics* **35**: 335-340.
- Lignereux, Y., S. Regodon and C. Pavaux. 1991. Cephalic typology in dog. *Rev. Med. vet. (Toulouse)* **142**(6): 469-480.

- Lignereux, Y., S. Regodon and C. Pavaux. 1992. Eine Methode zur Klassifizierung der Schädeltypen beim Hund. *Bayerisches landwirtschaftliches Jahrbuch* **69**: 43-49.
- Lindblad-Toh, K., C. M. Wade, T. S. Mikkelsen, E. K. Karlsson, D. B. Jaffe, M. Kamal, M. Clamp, J. L. Chang, E. J. Kulbokas, M. C. Zody, E. Mauceli, X. Xie, M. Breen, R. K. Wayne, E. A. Ostrander, C. P. Ponting, F. Galibert, D. R. Smith, P. J. de Jong, E. Kriksness, P. Alvarez, T. Biagi, W. Brockman, J. Butler, C. -W. Chin, A. Cook, J. Cuff, M. J. Daly, D. DeCaprio, S. Gnerre, M. Grabherr, M. Kellis, M. Kleber, C. Bardeleben, L. Goodstadt, A. Heger, C. Hitte, L. Kim, K. -P. Koepfli, H. G. Parker, J. P. Pollinger, S. M. J. Searle, N. B. Sutter R. Thomas, C. Webber and E. S. Lander. 2005. Genome sequence, comparative analysis, and haplotype structure of the domestic dog. *Nature* **438**: 803-819.
- Lockwood, C. A., J. M. Lynch and W. H. Kimbel. 2002. Quantifying temporal bone morphology of great apes and humans: an approach using geometric morphometrics. *J. Anat.* **201**: 447-464.
- Lohmann, G. P. 1983. Eigenshape analysis of microfossils: a general morphometric procedure for describing changes in shape. *Math. Geol.* **15**(6): 659-672.
- Lorenzini, R. and R. Fico. 1995. A genetic investigation of enzyme polymorphisms shared by wolf and dog: suggestions for conservation of the wolf in Italy. *Acta Theriol.* **3**(suppl.): 101-110.
- Lovejoy, C. O., M. J. Cohn and T. D. White. 1999. *Proc. Nat. Acad. Sci. U. S. A.* **96**(23): 13247-13252.
- Lu, K. H. 1965. Harmonic analysis of the human face. *Biometrics* **21**: 491-505.
- Lumer, H. 1940. Evolutionary allometry in the skeleton of the domestic dog. *Amer. Natur.* **74**: 439-467.
- Lüps, P. 1974. Biometrische Untersuchungen an der Schädelbasis des Haushundes. *Zool. Anz. Jena* **192**: 383-413.
- Lüps, P. and W. Huber. 1968. Biometrische Analyse des Barsoi-Schädel. *Arch. Julius Klaus-Stift. Vererbungsforsch. Sozialanthropol. Rassenhyg.* **43**: 67-74.
- Lüps, P. and W. Huber. 1969a. Metrische Beziehungen zwischen Kopf- und Rumpflänge beim Haushund. *Rev. Suisse Zool.* **76**: 673-680.
- Lüps, P. and W. Huber. 1969b. Versuch einer differenzierten biometrischen charakterisierung der schädelbasis beim Wolf und beim Haushund. *Mitt. Naturforsch. Ges. Bern* **26**: 21-29.

- Lynch, J. M. and T. J. Hayden. 1995. Genetic influences on cranial form: variation among ranch and feral American mink *Mustela vison* (Mammalia: Mustelidae). *Bil. J. Linn. Soc. Lond.* **55**: 293-307.
- MacLeod, N. 1999. Generalizing and extending the eigenshape method of shape space visualization and analysis. *Paleobiology* **25**(1): 107-138.
- Mai, S., K. Wei, A. Flenniken, S. L. Adamson, J. Rossant, J. E. Aubin and S.-G. Gong. 2010. The missense mutation W290R in *Fgfr2* causes developmental defects from aberrant IIIb and IIIc signaling. *Dev. Dyn.* **239**: 1888-1900.
- Mangasarian, K., Y. Li, A. Mansukhani and C. Basilico. 1997. Mutation associated with Coruzon syndrome causes ligand-independent dimerization and activation of FGF receptor-2. *J. Cell. Physiol.* **172**: 117-125.
- Mansukhani, A., P. Bellosta, M. Sahni and C. Basilico. 2000. Signaling by fibroblast growth factors (FGF) and fibroblast growth factor receptor 2 (FGFR2)-activating mutations blocks mineralization and induces apoptosis in osteoblasts. *J. Cell Biol.* **149**(6): 1297-1308.
- Marchelewski, T. 1930a. Craniology of the domestic dog. *Bulletin international de l'Académie polonaise des sciences et des lettres, Classe des sciences mathématiques et naturelles, B(II)* **1930**: 511-548.
- Marchelewski, T. 1930b. Genetic studies on the domestic dog. *Bulletin international de l'Académie polonaise des sciences et des lettres, Classe des sciences mathématiques et naturelles, B(II)* **1930**: 117-145.
- Marie, P. J. 2012. Fibroblast growth factor signaling controlling bone formation: an update. *Gene* **498**: 1-4.
- Marroig, G. and J. M. Cheverud. 2005. Size as a line of least evolutionary resistance: diet and adaptive morphological radiation in New World monkeys. *Evolution* **59**(5): 1128-1142.
- Marsh, K. L., J. Dixon and M. J. Dixon. 1998. Mutations in the Treacher Collins syndrome gene lead to mislocalization of the nucleolar protein treacle. *Hum. Mol. Genet.* **7**(11): 1795-1800.
- Masotti, C., C. O. Ornelas, A. Splendore-Gordonos, R. Moura, T. M. Félix, N. Alonso, A. A. Camargo and M. R. Passos-Bueno. 2009. Reduced transcription of TCOF1 in adult cells of Treacher Collins syndrome patients. *BMC Med. Genet.* **10**: 136.
- McGreevy, P., T. D. Grassi and A. M. Harman. 2004. A strong correlation exists between the distribution of retinal ganglion cells and nose length in the dog. *Brain Behav. Evol.* **63**: 13-22.

- Merriam, J. C. 1906. Recent discoveries of Quaternary mammals in southern California. *Science* **24**(608): 248-250.
- Merriam, J. C. 1908. Death trap of the ages. *Sunset* **21**(6), October.
- Merriam, J. C. 1911. The fauna of Rancho La Brea. Part I. Occurrence. *Memoirs Univ. Calif.* **1**(2): 200-213.
- Merriam, J. C. 1912. The fauna of Rancho La Brea. Part II. Canidae. *Memoirs Univ. Calif.* **1**(2): 217-272.
- Milenkovic, M., V. J. Sipetic, J. Blagojevic, S. Tatovic and M. Vujosevic. 2010. Skull variation in Dinaric-Balkan and Carpathian gray wolf populations revealed by geometric morphometric approaches. *J. Mammal.* **91**(2): 376-386.
- Miller, G. S. 1912. *Catalogue of the Mammals of Western Europe (Europe Exclusive of Russia) in the Collection of the British Museum*. British Museum (Natural History), London.
- Miller, G. S. 1920. Recent literature: remarks on Some South American Canidae by Einar Lönnberg. *J. Morphol.* **1**(3): 149-150.
- Minouchi, O. 1928. The spermatogenesis of the dog, with special reference to meiosis. *Jpn. J. Zool.* **1**: 255-268.
- Minoux, M. and F. M. Rijli. 2010. Molecular mechanisms of cranial neural crest cell migration and patterning in craniofacial development. *Development* **137**: 2605-2621.
- Morel, P. and W. Müller. 1997. Hauterive-Champréveyres, 11. Un campement magdalénien au bord du lac de Neuchâtel: étude archéozoologique (secteur 1). *Archéologie neuchâteloise* **23**: 1-152.
- Morey, D. F. 1992. Size, shape and development in the evolution of the domestic dog. *J. Archaeol. Sci.* **19**: 181-204.
- Morey, D. F. 1994. The early evolution of the domestic dog. *Am. Sci.* **82**: 336-347.
- Morriss-Kay, G. M. 2001. Derivation of the mammalian skull vault. *J. Anat.* **199**: 143-151.
- Morvan-Dubois, G., B. A. Demeneix and L. M. Sachs. 2008. *Xenopus laevis* as a model for studying thyroid hormone signaling: from development to metamorphosis. *Mol. Cell. Endocrinol.* **293**: 71-79.
- Murray, S. A. 2011. Mouse resources for craniofacial research. *Genesis* **49**: 190-199.

- Musil, R. 2000. Evidence for the domestication of wolves in Central European Magdalenian sites. Pp. 21-28 in S. J. Crockford, ed. *Dogs Through Time: An Archaeological Perspective*. British Archaeological Reports, International Series 889.
- Nickel, R., A. Schummer and K. H. Wille. 1984. Passiver Bewegungsapparat, Skelettsystem. Pp. 11-229 in R. Nickel, A. Schummer and E. Seiferle, eds. *Lehrbuch der Anatomie der Haustiere, Band 1, Bewegungsapparat, ed 5*. Paul Parey, Berlin.
- Nie, X., K. Luukko and P. Kettunen. 2006a. BMP signaling in craniofacial development. *Int. J. Dev. Biol.* **50**: 511-521.
- Nie, X., K. Luukko and P. Kettunen. 2006b. FGF signaling in craniofacial development and developmental disorders. *Oral Dis.* **12**: 102-111.
- Niklas, K. 1977. Applications of finite element analyses to problems in plant morphology. *Ann. Bot.* **41**: 133-153.
- Noack, T. 1916. Über die Schädel vorgeschichtlicher Haushunde im Römermuseum zu Hildesheim. *Zoologischer Anzeiger* **46**: 75-94.
- Nobis, G. 1979. Der älteste Haushunde lebte vor 14,000 Jahren. *Umschau* **19**: 610.
- Nöller, C., J. Hueber, H. Aupperle, J. Seeger, T. H. Oechtering, C. Niestroock and G. U. Oechtering. 2008. New aspects of brachycephalia in dogs and cats. Basics: insights into embryology, anatomy and pathophysiology. Pp. 713-715 in *Proceedings ACVIM Forum, San Antonio, Texas, USA 4-7 June, 2008*. American College of Veterinary Internal Medicine, Lakewood.
- Nowak, R. M. 1979. North American Quaternary *Canis*. *Monogr. Mus. Nat. Hist. Univ. Kansas. no. 6*.
- Nussbaumer, M. 1982. On the variability of dorso-basal curvatures in skulls of domestic dogs. *Zool. Anz.* **209**: 1-32.
- Nussbaumer, M. 1985. Size- and sex-related proportions of the facial skeleton in Bernese Mountain Dogs. *Z. Tierzucht. Zuechtungsbiol.* **102**: 65-72.
- O'Higgins, P. and N. Jones. 1998. Facial growth in *Cercocebus torquatus*: an application of three-dimensional geometric morphometric techniques to the study of morphological variation. *J. Anat.* **193**: 251-272.
- Okarma, H. and T. Buchalczyk. 1993. Craniometric characteristics of wolves *Canis lupus* from Poland. *Acta Theriol.* **38**: 253-262.

- Okumura, N., N. Ishiguro, M. Nakano, A. Matsui and M. Sahara. 1996. Intra- and interbreed genetic variations of mitochondrial DNA major non-coding regions in Japanese native dog breeds (*Canis familiaris*). *Anim. Genet.* **27**: 397-405.
- Olmstead, M. P. 1911. Das Primordialcranium eines Hunde-embryo. Ein Beitrag zur Morphologie des Säugetierschädels. *Anat. Hefte.* **130**: 339-375.
- Olsen, S. J. 1985. *Origins of the Domestic Dog*. University of Arizona Press, Tucson, AZ.
- Olsen, S. J. and J. W. Olsen. 1977. The Chinese wolf, ancestor of New World dogs. *Science* **197**: 533-535.
- Olson, E. C. and R. L. Miller. 1958. *Morphological Integration*. University of Chicago Press, Chicago, IL.
- Onar, V. and H. Güneş. 2003. On the variability of skull shape in German shepherd (Alsatian) puppies. *Anat. Rec.* **272A**: 460-466.
- Onar, V., S. Özcan and G. Pazvant. 2001. Skull typology of adult male Kangal dogs. *Anat. Histol. Embryol.* **30**: 41-48.
- Ostrander, E. A. and E. Giniger. 1997. Semper fidelis: what man's best friend can teach us about human biology and disease. *Am. J. Hum. Genet.* **61**: 475-480.
- Ovodov, N. D., S. J. Crockford, Y. V. Kuzmin, T. F. G. Higham, G. W. L. Hodgins and J. van der Plicht. 2011. A 33,000-year-old incipient dog from the Altai Mountains of Siberia: evidence of the earliest domestication disrupted by the Last Glacial Maximum. *PLoS ONE* **6**(7): e22821.
- Pang, J. -F., C. Kluetsch, K. -J. Zou, A. Zhang, L. -Y. Luo, H. Angleby, A. Ardalán, C. Ekström, A. Sköllermo, J. Lundeberg, S. Matsumura, T. Leitner, Y. -P. Zhang and P. Savolainen. 2009. mtDNA data indicate a single origin for dogs South of Yangtze River, less than 16,300 years ago, from numerous wolves. *Mol. Biol. Evol.* **26**: 2849-2864.
- Park, J. O.-J. Park, W.-J. Yoon, H.-J. Kim, K.-Y. Choi, T.-J. Cho and H.-M. Ryoo. 2012. Functional characterization of a novel FGFR2 mutation, E731K, in craniosynostosis. *J. Cell. Biochem.* **113**: 457-464.
- Parker, H. G., L. V. Kim, N. B. Sutter, S. Carlson, T. D. Lorentzen, T. B. Malek, G. S. Johnson, H. B. DeFrance, E. A. Ostrander and L. Kruglyak. 2004. Genetic structure of the purebred domestic dog. *Science* **304**: 1160-1164.
- Parker, H. G., B. M. vonHoldt, P. Quignon, E. H. Margulies, S. Shao, D. S. Mosher, T. C. Spady, A. Elkahoun, M. Cargill, P. G. Jones, C. L. Maslen, G. M. Acland, N. B. Sutter, K. Kuroki, C. D. Bustamante, R. K. Wayne and E. A. Ostrander. 2009. An expressed *Fgf4*

- retrogene is associated with breed-defining chondrodysplasia in domestic dogs. *Science* **325**: 995-998.
- Parsons, T. E., E. J. Schmidt, J. C. Boughner, H. A. Jamniczky, R. S. Marcucio and B. Hallgrímsson. 2011. Epigenetic integration of the developing brain and face. *Dev. Dyn.* **240**(10): 2233-2244.
- Patterson, D. 2000. Companion animal medicine in the age of medical genetics. *J. Vet. Intern. Med.* **14**: 1-9.
- Patterson, D. F., M. E. Haskins and P. F. Jezyk. 1982. Models of human genetic disease in domestic animals. *Adv. Hum. Genet.* **12**: 263-339.
- Perlyn, C. A., V. B. DeLeon, C. Babbs, D. Glover, L. Burrell, T. Darvann, S. Kreiborg and G. M. Morriss-Kay. 2006. The craniofacial phenotype of the Crouzon mouse: analysis of a model for syndromic craniosynostosis using three-dimensional MicroCT. *Cleft palate Craniofac. J.* **43**(6): 740-747.
- Phelps, E. M. 1932. A critique of the principle of the horizontal plane of the skull. *Am. J. Phys. Anthropol.* **17**: 71-98.
- Phillipp, U., H. Hamann, L. Mecklenburg, S. Nishino, E. Mignot, A. R. Gunzel-Apel, S. M. Schmutz and T. Leeb. 2005. Polymorphisms within the canine MLPH gene are associated with dilute coat color in dogs. *BMC Genet.* **6**: 34.
- Phillips, J. M. 1945. 'Pig jaw' in Cocker Spaniels. Retrognathia of the mandible in the Cocker Spaniel and its relationship to other deformities of the jaw. *J. Hered.* **36**: 177-181.
- Pidoplichko, I. G. 1969. *Late Paleolithic dwellings of mammoth bones in Ukraine*. Institute of Zoology of the Ukrainian Academy of Sciences, Naukova Dumka, Kiev.
- Piltz, H. 1951. Die postembryonale Entwicklung des Schädels zweier extremer Rassentypen des Hundes. *Z. Morphol. Anthropol.* **43**: 21-60.
- Pionnier-Capitan, M., C. Bemilli, P. Bodu, G. Célérier, J.-G. Ferrié, P. Fosse, M. Garcià and J. D. Vigne. 2011. New evidence for Upper Paleolithic small domestic dogs in South-Western Europe. *J. Archaeol. Sci.* **38**: 2123-2140.
- Pollinger, J. P., C. D. Bustamante, A. Fledel-Alon, S. Schmutz, M. M. Gray and R. K. Wayne. 2005. Selective sweep mapping of genes with large phenotypic effects. *Genome Res.* **15**: 1809-1819.
- Poplin, F. 1976. Is there a correlation between anomalous numbers of cheek teeth and elongation of skull in dog? *Anat. Histol. Embryol.* **5**(1): 21-34.

- Preuschoft, H. and U. Witzel. 2005. Functional shape of the skull in vertebrates: which forces determine skull morphology in lower primates and ancestral synapsids? *Anat. Rec. A Discov. Mol. Cell. Evol. Biol.* **283A**: 402-413.
- Pullig, T. 1952. Inheritance of a skull defect in Cocker Spaniels. *J. Hered.* **43**: 97-99.
- Raaum, R. 2006. DVLR v. 4.12. NYCEP Morphometrics Group, New York.
- Randi, E., V. Lucchini, M. F. Christensen, N. Mucci, S. M. Funk, G. Dolf and V. Loeschcke. 2000. Mitochondrial DNA variability in Italian and East European wolves: detecting the consequences of small population size and hybridization. *Conserv. Biol.* **14**: 464-473.
- Read, D. W. and P. E. Lestrel. 1986. Comment on uses of homologous-point measures in systematics: a reply to Bookstein et al. *Syst. Zool.* **35**(2): 241-253.
- Regodon, S., A. Franco, J. M. Garin, A. Robina and Y. Lignereux. 1991. Computerized tomographic determination of the cranial volume of the dog applied to racial and sexual differentiation. *Acta Anat. (Basel)* **142**: 347-350.
- Regodon, S., J. M. Vivo, A. Franco, M. T. Guillen and A. Robina. 1993. Craniofacial angle in dolicocephalic, mesocephalic and brachycephalic dogs - radiological determination and application. *Anat. Anz.* **175**(4): 361-363.
- Reynolds, H. S. 1909. The Canidae. Pp. 1-28 in W. B. Dawkins, ed. *A Monograph of the British Pleistocene Mammalia*. The Palaeontological Society, London.
- Richtsmeier, J. T. and J. W. McGrath. 1986. Quantitative genetics of cranial nonmetric traits in randombred mice: heritability and etiology. *Am. J. Phys. Anthropol.* **69**: 51-58.
- Richtsmeier, J. T. and S. Lele. 1990. Analysis of craniofacial growth in Crouzon syndrome using landmark data. *J. Craniofac. Genet. Dev. Biol.* **10**: 39-62.
- Richtsmeier, J. T. and S. Lele. 1993. A coordinate-free approach to the analysis of growth patterns: models and theoretical considerations. *Biol. Rev.* **68**: 381-411.
- Richtsmeier, J. T., J. M. Cheverud and S. Lele. 1992. Advances in anthropological morphometrics. *Annu. Rev. Anthropol.* **21**: 283-305.
- Richtsmeier, J. T., V. B. DeLeon and S. R. Lele. 2002. The promise of geometric morphometrics. *Yrbk. Phys. Anthropol.* **45**: 63-91.
- Richtsmeier, J. T., K. Aldridge, V. B. DeLeon, J. Panchal, A. A. Kane, J. L. Marsh, P. Yan, and T. M. Cole III. 2006. Phenotypic integration of neurocranium and brain. *J. Exp. Zool. Mol. Dev. Evol.* **306B**: 360-378.

- Rohlf, F. J. and D. Slice. 1990. Extensions of the Procrustes methods for the optimal superimposition of landmarks. *Syst. Zool.* **39**(1): 40-59.
- Rosas, A. and M. Bastir. 2002. Thin-plate spline analysis of allometry and sexual dimorphism in the human craniofacial complex. *Am. J. Phys. Anthropol.* **117**: 236-245.
- Rosas, A., M. Bastir, J. A. Alarcón and K. Kuroe. 2008. Thin-plate spline analysis of the cranial base in African, Asian and European populations and its relationship with different malocclusions. *Arch. Oral Biol.* **53**(9): 826-834.
- Rosenberg, K. F. A. 1966. Die postnatale Proportionsänderung der Schädel zweier extremer Wuchsformen des Haushundes. *Z. Tierzücht. Züchtungsbiol.* **82**: 1-36.
- Roybal, P. G., N. L. Wu, J. Sun, M. Ting, C. A. Schafer and R. E. Maxson. 2010. Inactivation of *Msx1* and *Msx2* in neural crest reveals an unexpected role in suppressing heterotopic bone formation in the head. *Dev. Biol.* **343**: 28-39.
- Ruvinsky, A. 2001. Developmental genetics. Pp. 431-459 in A. Ruvinsky and J. Sampson, eds. *The Genetics of the Dog*. CABI Publishing, Wallingford, UK.
- Sablin, M. V. and G. A. Khlopachev. 2002. The earliest Ice Age dogs: evidence from Eliseevichi I. *Curr. Anthropol.* **43**: 795-799.
- Sakai, D. and P. A. Trainor. 2009. Treacher Collins syndrome: unmasking the role of *Tcofl1*/treacle. *Int. J. Biochem. Cell Biol.* **41**: 1229-1232.
- Salmon Hillbertz, N. H. C. and G. Andersson. 2006. Autosomal dominant mutation causing the dorsal ridge predisposes for dermoid sinus in Rhodesian ridgeback dogs. *J. Small Anim. Prac.* **47**: 184-188.
- Salmon Hillbertz, N. H. C., M. Isaksson, E. K. Karlsson, E. Hellmén, G. R. Pielberg, P. Savolainen, C. M. Wade, H. von Euler, U. Gustafson, Å. Hedhammar, M. Milsson, K. Lindblad-Toh, L. Andersson and G. Andersson. 2007. Duplication of *FGF3*, *FGF4*, *FGF19* and *ORAOV1* causes hair ridge and predisposition to dermoid sinus in Ridgeback dogs. *Nat. Genet.* **39**: 1318-1320.
- Sampson, J. and M. M. Binns. 2006. The Kennel Club and the early history of dog shows and breed clubs. Pp. 19-30 in E. A. Ostrander, U. Giger and K. Lindblad-Toh, eds. *The Dog and its Genome*. Cold Spring Harbor Laboratory Press, Cold Spring Harbor, NY.
- Satokata, I. and R. Maas. 1994. *Msx1* deficient mice exhibit cleft palate and abnormalities of craniofacial and tooth development. *Nat Genet* **6**: 348-356.
- Satokata, I., L. Ma, H. Ohshima, M. Bei, I. Woo, K. Nishizawa, T. Maeda, Y. Takano, M. Uchiyama, S. Heaney, H. Peters, Z. Tang, R. Maxson and R. Maas. 2000. *Msx2*

- deficiency in mice causes pleiotropic defects in bone growth and ectodermal organ formation. *Nat. Genet.* **24**: 391-395.
- Sauka-Spengler, T. and M. Bronner-Fraser. 2008. A gene regulatory network orchestrates neural crest formation. *Nat. Rev. Mol. Cell Biol.* **9**: 557-568.
- Savolainen, P., Y. Zhang, J. Luo, J. Lundeberg and T. Leitner. 2002. Genetic evidence for an East Asian origin of domestic dogs. *Science* **298**: 1610-1613.
- Schäme, R. 1922. Die Grundformen des Haushundschädels. *Jahrbuch für Jagdkunde* **6**: 209-264.
- Schleidt, W. M. and M. D. Shalter. 2003. Co-evolution of humans and canids, an alternative view of dog domestication: *Homo homini lupus?* *Biol. Theory* **9**: 57-72.
- Schliemann, H. 1966. On morphology and development of the skull of *Canis lupus f. familiaris* L. *Gegenbaurs. Morphol. Jarhb.* **109**(4): 501-603.
- Schmitt, F. 1903. Über das postembryonale Wachstum des Schädels verschiedener Hunderassen. *Arch. f. Naturgesch.* **69**(1): 69-134.
- Schmutz, S. M., T. G. Berryere and A. D. Goldfinch. 2002. *TYRP1* and *MC1R* genotypes and their effects on coat color in dogs. *Mamm. Genome* **13**: 380-387.
- Schmutz, S. M., T. G. Berryere, N. M. Ellinood, J. A. Kerns and G. S. Barsh. 2003. *MC1R* studies in dogs with melanistic mask or brindle patterns. *J. Hered.* **94**: 69-73.
- Scott, J. P. 1968. Evolution and domestication of the dog. *Evol. Biol.* **2**: 243-275.
- Sears, K. E., A. Goswami, J. J. Flynn and L. A. Niswander. 2007. The correlated evolution of *Runx2* tandem repeats, transcriptional activity, and facial length in Carnivora. *Evol. Dev.* **9**: 550-565.
- Seiferle, E. 1966. Zur Topographie des Gehirns bei lang- und kurzköpfigen Hunderassen. *Acta Anat.* **63**: 346-362.
- Selden, J. R., P. S. Moorhead, M. L. Oehlert and D. F. Patterson. 1975. The Giemsa banding pattern of the canine karyotype. *Cytogenet. Cell Genet.* **15**: 380-387.
- Shapiro, M. D., M. E. Marks, C. L. Peichel, B. K. Blackman, K. S. Nereng, B. Jónsson, D. Schluter and D. M. Kingsley. 2004. Genetic and developmental basis of evolutionary pelvic reduction in threespine sticklebacks. *Nature* **428**: 717-723.
- Shapiro, M. D., M. A. Bell and D. M. Kingsley. 2006. Parallel genetic origins of pelvic reduction in vertebrates. *Proc. Nat. Acad. Sci. U. S. A.* **103**(37): 13753-13758.

- Sharpe, P. T. 1999. The mouse as a developmental model. Pp. 3-5 in P. T. Sharpe and I. Mason, eds. *Methods in Molecular Biology, Vol. 97: Molecular Embryology: Methods and Protocols*. Humana Press, Inc., Totowa, NJ.
- Shaughnessy, P. D., A. E. Newsome and L. K. Corbett. 1975. An electrophoretic comparison of three blood proteins in dingoes and domestic dogs. *Austral. Mammal.* **1**: 355-359.
- Shearin, A. L. and E. A. Ostrander. 2010. Leading the way: canine models of genomics and disease. *Dis. Model Mech.* **3**(1-2): 27-34.
- Sherwood, R. J., L. J. Hlusko, D. L. Duren, V. C. Emch and A. Walker. 2005. Mandibular symphysis of large-bodied hominoids. *Hum. Biol.* **77**(6): 735-759.
- Sholts, S. B., F. Flores, P. L. Walker and S. K. T. S. Wärmländer. 2011. Comparison of coordinate measurement precision of different landmarks types on human crania using a 3D laser scanner and a 3D digitiser: implications for applications of digital morphometrics. *Int. J. Osteoarchaeol.* **21**: 535-543.
- Shubin, N. H. 2002. Origin of evolutionary novelty: examples from limbs. *J. Morphol.* **252**: 15-28.
- Shubin, N., C. Tabin and S. Carroll. 1997. Fossils, genes and the evolution of animal limbs. *Nature* **388**: 639-648.
- Siegel, A. F. and R. H. Benson. 1982. A robust comparison of biological shapes. *Biometrics* **38**: 341-350.
- Simonsen, V. 1976. Electrophoretic studies on blood proteins of domestic dogs and other Canidae. *Hereditas* **82**: 7-18.
- Singleton, M. 2002. Patterns of cranial shape variation in the Papionini (Primates: Cercopithecinae). *J. Hum. Evol.* **42**: 547-578.
- Slice, D. E. 1996. Three-dimensional, generalized resistant-fitting and the comparison of least-squares and resistant-fit residuals. Pp. 179-199 in L. F. Marcus, M. Corti, A. Loy, G. Naylor and D. Slice, eds. *Advances in Morphometrics*. Plenum Press, New York.
- Sneath, P. H. A. 1967. Trend-surface analysis of transformation grids. *J. Zool.* **151**: 65-122.
- Sommer, O. 1931. Untersuchungen über die Wachstumvorgänge am Hundeskelett. *Archiv für Tierernährung und Tierzucht* **6**: 439-469.
- Stark, D. 1962. Der heutige Stand des Fetalizationsproblems. *Zeitschr. f. Tierz. und Zucht.* **47**: 129-155.

- Stockard, C. R. 1941. The genetic and endocrinic basis for differences in form and behavior as elucidated by studies of contrasted pure-line dog breeds and their hybrids. With special contributions on behavior by O. D. Anderson and W. T. James. *Amer. Anat. Mem.* No. 19. The Wistar Institute of Anatomy and Biology, Philadelphia.
- Stockhaus, K. 1962. Zur Formenmannigfaltigkeit von Haushundskädeln. *Zeitschr. f. Tierz. und Zucht.* **77**: 223-228.
- Stockhaus, K. 1965. Metrische Untersuchungen an Schädeln von Wölfen und Hunden. *Zeitschrift für Zoologische Systematik und Evolutionsforschung.* **3**: 157-258.
- Studer, T. 1901. Die prähistorischen Hunde in ihrer Beziehung zu den gegenwärtig lebenden Rassen. *Zürich Abhandlungen der Schweizer paläontologischen Gesellschaft* **28**: 1-137.
- Studer, T. 1906. Über einen Hund aus der paläolithischen Zeit Russlands. *Canis Poutiatini.* *Zool. Anz.* **29**: 24-35.
- Sutter, N. B. and E. A. Ostrander. 2004. Dog star rising: the canine genetic system. *Nat. Rev. Genet.* **25**: 289-293.
- Sutter, N. B., C. D. Bustamante, K. Chase, M. M. Gray, K. Zhao, L. Zhu, B. Padhukasahasram, E. Karlins, S. Davis, P. G. Jones, P. Quignon, G. S. Johnson, H. G. Parker, N. Fretwell, D. S. Mosher, D. F. Lawler, E. Satyaraj, M. Nordborg, K. G. Lark, R. K. Wayne and E. A. Ostrander. 2007. A single *IGF1* allele is a major determinant of small size in dogs. *Science* **316**: 112-115.
- Sutter, N. B., D. S. Mosher, M. M. Gray and E. A. Ostrander. 2008. Morphometrics within dog breeds are highly reproducible and dispute Rensch's rule. *Mamm. Genome* **19**: 713-723.
- Szabo-Rogers, H. L., L. E. Smithers, W. Yakob and K. J. Liu. 2010. New directions in craniofacial morphogenesis. *Dev. Biol.* **341**: 84-94.
- Takeshita, S., A. Sasaki, A. S. Publico, M. L. Moss and K. Tanne. 2001. The nature of human craniofacial growth studied with finite element analytical approach. *Clin. Orthod. Res.* **4**: 148-160.
- Tanabe, Y., S. Sugiura, M. Asanoma and K. Ota. 1974. Genetic polymorphism of leucine aminopeptidase in canine plasma. *Anim. Blood Groups Biochem. Genet.* **5**: 225-230.
- Tchernov, E. and F. R. Valla. 1997. Two new dogs, and other Natufian dogs, from the southern Levant. *J. Archaeol. Sci.* **24**: 65-95.
- The, T. K. and C. O. Trough. 1976. Sexual dimorphism in the basilar part of the occipital bone of the dog (*Canis familiaris*). *Acta Anat. (Basel)* **95**(4): 565-571.

- Thompson, D'A. W. 1961. *On Growth and Form*, ed. abr. J. T. Bonner. Cambridge University Press, Cambridge.
- Tito, R. Y., S. L. Belknap III, K. D. Sobolik, R. C. Ongraham, L. M. Cleeland and C. M. Lewis, Jr. 2011. Brief communication: DNA from early Holocene American dog. *Am. J. Phys. Antropol.* **145**: 653-657.
- Trainor, P. A. 2005. Specification of neural crest cell formation and migration in mouse embryos. *Semin. Cell Dev. Biol.* **16**: 683-693.
- Trainor, P. A., K. R. Melton and M. Manzanares. 2003. Origins and plasticity of neural crest cells and their roles in jaw and craniofacial evolution. *Int. J. Dev. Biol.* **47**: 541-553.
- Trainor, P. A., J. Dixon and M. J. Dixon. 2009. Treacher Collins syndrome: etiology, pathogenesis and prevention. *Eur. J. Hum. Genet.* **17**: 275-283.
- Trouth, C. O., S. Winter, K. C. Gupta, R. M. Millis and J. A. Halloway. 1977. Analysis of the sexual dimorphism in the basioccipital portion of the dog's skull. *Acta Anat. (Basel)* **98**: 469-473.
- Trut, L. N. 1999. Early canid domestication: the farm-fox experiment. *Am. Sci.* **87**: 160-169.
- Trut, L. N. 2001. Experimental studies of early canid domestication. Pp. 15-43 in A. Ruvinsky and J. Sampson, eds. *The Genetics of the Dog*. CABI Publishing, Wallingford, UK.
- Trut, L. N., F. Ya. Dzerzhinsky and V. S. Nikolsky. 1991. Intracranial allometry and morphological changes in silver foxes (*Vulpes vulpes*) under domestication. *Genetika* **27**: 1605-1611.
- Trut, L. N., I. Z. Plyusnina and I. N. Oskina. 2004. An experiment on fox domestication and debatable issues of evolution of the dog. *Russ. J. Genet.* **40**: 644-655.
- Trut, L., I. Oskina and A. Kharlamova. 2009. Animal evolution during domestication: the domesticated fox as a model. *BioEssays* **31**(3): 349-360.
- Tseng, Z. J. and X. Wang. 2010. Cranial functional morphology of fossil dogs and adaptation for durophagy in *Borophagus* and *Epiicyon* (Carnivora, Mammalia). *J. Morph.* **271**: 1386-1398.
- Tsuda, K. Y., Kikkawa, H., Yonekawa and Y. Tanabe. 1997. Extensive interbreeding occurred among multiple matriarchal ancestors during the domestication of dogs: evidence from inter- and intraspecies polymorphisms in the D-loop region of mitochondrial DNA between dogs and wolves. *Genes Genet. Syst.* **72**: 229-238.
- Turnbull, P. F. and C. A. Reed. 1974. The fauna from the terminal Pleistocene of Palegawra cave. *Fieldiana: Anthr.* **63**: 81-146.

- Valeri, C. J., T. M. Cole III, S. Lele and J. T. Richtsmeier. 1998. Capturing data from three-dimensional surfaces using fuzzy landmarks. *Am. J. Phys. Anthropol.* **107**: 113-124.
- van Hagen, M. A. E., J. van der Kolk, M. A. M. Barendse, S. Imholz, P. A. J. Leegwater, B. W. Knol and B. A. van Oost. 2004. Analysis of the inheritance of white spotting and the evaluation of KIT and EDNRB as spotting loci in Dutch boxer dogs. *J. Hered.* **95**: 526-531.
- Verginelli, F., C. Capelli, V. Coia, M. Musiani, M. Falchettia, L. Ottini, R. Palmirota, A. Tagliacozzo, I. De Grossi Mazzorin and R. Mariani-Costantini. 2005. Mitochondrial DNA from prehistoric Canids highlights relationships between dogs and South-East European wolves. *Mol. Biol. Evol.* **22**: 2541-2551.
- Vigne, J. D. 2005. L'humérus de chien magdalénien de Eralla (Gipuzkoa, Espagne) et la domestication tardiglaciaire du loup en Europe. *Munibe (Antropologia-Arkeologia)* **57**(1): 279-287.
- Vilà, C., P. Savolainen, J. E. Maldonado, I. R. Amorim, J. E. Rice, R. L. Honeycutt, K. A. Crandall, J. Lundeberg and R. K. Wayne. 1997. Multiple and ancient origins of the domestic dog. *Science* **276**: 1687-1689.
- Vilà, C., J. Maldonado and R. K. Wayne. 1999a. Phylogenetic relationships, evolution and genetic diversity of the domesticated dog. *J. Hered.* **90**: 71-77.
- Vilà, C., I. R. Amorim, J. A. Leonard, D. Posada, J. Catroviejo, F. Petrucci-Fonesca, K. A. Crandall, H. Ellegren and R. K. Wayne. 1999b. Mitochondrial DNA phylogeography and population history of the gray wolf *Canis lupus*. *Mol. Ecol.* **8**: 2089-2103.
- Vilà, C., J. Seddon and H. Ellegren. 2005. Genes of domestic mammals augmented by backcrossing with wild ancestors. *Trends Genet.* **21**: 214-218.
- von Cramon-Taubedal, N., B. C. Frazier and M. M. Lahr. 2007. The problem of assessing landmark error in geometric morphometrics: theory, methods and modifications. *Am. J. Phys. Anthropol.* **134**: 24-35.
- vonHoldt, B. M., J. P. Pollinger, K. E. Lohmueller, E. Han, H. G. Parker, P. Quignon, J. D. Degenhardt, A. R. Boyko, D. A. Earl, A. Auton, A. Reynolds, K. Bryc, A. Brisbin, J. C. Knowles, D. S. Mosher, T. C. Spady, A. Elkahoun, E. Geffen, M. Pilot, W. Jedrzejewski, C. Greco, E. Randi, D. Bannasch, A. Wilton, J. Shearman, M. Musiani, M. Cargill, P. G. Jones, Z. Qian, W. Huang, Z. -L. Ding, Y. Zhang, C. D. Bustamante, E. A. Ostrander, J. Novembre and R. K. Wayne. 2010. Genome-wide SNP and haplotype analyses reveal a rich history underlying dog domestication. *Nature* **464**: 898-902.
- Vriesendorp, H. M. 1972. The occurrence of dog histocompatibility antigens in other Canidae. *Gene Phaenen.* **15**: 73-78.

- Wagner, K. 1929. Rezente Hunderassen. Eine osteologische Untersuchung. *Skrifter Norske Videnskaps Akademi Oslo, I. Mat Naturv. Kl.* **9**: 157.
- Wang, X. and R. H. Tedford. 2008. *Dogs: their fossil relatives and evolutionary history*. Columbia University Press, New York.
- Wayne, R. K. 1984. *A comparative study of skeletal growth and morphology in domestic and wild canids*. Ph.D. dissertation. Johns Hopkins University, Baltimore, MD.
- Wayne, R. K. 1986. Cranial morphology of domestic and wild canids: the influence of development on morphological change. *Evolution* **40**(2): 243-261.
- Wayne, R. K. 1993. Molecular evolution of the dog family. *Trends Genet.* **9**: 218-224.
- Wayne, R. K. 2001. Consequences of domestication: morphological diversity of the dog. Pp. 43-60 in A. Ruvinsky and J. Sampson, eds. *The Genetics of the Dog*. CABI Publishing, Wallingford, UK.
- Wayne, R. K. and S. J. O'Brien. 1987. Allozyme divergence within the Canidae. *Syst. Zool.* **36**: 339-355.
- Wayne, R. K. and E. A. Ostrander. 2007. Lessons learned from the dog genome. *Trends Genet.* **23**: 557-567.
- Wayne, R. K., W. G. Nash and S. J. O'Brien. 1987a. Chromosomal evolution of the Canidae: I. Species with high diploid numbers. *Cytogenet. Cell Genet.* **44**: 123-133.
- Wayne, R. K., W. G. Nash and S. J. O'Brien. 1987b. Chromosomal evolution of the Canidae: II. Divergence from the primitive carnivore karyotype. *Cytogenet. Cell Genet.* **44**: 134-141.
- Wayne, R. K., N. Lehman, M. W. Allard and R. L. Honeycutt. 1992. Mitochondrial DNA variability of the gray wolf: genetic consequences of population decline and habitat fragmentation. *Conserv. Biol.* **6**: 559-569.
- Weidenreich, F. 1941. The brain and its role in the phylogenetic transformation of the human skull. *Trans. Amer. Phil. Soc.* **31**: 321-442.
- Werth, E. 1944. Die primitiven Hunde und die Abstammungsfrage des Haushundes. *Z. Tierzucht. Zuchtungsbiol.* **56**: 213-260.
- White, T. D. 2000. *Human Osteology. Second Edition*. Academic Press, San Diego, California.
- Whitney, L. F. 1948. *How to Breed Dogs*. Rev. ed. Orange Judd Publishing Co., Inc., New York.

- Wilkie, A. O. M. and G. M. Morriss-Kay. 2001. Genetics of craniofacial development and malformation. *Nat. Rev. Genet.* **2**: 458-468.
- Woodard, G. D. and L. F. Marcus. 1973. Rancho La Brea fossil deposits: a re-evaluation from stratigraphic and geological evidence. *J. Paleontol.* **47**: 54-69.
- Wriedt, C. 1929. Aufspaltung der Schädelform des Pekingnesers (vorläufige Mitteilung). *Zuchter* **I**(7): 203-204.
- Wroe, S. and N. Milne. 2007. Convergence and remarkably consistent constraint in the evolution of carnivore skull shape. *Evolution* **61**(5): 1251-1260.
- Wu, P., T. X. Jiang, S. Suksaweang, R. B. Widelitz and C. M. Chuong. 2004. Molecular shaping of the beak. *Science* **305**: 1465-1466.
- Wu, P., T. X. Jiang, J. Y. Shen, R. B. Widelitz and C. M. Chuong. 2006. Morphoregulation of avian beaks: comparative mapping of growth zone activities and morphological evolution. *Dev. Dyn.* **235**: 1400-1412.
- Wyrost, P. and J. Kucharczyk. 1967. Analysis of several parameters of the dog skull in regard to their morphological value. *Acta Theriol.* **12**(13/18): 293-322.
- Yamaguchi, A., T. Kmori and T. Suda. 2000. Regulation of osteoblast differentiation mediated by bone morphogenetic proteins, hedgehogs, and Cbfa1. *Endocr. Rev.* **21**(4): 393-411.
- Yelick, P. C. and T. F. Schilling. 2002. Molecular dissection of craniofacial development using zebrafish. *Crit. Rev. Oral Biol. Med.* **13**: 308-322.
- Zahn, C. T. and R. Z. Roskies. 1972. Fourier descriptors for plane closed curves. *IEEE Trans. Comput.* **C-21**: 269-281.
- Zajc, I., C. S. Mellersh and J. Sampson. 1997. Variability of canine microsatellites within and between different dog breeds. *Mamm. Genome* **8**: 182-185.
- Zedda, M., P. Manca, V. Chisu, S. Gadau, G. Lepore, A. Genovese and V. Farina. 2006. Ancient Pompeian dogs - morphological and morphometric evidence for different canine populations. *Anat. Histol. Embryol.* **35**: 319-324.
- Zelditch, M. L., D. L. Swiderski, H. D. Sheets and W. L. Fink. 2004. *Geometric Morphometrics for Biologists: A Primer*. Academic Press, London.
- Zeuner, F. E. 1963. *A History of Domesticated Animals*. Harper and Row, New York.

Appendix 1: *Canis lupus* sample

Species (n)	Abbr.	Collection	ID	Sex
Grey Wolf (120) (61 Female, 59 Male)	WLF	UAM	16825	Male
	WLF	UAM	16829	Female
	WLF	UAM	16837	Male
	WLF	UAM	16898	Male
	WLF	UAM	16907	Male
	WLF	UAM	16908	Male
	WLF	UAM	16910	Male
	WLF	UAM	16914	Female
	WLF	UAM	16916	Female
	WLF	UAM	16929	Male
	WLF	UAM	16934	Male
	WLF	UAM	16938	Male
	WLF	UAM	17013	Male
	WLF	UAM	17018	Male
	WLF	UAM	17025	Female
	WLF	UAM	17027	Male
	WLF	UAM	17030	Male
	WLF	UAM	17034	Male
	WLF	UAM	17035	Male
	WLF	UAM	17036	Male
	WLF	UAM	17062	Female
	WLF	UAM	17077	Female
	WLF	UAM	17080	Female
	WLF	UAM	17081	Female
	WLF	UAM	17089	Female
	WLF	UAM	17092	Female
	WLF	UAM	17095	Female
	WLF	UAM	17096	Male
	WLF	UAM	17123	Male
	WLF	UAM	17124	Male
	WLF	UAM	17127	Female
	WLF	UAM	17129	Female
	WLF	UAM	17145	Female
	WLF	UAM	17148	Female
	WLF	UAM	17151	Male
	WLF	UAM	17152	Female
	WLF	UAM	17154	Male
	WLF	UAM	17156	Female
	WLF	UAM	17186	Female
	WLF	UAM	17187	Female
WLF	UAM	17221	Male	
WLF	UAM	17225	Female	
WLF	UAM	17241	Female	

Species (n)	Abbr.	Collection	ID	Sex
Grey Wolf (continued)	WLF	UAM	17245	Male
	WLF	UAM	17250	Male
	WLF	UAM	17251	Male
	WLF	UAM	17252	Male
	WLF	UAM	17265	Male
	WLF	UAM	17267	Male
	WLF	UAM	17271	Male
	WLF	UAM	17293	Female
	WLF	UAM	17295	Female
	WLF	UAM	17298	Male
	WLF	UAM	17301	Female
	WLF	UAM	17310	Female
	WLF	UAM	17312	Female
	WLF	UAM	17333	Female
	WLF	UAM	17336	Male
	WLF	UAM	17337	Male
	WLF	UAM	17341	Male
	WLF	UAM	17348	Male
	WLF	UAM	17350	Male
	WLF	UAM	17351	Male
	WLF	UAM	17366	Female
	WLF	UAM	17368	Female
	WLF	UAM	17375	Female
	WLF	UAM	17377	Male
	WLF	UAM	17382	Female
	WLF	UAM	17387	Male
	WLF	UAM	17392	Female
	WLF	UAM	17397	Female
	WLF	UAM	17402	Male
	WLF	UAM	17403	Female
	WLF	UAM	17407	Male
	WLF	UAM	17410	Female
	WLF	UAM	17414	Female
	WLF	UAM	17415	Female
	WLF	UAM	17417	Male
	WLF	UAM	17421	Female
	WLF	UAM	17430	Female
	WLF	UAM	17433	Female
	WLF	UAM	17437	Female
	WLF	UAM	17438	Female
	WLF	UAM	17439	Male
	WLF	UAM	17441	Male
	WLF	UAM	18239	Male
WLF	UAM	18240	Female	
WLF	UAM	18241	Female	

Species (n)	Abbr.	Collection	ID	Sex
Grey Wolf (continued)	WLF	UAM	18243	Male
	WLF	UAM	18245	Female
	WLF	UAM	18246	Female
	WLF	UAM	18250	Female
	WLF	UAM	18255	Female
	WLF	UAM	18257	Male
	WLF	UAM	18285	Female
	WLF	UAM	18287	Female
	WLF	UAM	18294	Male
	WLF	UAM	18295	Female
	WLF	UAM	18301	Female
	WLF	UAM	18303	Male
	WLF	UAM	18305	Male
	WLF	UAM	18310	Female
	WLF	UAM	18312	Male
	WLF	UAM	18316	Female
	WLF	UAM	18323	Female
	WLF	UAM	18325	Male
	WLF	UAM	18326	Female
	WLF	UAM	18327	Female
	WLF	UAM	18330	Male
	WLF	UAM	18336	Female
	WLF	UAM	18345	Female
	WLF	UAM	18347	Female
	WLF	UAM	18354	Male
	WLF	UAM	18385	Male
	WLF	UAM	18386	Male
	WLF	UAM	18391	Male
	WLF	UAM	18392	Female
	WLF	UAM	21420	Male
	WLF	UAM	21422	Male
	WLF	UAM	21423	Male

Appendix 2: *Canis familiaris* sample

Breed (n)	Abbr.	Collection	ID	Sex
AFFENPINSCHER (1)	AFF	AMNH	212877	unknown
AFGHAN HOUND(3)	AFG	AMNH	165673	unknown
	AFG	AMNH	189373	Male
	AFG	NMNH	506608	Female
AIREDALE TERRIER (4)	AIR	AMNH	11154	unknown
	AIR	AMNH	63976	Male
	AIR	NMNH	289972	unknown
	AIR	ROM	13149	Male
AMERICAN PIT BULL TERRIER (1)	AMP	NMNH	546132	Female
AMERICAN WATER SPANIEL (1)	AWS	NHMLAC	30124	Male
AUSTRALIAN CATTLE DOG (1)	ACD	CAS	26738	unknown
BASENJI (2)	BAS	ROM	14070	Male
	BAS	ROM	14098	unknown
BEAGLE (2)	BEA	MCZ	47065	unknown
	BEA	ROM	3403270001	Female
BERGER PICARD (1)	BRP	MCZ	11178	unknown
BLOODHOUND (3)	BLO	NMNH	20837	unknown
	BLO	YPM	1942	Male
	BLO	YPM	4007	Female
BORDER COLLIE (11)	BCL	AMNH	10746	unknown
	BCL	AMNH	16257	Male
	BCL	AMNH	16258	Male
	BCL	AMNH	16259	Male
	BCL	AMNH	16260	Male
	BCL	AMNH	16261	Female
	BCL	AMNH	16263	Male
	BCL	AMNH	16265	Male
	BCL	AMNH	16266	unknown
	BCL	AMNH	78	unknown
	BCL	NMNH	22141	unknown
BORZOI (45)	BOR	AMNH	100450	Male
	BOR	AMNH	15837	unknown
	BOR	AMNH	180256	unknown
	BOR	AMNH	204177	Female
	BOR	AMNH	238447	unknown
	BOR	AMNH	80291	unknown
	BOR	MCZ	51733	unknown
	BOR	NHMB	1051148	Female
	BOR	NHMB	1051149	unknown
	BOR	NHMB	1051150	unknown
	BOR	NHMB	1051152	Male
	BOR	NHMB	1051153	Male

Breed (n)	Abbr.	Collection	ID	Sex
BORZOI (continued)	BOR	NHMB	1051154	Male
	BOR	NHMB	1051155	Male
	BOR	NHMB	1051158	Male
	BOR	NHMB	1051159	Female
	BOR	NHMB	1051160	Male
	BOR	NHMB	1051161	Female
	BOR	NHMB	1051163	Female
	BOR	NHMB	1051164	Male
	BOR	NHMB	1051165	Male
	BOR	NHMB	1051166	Female
	BOR	NHMB	1051167	Female
	BOR	NHMB	1051168	Male
	BOR	NHMB	1051169	Male
	BOR	NHMB	1051170	Male
	BOR	NHMB	1051171	Male
	BOR	NHMB	1051172	Female
	BOR	NHMB	1051174	Male
	BOR	NHMB	1051175	Female
	BOR	NHMB	1051176	Male
	BOR	NHMB	1051177	Female
	BOR	NHMB	1051178	Male
	BOR	NHMB	1051179	Female
	BOR	NHMB	1051180	Female
	BOR	NHMB	1051182	Female
	BOR	NHMB	1051183	Female
	BOR	NHMB	1051184	Female
	BOR	NHMB	1052706	Female
	BOR	NHMB	1053128	Female
	BOR	NHMB	1055706	Female
	BOR	NMNH	269321	Male
	BOR	NMNH	291144	Male
	BOR	RBC	2703	unknown
BOR	YPM	2573	Male	
BOSTON TERRIER (6)	BOS	MCZ	19745	unknown
	BOS	NHMB	1051960	Male
	BOS	NMNH	200888	Male
	BOS	RBC	26499	unknown
	BOS	RBC	713	unknown
	BOS	YPM	1524	Male
BOXER (60)	BOX	CAS	27978	Male
	BOX	MVZ	114572	Male
	BOX	NHMB	1051299	unknown
	BOX	NHMB	1051300	unknown
	BOX	NHMB	1051301	unknown
	BOX	NHMB	1051302	unknown

Breed (n)	Abbr.	Collection	ID	Sex
BOXER (continued)	BOX	NHMB	1051303	unknown
	BOX	NHMB	1051304	unknown
	BOX	NHMB	1051305	Male
	BOX	NHMB	1051306	Male
	BOX	NHMB	1051308	Male
	BOX	NHMB	1051309	Female
	BOX	NHMB	1051310	Male
	BOX	NHMB	1051311	Male
	BOX	NHMB	1051312	Male
	BOX	NHMB	1051313	Male
	BOX	NHMB	1051314	Male
	BOX	NHMB	1051317	Female
	BOX	NHMB	1051318	Female
	BOX	NHMB	1051321	Male
	BOX	NHMB	1051322	Female
	BOX	NHMB	1051323	Male
	BOX	NHMB	1051324	Female
	BOX	NHMB	1051325	Male
	BOX	NHMB	1051326	Male
	BOX	NHMB	1051327	Female
	BOX	NHMB	1051328	Female
	BOX	NHMB	1051330	Male
	BOX	NHMB	1051331	Female
	BOX	NHMB	1051332	Male
	BOX	NHMB	1051333	Female
	BOX	NHMB	1051334	Female
	BOX	NHMB	1051335	Male
	BOX	NHMB	1051336	Female
	BOX	NHMB	1051337	Female
	BOX	NHMB	1051338	Male
	BOX	NHMB	1051339	Male
	BOX	NHMB	1051340	Male
	BOX	NHMB	1051341	Female
	BOX	NHMB	1051342	Male
	BOX	NHMB	1051343	Female
	BOX	NHMB	1051344	Female
	BOX	NHMB	1051345	Male
	BOX	NHMB	1051346	Female
	BOX	NHMB	1051347	Male
	BOX	NHMB	1051348	Female
BOX	NHMB	1052275	Male	
BOX	NHMB	1052702	Male	
BOX	NHMB	1052704	Female	
BOX	NHMB	1052705	Male	
BOX	RBC		1275	unknown

Breed (n)	Abbr.	Collection	ID	Sex
Boxer (continued)	BOX	RBC	1276	unknown
	BOX	RBC	153	unknown
	BOX	RBC	154	unknown
	BOX	RBC	594	unknown
	BOX	RBC	595	unknown
	BOX	RBC	596	unknown
	BOX	RBC	717	unknown
	BOX	RBC	743	unknown
	BOX	RBC	995	unknown
BRITTANY (1)	BRT	MVZ	114371	Male
BULL TERRIER (25)	BLT	AMNH	70118	Male
	BLT	AMNH	77	unknown
	BLT	MCZ	25509	unknown
	BLT	NHMB	1050921	Male
	BLT	NHMB	1050922	Female
	BLT	NHMB	1050923	Male
	BLT	NHMB	1050924	Male
	BLT	NHMB	1050925	Male
	BLT	NHMB	1050926	Male
	BLT	NHMB	1050927	Male
	BLT	NHMB	1050928	Male
	BLT	NHMB	1050929	Male
	BLT	NHMB	1050930	Male
	BLT	NHMB	1050931	Female
	BLT	NHMB	1050932	Male
	BLT	NHMB	1050933	Male
	BLT	NHMB	1050934	Male
	BLT	NHMB	1050935	Female
	BLT	NHMB	1050936	Female
	BLT	NHMB	1050937	Male
BLT	NHMB	1050938	Male	
BLT	NHMB	1052350	Male	
BLT	NHMB	1053188	Male	
BLT	NHMLAC	30419	Male	
BLT	NMNH	21995	Female	
BULLDOG (21)	BUL	AMNH	35609	unknown
	BUL	AMNH	69453	unknown
	BUL	AMNH	69456	unknown
	BUL	MCZ	10729	unknown
	BUL	MVZ	107176	Male
	BUL	MVZ	79819	Female
	BUL	NHMB	1050370	unknown
	BUL	NHMB	1050371	unknown
	BUL	NHMB	1050373	unknown
	BUL	NHMB	1050374	Female

Breed (n)	Abbr.	Collection	ID	Sex
BULLDOG (continued)	BUL	NHMB	1050375	Female
	BUL	NHMB	1050376	Female
	BUL	NHMB	1050378	Female
	BUL	NHMLAC	30129	Male
	BUL	NHMLAC	30529	unknown
	BUL	NMNH	21989	Male
	BUL	NMNH	785	unknown
	BUL	NMNH	785(B)	unknown
	BUL	RBC	26505	unknown
	BUL	RBC	714	unknown
BUL	RBC	716	unknown	
CAIRN TERRIER (1)	CAI	NMNH	289967	Female
CHIHUAHUA (18)	CHI	AMNH	100132	unknown
	CHI	AMNH	90210	Male
	CHI	AMNH	90231	Female
	CHI	NHMB	1051988	Female
	CHI	NHMB	1051998	Female
	CHI	NHMB	1052001	Male
	CHI	NHMB	1052006	Male
	CHI	NHMB	1052007	Female
	CHI	NHMB	1052008	Male
	CHI	NHMB	1052009	Female
	CHI	NHMB	1052010	Female
	CHI	NHMB	1052346	Female
	CHI	NMNH	175867	Female
	CHI	NMNH	270172	Male
	CHI	RBC	1296	unknown
	CHI	RBC	2280	unknown
	CHI	RBC	597	unknown
CHI	YPM	1469	Female	
CHINESE CRESTED DOG (1)	CCD	NMNH	21077	Male
CHOW CHOW (28)	CHO	AMNH	63770	Male
	CHO	CAS	26735	unknown
	CHO	NHMB	1051756	unknown
	CHO	NHMB	1051757	Female
	CHO	NHMB	1051758	Male
	CHO	NHMB	1051759	Female
	CHO	NHMB	1051760	Female
	CHO	NHMB	1051761	Female
	CHO	NHMB	1051762	Male
	CHO	NHMB	1051763	Male
	CHO	NHMB	1051764	Male
	CHO	NHMB	1051765	Female
	CHO	NHMB	1051766	Female

Breed (n)	Abbr.	Collection	ID	Sex
CHOW CHOW (continued)	CHO	NHMB	1051767	Female
	CHO	NHMB	1051768	Female
	CHO	NHMB	1051769	Female
	CHO	NHMB	1051770	Female
	CHO	NHMB	1051771	Female
	CHO	NHMB	1051772	Male
	CHO	NHMB	1051773	Male
	CHO	NHMB	1051774	Male
	CHO	NHMB	1051775	Female
	CHO	NHMB	1051777	Female
	CHO	NHMB	1051779	Male
	CHO	NHMB	1051781	Male
	CHO	NHMB	1051782	Female
	CHO	ROM	14359	Male
	CHO	YPM	2347	Female
CLUMBER SPANIEL (1)	CLU	YPM	2664	Female
COLLIE (45)	COL	AMNH	35865	unknown
	COL	AMNH	99667	Male
	COL	AMNH	99673	unknown
	COL	AMNH	99679	Male
	COL	AMNH	99680	Male
	COL	MVZ	118988	Female
	COL	NHMB	1050799	unknown
	COL	NHMB	1050801	Male
	COL	NHMB	1050803	unknown
	COL	NHMB	1050805	unknown
	COL	NHMB	1050807	Female
	COL	NHMB	1050809	Female
	COL	NHMB	1050812	Male
	COL	NHMB	1050813	Male
	COL	NHMB	1050814	unknown
	COL	NHMB	1050815	Female
	COL	NHMB	1050816	Male
	COL	NHMB	1050817	Female
	COL	NHMB	1050818	Female
	COL	NHMB	1050819	Male
	COL	NHMB	1050820	Female
	COL	NHMB	1050821	Female
	COL	NHMB	1050822	Male
	COL	NHMB	1050824	Female
	COL	NHMB	1050825	Female
	COL	NHMB	1050826	Male
	COL	NHMB	1050828	Male
	COL	NHMB	1050829	Female
	COL	NHMB	1050830	Male

Breed (<i>n</i>)	Abbr.	Collection	ID	Sex
COLLIE (continued)	COL	NHMB	1050831	Female
	COL	NHMB	1050835	Female
	COL	NHMB	1050836	Male
	COL	NHMB	1050841	Male
	COL	NHMB	1050842	Male
	COL	NHMB	1050845	Female
	COL	NHMB	1050847	Female
	COL	NHMLAC	30128	Female
	COL	NHMLAC	30528	unknown
	COL	NMNH	241137	Male
	COL	RBC	1300	unknown
	COL	RBC	3806	unknown
	COL	RBC	557	unknown
	COL	RBC	715	unknown
	COL	ROM	16090	Male
	COL	YPM	2653	Male
DACHSHUND (3)	DAC	NHMLAC	30598	Female
	DAC	NHMLAC	31106	Male
	DAC	NMNH	22194	unknown
DALMATION (1)	DAL	NMNH	21996	unknown
DOBERMAN PINSCHER (5)	DOB	AMNH	140219	Male
	DOB	NMNH	349500	Female
	DOB	RBC	1017	unknown
	DOB	RBC	1563	unknown
	DOB	RBC	32	unknown
ENGLISH FOXHOUND (1)	ENF	YPM	2681	Male
ENGLISH MASTIFF (4)	ENM	NMNH	22249	Male
	ENM	ROM	3111230018	unknown
	ENM	ROM	3503210001	Male
	ENM	YPM	2419	Male
ENGLISH SETTER (3)	ENS	AMNH	100321	Male
	ENS	NMNH	22044	Male
	ENS	NHMLAC	31114	unknown
ENGLISH SPRINGER SPANIEL (4)	ESS	MCZ	44675	unknown
	ESS	CAS	26736	unknown
	ESS	ROM	13119	Female
	ESS	ROM	14303	Female
ENGLISH WHITE TERRIER (1)	EWT	MCZ	44674	unknown
FOX TERRIER (4)	FOX	MVZ	98106	Male
	FOX	NHMLAC	30126	Male
	FOX	NMNH	122760	Male
	FOX	ROM	13008	Female
FRENCH BULLDOG (17)	FRB	NHMB	1051888	Male
	FRB	NHMB	1051889	Male

Breed (n)	Abbr.	Collection	ID	Sex
FRENCH BULLDOG (continued)	FRB	NHMB	1051893	Male
	FRB	NHMB	1051894	Female
	FRB	NHMB	1051895	Female
	FRB	NHMB	1051896	Female
	FRB	NHMB	1051898	Female
	FRB	NHMB	1051899	Female
	FRB	NHMB	1051900	Female
	FRB	NHMB	1051901	Female
	FRB	NHMB	1051903	Male
	FRB	NHMB	1051904	Female
	FRB	NHMB	1051905	Male
	FRB	NHMB	1051906	Male
	FRB	NHMB	1051907	unknown
	FRB	NHMB	1051908	Male
	FRB	NHMB	1052279	Female
GERMAN SHEPHERD DOG (22)	GSD	AMNH	165623	unknown
	GSD	AMNH	204218	Female
	GSD	AMNH	99663	Male
	GSD	AMNH	99664	Male
	GSD	AMNH	99665	Male
	GSD	AMNH	99666	Female
	GSD	AMNH	99669	unknown
	GSD	MVZ	106177	Male
	GSD	NMNH	187987	Female
	GSD	NMNH	272209	Female
	GSD	NMNH	274104	unknown
	GSD	NMNH	347608	unknown
	GSD	RBC	1277	unknown
	GSD	RBC	520	unknown
	GSD	RBC	550	unknown
	GSD	RBC	599	unknown
	GSD	RBC	719	unknown
	GSD	ROM	14888	Female
	GSD	ROM	15611	Female
	GSD	ROM	3201530001	unknown
	GSD	YPM	2595	Male
	GSD	YPM	4006	Female
GORDON SETTER (1)	GOR	AMNH	6284	Male
GREAT DANE (23)	GRD	AMNH	35564	Male
	GRD	NHMB	1050403	Male
	GRD	NHMB	1050404	Female
	GRD	NHMB	1050405	unknown
	GRD	NHMB	1050406	Female
	GRD	NHMB	1050407	Female
	GRD	NHMB	1050408	unknown

Breed (n)	Abbr.	Collection	ID	Sex
GREAT DANE (continued)	GRD	NHMB	1050409	unknown
	GRD	NHMB	1050410	unknown
	GRD	NHMB	1050411	unknown
	GRD	NHMB	1050412	unknown
	GRD	NHMB	1050414	Female
	GRD	NHMB	1050415	Male
	GRD	NHMB	1050423	Male
	GRD	NHMB	1050427	Male
	GRD	NHMB	1050428	Female
	GRD	RBC	1350	unknown
	GRD	RBC	586	unknown
	GRD	RBC	744	unknown
	GRD	ROM	13034	Male
	GRD	ROM	14061	Male
	GRD	ROM	15758	Male
	GRD	YPM	1362	Male
GREYHOUND (26)	GRY	AMNH	228654	unknown
	GRY	MCZ	11107	unknown
	GRY	MCZ	44700	unknown
	GRY	MCZ	9334	unknown
	GRY	NHMB	1051237	unknown
	GRY	NHMB	1051245	Male
	GRY	NHMB	1051246	Male
	GRY	NHMB	1051250	Female
	GRY	NHMB	1051251	Male
	GRY	NHMB	1051252	Male
	GRY	NHMB	1051254	Male
	GRY	NHMB	1051257	Male
	GRY	NHMB	1051258	Male
	GRY	NHMB	1051259	Female
	GRY	NHMB	1051261	Female
	GRY	NHMB	1051262	Male
	GRY	NHMB	1051263	Male
	GRY	NHMB	1051264	Male
	GRY	NHMB	1051266	Male
	GRY	NHMB	1056115	Female
	GRY	NMNH	20805	unknown
	GRY	NMNH	22308	unknown
	GRY	NMNH	22690	unknown
	GRY	RBC	861	unknown
GRY	ROM	13007	Male	
GRY	ROM	13038	Female	
GRIFFON BRUXELLOIS(1)	GRF	ROM	14432	Male
IRISH SETTER (3)	IRS	AMNH	17432	Female
	IRS	NHMLAC	31092	Female

Breed (n)	Abbr.	Collection	ID	Sex
IRISH SETTER (continued)	IRS	NMNH	22252	unknown
IRISH TERRIER (2)	IRT	AMNH	90154	Female
	IRT	AMNH	90155	Male
IRISH WOLFHOUND (25)	IRW	AMNH	100080	unknown
	IRW	AMNH	100128	Male
	IRW	AMNH	64000	unknown
	IRW	AMNH	80022	Male
	IRW	AMNH	90250	Male
	IRW	NHMB	1051239	unknown
	IRW	NHMB	1051244	unknown
	IRW	NHMB	1051249	Male
	IRW	NHMB	1051253	Male
	IRW	NHMB	1051272	Female
	IRW	NHMB	1051281	Male
	IRW	NMNH	289976	Male
	IRW	NMNH	289977	Female
	IRW	NMNH	347441	Female
	IRW	NMNH	347480	Female
	IRW	NMNH	347609	Female
	IRW	NMNH	350000	unknown
	IRW	NMNH	396991	Female
	IRW	NMNH	398215	Female
	IRW	NMNH	398536	Male
IRW	NMNH	399049	unknown	
IRW	NMNH	505255	Female	
IRW	NMNH	524513	unknown	
IRW	ROM	16046	Female	
IRW	YPM	1458	Male	
ITALIAN GREYHOUND (2)	ITG	AMNH	6285	unknown
	ITG	NMNH	21998	Male
KERRY BLUE TERRIER (1)	KBT	ROM	11184	unknown
KING CHARLES SPANIEL (2)	KCS	MCZ	11209	unknown
	KCS	MCZ	44696	unknown
KOMONDOR (1)	KOM	CAS	26776	Female
LABRADOR HUSKY (1)	LHU	YPM	2600	Male
LABRADOR RETRIEVER (2)	LAB	CAS	26734	unknown
	LAB	CAS	26737	unknown
MINIATURE PINSCHER (1)	MNP	NMNH	49610	unknown
MINIATURE SCHNAUZER (1)	MNS	NMNH	289971	unknown
NEWFOUNDLAND (17)	NEW	AMNH	42899	unknown
	NEW	AMNH	69465	unknown
	NEW	AMNH	69467	Male
	NEW	AMNH	69468	unknown
	NEW	AMNH	69469	unknown

Breed (n)	Abbr.	Collection	ID	Sex
NEWFOUNDLAND (continued)	NEW	NHMB	1050481	Female
	NEW	NHMB	1050487	Male
	NEW	NHMB	1050488	Male
	NEW	NHMB	1050490	Male
	NEW	NHMB	1050494	Male
	NEW	NMNH	187985	Male
	NEW	NMNH	22365	unknown
	NEW	NMNH	23005	Male
	NEW	RBC	1561	unknown
	NEW	ROM	16327	Male
	NEW	YPM	1074	Male
	NEW	YPM	1468	Female
OLD ENGLISH SHEEPDOG (2)	OES	AMNH	132868	unknown
	OES	NHMLAC	31009	Male
OTTERHOUND (1)	OTT	NMNH	283103	Male
PEKINGESE (15)	PEK	AMNH	100188	Male
	PEK	AMNH	179936	unknown
	PEK	AMNH	204453	Male
	PEK	AMNH	20868	Male
	PEK	AMNH	34719	unknown
	PEK	AMNH	35171	unknown
	PEK	AMNH	90118	Female
	PEK	MCZ	11212	unknown
	PEK	MCZ	9333	unknown
	PEK	NHMB	1051962	Male
	PEK	NHMB	1051963	Female
	PEK	NHMB	1051964	Male
	PEK	NHMB	1053190	Female
	PEK	RBC	26497	unknown
	PEK	RBC	3996	unknown
POINTER (4)	POI	MCZ	23712	unknown
	POI	NMNH	187988	Male
	POI	NMNH	22563	unknown
	POI	YPM	2616	Male
POMERANIAN (4)	POM	AMNH	61588	Male
	POM	RBC	26496	unknown
	POM	RBC	3992	unknown
	POM	RBC	598	unknown
POODLE (1)	POO	MCZ	52234	Male
PUG (14)	PUG	NHMB	1051924	unknown
	PUG	NHMB	1051925	unknown
	PUG	NHMB	1051927	Male
	PUG	NHMB	1051932	Female
	PUG	NHMB	1051935	Male

Breed (n)	Abbr.	Collection	ID	Sex
PUG (continued)	PUG	NHMB	1051936	Female
	PUG	NHMB	1055712	Female
	PUG	NHMB	1055713	Male
	PUG	NHMLAC	30595	Male
	PUG	NHMLAC	30605	unknown
	PUG	NMNH	20190	Male
	PUG	NMNH	21664	Male
	PUG	RBC	31	unknown
	PUG	RBC	741	unknown
PULI (1)	PUL	MCZ	56784	Male
RAT TERRIER (1)	RAT	CAS	27834	Male
SALUKI (4)	SAL	AMNH	120450	unknown
	SAL	MCZ	34072	unknown
	SAL	ROM	10147	Male
	SAL	YPM	1602	Female
SCHIPPERKE (1)	SCH	MCZ_	20966	unknown
SCOTTISH DEERHOUND (2)	SCD	MCZ	25825	Female
	SCD	YPM	2666	Male
SCOTTISH TERRIER (2)	SCT	AMNH	90212	unknown
	SCT	ROM	16225	Female
SEALYHAM TERRIER (1)	SEA	MVZ	81374	unknown
	SEA	ROM	3401100003	Male
SHAR PEI (4)	SHP	CAS	26732	unknown
	SHP	NHMB	1051776	Female
	SHP	NHMB	1051778	Female
	SHP	NHMB	1051780	Male
SHETLAND SHEEPDOG (4)	SHS	MCZ	28251	Female
	SHS	MCZ	58252	Male
	SHS	NHMB	1050823	Female
	SHS	NHMB	1050827	Male
SIBERIAN BLOODHOUND (1)	SIB	YPM	1047	unknown
ST BERNARD (4)	STB	CAS	26742	Female
	STB	NMNH	86370	Female
	STB	ROM	11695	unknown
	STB	ROM	3311290006	Male
WELSH TERRIER (3)	WEL	NMNH	122749	Male
	WEL	NMNH	187984	Male
	WEL	NMNH	23224	Male
WEST HIGHLAND WHITE TERRIER (1)	WHW	MCZ	28816	unknown

Appendix 3: Cranial landmark definitions

(Landmark numbers refer to Figure 2.6)

Dorsal landmarks

- 1 Midline point on anterior incisive bone, dorsal relative to incisor alveolar borders.
- 2 Point at ventral-most extent of left incisive-maxillary suture, anterior to right canine.
- 3 Point at ventral-most extent of right incisive-maxillary suture, anterior to left canine
- 4 Point at anterior-most projection of right nasal bone.
- 5 Midline point at anterior-most extent of midline nasal suture.
- 6 Point at anterior-most projection of left nasal bone.
- 7 Point at junction of right nasal-incisive and incisive-maxillary sutures.
- 8 Midline point between landmarks 7 and 9 on midline nasal suture.
- 9 Point at junction of left nasal-incisive and incisive-maxillary sutures.
- 10 Point at dorsal-most border of right infraorbital foramen.
- 11 Point at dorsal-most border of left infraorbital foramen.
- 12 Point at anterior-most extent of right frontal bone (between left nasal and maxilla).
- 13 Midline point between landmarks 12 and 14 on midline nasal suture.
- 14 Point at anterior-most extent of left frontal bone (between right nasal and maxilla).
- 15 Point at ventral-most extent of right zygomatic-maxillary suture on maxillary process of the zygomatic.
- 16 Point at posterior-most extent of right maxillary bone at articulation with zygomatic bone, dorsal to the maxillary process of the zygomatic
- 17 Point at posterior-most extent of left maxillary bone at articulation with zygomatic bone, dorsal to the maxillary process of the zygomatic.
- 18 Point at ventral-most extent of left zygomatic-maxillary suture on maxillary process of the zygomatic.
- 19 Point at dorsal-most extent of right zygomatic bone along infraorbital margin (contact with right lacrimal).
- 20 Midline point at posterior-most extent of nasals.
- 21 Point at dorsal-most extent of left zygomatic bone along infraorbital margin (contact with left lacrimal).
- 22 Point at dorsal-most extent of frontal process of right maxilla.
- 23 Point at dorsal-most extent of frontal process of left maxilla.
- 24 Point at ventral-most extent of the lateral zygomatic process of right frontal.
- 25 Midline point between landmarks 24 and 26 on midline frontal suture.
- 26 Point at ventral-most extent of the lateral zygomatic process of left frontal.
- 27 Point at dorsal-most extent of medial frontal process of right zygomatic.
- 28 Point at dorsal-most extent of medial frontal process of left zygomatic.
- 29 Point at lateral-most extent of right zygomatic arch on temporal-zygoamtic suture.
- 30 Point at junction of right frontal-parietal suture with left parietal-temporal suture.
- 31 Point at junction of left frontal-parietal suture with right parietal-temporal suture.
- 32 Point at lateral-most extent of left zygomatic arch on temporal-zygoamtic suture.
- 33 Point at lateral-most extent of right nuchal crest, dorsal to mastoid process.
- 34 Point at junction of right parietal-temporal suture and nuchal crest.
- 35 Point at junction of left parietal-temporal suture and nuchal crest.
- 36 Point at lateral-most extent of left nuchal crest, dorsal to mastoid process.

Ventral landmarks

- 37 Midline point at anterior-most extent of alveolar bone separating first incisors.
- 38 Point at anterior-most margin of left palatine fissure.
- 39 Point at anterior-most margin of right palatine fissure.
- 40 Point at posterior-most extent of left C root (contact with alveolar bone).
- 41 Point at posterior-most margin of left palatine fissure.
- 42 Midline point at junction of midline suture and incisive-maxillary suture.
- 43 Point at posterior-most margin of right palatine fissure.
- 44 Point at posterior-most extent of right C root (contact with alveolar bone).
- 45 Midline point at junction of palatine and maxillary bones.
- 46 Point at posterior-most extent of left P4 root (contact with alveolar bone).
- 47 Point at posterior-most extent of the margin of the left major palatine foramen.
- 48 Point at posterior-most extent of the margin of the right major palatine foramen.
- 49 Point at posterior-most extent of right P4 root (contact with alveolar bone).
- 50 Point at posterior-most extent of suture between the left palatine and maxilla.
- 51 Midline point at posterior-most extent of palatine.
- 52 Point at posterior-most extent of suture between the right palatine and maxilla.
- 53 Midline point at the sphenoidal incisure, or the midline junction of the vomer and presphenoid.
- 54 Point at the ventral-most extent of the left pterygoid-palatine suture.
- 55 Point at the ventral-most extent of the right pterygoid-palatine suture.
- 56 Point at posterior-most extent of ventral zygomatic-temporal suture on left zygomatic arch.
- 57 Point at the anterior border of the left zygomatic process of the temporal bone, just medial to landmark 56, at the anterior-most projection of the rugose muscle attachment.
- 58 Midline point at presphenoid-basisphenoid suture.
- 59 Point at the anterior border of the right zygomatic process of the temporal bone, just medial to landmark 60, at the anterior-most projection of the rugose muscle attachment.
- 60 Point at posterior-most extent of ventral zygomatic-temporal suture on right zygomatic arch.
- 61 Point at lateral-most extent of left retroarticular foramen, lateral to the bulla.
- 62 Point at medial-most extent of tympanooccipital fissure just posterior to bulla at junction of left occipital and temporal.
- 63 Midline point on basisphenoid-occipital suture.
- 64 Point at medial-most extent of tympanooccipital fissure just posterior to bulla at junction of right occipital and temporal.
- 65 Point at lateral-most extent of right retroarticular foramen, lateral to the bulla.
- 66 Midline point at ventral-most extent of ventral margin of foramen magnum.
- 67 Point at lateral-most extent of left lateral margin of foramen magnum.
- 68 Midline point at dorsal-most extent of dorsal margin of foramen magnum.
- 69 Point at lateral-most extent of right lateral margin of foramen magnum.
- 70 Midline point at dorsal-most extent of external occipital protuberance.

Reference landmarks

- A Point at dorsal-most border of right infraorbital foramen. (LM #10)
- B Point at dorsal-most border of left infraorbital foramen. (LM #11)
- C Point at ventral-most extent of right zygomatic-maxillary suture on maxillary process of the zygomatic. (LM #15)
- D Point at ventral-most extent of left zygomatic-maxillary suture on maxillary process of the zygomatic. (LM #18)

Appendix 4: Landmark coordinate standard deviations (gray wolf, 20 trials)

Landmark	Standard Deviation (mm)		
	X	Y	Z
1	0.266	0.220	0.289
2	0.248	0.463	0.365
3	0.177	0.235	0.236
4	0.416	0.339	0.293
5	0.302	0.408	0.365
6	0.575	0.311	0.474
7	0.550	0.395	0.267
8	0.518	0.738	0.489
9	0.571	0.437	0.259
10	0.155	0.245	0.310
11	0.181	0.227	0.312
12	0.614	0.330	0.259
13	0.606	0.687	0.351
14	0.543	0.604	0.417
15	0.271	0.161	0.363
16	0.138	0.715	0.346
17	0.202	0.256	0.145
18	0.591	0.218	0.280
19	0.653	0.370	0.575
20	0.396	0.446	0.180
21	0.623	0.355	0.484
22	0.811	0.420	0.257
23	0.644	0.364	0.174
24	0.417	0.589	0.241
25	0.225	0.295	0.125
26	0.280	0.523	0.176
27	0.307	0.419	0.168
28	0.526	0.417	0.108
29	0.179	0.211	0.201
30	0.159	0.418	0.404
31	0.175	0.288	0.644
32	0.293	0.254	0.268
33	0.309	0.479	0.217
34	0.329	0.479	0.472
35	0.240	0.547	0.526
36	0.260	0.317	0.334
37	1.358	0.386	0.388
38	1.258	0.486	0.192
39	1.221	0.402	0.132
40	1.184	0.473	0.243
41	1.270	0.361	0.170
42	1.247	0.416	0.222

Landmark	X	Y	Z
43	1.246	0.352	0.219
44	1.177	0.299	0.169
45	0.867	0.411	0.163
46	1.399	0.386	0.509
47	0.971	0.475	0.240
48	0.920	0.325	0.208
49	0.971	0.341	0.277
50	0.464	0.799	0.203
51	0.613	0.609	0.205
52	0.703	0.443	0.108
53	0.773	0.427	0.073
54	0.886	0.385	0.247
55	0.721	0.707	0.608
56	0.578	0.903	0.367
57	0.651	0.917	0.357
58	0.591	0.537	0.145
59	0.577	0.374	0.392
60	0.624	0.228	0.173
61	0.581	0.547	0.215
62	0.487	0.439	0.345
63	0.762	1.580	0.827
64	0.494	0.380	0.267
65	0.571	0.298	0.138
66	0.473	0.415	0.123
67	0.514	0.528	0.457
68	0.397	0.445	0.114
69	0.381	0.419	0.585
70	0.304	0.602	0.134
Average	0.585	0.447	0.294

Appendix 5: Focus breed second principal components of shape variation

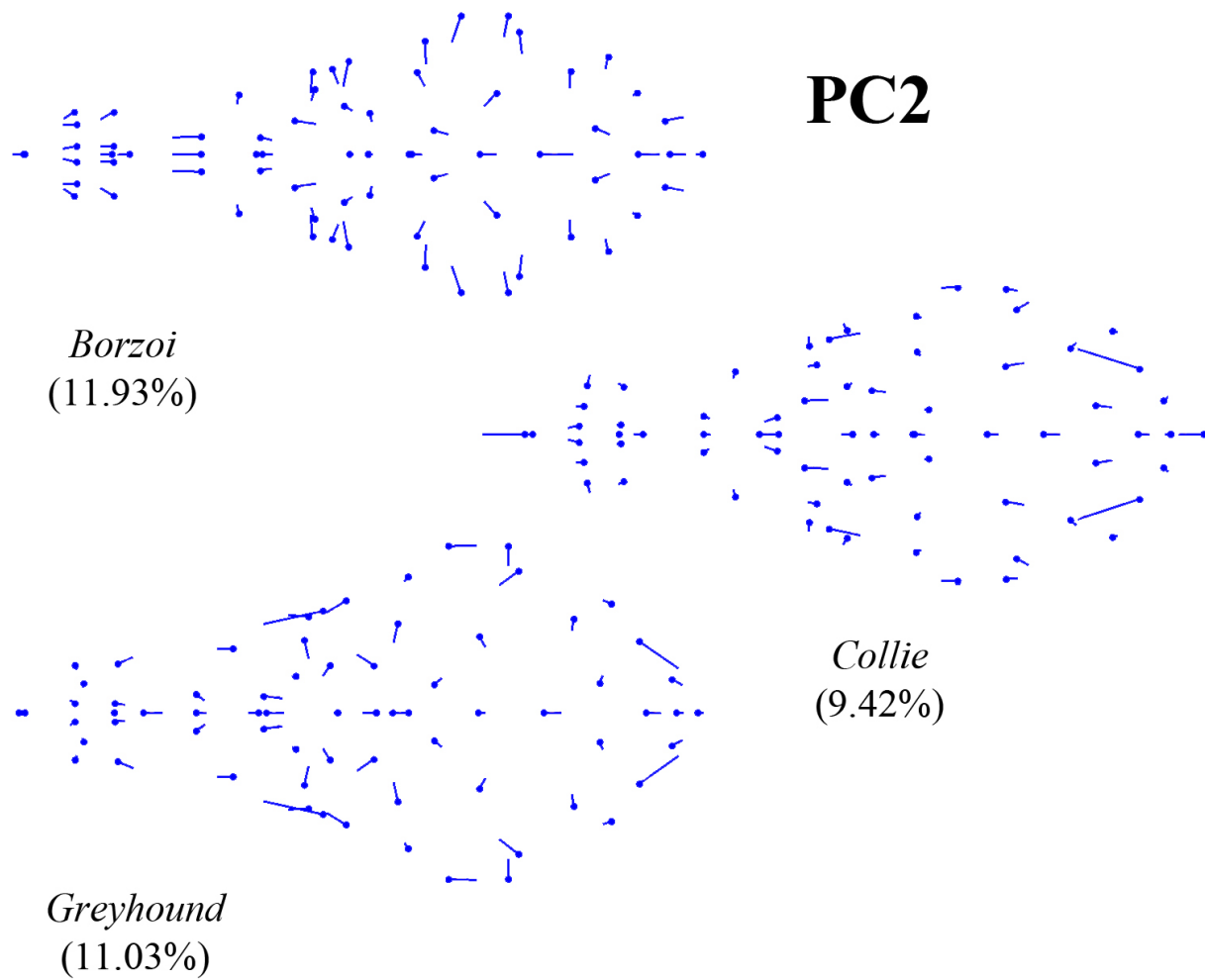


Figure A.1 Second principal components of shape variation for dolichocephalic breeds, dorsal view.

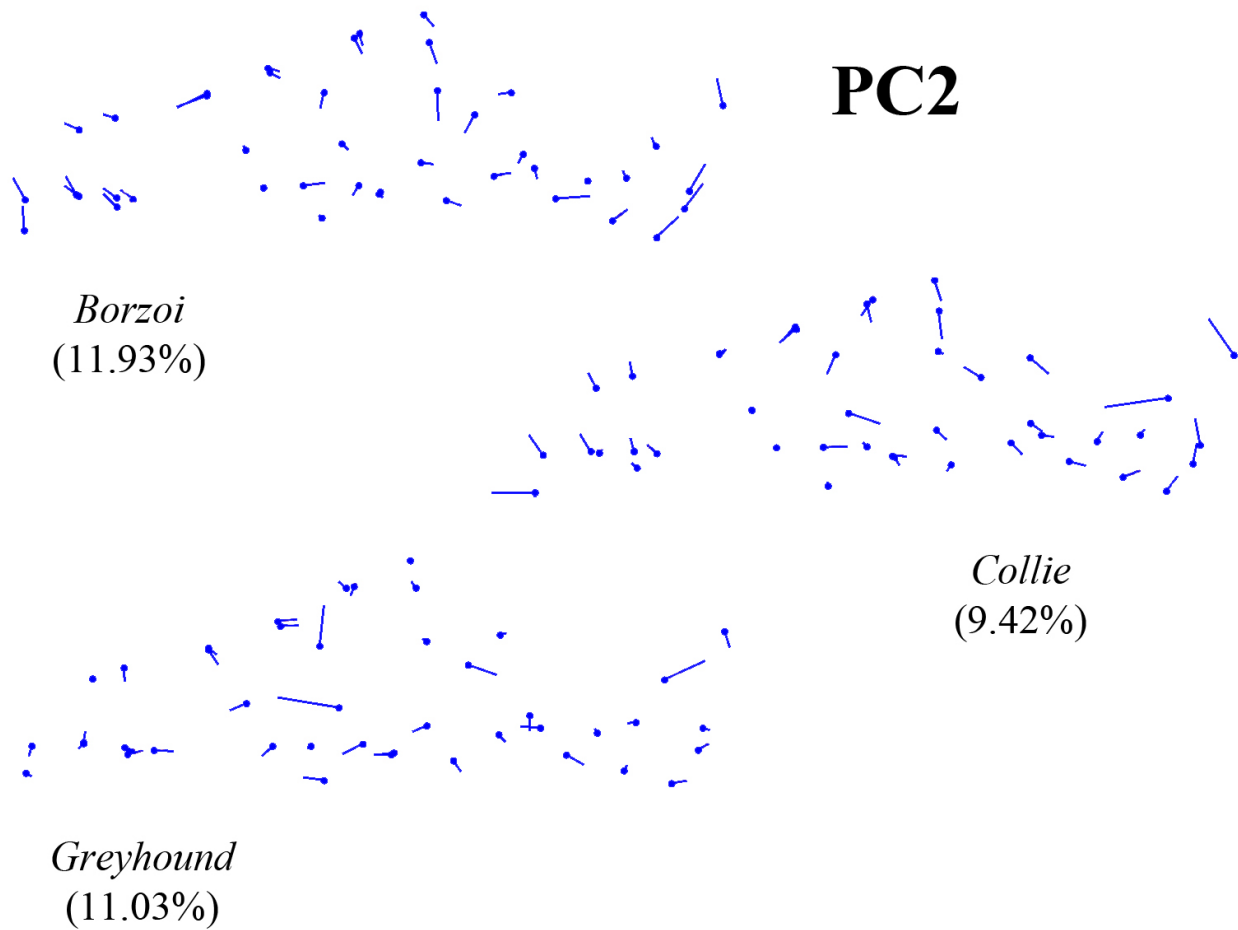


Figure A.2 Second principal components of shape variation for dolichocephalic breeds, lateral view.

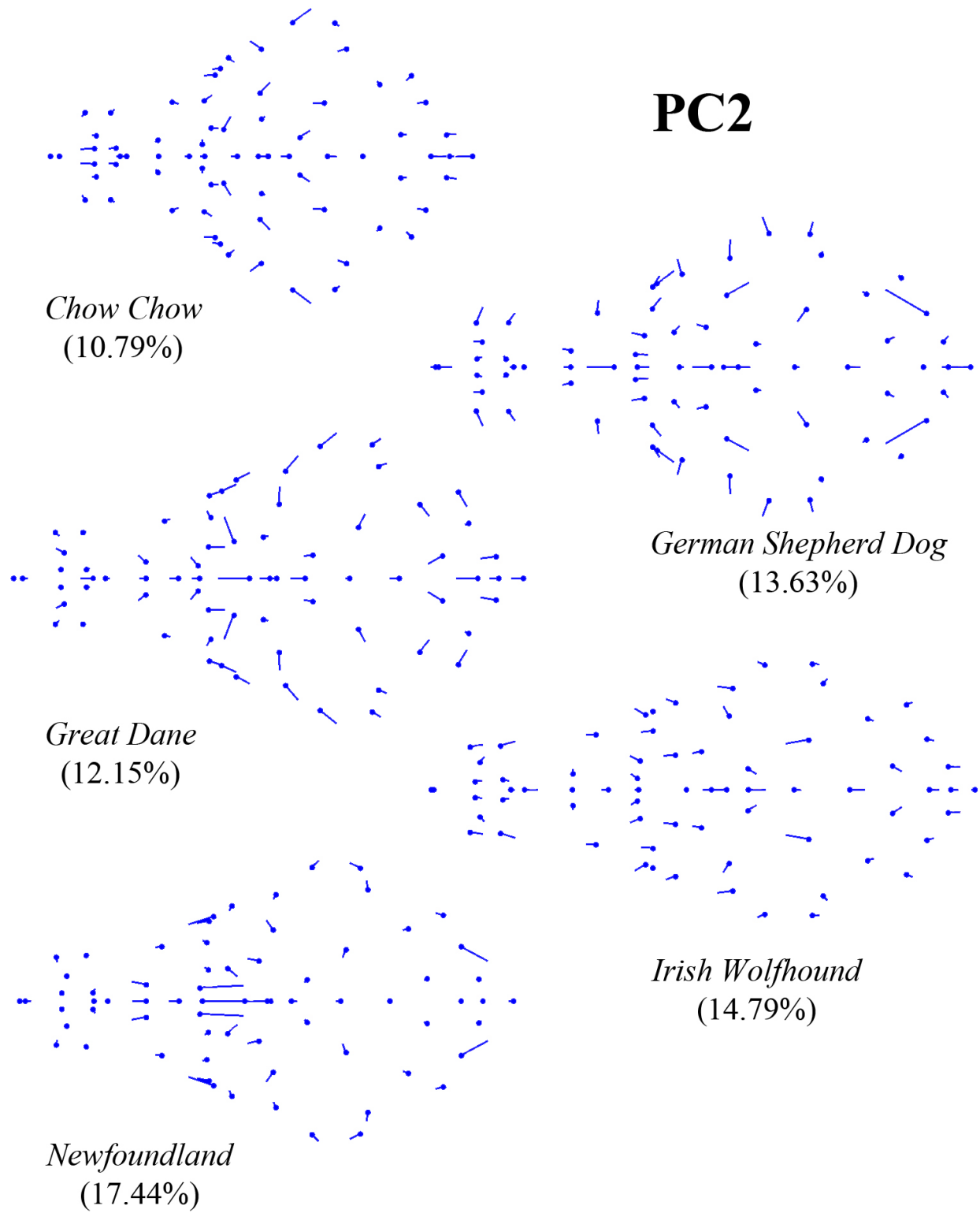


Figure A.3 Second principal components of shape variation for mesaticephalic breeds, dorsal view.

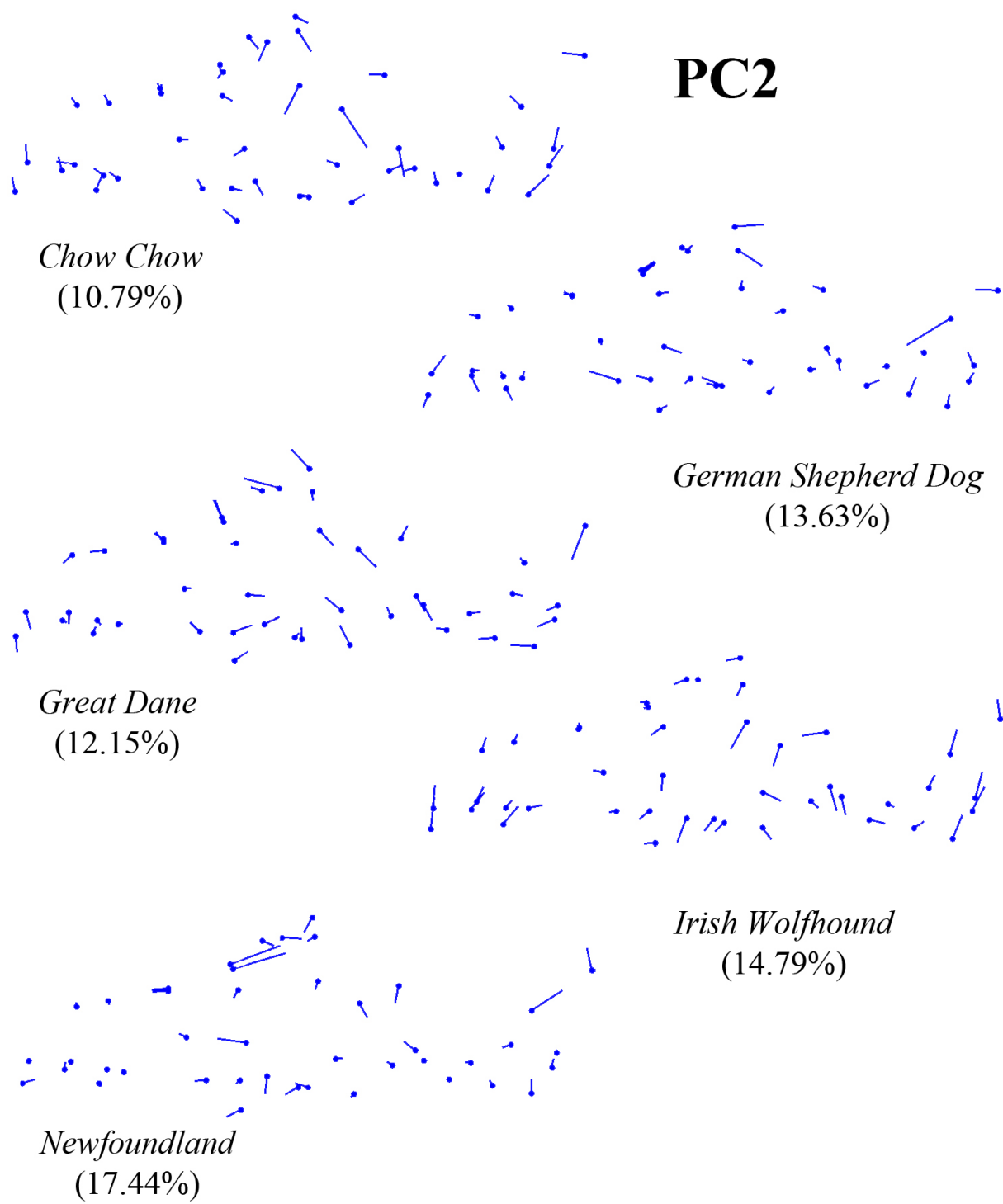


Figure A.4 Second principal components of shape variation for mesaticephalic breeds, lateral view.

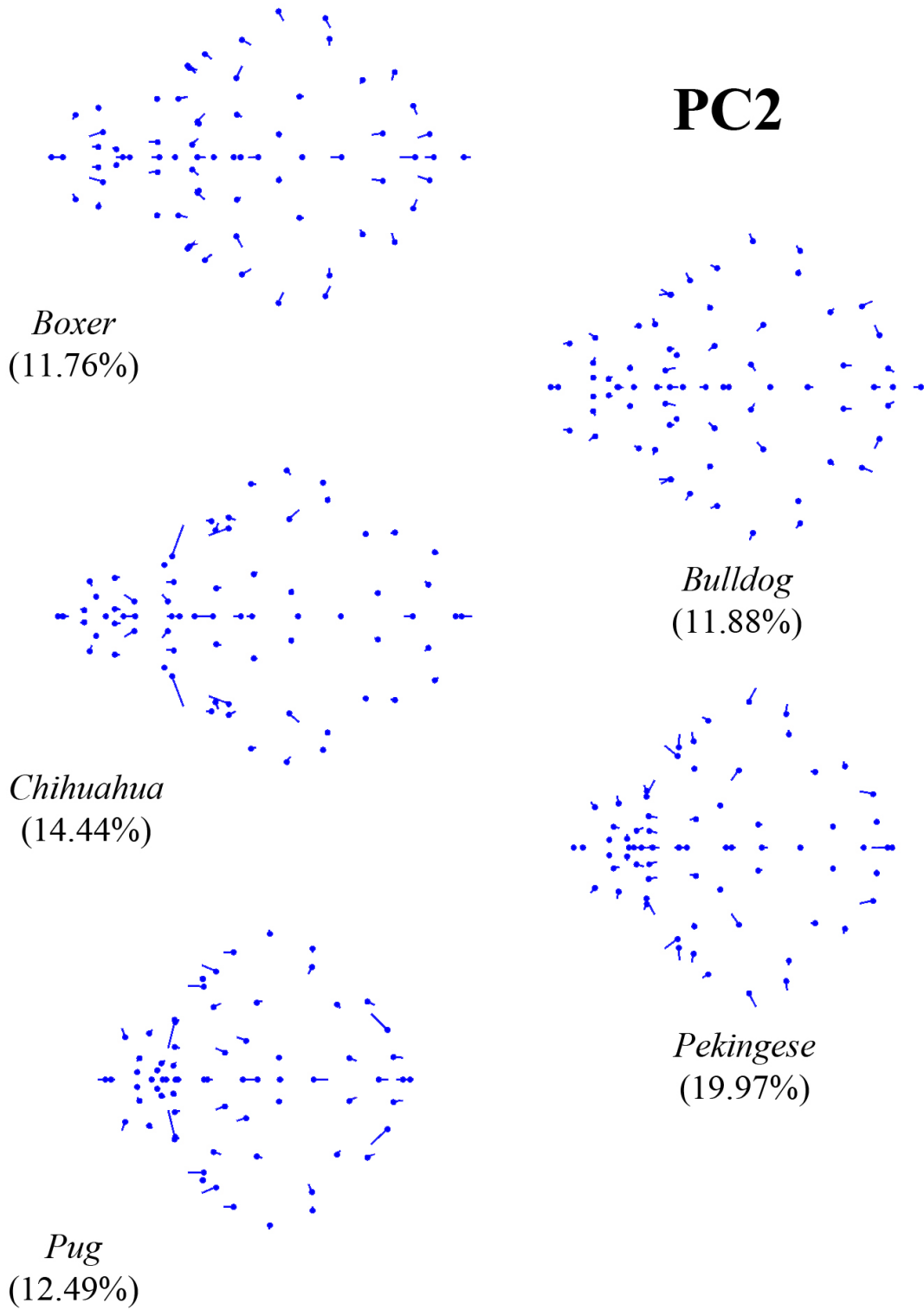


Figure A.5 Second principal components of shape variation for brachycephalic breeds, dorsal view.

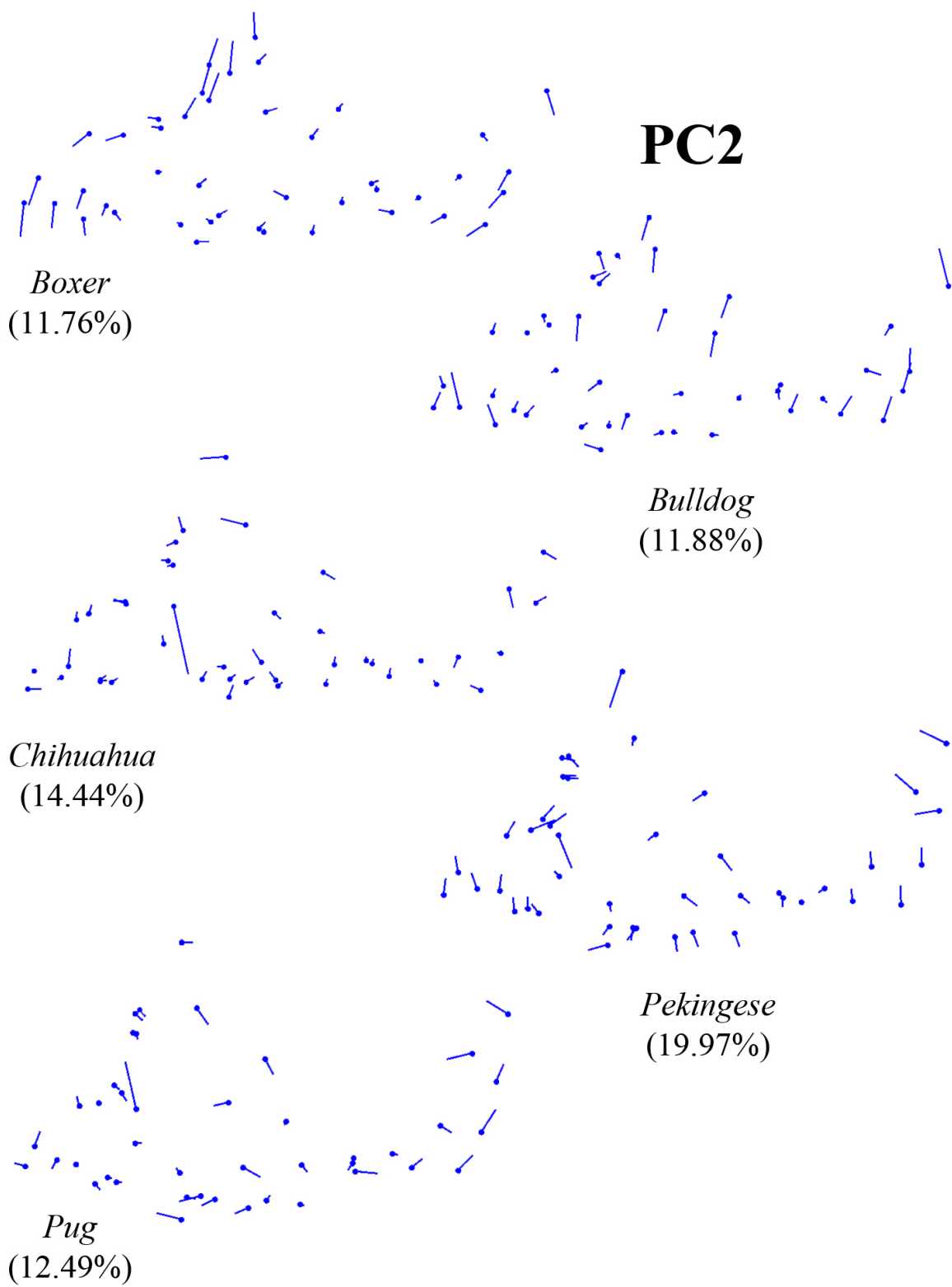


Figure A.6 Second principal components of shape variation for brachycephalic breeds, lateral view.

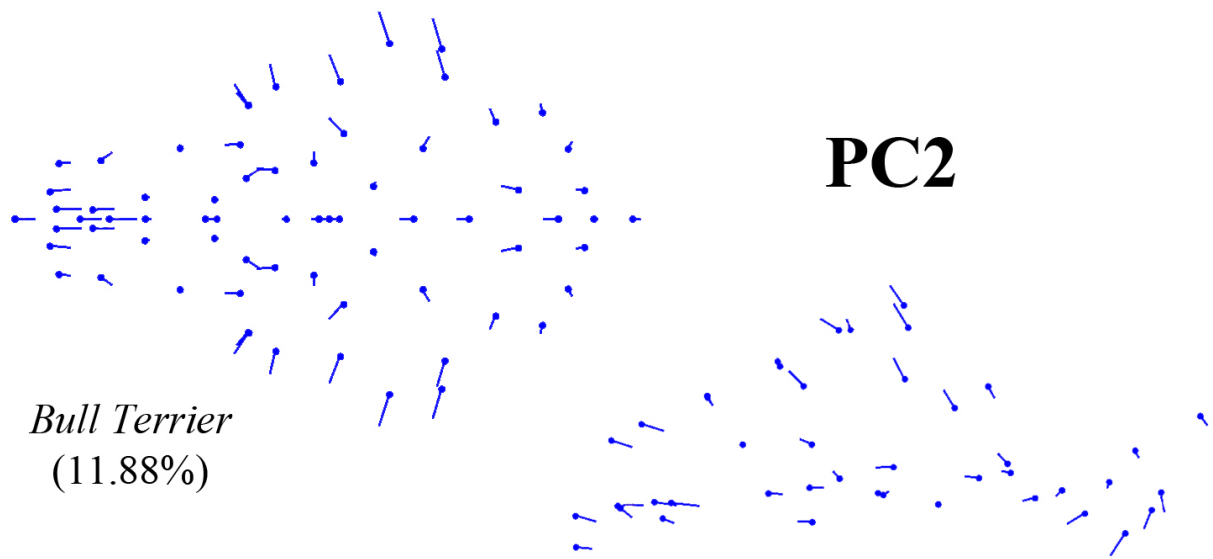


Figure A.7 Second principal components of shape variation for the Bull Terrier.



Figure A.8 Second principal components of shape variation for the French Bulldog.

Appendix 6: Discriminant function shape deformations: additional focus breeds

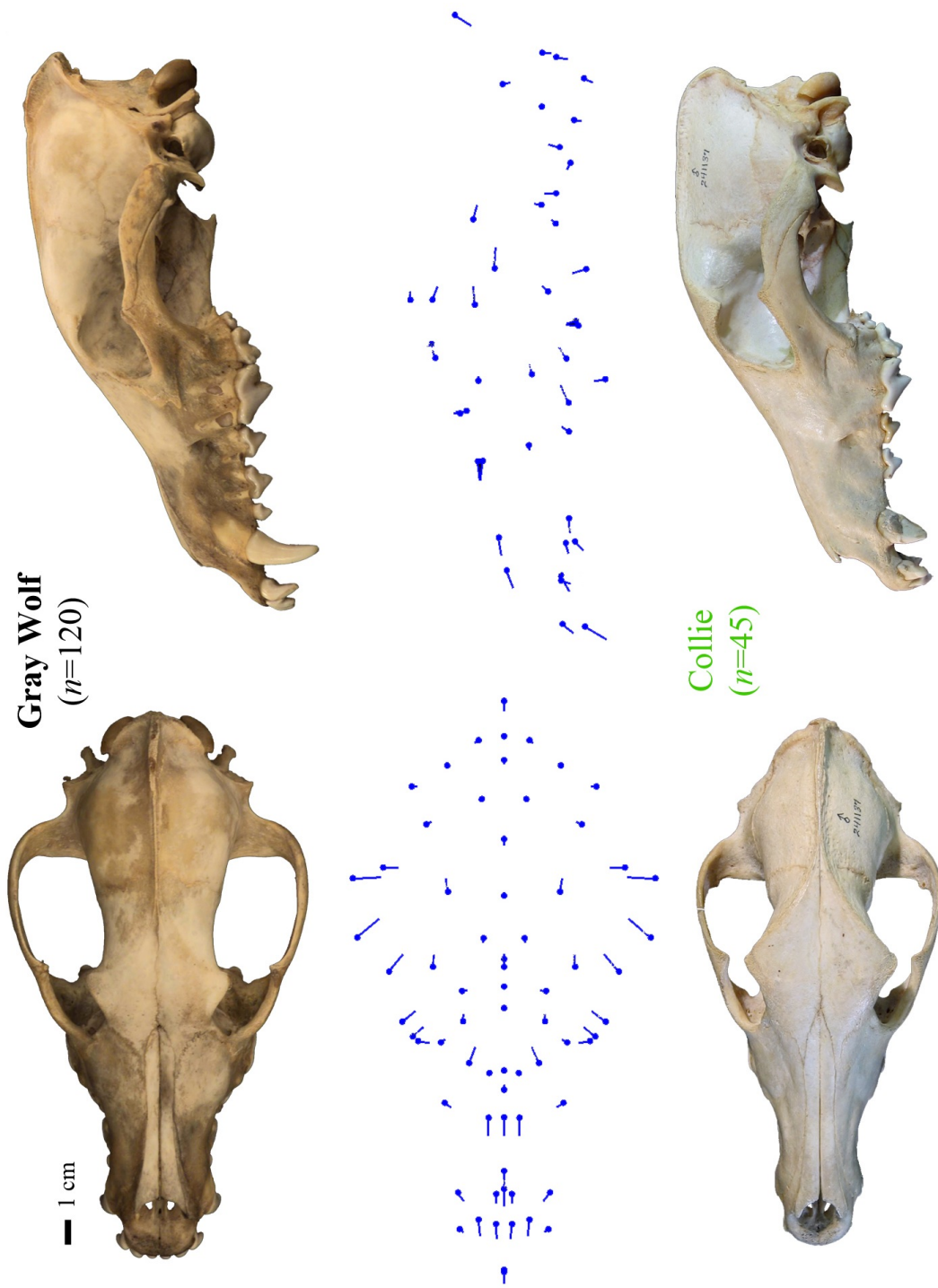


Figure 4.9 Shape difference between the average gray wolf cranium and the average Collie cranium.

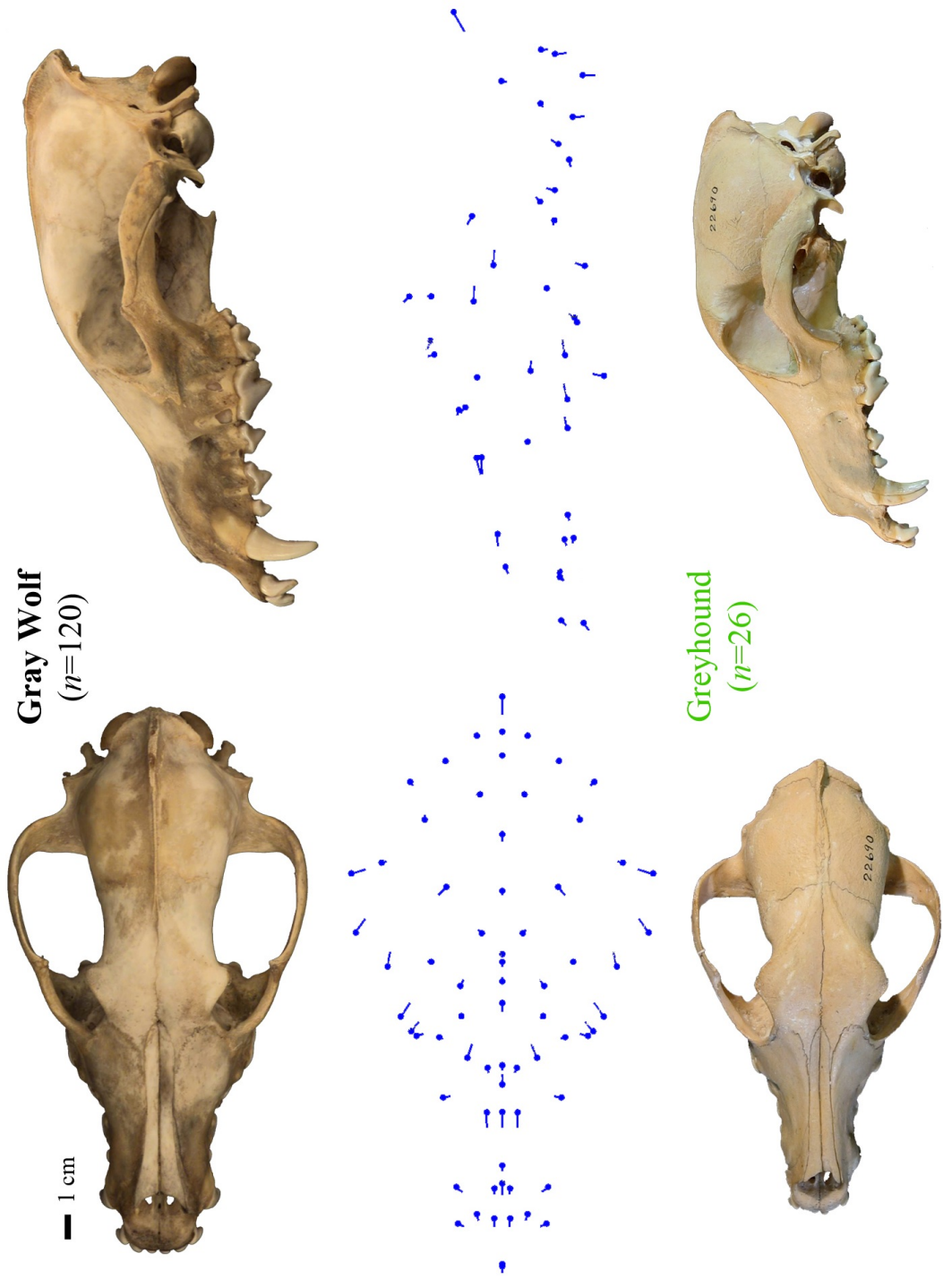


Figure A.10 Shape difference between the average gray wolf cranium and the average Greyhound cranium.

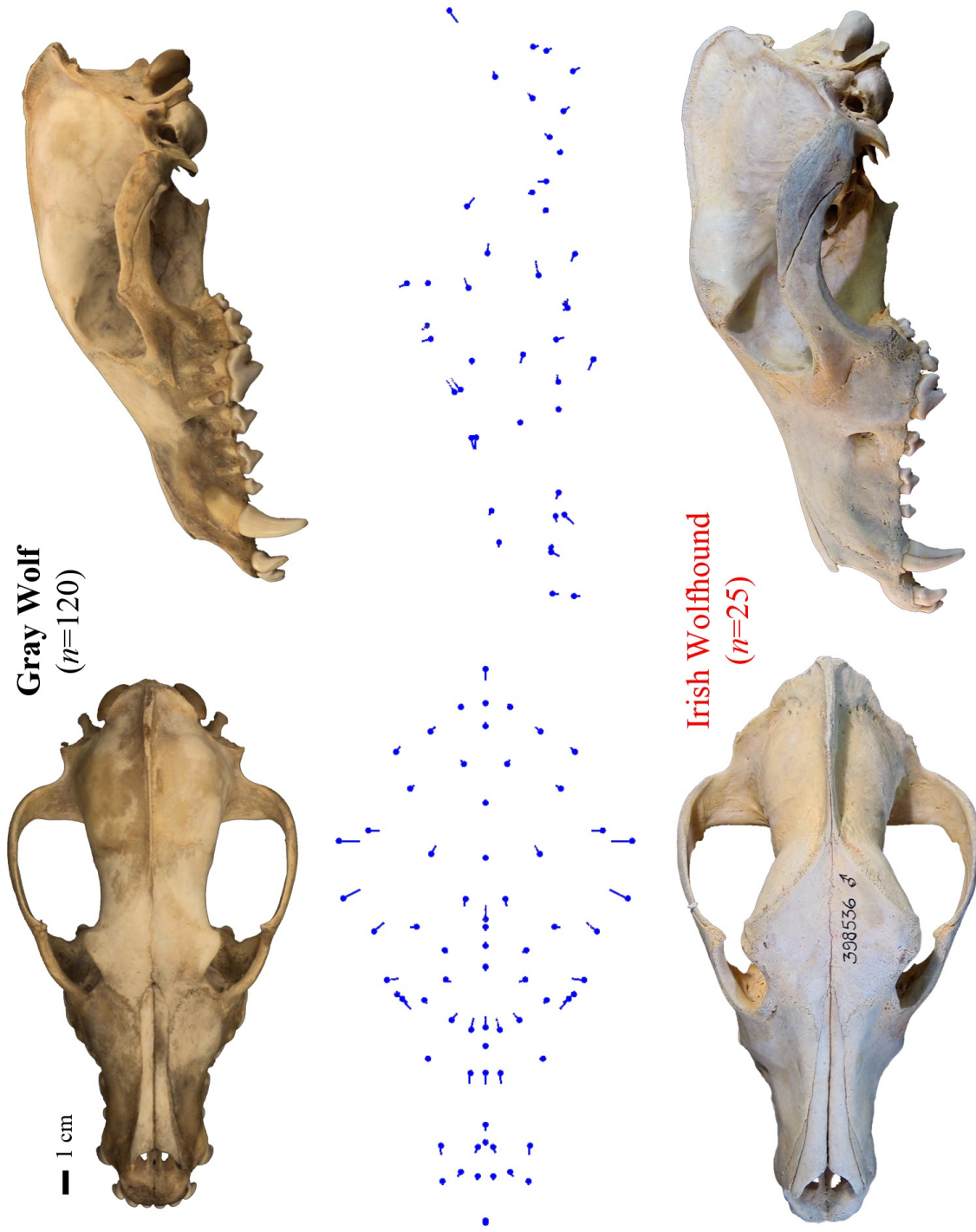


Figure A.11 Shape difference between the average gray wolf cranium and the average Irish Wolfhound cranium.

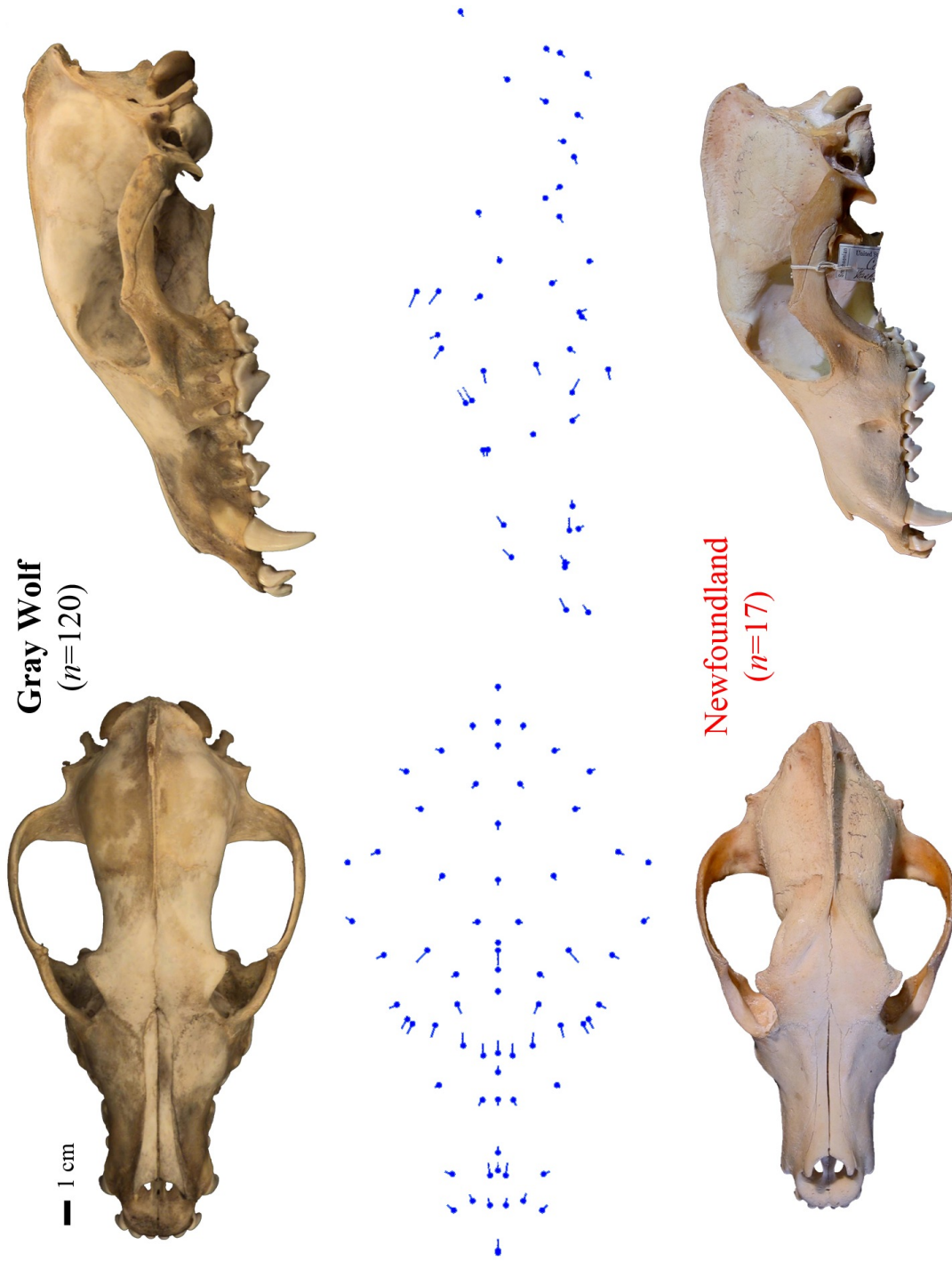


Figure A.12 Shape difference between the average gray wolf cranium and the average Newfoundland cranium.

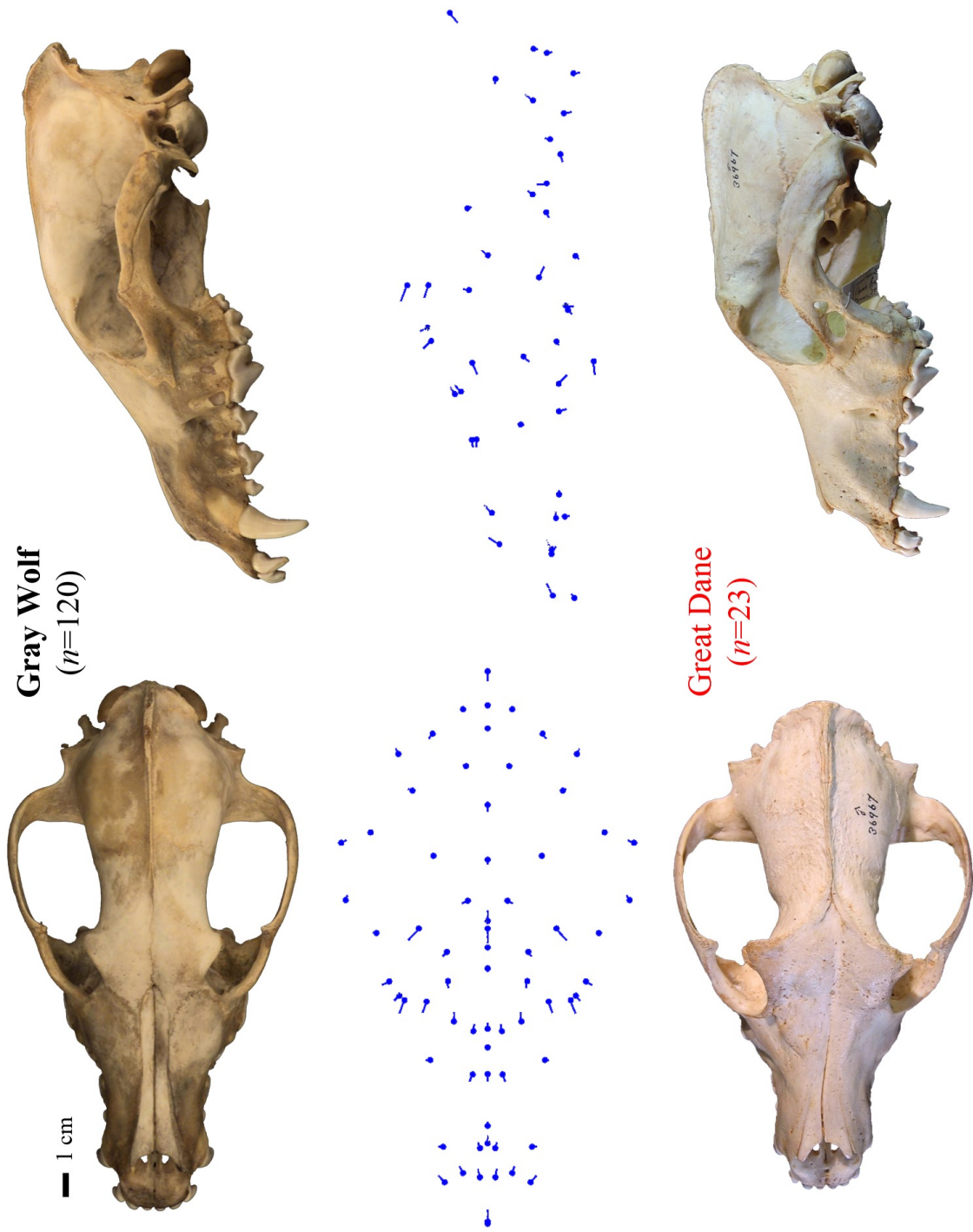


Figure A.13 Shape difference between the average gray wolf cranium and the average Great Dane cranium.

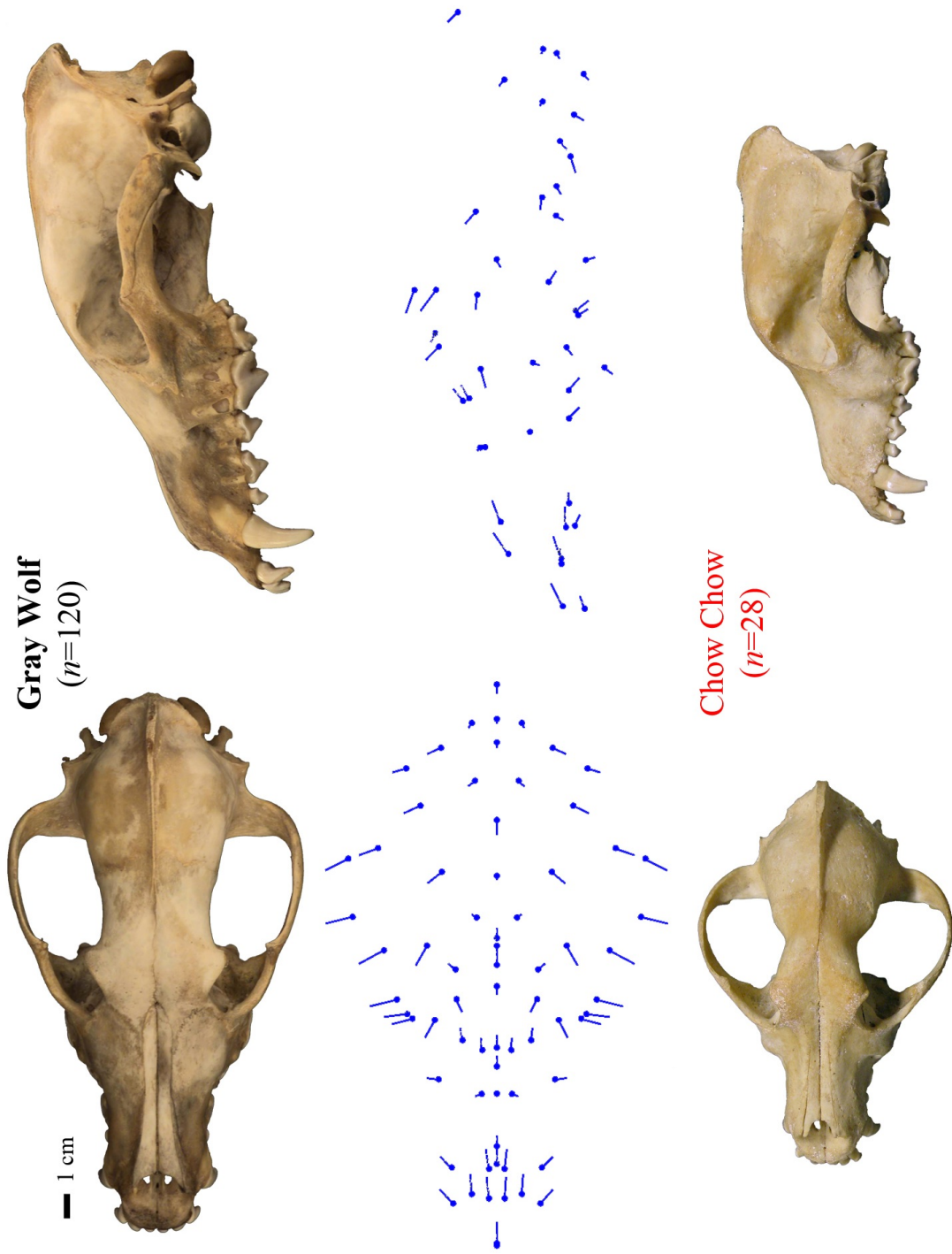


Figure A.14 Shape difference between the average gray wolf cranium and the average Chow Chow cranium.

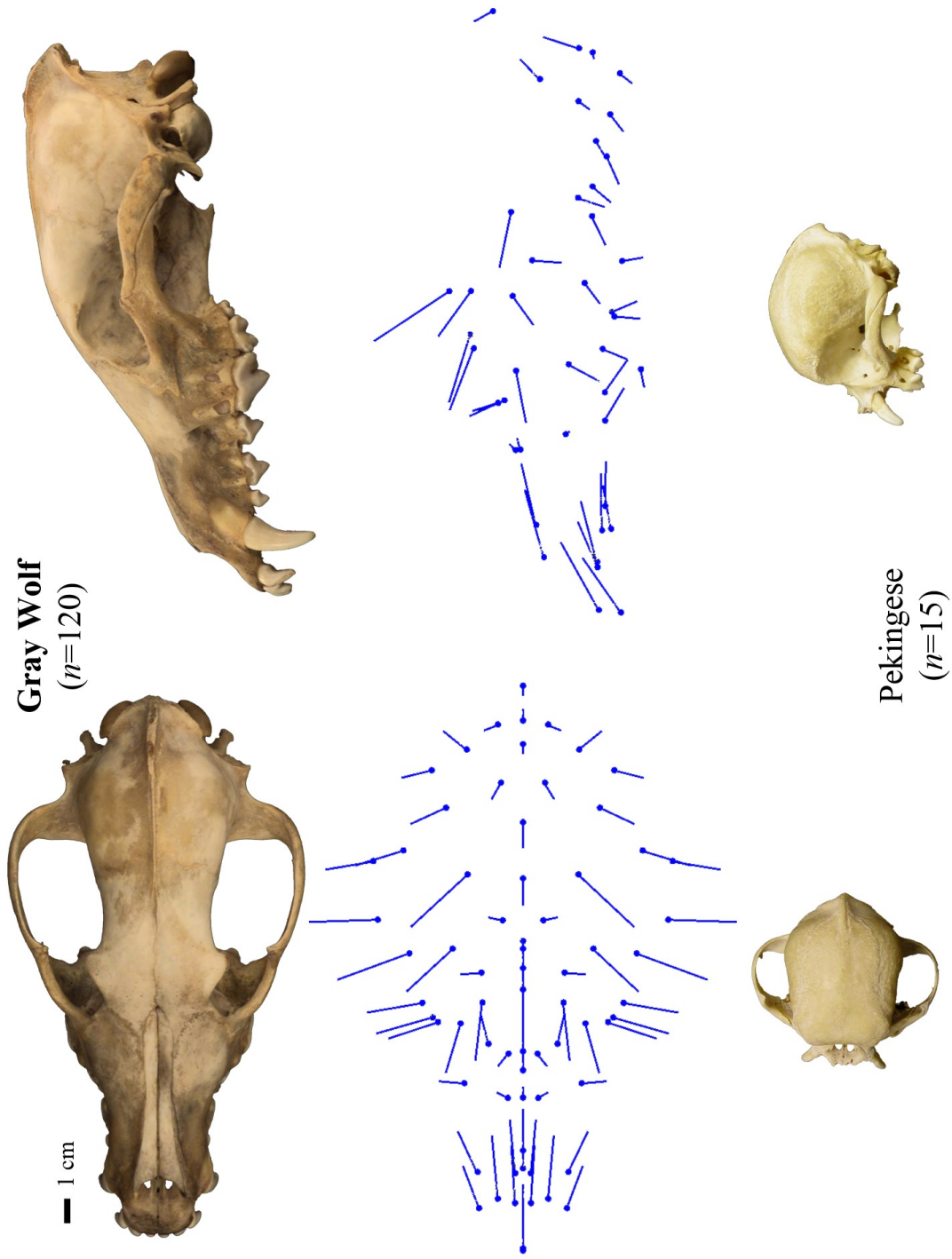


Figure A.15 Shape difference between the average gray wolf cranium and the average Pekingese cranium.

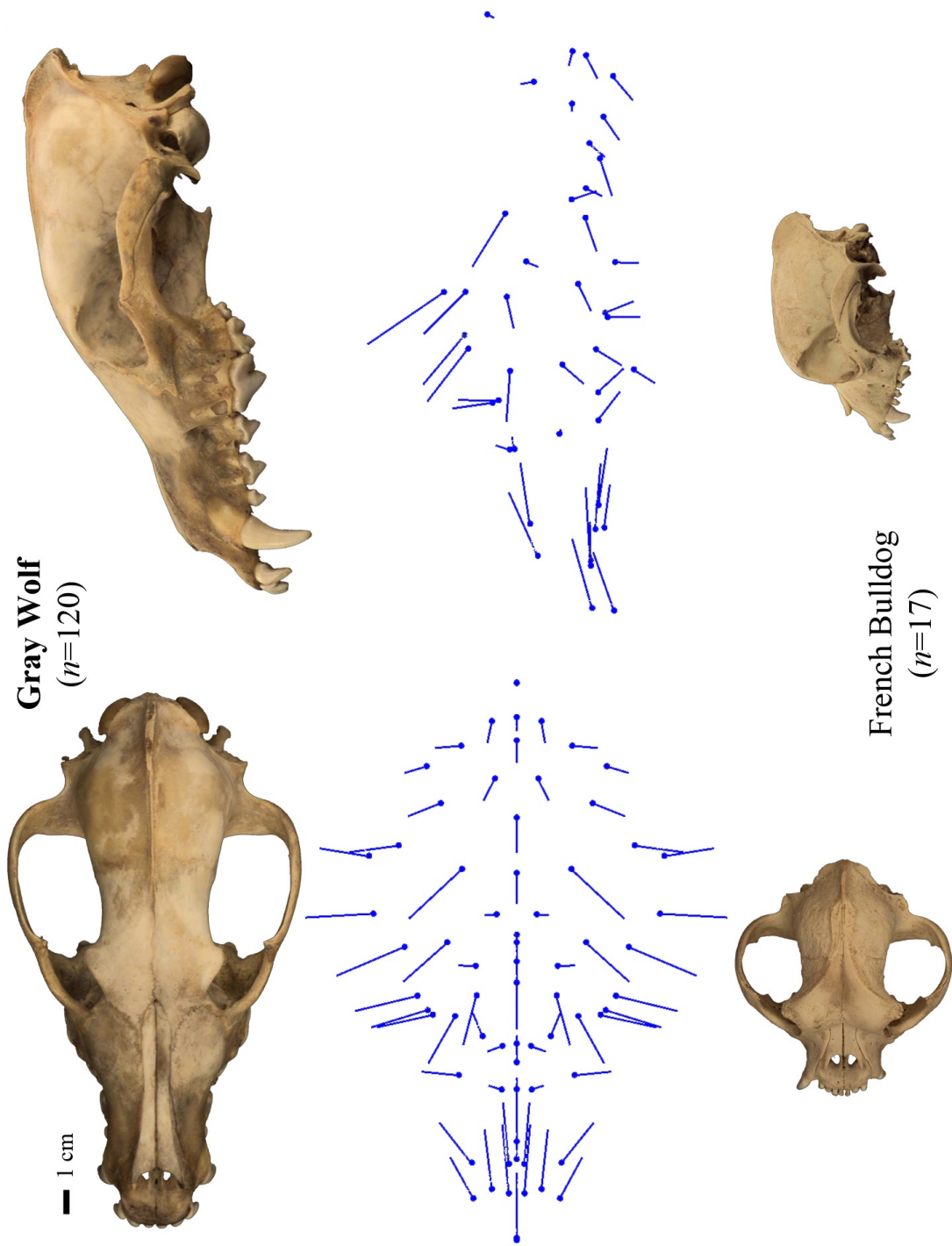


Figure A.16 Shape difference between the average gray wolf cranium and the average French Bulldog cranium.

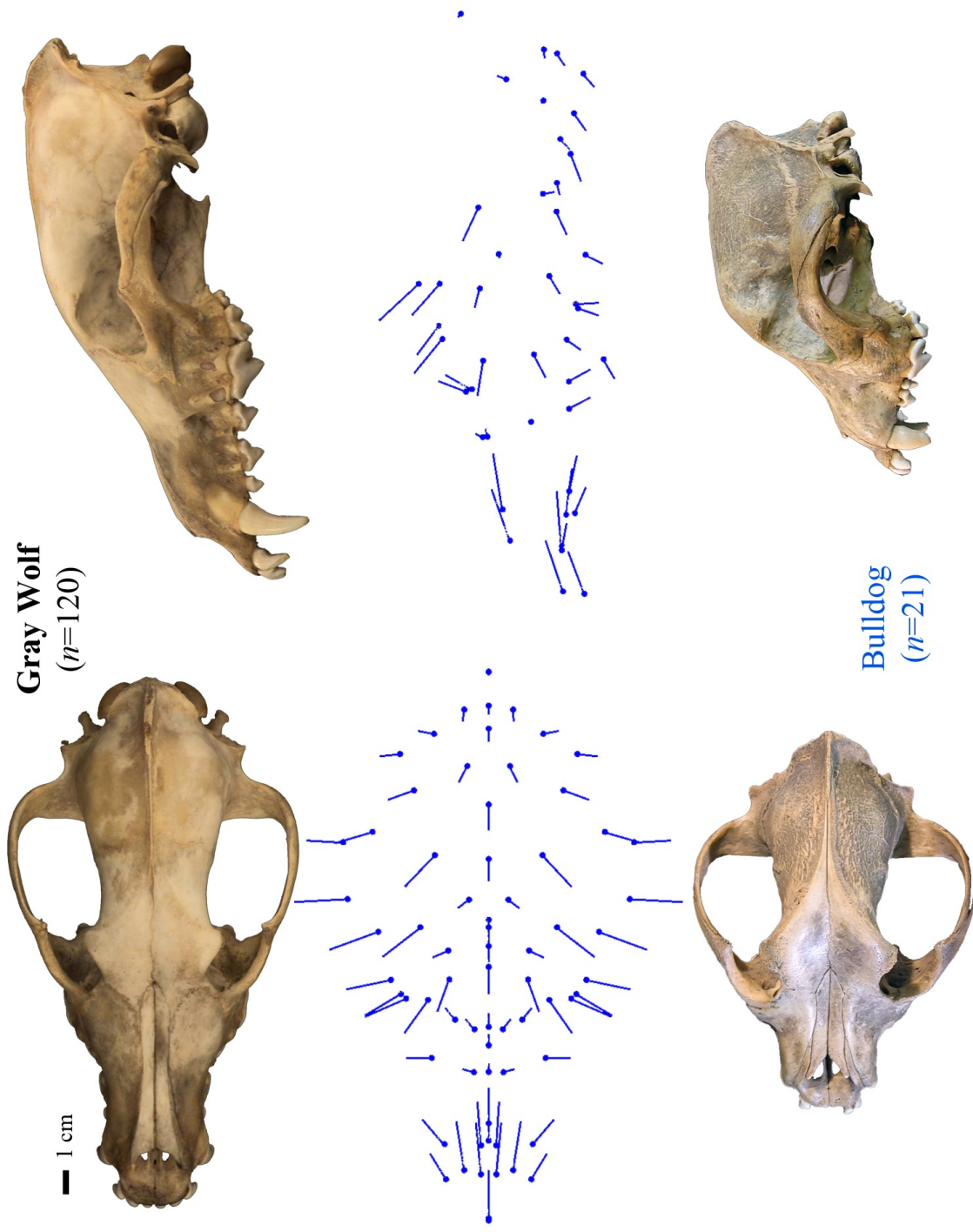


Figure A.17 Shape difference between the average gray wolf cranium and the average Bulldog cranium.

Appendix 7: Additional measures of disparity between breeds.

Mahalanobis distances (D) for pairwise discriminant function analyses of average cranial shapes for domestic dog breeds and the gray wolf. Breed abbreviations are explained in Appendix Two.

	BOR	BOX	BUL	CHI	CHO	COL	FRB	GRD	GRY	GSD	IRW	NEW	PEK	PUG	
WOLF	25.0331	27.1613	37.8139	54.5235	24.3988	21.1587	108.6832	27.8949	24.2091	26.8275	23.2883	28.2778	86.343	129.1008	
BLT	x	17.0572	16.7069	7.2124	12.0658	16.0276	15.3209	9.0481	9.3611	8.1339	12.2179	5.4281	9.3779	11.9918	
BOR		x	18.7504	22.2263	19.5998	13.7542	51.9169	18.4278	11.4304	11.405	12.5404	14.919	41.0348	40.893	
BOX			x	70.504	29.8655	29.8655	25.5921	25.5883	33.1358	28.0889	35.5665	21.4014	20.4949	25.9847	
BUL				x	11.3146	11.9781	6.1431	11.1361	14.7249	12.8958	14.3862	7.8399	9.2735	9.6484	
CHI					x	14.9268	15.6003	14.0903	12.1512	11.2374	16.4655	9.3423	7.2873	10.2293	
CHO						x	17.3226	7.6777	12.8358	8.8264	11.7378	7.041	15.8111	15.629	
COL							x	44.4574	15.5485	7.9014	11.7119	11.8472	28.0994	34.6199	
FRB								x	27.3027	37.4008	36.1755	44.4235	7.8203	6.8364	
GRD									x	10.4633	7.077	6.8559	20.8709	18.8266	
GRY										x	6.7616	8.179	21.4899	22.9311	
GSD											x	5.683	20.0649	20.3987	
IRW												x	26.435	26.7151	
NEW													x	17.9879	
PEK														x	
PUG															x



T-squared statistics for pairwise discriminant function analyses of average cranial shapes for domestic dog breeds and the gray wolf. Breed abbreviations are explained in Appendix Two.

	BLT	BOR	BOX	BUL	CHI	CHO	COL	FRB	GRD	GRY	GSD	IRW	NEW	PEK	PUG
WOLF	12965	9522	29509	25555	46531	13515	14652	175887	15018	12524	13381	11221	11907	99401	208959
BLT	x	5650	4926	594	1524	769	4129	2375	981	1117	774	1866	298	824	1291
BOR		x	127821	7073	8584	6631	4257	33257	5169	2153	1922	2527	2746	18943	17856
BOX			x	3009	12350	12421	158902	8676	10886	19917	12701	22323	6067	5041	7665
BUL				x	1241	1722	5297	535	1361	2519	1787	2362	577	725	782
CHI					x	2441	5956	2128	2005	1570	1250	2837	763	434	824
CHO						x	5915	3174	744	2221	960	1820	524	2442	2280
COL							x	24387	3680	1029	2027	2256	1526	8883	12798
FRB								x	7287	14379	12550	19969	5451	487	359
GRD									x	1336	563	563	147	3955	3085
GRY										x	545	991	687	4393	4785
GSD											x	378	302	3591	3560
IRW												x	718	6551	6405
NEW													x	2578	3134
PEK														x	49
PUG															x